Pottery fabrics from Malta

Characterising Late Punic/Early Roman fabrics from the Żejtun Villa and the sanctuary at Tas-Silġ

Emma Richard-Trémeau

Supervisor: Dr. Maxine Anastasi

Co-supervisor: Dr. Ing. John C. Betts

A dissertation presented to the Faculty of Arts in the University of Malta in part fulfilment of the degree of the Master of Arts by Research in Archaeology.

December 2022

FACULTY OF ARTS

DECLARATIONS BY POSTGRADUATE STUDENTS

(a) Authenticity of Dissertation

I hereby declare that I am the legitimate author of this Dissertation and that it is my original work.

No portion of this work has been submitted in support of an application for another degree or qualification of this or any other university or institution of higher education.

I hold the University of Malta harmless against any third party claims with regard to copyright violation, breach of confidentiality, defamation and any other third party right infringement.

(b) Research Code of Practice and Ethics Review Procedures

I declare that I have abided by the University's Research Ethics Review Procedures. Research Ethics & Data Protection form code 6382_1109 2020.

As a Master's student, as per Regulation 77 of the General Regulations for University Postgraduate Awards 2021, I accept that should my dissertation be awarded a Grade A, it will be made publicly available on the University of Malta Institutional Repository.

Contents

Introduction 2

I Literature Review 6

1 Fabric Studies in Malta 7

1.1 Fabric studies: General concepts 7

1.1.1 Defining fabric and fabric studies 8

1.1.2 Aims and methods of fabric studies 10

1.1.3 Theoretical considerations 15

1.2 Fabric studies for the Roman period in Malta 18

1.2.1 History of ware and fabric classifications 18

1.2.2 Developing scholarship in Malta: other periods 37

2 Understanding local production of pottery in Malta 41

2.1 Raw Material: the local geology 41

2.1.1 The local geology 42

2.1.2 Exploring other raw material 49

2.2 Localising pottery production 52

2.2.1 Considerations: where is the *local*? 52

2.2.2 Provenance studies: possibilities and limitations in Maltese case studies 54

2.3 Evidence for pottery production in Roman times 57

2.3.1 The missing workshops 58

2.3.2 Differing approaches to study local pottery production . . . 60

II Macroscopic and Fabric Analyses 66

3 The archaeological sites 67

3.1 Selecting the archaeological sites . . . 67

3.2 The Tas-Silġ Sanctuary . . . 70

3.2.1 The site and publications . . . 70

3.2.2 Phoenician, Punic and Early Roman occupations . . . 73

3.2.3 Tas-Silġ stratigraphic units . . . 77

3.3 The Żejtun Villa . . . 81

3.3.1 The site and publications . . . 81

3.3.2 Selecting units from the Żejtun villa and limitations . . . 85

4 Methodology 88

4.1 Assemblage description and sherd sampling . . . 88

4.1.1 General considerations for sampling . . . 88

4.1.2 The Żejtun Villa . . . 90

4.1.3 Tas-Silġ . . . 91

4.2 Macroscopic recording and catalogue . . . 93

4.2.1 Description . . . 93

4.2.2 Photographic and drawn record . . . 95

4.3 Microscopic analysis . . . 96

4.3.1 Sample preparation . . . 96

4.3.2 Sample description and classification . . . 97

4.4 Petrographic recording and classification . . . 101

4.4.1 Rationale and sample selection . . . 101

4.4.2 Sample preparation . . . 101

5 Results and preliminary interpretation **105**

5.1 Full assemblages description . . . 105

5.1.1 Macroscopic groups . . . 105

5.1.2 Assemblages fabric overview . . . 109

5.2 Macroscopic observations for the 70 sherds . . . 113

5.2.1 Typology of the samples . . . 113

5.2.2 Colour, surface finish and forming methods . . . 119

5.3 Microscopy and petrography . . . 126

5.3.1 Groupings summary and section structure . . . 126

5.3.2 Fabric 1 . . . 130

5.3.3 Fabric 2 . . . 139

5.3.4 Fabrics 3-4 . . . 146

5.3.5 Fabric 5 . . . 149

5.3.6 Fabric 6 . . . 156

5.3.7 Fabric 7 . . . 157

III X-Ray Fluorescence and data analysis **161**

6 Methodology **162**

6.1 X-Ray Fluorescence . . . 162

6.1.1 Sample selection for XRF . . . 162

6.1.2 Sample preparation and analysis . . . 166

6.1.3 Control samples: X-Ray Fluorescence (XRF) analysis from CRB laboratory . . . 169

6.1.4 Lack of calibration and implications . . . 169

6.1.5 Choosing variables . . . 175

6.2 Elemental composition: Data analysis . . . 177

6.2.1 Data transformation . . . 177

6.2.2 Analyses . . . 180
6.3 Experimental archaeology . . . 184

7 Results and preliminary interpretation 186
7.1 Descriptive statistics . . . 186
7.2 Bivariate analysis . . . 189
7.2.1 Correlation analysis . . . 189
7.2.2 Bivariate scatterplots . . . 191
7.3 Multivariate analysis . . . 196
7.3.1 PCA for Dataset 1 . . . 196
7.3.2 PCA for Dataset 2 . . . 201
7.3.3 Hierarchical clustering on PCs . . . 205
7.4 Terra Rossa experimental archaeology . . . 211

IV Discussion 214

8 Raw material provenance 215
8.1 Blue Clays and San Leonardo clays . . . 215
8.1.1 Fabric 1 . . . 215
8.1.2 Fabric 2 . . . 217
8.1.3 The question of quartz in local materials . . . 219
8.1.4 Fabrics 3, 4 and 6 . . . 219
8.2 Terra Rossa . . . 220
8.2.1 Fabric 5 . . . 220
8.2.2 Use of Terra Rossa in the Mediterranean . . . 221
8.2.3 Fabric 7: two fine vessels . . . 223
8.3 Other possible raw materials . . . 224
8.3.1 Marl samples . . . 224

8.3.2 Other quaternary and alluvial deposits 224

9 Chaîne opératoire and technology 227

9.1 Summary of the *chaînes opératoires* 227

9.1.1 Raw material treatment 227

9.1.2 Manufacturing methods and implications 229

9.1.3 Surface treatment 232

9.1.4 Firing methods 234

9.2 Technology and implications 237

9.2.1 Intended function, vessel efficiency and raw material choice 237

9.2.2 Workshops and archaeological sites 245

Conclusion 249

Bibliography 252

Appendices 284

A Pottery Catalogue 284

B Samples and SU lists 355

B.1 Results table and catalogue data (Digital Appendix) 355

B.2 Descriptions of diagnostic sherds for sampling (Digital Appendix) . 355

B.3 SU summary 355

B.3.1 Tas-Silġ 355

B.3.2 Żejtun 358

B.4 Geological samples 359

C Macroscopy and Fabric analysis tables and supplement 365

C.1 Microscopy . . . 365
C.1.1 Group A . . . 366
C.1.2 Group B . . . 367
C.1.3 Group C . . . 372
C.1.4 Group D . . . 374
C.1.5 Group E . . . 381
C.1.6 Group F? . . . 383
C.2 Petrographic raw data . . . 384
C.3 Experimental Archaeology supplement . . . 389
C.3.1 Marl-derived soils from Saint Peter's Pool . . . 389
C.3.2 Salt water vs tap water . . . 390

D Data analysis supplement 393

D.1 Analytical techniques . . . 393
D.1.1 XRF . . . 393
D.2 X-Ray Fluorescence Results . . . 394
D.2.1 CRB GmbH result . . . 394
D.2.2 Six samples test, XRF . . . 394
D.2.3 Spearman Correlation full results . . . 394
D.2.4 Multivariate Analysis datasets . . . 398
D.2.5 Data Transformation tables (Digital appendix) . . . 406
D.2.6 Method assessment: precision (Digital appendix) . . . 406
D.2.7 Method assessment: accuracy (Digital appendix) . . . 406
D.2.8 Raw data (Digital appendix) . . . 406

Abstract

Characterisation studies of pottery fabric are carried out to understand how pottery vessels are made. Combined with typological analysis, techniques such as Polarised Light Microscopy (PLM) or chemical techniques, including X-Ray Fluorescence (XRF), offer an insight into the stages of the *chaîne opératoires* of vessels. In Malta, Late Punic and Roman vessels have not been characterised widely, and assumptions about the techniques and raw materials used have only rarely been tested with these methods.

This research aims to compile a fabric classification for four stratigraphic assemblages from the Tas-Silġ sanctuary and the Żejtun villa. This study takes an interdisciplinary approach to assess the differences and similarities of fabric groups in regards to their *chaîne opératoire* and provenance of raw materials. A total of 70 sherds were recorded macroscopically and microscopically. Using PLM and XRF, a subset was then characterised. Sherds were compared to clays from the Maltese islands to assess the claim that the vessels could have been manufactured locally.

Seven fabric groups were identified. Two main fabric groups, Fabrics 1 and 2, were established for the plates and bowls; Fabric 1 compared well with the characteristics of the Maltese Blue Clays. One additional group, Fabric 5, was found to be associated with specific cooking vessel forms, and local Terra Rossa is proposed as a possible raw material. Differences between these fabric groups reveal variations in the raw material types and treatment, possibly including clay mixing. It is suggested that some distinctions between the raw materials could be explained by a procurement strategy based on the vessels' function. This research additionally opens the questions of when and how the *savoir-faire* of working Terra Rossa could have appeared in Malta.

In the future, the fabric classification proposed could be expanded with vessels from other archaeological contexts and chronological periods and serve as a basis for future characterisation studies.

List of Figures

1.1 Diagram illustrated the concept of fabric by Santacreu (2014: 109) 9

1.2 Diagram presenting the stages of the *chaîne opératoire*; from Gosselain (2018) 12

1.3 Montage of Sagona's photos of her ware classification cited most in this dissertation. The photos are reproduced from Sagona (2015b: 499-500, Figs. 1:247-248) 27

1.4 Microphotographs of Anastasi Fabric 1, image from Anastasi (2019: 36, Fig. 22) 32

1.5 Microphotographs of Anastasi Fabric 2, image from Anastasi (2019: 36, Fig. 22) 33

1.6 Microphotographs of Anastasi Fabrics 4 and 5, image from Anastasi (2019: 38, Fig. 23) 34

1.7 Photograph of sample M115/2 from FACEM (2020a) 36

1.8 Microphotograph of the main Maltese fabric (Fabric 2) according to Palmer; microphotographs from Palmer et al. (2018: 581; Fig. 7); PPL and XPL 40

2.1 Geological map of the Maltese Islands 43

2.2 Photograph of a clay slope at Għajn Tuffieħa 46

2.3 Photographs of clay models from G. Lanfranco (1978) 48

2.4 Photograph NAG/PA/01/31/1905 reproduced with courtesy of the National Archives of Malta (Gozo section) 48

2.5 Soil survey map first published by Lang (1960), georeferenced and modified with emphasis on the archaeological sites Tas-Silġ and Żejtun 50

2.6 Map of the proposed Punic roads or ways, image from Sagona (2002, 681) 53

2.7 Map and photograph of Il-Qarraba 54

2.8 Scatterplot presenting PCA results from Pirone (2017) 56

2.9 Photograph of Feature 7, Tal-Qares from Cutajar and Spiteri (2014) 59

2.10 Photograph of inscription of sample 34 from Tas-Silġ, rim of olla . 62

3.1 Map of the archaeological sites 68

3.2 Map of Żejtun with archaeological discoveries, from Pace et al. (2012: 62) 69

3.3 Map of selected archaeological sites in the South-Eastern part of Malta 70

3.4 Timeline of excavation campaigns at Tas-Silġ 71

3.5 Orthophotomosaic of the Northern part of Tas-Silġ 71

3.6 Plan of Tas-SilġTemple Period structures from Cazzella and Recchia (2012:19; Fig. 1) 73

3.7 Reconstruction of the Late Republican temple at Tas-Silġ, from Amadasi Guzzo (2011: 15, Fig. 7). 74

3.8 Plan of the Tas-Silġ from Bonanno and Vella (2015) 76

3.9 Plan of a part of Area A, Tas-Silġ. From Vella et al. (2015: 126) . 78

3.10 Plan of Area C, Tas-Silġ showing TSG96/2051 79

3.11 Timeline of excavation campaigns at the Żejtun villa 82

3.12 Plan of the Żejtun villa excavations modified from the publication of Vella et al. (2017: 113) 84

3.13 Orthophotomosaic of the Żejtun Villa, John Betts 85

3.14 Photo of areas A and G at the Żejtun villa, trench ZTN06/2116 (vine trench 9) and its fill (ZTN06/2107) after it was excavated. . 86

3.15 Photo of areas B at the Żejtun villa. 87

4.1 Flowchart of sampling procedure for the TSG96/352 Tas-Silġ assemblage 92

4.2 Photograph of ground sherd presenting the terminology described for the section colour when a double core was noticed 95

4.3 Diagram illustrating the process to correct and assemble images for the catalogue . . . 96

4.4 Photographs of the mounting procedure for sherds . . . 97

4.5 Microphotographs of sample 65 showing the difference between an unground and ground surface . . . 98

4.6 Photograph illustrating the different components described in the fabric descriptions. . . . 99

4.7 Illustration of the terminology to describe inclusions and voids in fabric analysis . . . 100

4.8 Flowchart of procedure including the microscopic analysis and the PLM analysis . . . 102

4.9 Photographs from sample preparations: slicing the pottery sherds to send for thin sections. . . . 103

5.1 Photographs of the four macroscopic Anastasi Fabric 1/ Crisp Ware variants identified. . . . 107

5.2 Photographs illustrating Anastasi Fabric 4 (left, sample 68) and Fabric 5 (right, sample 18). . . . 108

5.4 Żejtun villa, diagnostic sherds for SU ZTN06/549 and SU ZTN06/2107. Summarised data in Table B.7. . . . 111

5.5 Drawings: examples of profiles of plates found in the assemblages, Samples 21, 19 and 2. . . . 115

5.6 Drawings: examples of bowl shapes: Samples 16, 1, 50, 42, 41 . . . 116

5.7 Drawings: examples of profiles of miniatures found in the assemblages, Samples 6, 52 and 45. . . . 117

5.8 Drawings: examples of casserole and olla shapes, samples 13, 18, 46, 39, 5, 70 . . . 118

5.9 Close-up photographs of irregular vessel bases . . . 120

5.10 Photographs of sherds with surface treatments, irregular surface colours and firing defects. . . . 121

5.11 Photographs of cooking vessels . . . 124

5.12 Photographs of inscribed sherds; razing light . . . 125

5.13 Sample 52 microphotograph . . . 131

5.14 Microphotographs of group C members . . . 131

5.15 Microphotograph of sample 15 . . . 132
5.16 Microphotographs of group E members . . . 132
5.17 Microphotographs of group F members . . . 132
5.18 PLM photographs of sample 69 . . . 134
5.19 PLM photographs of samples 12 and 40 . . . 135
5.20 PLM photographs of samples 30, 37 . . . 136
5.21 Micorophographs of examples of members of group D . . . 141
5.22 PLM photographs of samples 4, 10, 25, 48 . . . 143
5.23 Sample 65 microphotograph . . . 146
5.24 PLM photographs of sample 65 . . . 147
5.25 Sample 62 microphotograph . . . 147
5.26 PLM photographs of sample 62 . . . 148
5.27 Microphographs of examples of group B members . . . 151
5.28 Microphotographs of sample 35, ground and unground . . . 151
5.29 PLM photographs of samples 13, 35, 46, 54 . . . 154
5.30 Sample 33 microphotograph . . . 156
5.31 PLM photographs of sample 33 . . . 156
5.32 Microphotographs of members of group A . . . 158
5.33 PLM photographs of samples 61 and 68 . . . 159

6.1 Map of the Maltese Islands with the main sample locations (geological samples) . . . 165
6.2 Photographs of XRF sample preparations and analysis . . . 168
6.3 Precision and accuracy as illustrated by Hein and Kilikoglou (2020: 5, Fig. 2) . . . 172
6.4 Scatterplots for the trial with six samples of untransformed and non-normalized percentages. . . . 174
6.5 Flowchart presenting the sequence of data treatment statistical analysis. . . . 184

6.6 Photograph of Terra Rossa briquettes during drying. Slabs are made of four briquettes to allow measuring shrinkage 185

7.1 Correlation matrix, Spearman correlation, for all variables 190

7.2 Scatterplot of CaO and Fe_2O_3 for dataset 2 (with outliers) 191

7.3 Scatterplots of Al_2O_3 and Fe_2O_3 for both datasets 192

7.4 Scatterplots of TiO_2 and CaO for both datasets 193

7.5 Scatterplot of ZrO_2 and Rb_2O for the Dataset 1. 194

7.6 Scatterplots of SrO and Ga_2O_3 for both datasets 194

7.7 Screeplot (Blue line) and broken stick (red line) for the PCA of dataset 1. 197

7.8 Bar chart of the loadings for each variable for the four first PCs. Data in Table D.4, Appendix D.2.4 198

7.9 Scatterplot of PCs scores for PC1 and PC2 199

7.10 Scatterplot of PCs scores for PC1 and PC2, ellipses are not statistically determined and are only here to improve readability. . . 200

7.11 Scatterplot of PCA 2 for dataset 2. 203

7.12 3D plot of the PC1, PC2 and PC3 205

7.13 Plot of the average silhouette for different k values (number of clusters chosen); here, three clusters. 206

7.14 Dendrogram of HCA, complete link, using the PC scores, cut at three clusters as indicated by RStudio. 209

7.15 Dendrogram of HCA, average link, using the PC scores, cut at three clusters as indicated by RStudio. 210

7.16 Photograph of manufactured briquettes after firing at 500°C. . . . 211

7.17 PLM photographs of sample LP A1. 212

7.18 PLM photographs of sample LP E1. 212

8.1 Photograph of vessel C70 from the Agora collection sitting on top of a brazier (American School of Classics Studies 1958) 222

8.2 Map representing the boundaries for Quaternary deposits falling into the "Valley fills" category as mapped on the Planning Authority (2021) 226

9.1 Ranges of temperatures achieved with different firing arrangements and procedures, from Gosselain (1992: 246) and Guo (2017: 182, Fig. 3) 235

9.2 Graphic summary presenting the discussion on the relationship between fabric, shape, and intended use. 242

List of Tables

1.1 Table presenting the main techniques used in characterization studies. 11

1.2 Table summarising the description of wares as defined by Blagg et al. (1990) 21

1.3 Table summarising some of the characteristics of the local classical wares as defined by Sagona (2015b). 24

1.4 Table presenting a simplified description of the three fabric classes for Roman amphorae described by Bruno and Capelli (1999) 29

1.5 Table summarising the seven local fabric classes for the Classical period as defined by Anastasi (2019) 31

1.6 Table of equivalence of Late Punic / Roman fabrics and wares as defined in the literature 34

1.7 Table listing the characterization and provenance studies for the Maltese Bronze Age. 38

2.1 Table presenting the characteristics of the five visible geological layers in Malta. 44

2.2 Table presenting the assumptions of Traditional Provenance studies by Wilson and Pollard (2001) 54

3.1 Table presenting final SUs selected from Tas-Silġ. The descriptions can be found in Vella et al. (2015: 81,55). Pottery reports include Sagona (2015b) and Frendo and Mizzi (2015) 80

3.2 Table presenting stratigraphic units chosen from the site of Zejtun. Information from Vella et al. (2017: 133-5) and SU sheet for ZTN06/549. 87

4.1 Table presenting the information recorded in the catalogue for every sherd 94

5.1 List of samples selected and their macroscopic group 113

5.2 Table of samples with their shape and typology. 114

5.3 Tables summarising the description of the microscopic analysis and the groups observed 127

5.4 Sample list sent for thin-sectioning and reason to add to the randomly selected samples. 128

5.5 Table of equivalence in the different scales of study: macroscopy, stereomicroscopy and PLM. These equivalencies are loose, as a few samples were misclassified. 129

5.6 Sample list for Fabric 1 based on the PLM and OM analysis. 130

5.7 Table of Group C characteristics 131

5.8 Table of Group E characteristics 132

5.9 Characteristics of PLM Fabric 1 133

5.10 Estimated firing temperature for samples sent to PLM analysis . . . 136

5.11 Sample list for Fabric 2 based on the PLM and OM analysis. 139

5.12 Characteristics of Group D and hypothetical subgroups 140

5.13 Characteristics of PLM Fabric 2 142

5.14 Estimated firing temperatures of the samples sent for PLM analysis 144

5.15 Sample 65 characteristics 146

5.16 Sample 62 characteristics 147

5.17 Sample list for Fabric 5 based on the PLM and OM analysis. 149

5.18 Characteristics of group B 150

5.19 Table of PLM Fabric 5 characteristics 152

5.20 Estimated firing temperatures of the samples sent for PLM analysis; Fabric 5 154

5.21 Sample 33 characteristics 156

5.22 Characteristics of group A 157

6.1 List of sherd samples analysed by XRF (marked with a x) and summary of OM and PLM analysis 164

6.2 List of geological samples used in the analysis 166

6.3 Samples sent for analysis to CRB laboratory, Germany 169

6.4 Means, standard deviation and relative standard deviation (in %) for the readings (n = number of readings) of Sample 21 and QL.B1. 171

6.5 Readings by the laboratory CRB XRF and the XRF used in this study using Sample 21 (S21) and QL.B1 which were analysed multiple times (see section 6.1.4). The difference is expressed in % (Diff in %). 173

6.6 Comparison of values for Cobalt in different dataset 175

6.7 Variables excluded from analysis 176

6.8 Agglomerative coefficient (AC) calculated using the Agnes R package for each clustering method. 183

7.1 Descriptive statistics for the pottery sherds and clays. 187

7.2 Descriptive statistics for each microscopic group of sherds (A-F). n= number of samples in the group. 188

7.3 Eigenvalues for the 10 first PCs (out of 20) as well as variance and cumululative variance (in %) 197

7.4 Table presenting the sherds and raw materials as classified by the Complete Link method (C) and Average Link method (A). The purple numbers are mismatches between methods. S: Samples. . . 208

7.5 Table presenting Dr Capelli's comments on the two Terra Rossa briquettes. 213

Acronyms

BCE Before Common Era.

CE Common Era.

CoFIPoMS Compiling Fabric Identity for Pottery from Maltese Sites.

HM Heritage Malta.

ICP-MS Inductively coupled plasma mass spectrometry.

PCA Principal Component Analysis.

PLM Polarised Light Microscopy.

PPL Plane-Polarised Light.

SCH Superintendence Of Cultural Heritage.

SU Stratigraphic Unit.

UoM University of Malta.

XPL Crossed-Polarised Light.

XRD X-Ray Diffraction.

XRF X-Ray Fluorescence.

XRF-EDS X-Ray Fluorescence Energy Dispersive Spectroscopy.

Acknowledgements

I want to thank my supervisor Dr Anastasi for her trust and constructive feedback. My supervision team has believed in me and encouraged me to strive. I want to express my gratitude to Dr Inġ. Betts, my co-supervisor, who supported me and my incessant daily questions at every step of these technical analyses. There were many stepbacks in this journey. However, we have always worked hard to find solutions and attempt to deliver the best science we can with the available means. Thanks also for the support when I was struggling; I have felt encouraged and valued throughout this degree.

My appreciation goes to Dr Claudio Capelli, who made part of this dissertation possible by analysing the samples with the polarised light microscope and discussing the results and classification with me at length and in great detail.

I wanted to thank Joseph Grech, who helped with the XRF methodology and entrusted me with the analysis. I am indebted to the staff from the Department of Metallurgy and Materials Engineering (DMME): Noel Tonna, Inġ. Mary Grace Micallef, Nicholas Gingell, Inġ. James Camilleri and Daniel Dimech. They have allowed and trusted me to use equipment to prepare all my samples, supported me in different analyses, tackled numerous questions and technical problems, and were kind and curious about my research.

I am grateful to all members of the Department of Classics and Archaeology, but all particularly to the scientific support of Maria Vella and the administrative support of Louisa Borg. They have supported my research with their skills, always ready to help. Thank you to Prof. Nicholas Vella for providing funding for analyses abroad

and permitting me to perform a better analysis. At the department, I would also like to thank everybody who has given me free time to help and prepare samples for analysis. Thanks to Nigel and Thornton, in particular, for helping with embedding samples and sample crushing and Imanuel, Meadow and Andrew for giving a hand in crushing the material.

In these last two years, numerous collaborations with the department have helped me. Special thanks to Iris for letting me use her work and Luke for working on his dissertation on Blue Clays with me. Thanks to Kellian for producing high-quality work, helping me with my photographs, and working with me on experimental samples. Finally, a special note for Alexandra, who has spent one year working alongside me on the clay samples and pottery and helping me with the XRF and additional analyses. She has made this work enjoyable by sharing her knowledge and friendship.

I am grateful to Matthew Grima from Heritage Malta for discussing my methodology with me. Special thanks to Dr Gianmarco Alberti, who has kindly advised me on my statistical analysis. These discussions were enriching and pushed me always to do better work.

During this work, I have contacted many scholars for information or advice. Our communication is acknowledged throughout this work, and I thank all of them for their time. I am also grateful to the staff of the Fitch Laboratory at the British School at Athens for teaching me what I need to understand the complexity of pottery manufacture and the petrographic data. The training I have received at Fitch is invaluable, and I hope to continue to further the skills I have started to learn.

The CoFIPoMS project is funded by the Research Excellence fund and the Research Seed fund. I was fortunate to benefit from the funding of this more comprehensive project to carry out the analyses and was trusted to manage this fund by my Head of Project, Dr Inġ. Betts. None of the petrographic and XRF work would have been possible otherwise. Finally, I am grateful to the Maltese Superintendence of Cultural Heritage for allowing me to conduct destructive analyses on the sherds;

and to the Environment and Resource Authority for allowing me to sample Blue Clay around the Maltese islands.

Last but not least, I must thank the people who have stayed by my side in this task. These include my friends, who have endured my highs and lows, and were always happy to help and hold these engaging discussions. My thanks would not be complete without acknowledging the constant backing of my family, particularly my dad and brothers. They have always been open-minded, enthusiastic, curious and encouragIng. My dad has always supported me in my choices and gave me the means and will to achieve my goals.

The most valuable help comes from my partner, Arthur, who hears me talk constantly about my passion for archaeology but also the challenges I face every day. His unconditional support these last two years has been instrumental to my achievements.

To the memory of my mum, whose passion, perseverance and kindness still inspire me every day.

Introduction

Background

For an archaeologist, there is no need to introduce what a piece of pottery is, as, for many in the profession, their first find was likely a sherd. Often cited as the most prevalent type of find on sites with sedentary occupation (Hunt 2017a: 3), pottery has been an inherent part of the discipline, and its study has followed both the theoretical waves and technical advances in the field of research.

The current approach to the study of pottery is interdisciplinary, as exemplified by recent publications such as *The Oxford Handbook of Archaeological Ceramic Analysis* (Hunt 2017b), which covers matters from statistical modelling to ethnographic research. Pottery characterisation, for example, can enhance knowledge of pottery manufacture, from the provenance of material to the distribution of goods. These interdisciplinary approaches make it possible to hypothesise on the craftspeople's behaviour at several stages of the *chaîne opératoire*, and what might constrain or favour specific choices and gestures in their unique environmental and social context (Santacreu 2014: 2).

In Malta, Punic and Roman pottery classes have interested scholars since the first vessel classification carried out by Caruana (1899). However, the manufacture and provenance of sherds from these periods have more rarely been approached through characterisation. There is, therefore, a prospect of better understanding the local making of vessels through the application of characterisation techniques.

Geographical and chronological context

This dissertation focuses on pottery found in the South East of the Maltese islands, specifically on the assemblages from two archaeological sites: the sanctuary at Tas-Silġ and the Żejtun villa. The assemblage comprises vessels described as 'local vessels' in published post-excavations studies (Bechtold 2017; Sagona 2015b). 'Locally produced' here means produced in the Maltese islands. As there is no direct evidence of pottery production at the two archaeological sites and little clay in the surroundings, pottery might have been transported over

distances across the islands. As more studies and assemblages are published, they could offer a higher resolution and more insight into the local production and distribution of vessels at a regional or settlement scale. However, it is not within the scope of this work.

Chronologically, this dissertation will mainly focus on Malta's Late Punic and Late Republican periods (or the 'Early Roman Period'). For the Maltese islands, the Late Punic period, sometimes called the Hellenistic period, is defined from the end of the fourth to the third-century Before Common Era (BCE). The Late Republican or Early Roman period is defined as the end of the 3rd to the 1st century BCE. The early Roman period is determined by chronological markers and historical events. The Roman Republic is said to have seized Malta during the second Punic war in 218 BCE (Bonanno 2005: 138). The Late Republican period ended with Octavius becoming Augustus, sole ruler over Rome in 27 BCE (Bonanno 2005: 193). These historical dates mark political changes rather than depict socio-cultural affinities: a chronological nomenclature based on historical events should not prevent a discussion of cultural and material continuity and change. The annexation of Malta to the Republic certainly did not alter pottery manufacture from one day to another. Many scholars highlight continuity on the islands until the imperial period and the first century BCE (Cardona 2021: 232).

Scholars have named these periods differently. For instance, Sagona (2002: 4), in her work on pottery, calls the whole era 'Punic', privileging cultural affinities and continuity rather than political change. This can, however, prevent a greater emphasis on shorter-term changes which becomes impossible to describe when a period spans many centuries.

Research aims and objectives

The main aim of this study was to investigate the local manufacture of pottery during the Late Punic/Early Roman periods in Malta through an interdisciplinary study of fabric.

The following objectives were set out:

- Identify and review the literature on Late Punic/Early Roman fabrics and clay analysis in the Maltese islands, focusing on previous classifications and the methods employed.
- Investigate the variations in pottery fabric of a targeted pottery assemblage by classifying them using macroscopic, microscopic, petrographic and chemical analysis.
- Assess these variations by looking specifically at differences in *chaîne opératoire* and technological choice
- Assess the claim made that these vessels could have been produced with local material by comparing their composition to locally sourced raw material

Scope

This research is part of a broader research project named Compiling Fabric Identity for Pottery from Maltese Sites (CoFIPoMS) led at the University of Malta (University of Malta 2021), a continuity of the MaltaPot project (University of Malta 2020).

Significance of the research

This study can contribute to understanding how pottery was manufactured, including the provenance of raw material, in the Maltese islands during the Late Punic/ Early Roman period. Although it focuses on specific stratigraphic units, this case study can classify pottery based on techniques that have not been widely used in local scholarship. Future researchers will then be able to compare their assemblages and expand or correct the classification, adding variations across geographical areas and site-specific contexts. Hopefully, the preliminary work on the clay material led during this research, and more widely within the CoFIPoMS project, will highlight and start tackling the lack of specialist knowledge on raw materials in Malta, their diversity and their properties.

Dissertation structure

Part I starts with two chapters reviewing the literature about the manufacture of pottery in Malta and how it has been investigated in the past. Chapter 1 looks specifically at the fabric studies in Malta, introducing the general aims of fabric studies and then looking at which methods have been applied in Maltese scholarship. The second chapter looks at how archaeologists have assessed the provenance of sherds in Malta.

Part II presents the typological and fabric analysis carried out in this dissertation. Chapter 3 describes the two archaeological sites under study and how the assemblages were selected. Chapter 4 lays out the methodology for these analyses. The results, including the fabric classification, are presented in Chapter 5.

Part III comprises the X-Ray Fluorescence analysis and data analysis. Chapter 6 describes the methodology for both these analyses, and Chapter 7 describes the results.

Finally, Part IV of this dissertation discusses the results, bringing the analyses together to answer questions about provenance, the *chaînes opératoires* and technological choices.

Part I

Literature Review

Chapter 1

Fabric Studies in Malta

1.1 Fabric studies: General concepts

Until the 1950s, the study of ceramics focused on vessel types and their classification (Pollard and Heron 2008: 99), during what has been termed the *typological phase* of the discipline (Orton and Hughes 2013: 7). Researchers ordered vessels in classes based on shape or style, broadly equated with cultural complexes (Johnson 2009: 36-37). Typological analysis is still a helpful tool today; however, at the time, differences in artefacts were taken to reflect culture groups (Fowler 2010: 355-356). 'Culture' was portrayed as static, and changes in the material record were explained according to external factors such as invasion. The aims of pottery studies were, on the one hand, to define these 'cultures' and, on the other hand, to use typology and seriation to date sites and artefacts (Renfrew 1977: 3).

It is not to say that the understanding of pottery fabric did not attract scholars. As early as the nineteen century, the fabric of vessels was of interest. Brongniart (1844: 15), for example, described the pastes[1] of Roman and Greek vessels from the archaeology museum of Sèvres, France, looking at their characteristics and assumed provenance. He stated that no "lead", "copper", or "tin" have been identified in

[1] from the french "Pâtes"

the glaze of European potteries from before the thirteen century BCE.[2]. According to the author, these statements are based on a laboratory study, but he does not describe the experiments he led. This example highlights that the scope of studying pottery fabrics was understood early in the history of the discipline.

The systematic study of fabrics using scientific methods was formalised in the 1950s. Shepard's book in 1956 was instrumental in framing how ceramic research should be conducted and how to integrate scientific methods within pottery studies (Tite 2016: 8). In her book, Shepard illustrates how to describe the physical properties of ceramics and the use of different methods such as petrography and X-Ray diffraction to study both the composition and manufacture of pottery vessels (Shepard 1956: 146-168).

1.1.1 Defining fabric and fabric studies

Peacock (1977b), and his students were pioneers in stressing the benefits of fabric studies. Their work is still widely cited for their methodology to describe and record fabric through their fabric recording form(Degryse and Shortland 2018: 3). Peacock (1970: 375) defined "fabric" as the material which makes up ceramic vessels and proposed a standardised recording system with macroscopic criteria (e.g. hardness) and frequency, size or distribution of inclusions (Peacock 1977a: 29). This record is strengthened by petrographic and, if necessary, chemical analysis.

Whitbread (2016: 200) defined fabric as the "arrangement, size, shape, frequency, and composition of the material constituents of the ceramic". His first work, from 1995 on Greek amphorae, aimed to standardise pottery classification (Whitbread 1995: 368). Whitbread describes a systematic way, adapted from the studies of rocks, to record fabric, classify thin section analysis and describe fabric constituents. These constituents are both the micro mass (the matrix), the inclusions, and voids (Whitbread 1995: 380-383). This definition considers

[2]dated with nineteen-century methods; from the french "on n'a trouvé ni plomb, ni cuivre, ni étain, dans aucune Poterie Européene fabrique avant le XIIIe siècle" (Brongniart 1844: 17)

qualitative and semi-quantitative aspects of the constituents (e.g. frequency) and includes voids/pores as features of the fabric. Those are sometimes omitted from textbook definitions despite being informative on manufacturing techniques (e.g. Orton and Hughes, 2013: 71).

One approach to conceptualise fabric is given by Santacreu (2014: 109) who differentiates *Fabric* from *Paste*, sometimes used interchangeably (Orton and Hughes 2013: 71). The paste describes the characteristics of the unfired material after processing (e.g. levigating or tempering). The fabric, on the contrary, is the material resulting from the whole sequence of production, the *chaîne opératoires*, including firing, which impacts composition (Figure 1.1). Pottery fabrics are thus a set of physical and chemical characteristics resulting from *active* processes which have economic and social dimensions (Santacreu 2014: 110-111). Looking at fabric, these actions can be studied to gain insight into technological choices and their complexity (Roux 2016: 101).

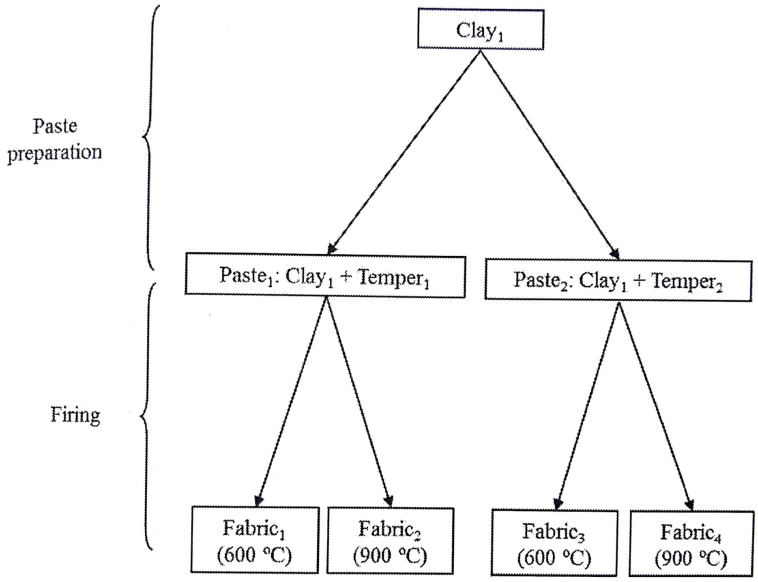


Figure 1.1: Diagram illustrated the concept of fabric by Santacreu (2014: 109)

Fabrics should be differentiated from *Wares*. The term *Ware* is sometimes used loosely to integrate some characteristics of fabric; this will be explored in the work of Sagona (2002; 2015b) in Section 1.2. The term *Ware* has been used in the past to describe groups of ceramics that were assumed to be made of the same recipe (Kipfer 2008), with the same technology or produced in the same workshop (Darvill 2008). Shepard (1956: 318) already noted that the term *ware* was often "loosely employed" for both broad classes of vessels (e.g. "earthenware"), or groups of pottery sharing similarities in manufacture or surface treatment. Rice (2015: 230) underlines the need for defining these terms clearly when using them as classification units. Ware categories can be used as broad classes with defined characteristics in a pottery classification system (Rice 2015: 230-231). However, the unit descriptions and hierarchy have to be "systematic and coherent" (Santacreu et al. 2016: 184). The classes termed *Wares* might therefore integrate the vessel fabric as a characteristic, or even the primary variable, of classification (Degryse and Shortland 2018: 3), but this has to be clear in the classification methodology.

1.1.2 Aims and methods of fabric studies

Fabric studies have varied research interests and employ multiple techniques such as those cited in table 1.1. A full description of available techniques can be found in Cuomo Di Caprio (2017a), Henderson (2000), and Pollard and Heron (2008) and a list in Kolb (2014). This section will therefore focus mainly on the methods chosen for this dissertation.

The first step in fabric studies is the creation of a fabric classification based on the similarities and differences in observations (Whitbread 2016: 392). These archaeological categories, not emic categories, can not necessarily be equated to production centres (Santacreu et al. 2016: 185), but aim at grouping sherds resulting from similar manufacturing processes and raw materials (Quinn 2013: 71). The characterisation of these fabric groups then describes the process of identification of the material characteristics and physicochemical properties of the

various components (Degryse and Shortland 2018).

Name	Acronym	Analysis type	Properties investigated
Inductively Coupled Plasma Mass Spectrometry	ICP-MS	Bulk analysis	Major/minor/trace elements
Instrumental Neutron Activation Analysis	INAA	Bulk analysis	Major/minor/trace elements
X-Ray Fluorescence	XRF	Bulk analysis	Major/minor/trace elements
X-ray Emission Induced by Protons	PIXE	Point/bulk analysis	Major/minor/trace elements
Proton Induced Gamma Emission	PIGE	Complement PIXE for light elements	
Scanning Electron Microscopes combined with Energy Dispersive X-ray Spectroscopy	SEM-EDX/EDS	Surface analysis (mainly)	Major/minor elements
Raman spectroscopy		Surface analysis (mainly)	Molecular bonds
X-Ray Diffraction or X-Ray Powder Diffraction	XRD or XRPD	Bulk analysis	Mineral phases
Fourier-transform infrared spectroscopy	FTIR	Bulk analysis	Molecular bonds
Polarised light microscopy	PLM	Component description	Mineralogical composition
Optical microscopy	OM	Inclusion and matrix	Visual characteristics

Table 1.1: Table presenting the main techniques used in characterization studies. Summarised from the tables in Cuomo Di Caprio (2017b) for each method and Ruvalcaba-Sil (2018) for PIXE. The acronyms are excluded from the list of Acronyms in the Front Matters.

Manufacture

Fabric studies can aim at explaining manufacture and technological choices, inferring into the specific actions taken when producing a vessel (Cuomo Di Caprio 2017b: 529). The purpose is to reconstruct the steps of the *chaîne opératoire*[3] (Figure 1.2), and "the dialogue that the potter has with the raw clay to improve its characteristics" (Eramo 2020: 164). Studying manufacture from finished deposited vessels assumes that 1) different manufacturing stages leave diagnostic traces; 2) other stages do not eliminate these physical diagnostic traces. Interpreting the decisions of the potter has substantial theoretical implications (Section 1.1.3), as some cultural variables that could influence a technological action, consciously or unconsciously, cannot be observed directly (Rice 2015: 212-213).

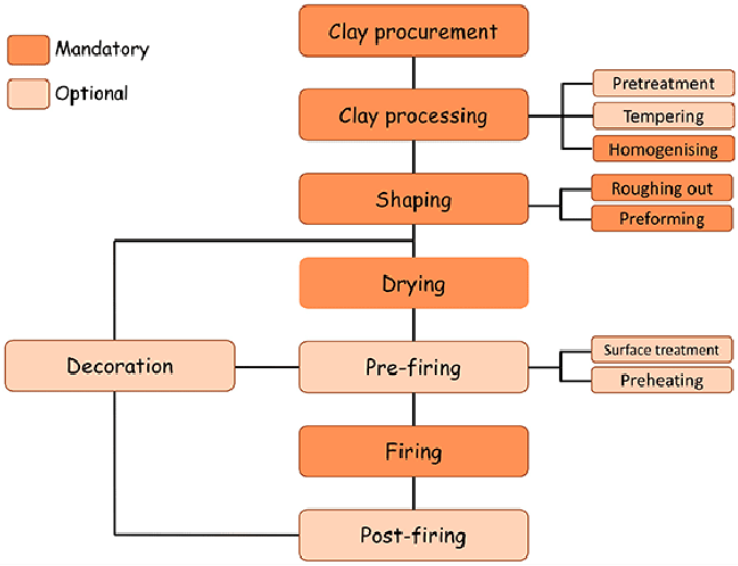


Figure 1.2: Diagram presenting the stages of the *chaîne opératoire*; from Gosselain (2018)

One example of such analysis is the study of adding a temper to a pottery paste. Tempering refers to the addition of non-hydroplastic, particulate material to the paste (Cuomo Di Caprio 2017a: 63), presumably to change the characteristics of the paste (e.g. improve workability) and/or the final product (Rice 1987: 74-75). It is challenging to differentiate temper from natural inclusions already in

[3]The stages of the *chaîne opératoire* are described in detail in Roux (2019)

the raw material. Raw material processing, such as crushing, sorting or levigating, affects natural inclusions. Both natural inclusions in the raw material and temper will affect the vessels' chemical composition and physical properties (Roux 2016: 30-31).

For instance, calcite ($CaCO_3$) can be found naturally in clays, such as in Maltese clays (Pedley and Clarke 2002). Calcite might be added purposely to decrease the plasticity of certain clays (Santacreu 2010: 32). Some calcite forms might also increase mechanical and thermal stress resistance in low-fired cooking vessels (Hoard et al. 1995: 831). However, these properties depend on many factors: the mineral form, the temper distribution and frequency, and the firing temperature; and might not have mattered to the potter (Tite et al. 2001: 322). Careful examination of the size, angularity and distribution can help differentiate between natural inclusion and temper, supported by a good knowledge of the surrounding geology (Santacreu 2010: 21 for calcite). Models based on the continuity of grain size distribution have also been elaborated (Roux, 2016: 139, Eramo, 2020: 12-16).

Temper and natural inclusions can be identified by Polarised Light Microscopy (PLM). PLM, adapted from geological studies (Peacock 1977a: 26), requires the use of a specific microscope (described by Quinn 2013: 4; Degryse and Braekmans 2016: 234). The samples are prepared as thin sections, where thin slices (30 μm) are mounted on microscope glass slides. In PLM, the light source below the sample is polarised: the light waves are filtered, and only one orientation is allowed to pass through (Cuomo Di Caprio 2017b: 545). This setup differs from ordinary light waves, which oscillate in all directions. Plane-Polarised Light (PPL) describes when one filter is used to observe colour, grain boundaries or cleavage (Degryse and Braekmans 2016: 238-329). Crossed-Polarised Light (XPL) when two filters are to study double refraction (birefringence) of the minerals, which produces "interference colour" which can be diagnostic (Cuomo Di Caprio 2017b: 545). This characterisation method requires considerable training and practice. Stoltman (2001: 299) mentions two years of close to full-time study to identify efficiently and accurately. However, Quinn (2013: 73) highlights that a less inexperienced researcher can still operate primary visual classification on thin

sections even if unable to characterise the minerals fully.

PLM is primarily a qualitative analysis, including sometimes ratios, sizes and frequencies. Still, studies have also used point counting and statistical analysis to quantify differences between fabric classes (Quinn 2013). PLM has long been used in archaeology to study stages of the *chaîne opératoire* from clay processing (Eramo 2020; Shepard 1956), forming (Thér 2020: 172) and firing (Rice 1987: 426). Some of these processes can be primarily assessed with a stereomicroscope, which does not allow the characterisation of minerals, and confirmed or rejected by PLM, saving time and cost.

Provenance

One other aim of characterization studies is to provenance the raw material of vessels (Waksman 2016: 149). PLM allows the identification of potential local sources if the local geology is well studied and has "mineralogical-petrographic markers" (Montana 2020: 4). Provenance studies are, however, often performed or refined by using bulk chemical analysis and subsequent statistical assessment (Waksman 2016; see Table 1.1).

X-Ray Fluorescence (XRF) is a method which analyses the bulk elemental composition of samples. Detailed accounts of XRF principles can be found in Pollard et al. (2007) and Shackley (2018), and its application to ceramic studies is summarised in Hall (2016).[4] XRF is an analysis of "mass components" (Shackley 2011: 10) and therefore will not differentiate between the surface (e.g. slip), the natural elements of raw materials or those who have been added during the production process. Statistical analyses of XRF data enable the classification of samples, the verification of existing groups, and the assessment of their significance. Clustering methods are common analyses (Hall 2016: 353), and are described in Glascock (2016: particularly 10-12). The dataset can include the analysis of hypothetical raw materials, assuming that markers are carried out from the source to the vessel. The methodological assumptions of provenance

[4]XRF and its functioning are summarised as a reference for the reader in Appendix D.1.1.

studies are explored in section 2.2.2.

Pottery research should combine several techniques to understand manufacture and provenance (Degryse and Braekmans 2016: 234). Researchers promote an "integrated approach" (Quinn 2013: 7) where the results of one analysis enrich the interpretation of another (Stoltman 2001: 296). For example, understanding what minerals might have been added as temper using PLM allows grasping the limitations of a bulk chemical analysis when comparing directly to raw materials (Degryse and Braekmans 2016: 298).

1.1.3 Theoretical considerations

It is outside the scope of this work to develop new theoretical approaches to interpreting pottery manufacture. It is, however, necessary to mention a few theoretical points as the methods and interpretations of fabric studies have been embedded in different theoretical frameworks, which have shifted over time. As Arnold (2011: 63) points out, archaeologists interpret objects from the way they look at "the relationships between artefacts and behaviour". Although not always acknowledged, the understanding of technology is related to broader concepts such as culture, social organisation, economic rationality or human-environment relationships. These points have been summarised by Santacreu (2014), who offers an extensive bibliography for every approach. Pottery research has been reconciling these different approaches (Pollard and Heron 2008: 408), acknowledging that these ideas might all offer valid interpretative frameworks depending on the assemblages and unique situations under study. The theoretical schools presented here are the ones that still mainly influence the interpretation of pottery production.

Functionalism

Functionalism, which developed in the first part of the twentieth century, is a wide array of theories that look at societies as systems. Cultural forms (including

material culture) are interpreted according to the function they perform in these systems (Johnson 2009). Functionalist theories for material culture studies stress the ability of humans to assess their needs and adapt technology accordingly. For functionalists, all humans perceive the environment and physical properties in the same way and share similar cognitive schemes (Santacreu 2014: 129-130). Craft people are seen as economically rational and, therefore, predictable (Trigger 2006: 386-392). They can optimise their resources and every step of the manufacturing process, considering the physical constraints of the raw materials and environment. For instance, when referring to calcite temper in Section 1.1.2, calcite tempering can increase mechanical stress and prevent breakage (Hoard et al. 1995: 831). The choice of adding calcite is made, consciously or not, to optimise the efficiency of vessels. These interpretations have to be approached with caution. Rice (1987: 328) emphasises that actions are performed within unique historical and cultural contexts where potters interact with material properties differently. Although the material characteristics of vessels should not be ignored, ethnoarchaeologists have widely noted that material culture is not always produced efficiently. Santacreu (2014: 185) gives the example of grog in cooking pots, which does not significantly impact its technological efficiency. Archaeologists might encounter what they think might be "illogical choices" (Skibo and Schiffer 2008: 21) in terms of performance and might be tempted to brand these choices as "cultural". However, all actions are embedded in cultural frameworks, efficient in the view of archaeologists or not, including the assessment of material characteristics, suitability, and performance by the potter.

Human-environment relationships

Cultural ecology and functionalist theories have influenced processual archaeologists, which interpreted "culture" as an adaptive mechanism to a set environment (Fowler 2010: 357). Ceramic ecology approaches have, more generally, given the environment a predominant role in ceramic production. The approaches under this umbrella have often postulated that general laws on human-environment relationships could be drawn, including about ceramics

(Santacreu 2014: 143). For example, Arnold (1980) modelled the expected distances from production to raw material source using ethnoarchaeological research with the assumption that potters would travel similar distances on similar terrains to get their raw material (Section 2.2.1).

Ceramic ecology approaches can be reductionist in interpretation, and general laws on behaviour can risk hiding the historical and cultural specificity of the social groups under study (Santacreu 2014: 143). The interpretative framework, however, can still be helpful to question and interpret the archaeological record (Santacreu 2014: 142), particularly when understanding the constraints and potential of one environment (Rice 1987: 314). A modern ceramic ecology approach would emphasise looking at "all aspects of ceramic production" (Kolb 2020: 2059).

Archaeology of practice

The theoretical movements which have looked at the social theory of knowledge and practice theory have been popular in understanding actions and choices in studies of craft production. Intending to bridge the long-lasting debate on *structures* and *individuals*, these theories have been drawn from sociologists such as Bourdieu (1990) and have been adapted to understand manufacture. Dietler and Herbich (1998: 245-247) summarise how Bourdieu's concept of *habitus* can be tied with the analysis of the *chaîne opératoire*. The habitus is the set of conscious and unconscious expectations acquired through socialisation that regulate our daily lives. By doing and acting, people dynamically reproduce these norms; they might maintain them as such or modify them, consciously or unconsciously, by acting. People as social beings are both produced by their habitus and producing it. The learnt dispositions regulate what people define as natural or the field of their possibilities, including in craft-making (Santacreu 2014: 199).

This approach has emphasised how practice, including craft practice, responds to social demands or constraints at every level of the *chaîne opératoire*. Making an

object and the production stages are never detached from broader social considerations, including unconscious and naturalised ones. Of note, the theory of practice does not deny the role of the natural and biological environment; they are part of what the *habitus* will respond to (Santacreu 2014: 199). The importance of transmission of knowledge and how *savoir-faire* is maintained by interaction is significantly linked to this theoretical school.

1.2 Fabric studies for the Roman period in Malta

1.2.1 History of ware and fabric classifications

This section reviews previous classifications of Late Punic and Early Roman fabrics from the last thirty years. This section additionally highlights how local pottery classifications would benefit from characterisation. Fabric as a valuable tool for understanding technology or provenance has been recognised since the island's first classification of classical pottery. Caruana (1899: 3), for instance, mentioned that the local fabric could be defined as "coarse and gritty clay" for the Classical period.[5] Caruana (1899: 8) writes that paste or fabric is part of his classification, although he does not give any further description.

The study of local pottery from the Roman period lacked, until the work of recent scholars (Anastasi 2019; Sagona 2002), a national fabric classification. Various grouping systems have been used concomitantly. This variety of classifications reflects different research aims, methods and assemblages under study, which are explored in this section.

First classification of wares: The Ħall-Millieri assemblage

As outlined in Section 1.1, pottery fabric is sometimes one variable used when defining ware groups. This approach has been taken in several pottery reports in

[5] as defined in the late nineteenth century.

Malta.

Blagg et al. (1990) recovered an assemblage from the excavation at Ħal Millieri church. The assemblage of Ħal Millieri is secondary and is challenging to date or relate to a primary deposition context. The report's aim was not to produce a fabric classification but to publish a detailed report on the pottery assemblage, as only a few of these reports existed in Malta. The pottery report classified Prehistoric, Roman and Medieval pottery, but only Roman pottery is explored here. Since the assemblage is secondary, the pottery is dated as 'Roman', mostly by forms and thanks to the imports (Blagg et al. 1990: 54). The dates span from the first century BCE to the sixth-century Common Era (CE). The authors classified the pottery assemblage into seven Roman coarsewares, including "Miscellaneous coarse wares" and one hand-made cooking ware, summarised in Table 1.2. It is argued that most of these wares could be locally manufactured, but other hypotheses are considered, such as a Sicilian provenance (Blagg et al. 1990: 79). The authors treat amphorae and lamps separately, although the fabrics overlap. The only fine ware described as imported is identified as African Red Slip (Blagg et al. 1990: 54).

Fabrics A and B have the most systematic and complete fabric descriptions. These two are variations of the categories "Red Coarsewares" and differ from each other by their texture, Fabric B being coarser than Fabric A. The description of this ware includes matrix colour systematically described using the Munsell Colour Chart, which allows repeatability even decades after (Whitbread 2016: 203). The descriptions include very brief inclusion accounts and indications of hardness/texture. The other coarseware groups are described in less detail, although the same variables are described more or less extensively (colour, texture and inclusions). Other aspects, such as surface treatment, are included in a few descriptions.

The major limitation of using the Ħal Millieri ware descriptions for secondary fabric research is that some fabrics classes overlap the ware categories. Blagg et al. (1990: 59) themselves noted that the group 'Cream-coated coarsewares' is made

of several fabrics, possibly overlapping with the 'Buff Coarsewares'. There is an emphasis on macroscopic and visual characteristics such as surface colour and treatment rather than fabric. Although these are important in pottery studies and might be related to the chemical composition (Hall 2016: 345) and properties of the vessels (Rice 2015: 333), the material making up these wares could still be the same. Colour description, for instance, can be misleading when used to interpret fabric composition as differing firing conditions might produce a range of colours on the same material (Quinn 2013: 76). For instance, the grey or greenish wares could represent a firing variation of other Coarsewares as calcareous raw materials can fire grey in reducing atmospheres (Santacreu 2014: 95).

Only a short description of inclusions is provided, and only one group was characterised. A sample of hand-made cooking wares was subjected to PLM, which revealed the presence of grog and microfossils, suggesting a local origin (Blagg et al. 1990: 66). The authors acknowledge the necessity of further studies in petrography and "heavy mineral" analysis to confirm these primary results and understand the provenance of the vessels (Blagg et al. 1990: 79). Therefore, this report already stressed the significance of characterizing Roman sherds, which has not been fully explored since then. This report exemplifies the problem of setting boundaries between the common fabric classes and sub-classes in Malta, which could be improved by characterising the matrix and inclusions.

Ware type	Sub category	Texture / hardness	Matrix colour	Inclusions	Surface colour	Surface treatment / Manufacture
Red coarsewares:	Fabric A	Fine and sandy	Dark orange red (Munsell 2.5 YR 5/6-5/8),	Limestone and small black inclusions	Dark red to reddish grey (Munsell 5 YR 5/2). Variations on vessels (firing)	
	Fabric B	Coarse and hard	Red to light red in colour (Munsell 10 R 5/6-6/6)	Frequent limestone inclusions ("grit")	Greyish brown / Light brownish grey (Munsell 10 YR 5/2-6/2)	
Buff Coarsewares		Fairly fine and hard	Buff or orange buff	Small limestone inclusions	Buff or orange buff	Occasional painted bands and wiped or brushed (striations)
Pale Green Coarsewares		Fine/ fairly fine and sandy	Pale greenish buff or Pale greenish brown	Sparse limestone inclusions	"Greenish"	Some combed decorations
Cream-coated Coarsewares (commonest)		Coarser fabric	Varied colours (red to orange buff) and reduced grey core	Fine sand inclusions and occasionally large limestone inclusions ("grit")	Cream slip, or wash, possible salt-coating	
Grey-coated Coarsewares		Coarse	Similar than Cream-Coated Coarsewares		Grey or greyish green	
Ribbed Coarsewares		Fairly fine	Light creamy buff, light brownto red colour			External ribbing
Handmade Cooking-pots		Coarse and crumbly	Greyish browncolour with high variation	Microfosils (foraminifera, ostracoda and algae), grog (examined by petrography)	Similar to matrix, varied	Both surfaces smoothed and lightly burnished

Table 1.2: Table summarising the description of wares as defined by Blagg et al. (1990). This table excludes the imported fine ware, Misc Coarsewares, Amphorae (which overlap coarsewares) and lamps. The terms are reported as in text (Blagg et al. 1990: 54-66). These wares are noted as possibly local (Bonanno and Vella 2012: 79).

A first national framework by Sagona (2002)

Regional frameworks for pottery classifications are achieved when different sites and stratified assemblages are brought together (Orton and Hughes 2013: 41). This was first carried out by Sagona (2002), who aimed at studying typology and ware types across the Maltese islands. The work published in 2002 is the first cross-site study including a large assemblage to construct a typology, dating system and ware classes for the Maltese Punic and Roman periods.

Sagona (2002) studied many vessels (exact number unknown), many complete, found in funerary contexts and stored in museum stores or unpublished reports. Her work aimed to study the tombs, including the rock-cut features and assemblages. She gathered information on 761 hundred tombs in the Maltese islands. She created a ware classification, which was later enriched by the study of the pottery of the sanctuary at Tas-Silġ (Sagona 2015a). The classification described 14 wares stretching over six chronological periods (see Punic/Roman ones in Table 1.3). The author herself has outlined some inherent problems with the assemblages (Sagona 2002: 86) which have been discussed by Anastasi (2010: 11). Limitations include the lack of stratigraphic excavations for many of the tombs, subsequent re-use of the sites or missing contextual information due to their excavation by antiquarians.

Ware	Phase	Hardness / feel	Break	Texture	Surface colour, treatment and decorations	"Clay colour"	Inclusions and voids
Coarse pink-buff (hand-made)	Phoe-nician, Punic	Friable - moderately hard	Uneven, rough	Very coarse - better finish	Yellowish slip, slurry finish, self-slipped, plain, straw-wiped, burnishing	Uneven: Mid-brown, pinks, dark reddish grey	heavily gritted: mixed medium-large inclusions, SM angular and SM gravel size. Large voids, folds, shrinkage cracks
Coarse Grey CW	II to early III	Hard, crisp	Jagged, irregular	Coarse	Reddish-yellow - pink / brown - reddish. SM Slip green to yellow; Red paint yellow	Grey core	Heavily gritted and voids SM noted
Thick - slipped CW	III to Early IV				Pale thick slip pink to yellowish, burnishing, smoothing. Rare decoration	SM dark brown, even section or red margin	Fine- medium mixed gritty. Fine voids, SM blisters
Crisp Ware	From III	Hard-baked, crisp	Sharp, angular	Fine to coarse	Greens to reds, mottled. Slip, matt, refined / thick / wash. Green - pinks - yellows.SM painted lines	Wide range, even to uneven sections	Fine - medium mixed gritty, SM ochre and grog?
Buiscuit ware	III to IV	Very hard, crisp	Sharp	Medium to coarse.	Green to yellows. Matt, 2015: often slipped	Reddish yellow/pinkish	Crushed yellow grit, angular yellow (limestone?)
Soft reddish yellow ware	From IV	Friable, soft texture	Dull		Pale slip, matt (yellow - off white - pink), Painted bands (not TS)	Reddish-yellow or orange clay	SM fine to large gritty (moderate number)

Ware	Phase	Hardness / feel	Break	Texture	Surface colour, treatment and decorations	"Clay colour"	Inclusions and voids
Soft brown ware	III to IV	Soft and friable	Not sharp breaks	Fine to medium	Smoothed, self slipped or wet smoothed, SM burnished	Brown and pinkish brown, even section	medium mixed gritty, grog? Fine chaff
Hand-made coarse ware	Late Roman ?	Compact and hard-fired	Jagged	Coarse	Red, brownish. Slip, mottled red/black, smoothed and wiped surfaces	"Darker in section"	Frequent medium to coarse gritty inclusions
Crisp black gritty ware	Post Punic	Compact, hard-fired, sandy	Very sharp		Greenish yellow to red. Self-slipped, wet-smoothed, thin slip (pale yellow), rarely red slip		Black grit, shiny and fine. Either angular, elongated AND/OR like sand, SM on surface. SM golden micaceous ones.
Red bricky ware (+ refined version)	From IV	Thoroughly fired	Sharp, angular	Medium to coarse	Red to reddish brown. Self-slipped, thin wash (darker), wet smoothed (drag lines), matt	Darker core	Angular white and yellowish grit. Some voids
Late red bricky ware	Post Punic?	Compact and hard fired	Sharp and angular		Red to reddish yellow. Self-slipped or slipped red		Grit (not white)
Red Ware, soft and eroding	Late to Post Punic	Eroding, soft, friable	Eroding, dull	Coarse or medium	SM Pale yellow to pink 5YR 8/4 slip, matt, SM self-slipped or plain	Red hues	Fine - small gritty and SM mica?

Table 1.3: Table summarising the characteristics of some local wares defined by (Sagona 2015b) using her terminolgy for colours, firing and production technique. Yellow cells: Crisp Ware variants. SM:Sometimes.

Sagona's work does not aim to be a fabric but a ware classification. Her descriptions are based on macro-scale observations, focusing on visual characteristics such as colour, surface treatment and shape. Her ware definition can be ambiguous as her groupings are sometimes equated with fabrics but include surface treatment. For instance, the "Thick-slipped Crisp Ware" is a category based on the surface treatment and fabric, using both attributes of the slip and the texture of fabric (Sagona 2002: 79). On the contrary, other variants of Crisp Ware are defined by specific inclusions, such as Crisp Ware with red inclusions or Crisp Ware with Black grits (Sagona 2002: 83). These Crisp Ware categories (Figure 1.3) can, however, according to the description, still have a slip. The boundaries between the groupings are sometimes misleading, and categories overlap. Overlapping classes is a challenge for fabric classifications because of the highly varied nature of raw material and production processes (Whitbread 2016: 202). These variations within the material can be substantial in areas with no specialised centres with systematised production (Quinn 2013: 76). However, Sagona's classes/variants were not created following one criterion (surface treatment or inclusions or forms), making this overlap more likely.

Looking at fabric, Sagona refers to the "clay" matrix texture or colour, and she occasionally mentions microstructure such as the presence of voids in the early Reddish Yellow Gritty Ware (Sagona 2002: 78). Inclusions are occasionally described by their texture, size or colour as, for example, the angular black grit of the Crisp Black gritty ware (Sagona 2002: 81). The fabric descriptions lack a systematised approach to description as it is today recommended for fabric classes (Orton and Hughes 2013; PCRG 2010; Peacock 1977a; Quinn 2013: 159). Systematic descriptions are time-consuming when the fabric is not the main focus of research and if the analysis is conducted macroscopically.

The recording terms for the fabric descriptions used are not explained in detail in her volume, contrasting with the more explicit methodology for typology (Sagona 2002: 85-86). For instance, the terms "medium" or "mixed inclusions" are not related to a specific scale or previous publications for the reader to refer to, and vague descriptive terms such as "evenly fired" or "well levigated" are more likely to

be subjectively interpreted (Whitbread 2016: 204). The exception is the Munsell Colour Chart, ensuring some repeatability (see Whitbread 2016: 203 on subjective terminology). Sagona's 2002 work highlighted the need for better fabric-focused descriptions, including a systematic way of describing its components and defined boundaries between the groups.

Sagona recognises one generic class, the Crisp Ware (Figure 1.3), and traces it back to Phoenician influences (Sagona 2015b: 43). This generic category is recognised across many classifications for Malta's Late Punic/Roman period (see Table 1.6). However, researchers disagree on the possible variants. Characterisation studies of this generic group could establish if it is a coherent group or if sub-groups exist and assess if different technological processes, raw material or provenance can explain these groupings (Quinn 2013).

Some of the shortcomings of the 2002 publication were addressed in 2015 when Sagona published the pottery report of the excavation of Tas-Silġ (Sagona 2015b). For the Punic and Roman periods, eleven ware groups (see Table 1.3) are re-defined, but most descriptions are similar to those published in 2002. Her descriptions are organised in systematic sections such as "Fabric and Manufacture" or "Date", briefly described in the methodology (Sagona 2015a: 5). The different sections, however, still do not refer to standards apart from the Munsell colour chart. Some small pictures are provided for identification support (Sagona 2015b: 497-500), some of which are given in Figure 1.3. The description of the colour and shape of the inclusions has expanded, such as for the Crisp Ware variant "Black Gritty Ware" (Figure 1.3), where inclusions are described in terms of size, location (e.g. on the surface) and shape (Sagona 2015b: 72-73).

Fabric classification was, again, not the report's aim, and the sherds were studied macroscopically. Sagona gives an overview of the 80,000 sherds of pottery found in the trenches excavated at Tas-Silġ, using selected stratigraphic units and forms (Sagona 2015b: 4). The report also spans several chronological periods. This example highlights that classifications and fabric descriptions are imbued by the researcher's specialism, methodology and approaches to assemblages but also the

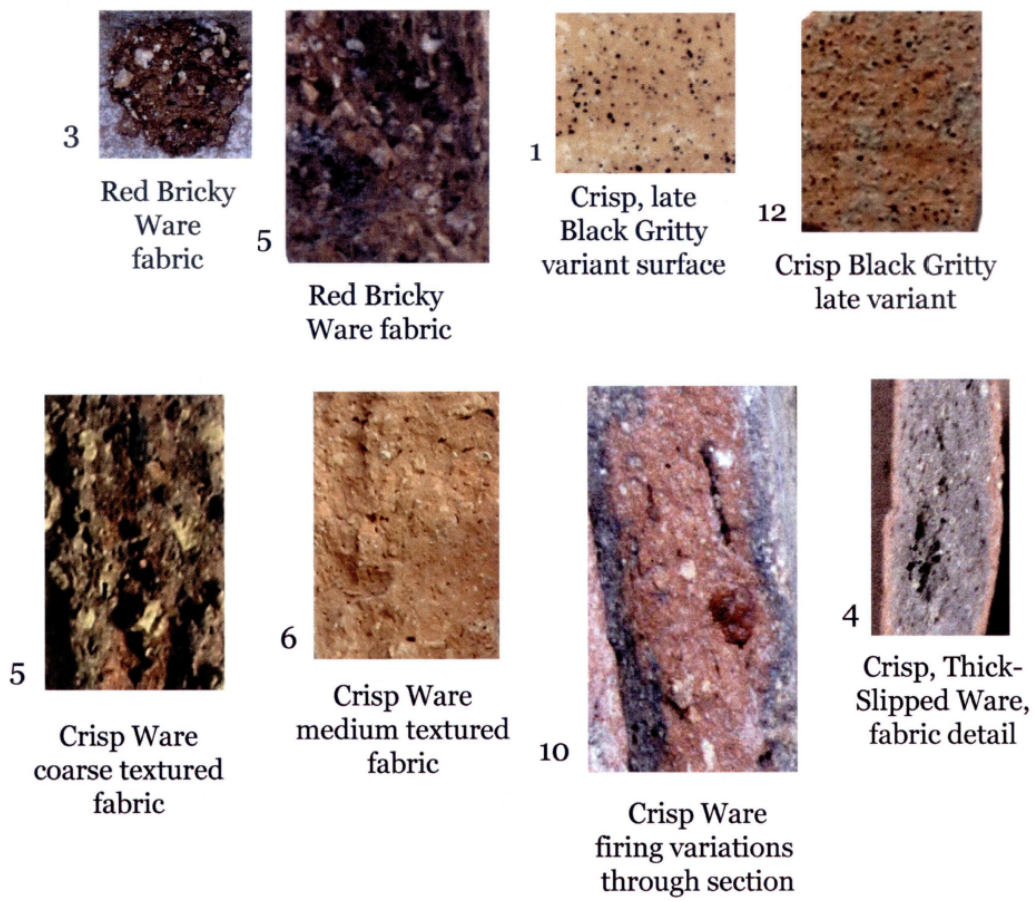


Figure 1.3: Montage of Sagona's photos of her ware classification cited most in this dissertation. The photos are reproduced from Sagona (2015b: 499-500, Figs. 1:247-248)

amount of work, time and resources available (Whitbread 2016: 202). Sagona (2015b: 77) highlights herself the limitations of macroscopic classification. She has argued that her ware groupings should be supported by some chemical and mineral characterisation, such as PIXE, to clarify the boundaries of her ware types. Other shortcomings of her approach for differentiating "local" from imported pottery are discussed in section 2.3.

The Missione's work: Tas-Silġ and San Pawl Milqi

The work of Quercia on Punic-Roman material excavated by the *Missione Archeologica a Malta* at Tas-Silġ provided a baseline for studying pottery of these periods in Malta (Quercia 2002; 2005; 2011). Quercia, however, mainly worked on typology, form and use and did not focus on the fabric of the vessels. Other published work on pottery from the *Missione* includes the work by Bruno and Capelli (2000), expanded in Bruno (2009). This study looked at Late Punic/Roman amphorae found at San Pawl Milqi and Tas-Silġ. This is the only published work systematically using PLM for the Roman period in Malta. Bruno (2009: 108) mentions that further characterisation work on the Tas-Silġ assemblages was ongoing, but to date, they still await publication.

The study of the amphorae from Tas-Silġ and San Pawl Milqi led Bruno and Capelli (2000) to differentiate three fabric classes, also noted on other vessels (Bruno 2009: 111). Bruno and Capelli (2000: 60) studied 20 thin sections selected from a few hundred sherds observed macroscopically and microscopically. The three groups they identify are summarised in Table 1.4. Fabric A is reminiscent of this generic fabric described by other authors, such as Sagona's Crisp Ware (Table 1.6). The authors characterise components, such as fine quartz, which is not observable macroscopically. Fabric B, the glauconitic group, could be similar to the black grit variant of Crisp Ware (Sagona 2015a: 72-73; Anastasi 2019). According to the authors, fabric C contains round quartz and volcanic minerals, which are not found in Malta. However, this fabric is found in amphorae types considered local to Malta, as argued by Bruno (2009: 111). Moreover, votive inscriptions associated with the temple were also found on vessels made of a similar fabric, opening the possibility that volcanic temper could have been imported.

The fabric classification by Bruno and Capelli (2000) provides short petrological descriptions with identification of inclusions and their description with their relative frequencies and their actual maximum size. These descriptions follow the systematic class description expected of PLM analysis (Quinn 2013: 79-80). The identification provides clear boundaries between the fabric classes: the presence of

Fabric Group	Frequent inclusions	Less frequent inclusions
A - "Generico"	Subangular inclusions or patches of clay, undetermined foraminifera ("dissociated" by firing)	Rare and fine (<0.1mm) angular quartz or feldspar inclusions. Very rare Mica.
B - "Glauconitico"	Microfossils (foraminifera) and fragments of limestone. Abundant glauconite (0.2-0.4mm) as main characteristic.	Rare subangular inclusions or patches of clay, minimal quantities of quartz and feldspars, no mica
C - "Vulcanico-quarzoso"	Foraminifera, round quartz (0.2-0.7mm) with shiny surfaces (sometimes eroded). Subangular and rounded clasts of volcanic rocks (and derived minerals) measuring between 0.2mm-1 mm with lava fragments up to 2mm. Agglomerates of phenocrysts of feldspar (plagioclase), clinopyroxene, olivine within vitreous cloudy mineral matrix. Single minerals of feldspar and clinopyroxene.	Minimum quantities of limestone, calcarenites, flints and acid metamorphites. Angular quartz nearly absent

Table 1.4: Table presenting a simplified description of the three fabric classes for Roman amphorae as described by Bruno and Capelli (1999). These descriptions are translated and summarised from the Italian.

Glauconite (Fabric B) and volcanic material and round quartz (Fabric C). Bruno and Capelli (2000: 60) combine their results with a typological approach; for example, Amphora type 1 is only found in Fabric A (frequent) and B (less frequent). The main limitation is that the lack of microphotographs hinders repeatability, a problem in many printed journals. It is hoped that the development of recent online databases will enable the sharing of microphotographs (Orton and Hughes 2013: 96, 286-287).

To summarise, the work carried out by Bruno and Capelli (2000) highlights the importance and value of PLM characterisation of fabric and identification of inclusions and the new set of questions and interpretations that might emerge. The composition of Fabric C, for example, questions on the import of temper or of the provenance of vessels which were believed to be Maltese.

Current Local Classification: Anastasi's proposition and recent works

The first work to bring this literature together was carried out by Anastasi (2015) and then published in Anastasi (2019). Anastasi has identified seven fabric classes in Malta spanning the Late Punic and Roman periods as represented in Table 1.5. This classification was conducted during a typological study of more than 10,000 sherds from three sites around the Maltese islands discovered during development-led and research excavations. The sherds range from residual fragments from the fourth to the first-century BCE to stratified sherds from the first to the fourth-century CE. The fabric classification was performed using a hand lens, permitting a detailed description of the inclusions. Anastasi is the first since Bruno and Capelli (2000) to focus on a fabric classification rather than a ware classification looking at fabric in its own right and identifying how her work relates to wares and fabrics identified by earlier works. Anastasi (2019) provides a local framework that can be used and expanded spanning sites across Malta and Gozo.

	Period and relation to other groups	Colour of matrix	Texture / hardness	Most frequent inclusion	Other inclusions	Use of fabric
1	Whole Classical period	pale red/orange clay, SM reduced pale grey core.	coarse, small to large voids	white or yellow lime, foraminifera	red iron ore grains	Generic, used across forms: coarse/table ware and egg shaped amphorae (eg. Malta Type 1)
2	From LP, very common during LR. similar to 1, but finer matrix and peppered glauconite tempering		soft to medium hard	white or yellow lime fragments, white foraminifera, and fine, round and shiny glauconite granules		coarse ware (eg plate,bowl...), fine ware with thinner walls, Malta Type 1 and 2 amphorae. Common in particularly Gozo
3	LR/EI.combination of 1 and 2			lime and foraminifera, angular crystalline such as gypsum or calcite	glauconite	coarse ware bowls and plates from centraland southern Maltese contexts
4	Common (RP)	hard-fired red to dark orange clay		matt black spherical	white or yellow limey, fossils	local red-slipped fine wares, thin walled wares and cooking wares
5	4/3rd century BC, rare in RP. Coarser version of 4	rust coloured red/brown to brick red coloured clay	Coarse, visible voids	fine to large coarse white and yellow lime, foraminifera, fossils	glauconite inclusions	noted in round bottomed cooking pots - Quercia's olla typeB
6		dark orange/ brown clay		yellow and white foraminifera and fossil, fine angular gypsum and fine black volcanic sand	rounded quartz granule (observed by Bruno and Capelli)	two amphora rim sherds from Melita and Foreman (Malta Type 2)
7	Probably continuous	pale pink, rey, brown, black	coarse limey	lime, foraminifera, microfossils, gritty inclusions		Cooking ware

Table 1.5: Table summarising the seven local fabric classes for the Classical period as defined by Anastasi (2019). LP: Late Punic, LR: Late Republican, EI: Early Imperial, RP: Roman Period. SM: Sometimes

The fabric descriptions include microphotographs and descriptions of inclusions and proposed identifications (Anastasi 2019: 36, 38). Since the fabric classes were defined with a handheld lens, there are areas for improvement in identifying inclusions (Anastasi 2019). Since the aim of the work by Anastasi (2019) was not to characterise fabrics, polarised light microscopy and chemical analysis were not used to support the identifications. The author does not claim to be exhaustive and stresses that her work should be considered as a "nudge to better record and understand a large body of data that is often overlooked" (Anastasi 2019: 30).

Anastasi's classification also identifies one generic group, Fabric 1 (Figure 1.4), the commonest fabric during the Classical period with the most macroscopic variations (Anastasi 2019: 35). This heterogeneity could be explored by PLM and/or chemical study as mentioned in section 1.2.1.

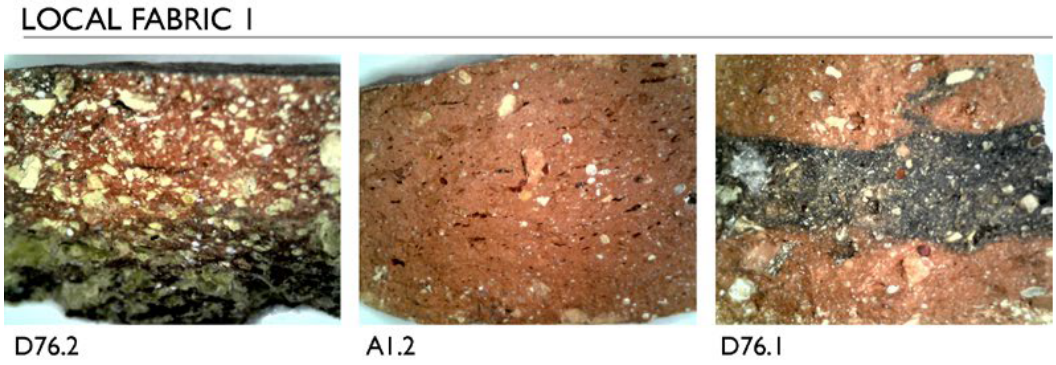


Figure 1.4: Microphotographs of Anastasi Fabric 1, image from Anastasi (2019: 36, Fig. 22)

Recent student dissertations have explored Anastasi Fabric 2 (Figure 1.5), a glauconitic group (Asciak 2019; Grech 2019), and emphasised the need for identification of inclusions using characterisation techniques. In both dissertations, some black inclusions, interpreted visually as glauconite, were identified by SEM-EDS as magnetite (Asciak 2019: 124), wüstite or hematite (Grech 2019: 69). Some samples did not display glauconite peaks on X-Ray Diffraction (XRD) results (Asciak 2019: 117). Magnetite, for instance, is frequently found in Blue Clay in the Maltese Islands, as indicated in recent unpublished XRD results (Humann 2021). These results are pretty significant, as

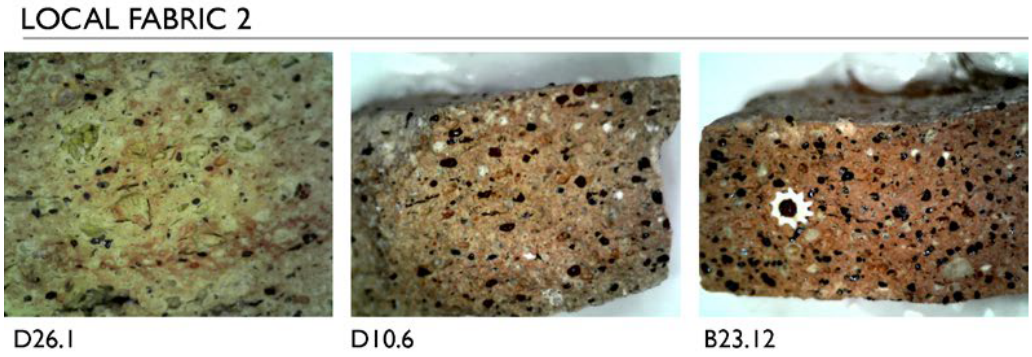


Figure 1.5: Microphotographs of Anastasi Fabric 2, image from Anastasi (2019: 36, Fig. 22)

the presence of glauconite was the boundary marker for Fabric 2 in Anastasi's classification. Therefore the visually homogeneous assemblage might contain mineral variations, which could be caused by differences in raw material sources or processing. This example stresses that macroscopic and microscopic identifications have limitations, and mineral and/or chemical characterisation need to be included in fabric group definitions.

At least two fabric classes could benefit from characterisation: Fabrics 4 and 5 (Figure 1.6). There are, for now, no clear-cut boundaries between the two since Fabric 5 is defined as the "coarser version of Fabric 4" (Anastasi 2019: 37). These fabrics could be equated to Blagg et al. (1990: 54-55) Fabric A (finer) and B (coarser) and the coarser Red Bricky ware (cooking ware) and the finer Late Red Brick Ware from Sagona (2015a: 74-77; Figure 1.3 and table 1.6). These are systematically recognised as different from Fabric 1 / Crisp Ware because of their colour (red) and texture. Visually, the sherds have a spectrum of inclusion frequency and size, with no asserted boundary between the fine and the coarse sherds. "Coarse" and "fine" can be quite relative to the assemblage under study (Whitbread 2016: 201).

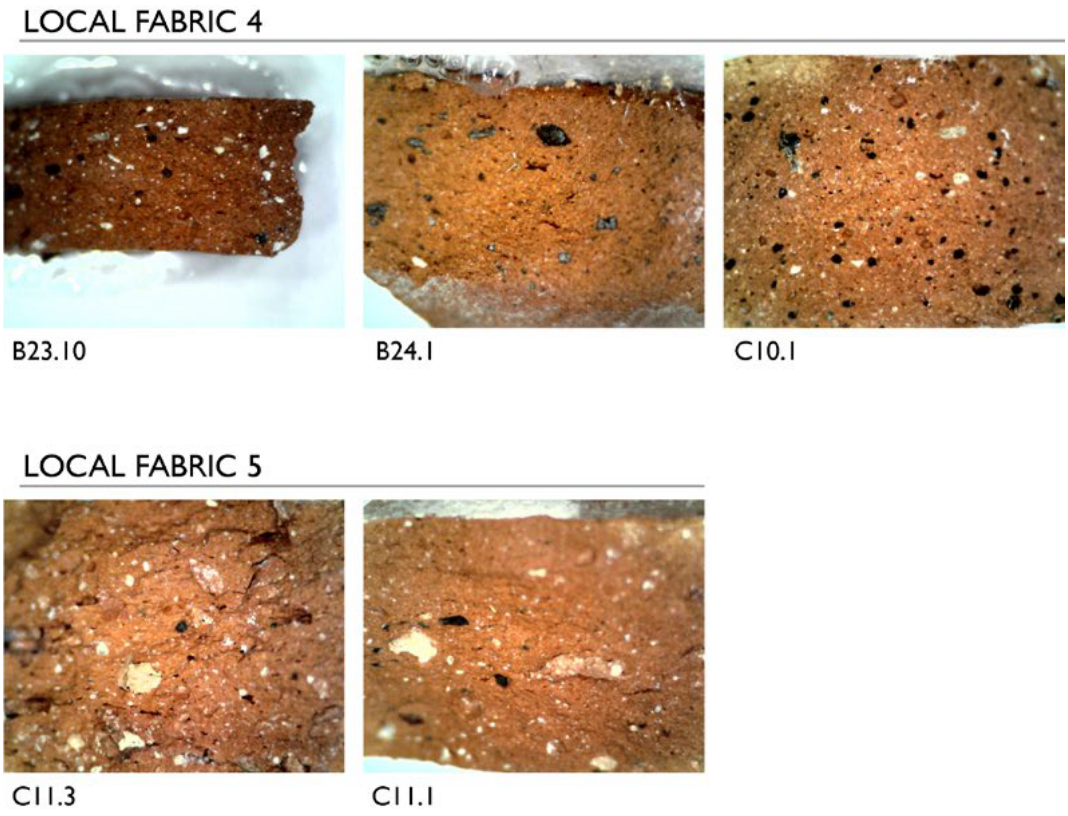


Figure 1.6: Microphotographs of Anastasi Fabrics 4 and 5, image from Anastasi (2019: 38, Fig. 23)

Anastasi (2019)	Bruno and Capelli (2000)	Sagona (2015a)	Blagg et al. (1990)
Fabric 1	Group A	Crisp ware and variants	Buff, Pale, Green and Cream-coated coarsewares, two main amphorae fabrics
Fabric 2	Group B	Black gritty ware	
Fabric 3			
Fabric 4		"Late Red Bricky ware", potentially "Fine Roman Ware"	Fabric A
Fabric 5		Bricky red ware'	Fabric B of Hal Millieri
Fabric 6	Group C		
Fabric 7		'Coarse pink-buff, hand-made ware and 'Hand-made coarseware'	Handmade Cooking-pots

Table 1.6: Table of equivalence of Late Punic / Roman fabrics and wares as defined in the literature. Most equivalences were already identified in Anastasi (2019) in her fabric description. Blue text for complementary equivalence.

FACEM

The FACEM database (Bechtold et al. 2020) currently has eight releases and one publication on Maltese Punic fabrics (Schmidt and Bechtold 2013). FACEM intends to present an open-access database of fabrics in the Mediterranean from the 6th to the 2nd century BCE. In Maltese fabrics, the samples date to the fourth century BCE, overlapping Sagona's work and slightly earlier than most samples of this dissertation. FACEM proposes five amphorae fabrics, two coarseware fabrics and one hand-made fabric. For the coarse fabrics (MALTA-C-1; MALTA-C-2) and the hand-made fabric (MALTA-HP-1), all samples (18 in total) were extracted from four stratigraphic contexts from the Żejtun villa, dated to the fourth century BCE. The two coarsewares are similar in description to Anastasi Fabric 1 on the macroscopic scale. However, the presence of mica, for example, in Sample M 115/2 on the website and illustrated in Figure 1.7, is not indicated in Anastasi (2019: 35). The website presents a description for each sample, including its typology, illustration and petrographic information, and microphotographs at different magnifications. The microscopic information follows standards close to those established by Orton and Hughes (2013) and Peacock (1977a).

This database provides comparative material from Malta and other places in the Mediterranean. This type of open-access database should be considered the future of fabric publication (Quinn 2013: 37), although they should be accompanied by papers discussing the significance of the groupings. The publication of multiple images and additional data, such as the individual description of sherds with illustrations, is impossible in a word-count-restricted academic paper. These databases can be a way of bridging multiple classifications together and give a basis for identifying imports.

The database also provides maps of where the fabrics have been identified, which could be a study of the movement of goods as the database builds up. For the Maltese coarsewares and hand-made ware, this is now restricted to finds from Malta. However, some amphorae fabrics, such as MALTA-A-1, have been identified

elsewhere in the Mediterranean, such as Pantelleria. Schmidt and Bechtold (2013), a paper associated with FACEM, describes the fabric groups rather than individual samples as presented on the database, allowing a more general understanding of the fabrics.



(a)

Inclusions	
quartz	singular, well rounded, subangular, subspherical, elongate, clear, white, grey, 0.08-0.28
mica	very frequent, angular, spherical, elongate, white, <0.04
calciumcarbonate	very frequent, well rounded, very spherical - subspherical, yellowish, white, <0.04-0.32
carbonate pseudomorphoses	singular, rounded, subspherical, white, 0.15-0,24
reddish inclusions	very frequent, well rounded - subrounded, very spherical - subspherical, elongate, red, reddish brown, <0.04-0.45
black inclusions	infrequent, spherical - subspherical, elongate, black, 0.04-0.1
foraminifera	frequent, well rounded, very spherical, subspherical, very elongate, white, grey, 0.12-0.52
more inclusions2	frequent, subangular - very angular, spherical - subspherical, elongate - subelongate, yellowish brown, reddish, 0.08-1.2

(b)

Figure 1.7: Photograph from FACEM (2020), sample M115/2 (Fabric Malta-C-1), photograph of section with magnification 8 on the left and the inclusion description provided on the right.

New data on three of these Maltese amphorae fabrics as found in sites in the central Mediterranean were published by Bechtold (2018). For the 3rd and 2nd century BCE, Bechtold (2018: 266-267) highlights the presence of Maltese domestic amphorae in Pantelleria made of fabric Malta-A-1, Lilybaeum and Ibiza as well as less prevalent open forms. Bechtold (2018: 269) proposes that, during the 3rd century BCE, an increased political and economic control from Carthage on the central Mediterranean was a reaction to the growing power of Rome. This could have caused population movement, with the inhabitants of Malta carrying their domestic vessels with them. This study highlights the significance of identifying characteristics of Maltese fabrics and forms to better understand processes such as trade or population movements. Bechtold (2018: 259), however, highlights the need for systematic archaeometric analysis to support these arguments.

1.2.2 Developing scholarship in Malta: other periods

Fabric classification and characterization have been carried out for other periods and there has been an increase in publications of fabric studies in the last decade. Some of these studies can help frame the practice for studying Late Punic and Roman sherds in offering comparative materials when looking at locally produced vessels. A project named MaltaPot, focusing on the Maltese pre-temple Neolithic, has recently been led at the University of Malta and is awaiting publication (Brogan 2021a,b; University of Malta 2020). This project, which has used different techniques (XRF, XRD, SEM-EDS, OM, PLM), can potentially improve the archaeological understanding of the provenance and manufacture of locally excavated Neolithic vessels.

The Maltese Bronze Age

The Maltese Bronze Age pottery has been the most extensively published with a focus on the sites of Borġ in-Nadur (Barone et al. 2015; Raneri et al. 2015) and Qlejgħa tal-Baħrija (Tanasi et al. 2019; 2020a,b). Barone et al. (2015) and Tanasi et al. (2019; 2020a) both set out to elaborate their PLM fabric classifications with at least one chemical technique such as XRF or Inductively coupled plasma mass spectrometry (ICP-MS). They combine two characterisation methods targeting technological questions, mineral identification and bulk chemistry for fabric classification and provenance. Thus, these papers use the "integrated approach" as advocated by Quinn (2013: 7; section 1.1.2). These papers, reflecting what would be expected of fabric classification, present the following: description of the sherds and their typology, detailed qualitative PLM description and microphotographs, which allow for other authors to elaborate, replicate and build on these fabric descriptions. For example, this allowed the papers of Tanasi et al. (2019) and Tanasi et al. (2020a) to expand on the publication by Barone et al. (2015) for the Borġ in-Nadur phase (Tanasi et al. 2020a: 132).

These papers also use chemical techniques to study fabric and engage in provenance studies comparing them to Maltese and sometimes Sicilian clays. They use descriptive, bivariate, and Principal Component Analysis (PCA), an exploratory unsupervised multivariate method, to observe patterns in differences in composition. In these papers, PCA allowed the researchers to observe that one fabric class had subtle differences across two sites highlighting that chemical data can be used to study raw material use and differences in procurement (Tanasi et al. 2020a: 133). The samples used are described in Table 1.7, and more about provenance is explored in Section 2.2.2.

Authors	Raneri et al. (2015) and Barone et al. (2015)	Tanasi et al. (2019) and Tanasi et al. (2020a)	Tanasi et al. (2020b)
Research interest	Fabric classification, technology and provenance	Fabric classification, technology and provenance	Provenance
Analysis	PLM, XRF, XRD	PLM, XRF (and pXRF), LA-ICP-MS	pXRF
Number of sherds sampled	Same sherds: 28	Same sherds: 37	274
Site studied	Borġ in-Nadur	Qlejgħa tal-Baħrija	Qlejgħa tal-Baħrija
Comparative geological samples	2 Ġnejna samples, 15 Sicilian samples	samples from Ġnejna, same as analysed by Barone et al. (2015)	14 Għajn Tuffieħa samples
Other comparative material	Possible Maltese imports from Sicilian sites		Sample includes 1 from Tas-Silġ and 1 from Borġ in-Nadur and few Punic sherds

Table 1.7: Table listing the characterization and provenance studies for the Maltese Bronze Age

Phoenician amphorae

Anastasi et al. (2021) published a study of amphorae from the seventh-century BCE cargo found in Xlendi Bay off Gozo. The sherds were studied using PLM and classified into three fabric groups for which qualitative PLM descriptions, identifying the minerals and XPL microphotographs are given. The study builds on a typological analysis of the full cargo to understand how and where the different amphorae might have been produced (Gambin et al. 2021). Fabric II could be of Maltese origin and is used for a type of amphorae which was not uncovered in Malta before (Anastasi et al. 2021: 3-4).

In the description of fabric II, a wide range of firing conditions and a lack of evidence for wheel-throwing were noted. The authors suggest the group is consistent with a Maltese origin and Maltese geology with, for example, varying Fe/Ca ratio in the matrix, little quartz or the presence of micro-fossils (Anastasi et al. 2021: 3). This paper adds to the literature on inclusions and technological processes of locally made vessels. It exemplifies that PLM can be used for specific typologies and to understand their production, associated fabric groups and types, and possibly analyse their provenance.

Later periods

Palmer's work on post-medieval pottery has combined PLM, chemical analysis, archival study and typology (Palmer 2020; Palmer et al. 2018). His work targets pottery from the 17th to early 20th century, considered of Maltese origin, excavated at the Dockyard Creek and the Inquisitor's Palace (Palmer et al. 2018: 577). This encompassed well-known shapes such as traditional braziers (*kenur tal-fuar*). He conducted petrographic and chemical analysis where he included some data from the Bronze Age analysis (clays and ceramics) from Barone et al. (2015). Palmer classified the sherds and identified both local groups of pottery (Fabrics 2 in Figure 1.8; and 4)[6] and pottery likely produced close to Messina (Fabric 1) and Syracuse, Sicily (Fabrics 3 and 4). The paper presents typological

[6]Note that the numbering for the fabric groups in each paper is independent.

information, drawings and photographs of sherds, coloured microphotographs (PPL and XPL), detailed analysis of fabric groups and individual sherds (including frequencies of minerals) and statistical analysis. The inclusions identified are described allowing future studies to have comparative material. Palmer's publication illustrates an "integrated approach" (Quinn 2013: 7) to understand the fabric groups and technological processes, as well as provenance, of pottery found in Malta. The reuse of datasets from earlier periods, for example, the use of Barone et al. (2015), highlights the need for quantitative analysis to report and publish their data collection methods, data transformation and raw data transparently.

These archaeometric results were published in 2018 (Palmer et al. 2018). In another paper, Palmer discusses these findings looking at the vessel's function, fabric analysis at the macro and microscopic level (stereomicroscope) and a discussion of archival evidence on pottery production including sculptural evidence (Palmer 2020: 447) or looking at census, to analyse production scale and organisation (Palmer 2020: 449). This data type is unavailable for the Punic and Roman periods; however, Palmer's work is indicative and gives examples of clay procurement strategies in the Maltese landscapes.

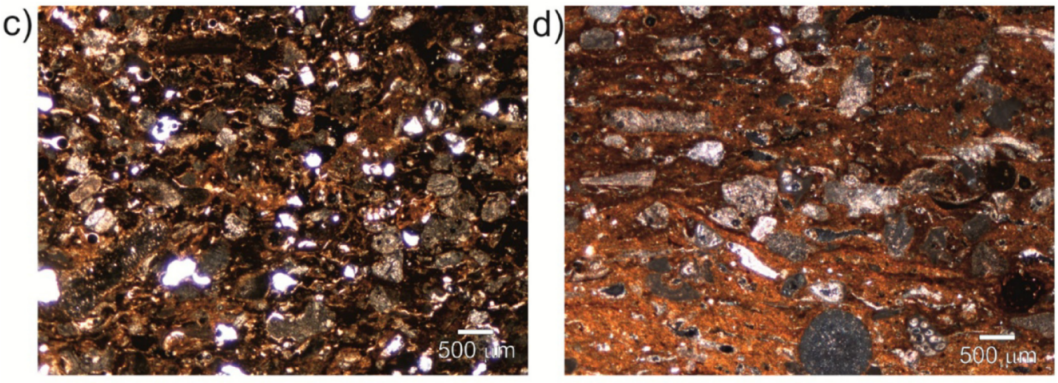


Figure 1.8: Microphotograph of the main Maltese fabric (Fabric 2) according to Palmer; microphotographs from Palmer et al. (2018: 581; Fig. 7); PPL and XPL

Chapter 2

Understanding local production of pottery in Malta

This chapter reviews the literature on local pottery production in Malta, the type of material available, and the studies carried out in the past. The case studies overlap with the previous chapter on pottery classification, as fabric classification and technological studies often integrate hypothetical sherd provenance and sometimes include chemical analysis (Palmer et al. 2018; Tanasi et al. 2019: for example). This chapter looks specifically at raw material procurement, how archaeologists have inferred provenance in the Maltese scholarship, and some assumptions behind chemical analysis.

2.1 Raw Material: the local geology

"Raw materials are necessary to make pots", asserted Arnold (2011: 63). As evident as this statement sounds, Arnold emphasizes that archaeologists must consistently explore the relationships between pottery production and the landscape. Identifying local raw material originates in a knowledge of the local geology and the use of these resources across periods (Montana 2020: 7-8). An in-depth survey of the availability and suitability of the soils around the islands is

needed to better understand possible procurement strategies in Malta. Blue Clay and the derived soils are interpreted as the primary source of raw material for pottery production in archaeological periods (Anastasi 2019: 32).

There is no systematic relationship between local raw materials and local production. Shepard (1956: 339) highlighted that local potters might import foreign materials or foreign/itinerant potters might travel with their "native materials". Potters might also use opportunistic material, such as recycling broken imported vessels for chamotte. With these limitations in mind, locally produced vessels are understood, in this study, as *pottery made with locally available raw materials (clays)*.

2.1.1 The local geology

The Maltese islands comprise five exposed geological layers (Figure 2.1) described by Pedley and Clarke (2002) and recently summarised by Chatzimpaloglou et al. (2020), French and Taylor (2020), and Scerri (2019). These layers were successively deposited during the late Oligocene and Miocene, between twenty-three and five million years ago, below sea (Pedley and Clarke 2002: 17). Table 2.1 outlines the principal characteristics of each layer (table 2.1). Minerals from any of these layers might get included, intentionally (e.g. tempering) or not (erosion and transport), in the pottery raw material. A new geological map was published in December 2022 with a higher resolution; however, the Blue Clay layer is still described as one layer (Continental Shelf 2022).

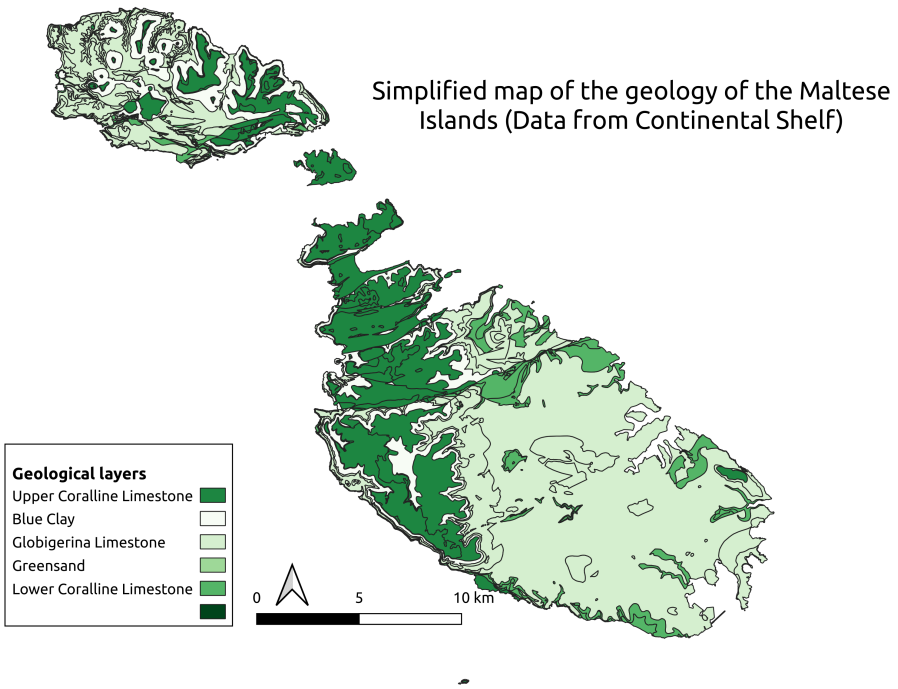


Figure 2.1: Simplified Geological map of the Maltese Islands, map made from GIS data available on the Maltese Inspire Geoportal (MITA 2021). Colours do not represent the International stratigraphic chart because the geological layers date mostly from the Miocene, and no colour gradients would be represented.

Layer	Period	Members and characteristics	Other inclusions
Lower Coralline Limestone	Chattian (Late Oligocene)	*Members*: Magħlaq; Attard; Xlendi; Il Mara. Layered units deposited in shallow sea with varied marine environments, formed mostly by reef organisms and derived sediments. Varied fauna and fossil content (eg low for Magħlaq but sea urchin for Il-Mara). Resistant material which form cliffs.	Foraminifera, Micrite
Globigerina Limestone	Aquitanian to Langhian	*Members*: Lower, Middle and Upper Globigerina and Conglomerates. Deposited in deeper marine environment until shallowing of the sea for Upper Globigerina . Describe as calcareous "mudrocks" by French and Taylor (2020: 197). Contain planktonic fossils and other fossils (eg. scallops) and traces of "burrowing". Softer material which form slopes.	Micrite, Foraminifera, Francolite (rubley conglomerate contain phosphate), chert outcrops
Blue Clay	From Langhian to Tortonian	Deposited in deep sea with "low-energy" environment, similar conditions than Globigerina limestone but with an input of clay minerals from the land. Weather easily and form clay slopes. The banding depends on fossil content with maximum 10% of calcium carbonates for darker bands and 20-40% for lighter bands	Clay minerals (Kaolinite), carbonates, quartz, fossils (molluscs fragments, foraminifera). Glauconite and phosphate sand closer to the Greensand formations.
Green Sand	From Langhian to Tortonian	Deposited in shallow sea with more energy after a period of erosion of Blue Clay. Termed "argillaceous sandstone" by French and Taylor (2020: 197) and "marly limestone" by Scerri (2019: 41). Friable material, often concealed by Upper Coralline Limestone.	Fossil (eg. sea urchins), glauconite (potassium-iron-aluminium-silicate mineral), quartz sand, iron oxides, clay minerals and lime
Upper Coralline Limestone	Tortonian to Messinian	*Members*: Għajn Melel; Mtarfa; Tal-Pitkal; Ġebel Imbark; Deposited in shallow sea with varied marine environments, containing Rhodoliths (algae) and fossils different according to members. Hard but porous material.	Micrite, glauconite, apatite, haematite, feldspar, dolomite, calcite (French and Taylor 2020: 197).

Table 2.1: Table presenting the characteristics of the five visible geological layers in Malta. Timeline can be found in Gauci and Scerri (2019: 50). Information from French and Taylor (2020), Pedley and Clarke (2002), and Scerri (2019). Described eldest to youngest.

Blue Clay

Chemists and geologists use the term *Clay* differently (Rice 1987: 37). Chemists refer to clays as specific minerals with a particular structure, a type of phyllosilicate. Sedimentologists, on the other hand, often use the category "Clay" as a particle grain size when describing soils (Pollard and Heron 2008: 102); whilst geologist looks at claystone or mudstone rather than the product of rock erosion. Archaeologists adopt both the above definitions and the potter's definition of clay: a material which is dug or collected from the ground and is a mixture of minerals, including clay minerals, and other material such as organic material (Cuomo Di Caprio 2017a: 37). The emphasis of the potter is on the characteristics of clays: it is plastic when wet, retains shape and becomes hard when fired.

Kaolinite is the primary clay mineral present in Blue Clay, whilst illite, smectite, and chlorite can occur in smaller proportions (John et al. 2003: 221). Blue clay includes other minerals such as carbonates, quartz and glauconite, particularly close to the Greensand layer (French and Taylor 2020: 197); tourmaline, rutile or augite (Molitor 1988: referencing Hyde 1955). The CoFIPoMS project has recently performed more XRD readings of a few clay samples from Malta and Gozo (University of Malta 2021). The preliminary data confirm the presence of these minerals, except for tourmaline, but gypsum and magnetite were also found in most samples (Humann 2021).

The high content of calcium carbonate ($CaCO_3$) has driven some researchers to qualify Blue Clay as marls (Sagona 2002: 2, for example) or marly clays. According to Cuomo Di Caprio (2017b: 72), marls contain around forty to sixty per cent of calcium carbonates. As mentioned in Table 2.1, the calcium carbonate content varies with the deposited dark/light-coloured bands of the clay. It derives from skeletal remains such as *Foraminifera*, and the colour differences are visible on clay slopes like in some parts of Għajn Tuffieħa as seen in Figure 2.2. Some bands might contain up to fifty per cent of $CaCO_3$ (Pedley and Clarke 2002: 41). Other researchers suggest an average of around 25% (Scerri 2019: 40).



Figure 2.2: Photograph of a clay slope at Għajn Tuffieħa. The light bands contain a higher carbonate content.

Understanding the composition of clays supports apprehending their suitability as a raw material to make pottery as their characteristics can affect production choices (Gualtieri 2020). Clays are complex materials whose characteristics are difficult to analyze without direct observations and experiments (Santacreu 2014: 118). Kaolinite-based clays, for instance, are described in the literature as refractory (Cuomo Di Caprio 2017b: 53), needing firing at high temperatures. Carbonates might, however, act as a flux and lower the temperature necessary to fire pottery (Gualtieri 2020: 7). There are, in Malta, very few records of systematic experimental archaeology describing the workability of Blue Clay for pottery, either qualitatively or quantitatively.[1] However, there have been studies on the characteristics of selected samples by, for example, civil engineers (Cassar 2020; Debono 2012). Most assumptions about Maltese clays' characteristics when working for making vessels have yet to be tested through experimentation.

[1]A BA dissertation by Borg (2005) had attempted the making and firing of vessels made with clay collected at Għajn Tuffieħa

Blue Clay slopes are no longer sourced for making pottery, as they are primarily situated in Natura 2000 zones, preventing raw material extraction. This aims to preserve vegetation and protected species (Jonathan Henwood, ERA, *pers comm* 2nd of July 2021). The lack of locally sourced pottery production prevents archaeologists from gathering information from modern production practices and strategies to prepare the raw material for pottery manufacture (Montana 2020: 12). Cuomo Di Caprio (2017a) describes kaolinite-rich clays as stiff and low in plasticity, which tends to be confirmed by the plasticity index of samples from Mellieħa, for example (Cassar 2020: 108).

On the contrary, Bruno (2009: 90) depicts Maltese clays as highly plastic based on the end products made by craftspeople. She mentions, for example, the Maltese tradition of making pasturi, the clay nativity figures used in Christmas dioramas in parts of the Mediterranean. The production of these figurines necessitates a material plastic enough, or treated adequately, to create details (see Figure 2.3). Some pasturi makers used, until the 1960s, local clays, among other materials (Lanfranco 1978: 292). Lanfranco (1978: 293) describes, for example, that the craftspeople had to beat their material with timber to be able to mix it with water.

Present and past practices can enhance our understanding of the suitability of clay sources for making material culture. It was reported by a local journal that a workshop from Għasri (Gozo) used to source clay from "the old hill" - "La Veċċa", also called Ta-Leveċa (Attard 2010: 17). Similarly, this hill was used by potters until recently as a source of raw material. Indeed, the archives from Gozo contain photographs of Karmnu Sacco 'Il-fuħħari', from Wara San Frangisk in Rabat (Figure 2.4). According to the archives, a photograph from the 1940s portrays the potter selling vessels made from Laveċċa clay (National Archives n.d.: 168).



(a) (b)

Figure 2.3: Photographs of clay models from Lanfranco (1978). Left is a clay modelled figure of Christ Risen (Lanfranco 1978: 296). Right, are pasturi from a Christmas Crib made in mass process with moulds (Lanfranco 1978: 294).



Figure 2.4: Photograph NAG/PA/01/31/1905 reproduced with courtesy of the National Archives of Malta (Gozo section)

2.1.2 Exploring other raw material

The Oxford Anthropological Expedition of the 1920s is one of the only ethnographic sources describing the use of local raw materials for the manufacture of vessels in Malta (Anastasi 2019; Palmer 2020: 446). They describe two production sites at "Birchircara" and Żejtun. The Żejtun workshop is said to have imported its clay from Gozo, whereas, for "Birchircara", it is collected from the surface close by (Buxton and Hort 1921: 131). The modern town of Birkirkara is situated around five kilometres away from the border of the Blue Clay layer. Surface soil containing clay minerals or a significant fraction of fine-size material could have been available in the Msida Valley, which is today developed. In a press article of the *Times of Malta*, an old pasturi shop, "Orslika", is described and the journalist mention that clay used to be collected from Msida valley for this shop, not mentioning where this information comes from (Cachia 2011). However, if this information is accurate, this potential raw material is no longer available for archaeologists to study. Still, this example shows that archaeologists should not restrain themselves to the geological map of Malta to find suitable clays.

As mentioned in section 2.1.1, the definition of raw materials as clay can be problematic because of the varied definitions and the gap with what potters might find suitable to make vessels (Rice 1987: 37-51 for an explanation of each). Properties such as plasticity, which is essential for making vessels, are partly derived from the clay minerals and their structure when mixed with water (Montana 2020: 8). Rice (2015: 43) suggests that soil with a fine texture, with as little as 15% of fine particles, can exhibit plasticity. There have been no surveys of the varied soils in Malta to disprove that they could be used as raw material for making vessels. Areas like the eastern part of Malta, with a limited amount of Blue Clay, should be explored as other soils might have been exploited.

Bruno (2009: 23,91) states that "surface terrains" were used for pottery making, citing Ciantar's version of *Malta Illustrata*. From her description (Bruno 2009: 23), she might be referring to Terra Rossa soils in Lang's classification system (Figure 2.5). Lang (1960) classified the soils in Malta according to their composition. A

more recent soil classification, MALSIS (MALtese Soil Information System), was created (Vella 2003), but the data is not easily accessible. These red soils include soils derived from limestone erosion (Chatzimpaloglou et al. 2020; Farres 2019: 31). No publications indicate that they have been tested for pottery manufacture. The soil history of the Maltese Islands is complex, and the soils available to the craftspeople in Roman times might have differed from today. Lang's and MALSIS maps are a limited tool to understand the types of soils that the craftspeople in Roman times could have exploited. Some of these soils have been heavily transformed by human activity (e.g. farming). Bruno (2009: 64-65), in reviewing more recent historical sources, cites many instances of soil modification of soils such as soil mixing and movements across the islands and even soil import from Sicily or ground from Sicilian and local stones.

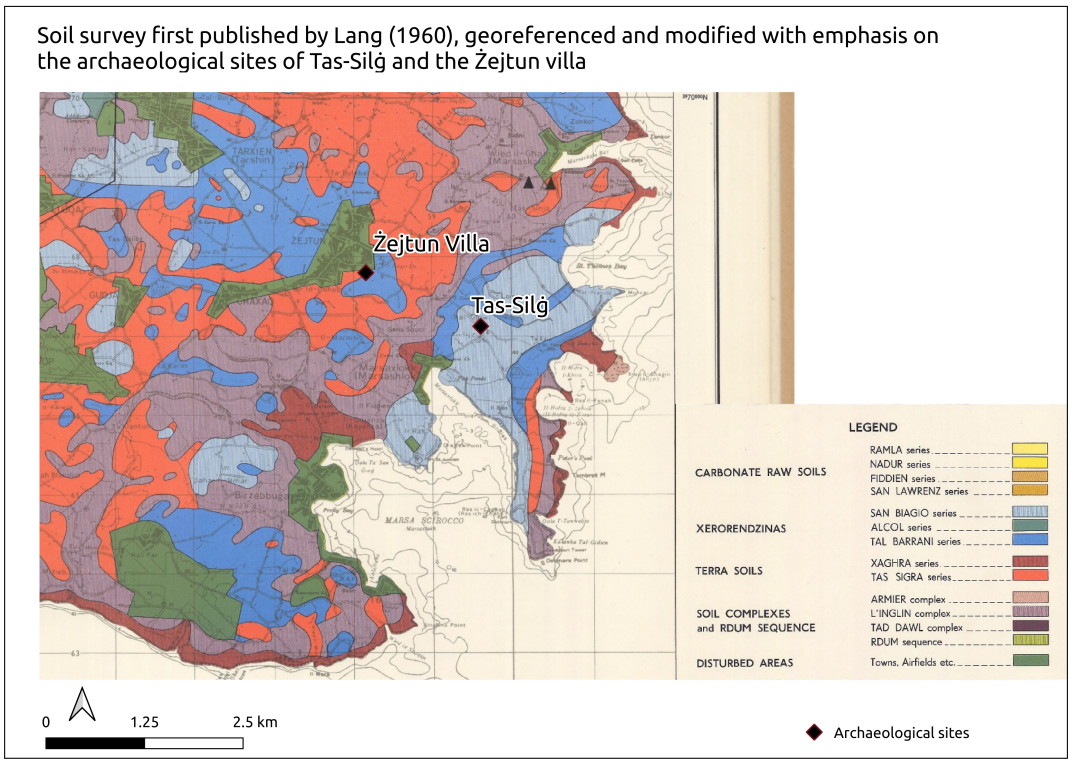


Figure 2.5: Soil survey map first published by Lang (1960), georeferenced and modified with emphasis on the archaeological sites Tas-Silġ and Żejtun. The map was modified and georeferenced to add the two archaeological sites.

In a recent publication (French et al. 2020), one sediment core was taken close to Il-Ballut Reserve in Marsaxlokk, less than one kilometre from Tas-Silġ (Hunt et al. 2020: 58). The core seemed to have a similar top-soil complex to the current farming soils around Tas-Silġ (following Lang's data, the San Biagio series). The

core goes down to 3.86 metres through different soil horizons (Hunt et al. 2020: 58). From the three overlapping carbon dates that were obtained (cc. 419-556 CE and cc. 435-670 CE), the soils have been most likely mixed (French and Taylor 2020). The lowest part of the column is described as *Terra Rossa* soils (French and Taylor 2020: 197) and some samples are described as possible weathering of Blue Clay (French and Taylor 2020: 209).

The term "clay" in the description should be understood as the particle size rather than minerals, meaning that some of the soils from the core are fine-grained. Prof. C. Hunt (*pers. comm. to Dr Ing.J. Betts*, 9 February 2021) mentioned that the cores near Marsaxlokk were sampled in particularly sticky clays; these soils have never been investigated for pottery manufacture.

Similarly, near Marsaxlokk areas, other types of soils have yet to be studied as a potential raw material for making pottery and/or temper. The soil created by the erosion of marly interbeds of the Globigerina limestone (Scerri 2019: 37), for instance, would contain some clay minerals such as smectite, although not necessarily enough to make them plastic for pottery (*pers. comm.* Dr A. Misfud 5 March 2021). More generally, soils deriving from some limestones in Malta have a high clay content (grain-size) and are close to the Blue Clay derived soils in terms of plasticity index (Debono 2012: 76, 82,83; on Upper Globigerina). Other potential sources of clays that need to be kept in mind are: deposited clays in caves such as Għar Ħasan or Għar Dalam (*pers. comm.* Dr M. Pedley 5 March 2021); or valley floors such as Wied Żembaq.

Further surveying and experimental archaeology might be necessary to assess if these soils were accessible in different periods and suitable for pottery manufacture. These examples highlight that the diversity of soils in Malta might impact provenance studies; one should remember that potters might have had access to a different environment and other possible raw materials which are not Blue Clay soils.

2.2 Localising pottery production

2.2.1 Considerations: where is the local?

Druc (2013: 487) stresses that the term "local" is not an objective concept. When looking at Malta, one can agglomerate everything inside the shores as local into one or two entities, the Maltese islands or Malta and Gozo. However, this definition of "local" might not be representative of more complex networks and even less of what people might have considered as made locally in the past. The scales of "local" that archaeologists create, such as Maltese or non-Maltese, from a specific region in Malta, from a settlement or considering a production area, might not represent emic conceptions of locality or local identity.

The term *local* can designate microregions (the Maltese Islands) or a bounded production or distribution area. Local areas of production, which include the distances in which a craft-person sources their material, might differ from the local area of distribution (Arnold 1980). In Malta, the raw material, if only Blue Clay is considered (see section 2.1), does not cover the islands, and procurement might also be restrained by other activities taking place over the layers (e.g. farming). Therefore, the sourcing of raw materials could overlap different areas of production. This dissertation will take "local" as a broad meaning of the microregion "the Maltese Islands". As there is no comparative archaeometric data for Roman ceramics on the islands, the patterns observed for the sites of Tas-Silġ and Żejtun can not be contrasted with other potential production or distribution zones.

Arnold (1980: 149) proposed a seven-kilometre threshold as a "preferred territory of exploitation", whilst other researchers have defined that fifteen kilometres or half a day of travel should be considered as "local" procurement (Santacreu 2014: 135 references within). Arnold (2011: 89) mentions that carts might have expanded this threshold to twenty kilometres in Roman times. Santacreu (2014: 135) also proposes that a vessel is "locally produced" when it is compatible (mineral and chemical) with the closest accessible resources.

In Malta, a possible road network was proposed by Sagona (2002: 681; Figure 2.6) for the Punic period, which has not been recently updated with development-led discoveries. However, it is unknown how potters would transport clay from the sources or if they would have created workshops close to the clay hills themselves. The "distance"-models do not necessarily apply unambiguously to Malta, where the sea probably played an essential role in local trade and procurement strategy. Clay in Malta can be obtained on slopes close to the shore (see section 2.1), for instance, at Il-Qarraba (Figure 2.7), where the clay slopes dip straight in the seawater and clay can be collected from the shore. Anastasi (2015: 33) discusses the scales of interaction as described by Tartaron (2013) and suggests that for "Coastscape" or "microregion" interactions, such as local trade, land and coast travel should be considered. Explaining procurement of raw materials in the archipelago would, thus, need to integrate both sea and land travel.

To summarise, the category *local* is not unambiguous even in archaeological terms, and different scales might be addressed. For this study, *local* will mean from the Maltese islands.

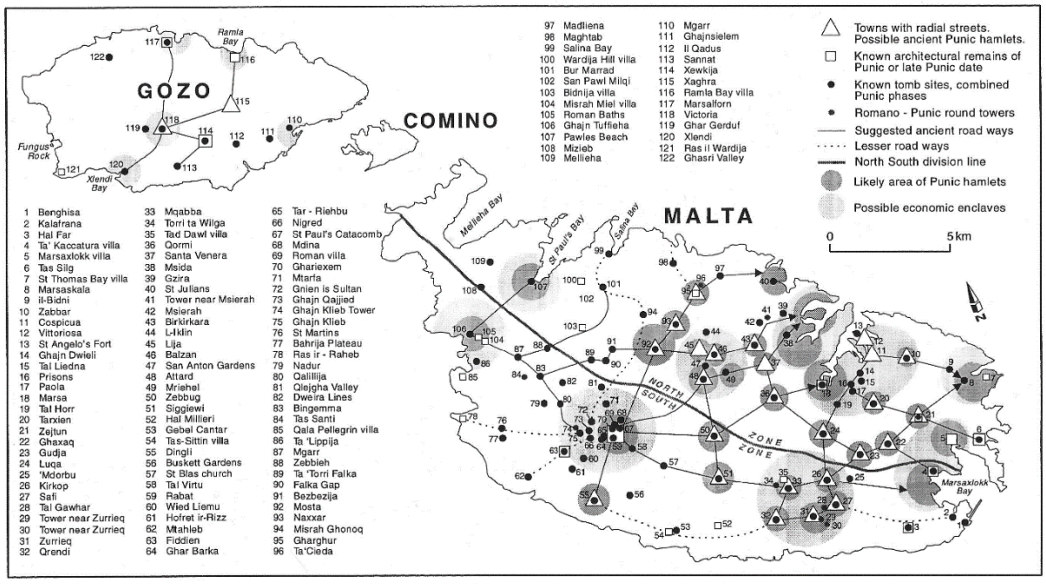


Figure 2.6: Map of the proposed Punic roads or ways, image from Sagona (2002, 681)

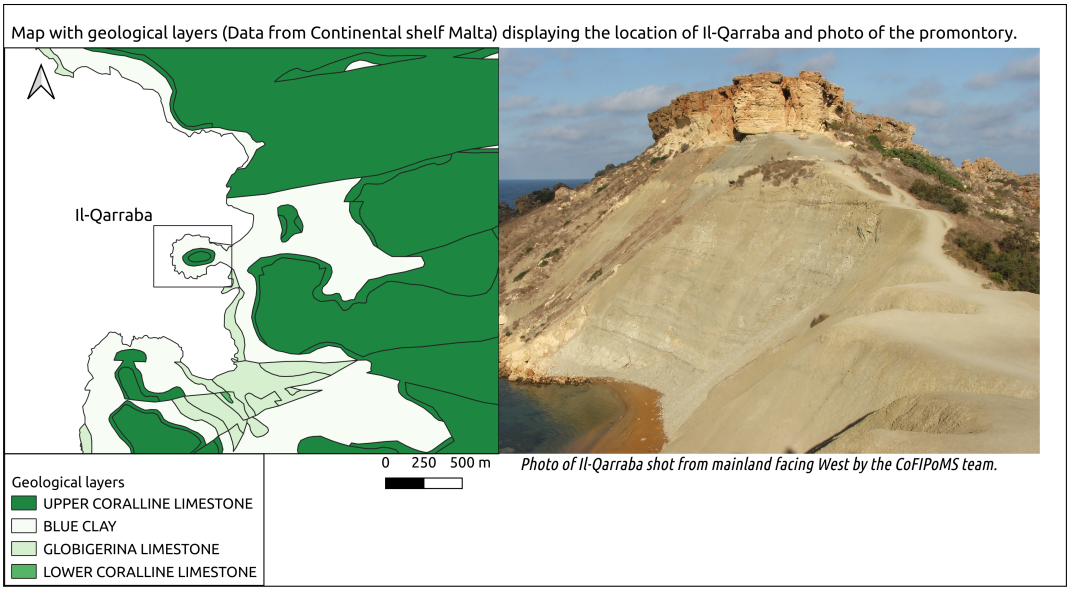


Figure 2.7: Map and photograph of Il-Qarraba. The photograph illustrates the clay slope dipping in the water, which can be collected from the shore. The geological map illustrates the Blue Clay layer making up most of the promontory.

2.2.2 Provenance studies: possibilities and limitations in Maltese case studies

This section summarises some of the main assumptions behind chemistry-based provenance studies (Table 2.2) and cites recent publications on Bronze Age Malta.

1	some chemical or isotopic characteristic of the geological raw materials is carried through unchanged into the finished object
2	the fingerprint varies between potential geological sources available in the past, and this variation can be related to geographical occurrences of the raw material
3	such characteristic fingerprints can be measured with sufficient precision in the finished artefacts to enable discrimination between competing potential sources
4	no mixing of raw materials (before or during processing), or that the mixing can be accounted for adequately
5	postdepositional processes either have a negligible effect or that the alteration can be detected
6	any observed patterns of exchange or trade of the finished products are interpretable in terms of human behaviour

Table 2.2: Table presenting the assumptions of "Traditional Provenance" as worded by Wilson and Pollard (2001) and later Kolb (2014).

The provenance assumptions are not universal laws and must be evaluated for every

study and local environment (Hein and Kilikoglou 2020: 2). This requirement is not yet filled for the Maltese Islands as no extensive survey and systematic sampling has taken place for provenance studies within the archipelago. Blue Clay is one geological layer (section 2.1), and the variations within have not been widely studied, apart from the banding observed in cases (Scerri 2019: 40). It is possible to have chemical variations between different areas of one geological bed (Bishop et al. 1982: 294). Still, these would need to be assessed for Maltese clays.

Recent cross-period studies such as Pirone and Tykot (2017), and Tanasi et al. (2020b), as well as the MaltaPot project (University of Malta 2020), have all included semi-quantitative XRF (MaltaPot) or pXRF on sherds and clay samples in an attempt to provenance pottery sherds. Tanasi et al. (2020b: 118), based on the study by Pirone and Tykot (2017: 24), have shown that there can be considerable variations within clay outcrops of Rubidium (Rb), Strontium (Sr) and Zirconium (Zr). As can be observed in the PCA plot (Figure 2.8), the Ġnejna slope samples (black) cluster in A with Selmun Bottom samples (purple) and Ġnejna Bay Top (red) is closer to Selmun Top samples (Blue). This tends to suggest that the provenance postulate within the Maltese islands might be challenging to assert as variations within one source (i.e. Selmun) are not smaller than between two sources. However, this analysis only considered a few trace elements rather than the total composition of the clays.

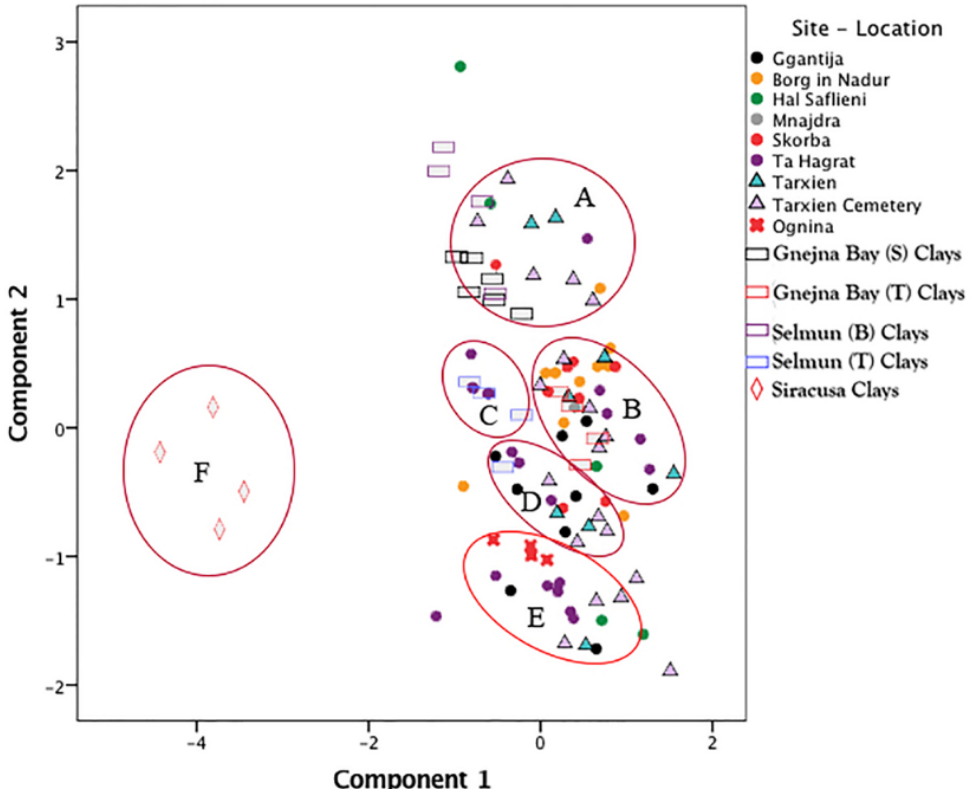


Figure 2.8: Scatterplot presenting PCA results from Pirone and Tykot (2017: 212). Horizontal rectangles represent the clay samples. The ellipse were drawn artificially in his PhD.

In these studies, the Maltese clays seem to cluster away from the sampled Sicilian clays from Siracusa. This strengthens the interpretation that the sherds were produced with Maltese clays (Pirone 2017: 14). Other studies which highlight the potential differences between the diverse Sicilian clays and Maltese Blue Clay include Barone et al. (2010) with clays from Licata, and Barone et al. (2015) from Siracusa. The main issue in provenancing sherds between Malta and Sicily comes from the latter having a diverse geology (Tassi et al. 2012). A few samples from Malta and a sample in Sicily from an area with different underlying geology are insufficient to prove the provenance postulate: that all Sicilian clays would differ in composition from Maltese clays. This was not the scope of the research by Pirone (2017) and Tanasi et al. (2020b), who explored the possible provenance of specific sherds. However, in the future, more studies should be done on studying these local variations to reinforce the claims that the chemical composition of sherds differs from other areas in the central Mediterranean and create reference groups.

Semi-quantitative pXRF analysus is the central element of the studies by Pirone and Tykot (2017) and Tanasi et al. (2020b) and limitations of semi-quantitative analyses have been explored by Holmqvist (2016) and Speakman et al. (2011). According to Hunt and Speakman (2015: 627), some of the limitations of the handheld XRF include less powerful X-Ray tubes, the lack of vacuum and other limitations common to ED-XRF which are Bremsstrahlung radiation which affects low-2 elements quantification. These analyses are most valuable when an established data structure exists, such as fabric groups created with petrography (Holmqvist 2016: 372).

Bruno (2009: 109) states that some clays from the Ragusa formation could be similar to the Maltese clays, and this claim should be assessed with chemical and petrographic analyses. From the Hyblean plateau (Montana et al. 2011: 477 for geological map), only Syracusan clays have been tested before, and these are not part of the Ragusa formation (Barbera et al. 2014: 190 for map). More studies must include a systematic collection of clays from both areas.

Comparative material for provenance analysis can include sherds of assumed local provenance (Pollard and Heron 2008: 100), such as the *kenur tal-fuħħar* in the study of Palmer et al. (2018: 579). This typology was assumed to be Maltese because it was common until recently in the Maltese islands with no direct comparative material. Other analyses could target wasters of production or samples of known provenances, such as ones carrying stamps (Waksman 2016: 151). If these are unavailable, it is still possible to sample from the different main fabrics from a site to define different production areas until further data from workshops are available (Waksman 2016: 150).

2.3 Evidence for pottery production in Roman times

No chemical analysis has been carried out comparing Late Punic/Roman sherds and Maltese Clays. The study by Bruno and Capelli (2000), cited in section 1.2, had

stated using PLM that some amphorae had a mineral composition consistent with the local geology with their calcium-rich matrix, fossils and sometimes glauconite. This study aside, archaeologists have relied on other types of evidence to state that sherds were produced locally such as the abundance of certain forms. This section reviews the evidence put forward to infer local production in the Punic and Roman periods in Malta and concludes by reviewing the only chemical characterisation study available including Punic sherds of the Maltese Islands (Mommsen et al. 2006).

2.3.1 The missing workshops

The direct material evidence for pottery production, such as kilns, is limited in Malta. Anastasi (2019: 21-23) examines the possible pottery production sites for the Roman period. Her study of the pottery from a site at Foreman Street (Rabat, Gozo) is the only published assemblage which could be derived directly from a production area. No kilns were found, but some deposits were interpreted as a dump of pottery production material (Anastasi 2015: 118). This hypothesis was suggested because of the numerous pottery wasters, sherds and ash. The site was excavated in 2008 during an assessment for development as earlier remains were exposed in the mid-1990s (Asciak 2019). Anastasi (2019: 4) suggests a date end second century CE/ Mid third century CE for the pottery.

Anastasi (2019: 9, 21-23) mentions two other sites excavated during development-led archaeology. The first includes a possible kiln in a rural site at Tal-Qares, Mosta. The second is a pit filled with ash in Żebbiegħ, which the excavator recorded as "probably a classical pottery kiln" (Cutajar 2006). They also recorded deposits mixing ash and ceramics. For Żebbiegħ, no publication is available, and a review of the sites and the material evidence is waiting. The online record mentions a Medieval and a classical occupation for the site. Therefore, with the current evidence, it is impossible to assess if Roman pottery was produced in the vicinity.

A brief report for Tal-Qares is available online. One feature (Feature 7) is described as a kiln, probably Early Roman (Cutajar and Spiteri 2014: 7) and is illustrated in

Figure 2.9. The grey and pink surfaces of the stones suggest that the structure was used for firing. The excavators attribute an Early Roman date to the site, based on the structural remains of the possible "villa", and mention a large number of cooking pots (Cutajar and Spiteri 2014: 8). No stratigraphic relationship can be established from the online report, and there is no mention of the deposits or finds within the feature, which could give dating elements or information about what the structure contained or if it was disturbed. Without the mention of wasters or ash deposits mixed with ceramic finds, it is not possible with the current evidence to assert that this was a pottery production site.



Figure 2.9: Photograph of Feature 7, Tal-Qares from Cutajar and Spiteri (2014: 15). This feature has been identified as a kiln by the excavators.

Anastasi (2019) and Sagona (2015a: 3) remark that Caruana (1899: 22) mentions one potential production site in the vicinity of Marsaxlokk discovered in 1883 and one in Gozo. No documentation is available, but he believed the Marsaxlokk site was a "Greek Factory" after numismatic evidence, standing close to "Phoenician ruins". He described three potential ovens, pottery, and bricks, but these remains have never been identified.

Several explanations could be put forward for this lack of kilns in the archaeological record in Malta. Stone-built features might not have withstood stone robbing, which has been common in archaeological sites (Bonanno 2007: 107). Kilns might also not have been permanent stone-built structures and might

not have survived in the archaeological record. Modern towns are often built on older and long-lived settlements (Sagona 2002: 268), and therefore, the evidence from Late Punic and Roman settlements depends largely on sites excavated development-led archaeology. Finally, since workshops can be a nuisance in settlements because of the smoke, they are often found outside town boundaries (Peacock 1982: 38), which, in the case of Malta, could result in being on unexcavated farming land.

Rice (2015: 339) mentions that the presence of firing wasters can indicate local production when workshops are missing. Misfired sherds can still be functional and might not necessarily represent a production waste. Cuomo Di Caprio (2017a: 336) defines wasters and misfired sherds as distorted, bloated or displaying bubbly surfaces. Their colours would vary from greenish to brownish, caused by over/under firing. Although wasters have yet to be systematically studied in Malta, Anastasi (2015: 147) mentions misfired vessels in Tas-Silġ, and Sagona (2015b: 79) mentions "blisters" in the assemblage, belonging to Crisp Ware, strengthening the argument that this generic group might be local.

2.3.2 Differing approaches to study local pottery production

The abundance criterion and comparative material

How have archaeologists inferred local production if workshops have not been found in Malta? Archaeologists traditionally rely on vessel types, their frequency at a given site and region and their comparative material in other assemblages and publications. They additionally rely on the number of similar vessels at one site or across a region (Druc 2013). This last approach is called the "abundance criterion" (Bishop et al. 1982: 301) or "criterion of relative abundance" (Rice 1987: 177). The principle is that the frequency of objects decreases away from their source.

In her local classification, Sagona (2002) does not state how she distinguishes the local wares from the imported ones. Imported vessels are recognised when the vessel shape lacks a local development. By extension, the ware and fabric which make up

these least represented vessels are labelled imported. As such, Imported Pink Buff Ware is used only for some "unguentaria [...] and some flasks" (Sagona 2002: 82). Imported [?] Red Bricky Ware (Sagona 2002: 83) and other non-prevalent fabric are compared to material in the Mediterranean such as the Aegean, Tarsus and Italy (Sagona 2002: 82-83). In contrast, Crisp ware is the most predominant ware across forms, including those described as Maltese. Sagona additionally looks at shapes with no comparative material abroad or local development across periods (Sagona 2015a: 244).

Similarly, Quercia (2002: 407, 411) established local forms looking at the most attested forms at Tas-Silġ and compared with sites across the Mediterranean such as plate types (Quercia 2011: 435). For instance, for plate type 1:2 (Late Punic, first half of the third century), he highlights how frequent they are at Tas-Silġ and infrequent in funerary, as well as the lack of comparative material outside Malta. He then concludes: "It is probable that this type should be considered as local" (Quercia 2011: 435). This implies that the abundance of vessel types was central in defining them as locally produced in the local literature.

Astarte inscriptions as evidence of local manufacture

The inscriptions to Astarte, among other inscriptions, are often cited as evidence for local production in Malta (Bonanno et al. 2000; Sagona 2002: 45; Quercia 2002: 417; Quercia 2005: 352; Bruno 2009: 3; Anastasi 2010; Sagona 2015b). Some of the inscriptions found at Tas-Silġ, and a few other sites across the Maltese islands (Anastasi and Vella 2021), suggest a dedication to the goddess Astarte (Frendo and Mizzi 2015: 550). The evidence that this goddess was worshipped at the temple site includes inscriptions of her name, also found on structural elements made in limestone (Amadasi Guzzo 1993: 205), strengthening the link between the vessels and the temple. Quercia (2002: 417) suggests a local workshop close to the temple, but the evidence is yet to be published.

The vessels were inscribed before firing. Therefore, a targetted vessel production for the temple is suggested. On the inscription in Figure 2.10, some clay displaced

when incising was left on the sides of the inscriptions, forming small lumps that hardened during firing. Inscriptions are found on varied vessels (Frendo and Mizzi 2015: 527, Quercia 2002: 417), mostly bowls, plates and on various wares (Sagona 2002: 79,82), mainly Crisp Ware, but also Cooking pots made of Bricky Red Ware. These inscribed sherds have yet to be characterised and compared with other members of their ware groups to assert that they are homogeneous in composition and that this "cross-provenancing" can be carried out.



Figure 2.10: Photograph of inscription of sample 34 from Tas-Silġ, rim of olla

Anastasi Fabrics 4 and 5: the question of provenance

Anastasi Fabrics 4 and 5 (Sagona Bricky Red Ware; Figures 1.6; 1.3), observed in specific types of fine wares and cooking vessels have been more controversial in terms of provenance. Anastasi (2019: 37) suggests that fabrics 4 and 5 are local because of the prevalence of the shapes which are made of these fabric groups. Anastasi (2019: 37) adds that these fabrics contain glauconite, *foraminifera* and lime, consistent with the geology in Malta. Quercia, who first published the classification for *olla*, *pentola* and *tegame* - often made of Anastasi Fabric 5 -

had proposed that the shapes are locally produced because they are prevalent and have a local development across time-periods (Quercia 2002: 407, 411, 413).

These inclusions would necessitate characterisation to ensure their identification (see section 1.2 for the discussion on Fabric 2 and black inclusions). The presence of *Foraminifera* and their identification have been considered as a possible indicator of provenance for sherds (Molitor 1988; Wilkinson et al. 2016). Previous studies mention calcareous microfossils in other vessels interpreted as locally produced, particularly *Globigerina* and *Globigerinoides* (Anastasi et al. 2021: 3, Bruno and Capelli 2000: 60, Anastasi 2019 and earlier periods Tanasi et al. 2020a: 125). *Foraminifera* are common to Maltese clays (Murray 1890), however, there are similarities between sedimentary geologies such as Malta and southern Sicily (Molitor 1988: 110; DiGeronimo et al. 1981).

Sagona had first labelled these ware groups as imported (Sagona 2002). This is an example of the limitations of the abundance criterion. Sagona (2002: 83) classified Bricky Red Ware as Imported [?] because 1) the forms found in this ware group had parallels elsewhere in the Mediterranean and 2) this ware was rarely found in tombs (Bonanno et al. 2000: 95). However, the under-representation of this ware in tombs could be a bias from the archaeological record, as most of the vessels are cooking shapes and the sites analysed by Sagona are only funerary where cooking forms might be under-represented (Anastasi 2019: 37). In the preliminary report for the excavations at Tas-Silġ (Bonanno et al. 2000: 95), Sagona questions the provenance of the Bricky red ware or Late Red Bricky ware as inscriptions to Astarte were found on this ware, suggesting a local provenance. Sagona proposes a possible itinerant craft person travelling with their clay. The temple is close to Marsaxlokk, an important maritime route (Vella and Anastasi 2019), and itinerant craftspeople could have produced vessels in the area. Bruno (2009: 130) proposes that, in general, items were likely sold at Tas-Silġ with the site acting as a possible "emporium" during the Late Republican period (Bruno 2009: 138). However, these cooking vessels in Fabric 4 and 5 were excavated in many other sites in Malta (Anastasi 2019) and are not constrained to Tas-Silġ.

Examples of Sagona's ware types from Tas-Silġ and their possible provenance were studied with NAA by Mommsen et al. (2006). This study is the only bulk-chemical study including Punic sherds and includes sherds dating as early as the Temple Period. The samples include examples from the ware types Crisp Ware or Biscuit Ware, five "Bricky Redware" sherds (Anastasi Fabric 5), although one is described as "Fine" (Mommsen et al. 2006: 83, Anastasi Fabric 4 or 5?). Some of these sherds would likely date from the Roman period as Sagona does not differentiate Late Punic from Early Roman in her methodology (Sagona 2015b: 4).

The five Bricky sherds are from two stratigraphic units. The context of most sherds (TSG96/34 - Group AG28) is a secondary ash deposit and part of a group of deposits interpreted as levelling activities stratigraphically dated to the Late Roman/Medieval period (Vella et al. 2015: 149). These sherds are therefore not from secure contexts, and the lack of illustrations makes a secondary typological analysis impossible.

The NAA results are analysed using Mahalanobis distance, which measures the distance between points in multivariate space. This statistical method and the assumptions have been reviewed in Baxter (2001). In the results, the sherds are grouped into two groups SILA and SILB, which are then compared with sherds from Segesta in Sicily. Most sherds, including Crisp Ware, are grouped as SILA. The authors suggest a similar raw material for SILA with different recipes explaining some of the variations observed. Only the five sherds of Red-Bricky Ware were classified as the homogeneous group SILB. Based on the groupings alone, a local origin is not supported for SILB (Mommsen et al. 2006: 86). However, the authors suggest that the vessels of SILB must have been locally manufactured, not necessarily with local material, because of the Astarte inscriptions on similar vessels (Bonanno et al. 2000: 95). This study highlights that chemical groupings results should be interpreted within the broader archaeological record but does not resolve the question of the provenance and the manufacture of Fabric 5 and 4. Research needs to be conducted to understand why these sherds differ from the main generic fabric and if they could be made with local clays.

To summarise, this chapter has reviewed the known raw materials available in Malta, including lines of enquiry for materials which have not been studied and how they could be investigated, from systematic sampling and secondary ethnographic investigation to experimental archaeology. The assumptions for pottery provenance studies using chemical analysis were then considered, and the problem of yet non-quantified variations within Maltese clays was highlighted. Finally, the available evidence for local production in the Late Punic-Roman period has been examined, also looking at how archaeologists have studied local production in Malta. The case study of the Bricky Red Ware has highlighted the debate around the provenance of these particular vessels and the limitations of traditional evidence, such as the abundance criterion to assess the source of raw material of a vessel.

Part II

Macroscopic and Fabric Analyses

Chapter 3

The archaeological sites

3.1 Selecting the archaeological sites

To investigate the variations in fabric classes in the Late Punic and Early Roman period in Malta, two sites excavated by the University of Malta (UoM) were selected as case studies: part of the sanctuary of Tas-Silġ and the Żejtun villa. Both excavations were carried out stratigraphically following the single context recording system (Bonanno and Vella 2012: 19; Bonanno and Vella 2015a: 4). UoM has selectively published the excavation results in recent years (Bonanno and Vella 2015c; Vella et al. 2017), presenting a description and interpretation of the chronology of the sites, but the complete account of the Żejtun villa is yet to be published. Choosing to study samples from UoM excavations ensured that the material and documentation were easily accessible.

These sites are located in the island's southeastern part (Figure 3.1), only 1.6 kilometres away from each other (Vella et al. 2017). The harbour of Marsaxlokk would have been strategic in antiquity thanks to its geographical location and accessibility as a naturally sheltered harbour. Bonanno (2011: 53) has suggested that the inner harbour of Marsaxlokk is similar to the *cothon* found at Motya. He also underlines that the sanctuary at Tas-Silġ is cited in Cicero in his speech against Verres and might have been known in the central Mediterranean (Bonanno

2011: 145). Additionally, Bruno (2009: 121) mentions old discoveries in the Bay and around Delimara, pointing to cargoes around the area.

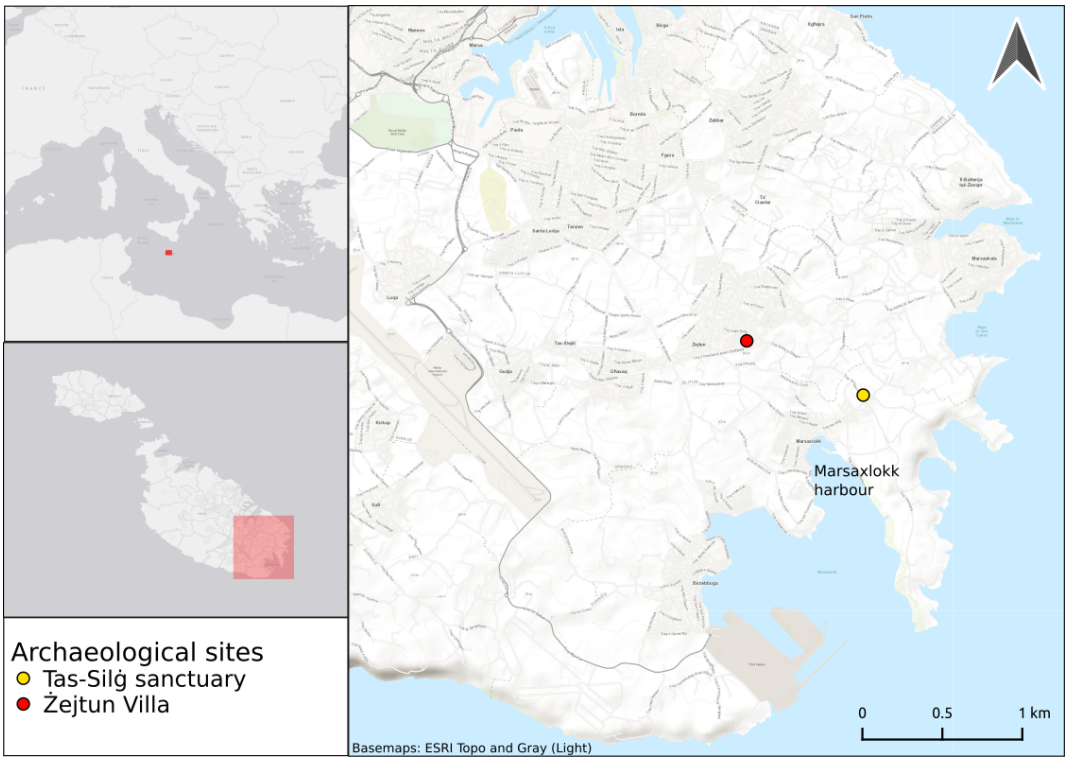


Figure 3.1: Map showing the location of the two archaeological sites with insets from Malta and the Mediterranean.

Other sites in the area include a Roman villa in Marsaxlokk (Bruno 2009: 48), burial grounds from the Punic, Roman, and later periods (Pace et al. 2012: 61, 63; Abela 2012; Said-Zammit 1993). In the broader region, sites are numerous such as the villa of Ta' Kaċċatura, the Roman baths close to Żabbar discovered in the 1930s (Sagona 2015a: 313) and some cisterns cited by Bruno (2009: 120). Other Late Punic and Roman sites keep being discovered in the Marsaxlokk region, such as the Marnisi villa, currently excavated by UoM in collaboration with the Superintendence Of Cultural Heritage (SCH). Selected sites are represented in Figure 3.3. A map for the Żejtun local council was published in Pace et al. (2012: 62) and is reproduced in Figure 3.2 and some of the sites, up to 2006, are mentioned by the Malta Environment and Planning Authority (2006: 212). The detailed chronology of all these sites, and their relationship, still need to be fully established.

The similarities in pottery production in the region have been discussed by Anastasi (2015). Plates and bowls, which are the predominant forms at Tas-Silġ and to some

extent Żejtun, share a similar typology (Anastasi 2010: 121; Anastasi 2012: 31; Vella et al. 2017: 125). Inscribed sherds, interpreted as offerings or dedications to the goddess Astarte, common at Tas-Silġ, were found in the Żejtun Villa suggesting links between the two sites. Inscribed vessels have been found in different contexts across the Maltese islands, for example, at Ras ir-Raħeb, Għar ix-Xih and tombs (Anastasi and Vella 2021: 30). The economic production of the two archaeological sites under study should not be looked at in isolation. Bruno (2009: 130) suggests that the relation between Tas-Silġ and surrounding agricultural lands could be an economic one, with the temple gaining income from the agricultural land around in a similar situation to Delos.

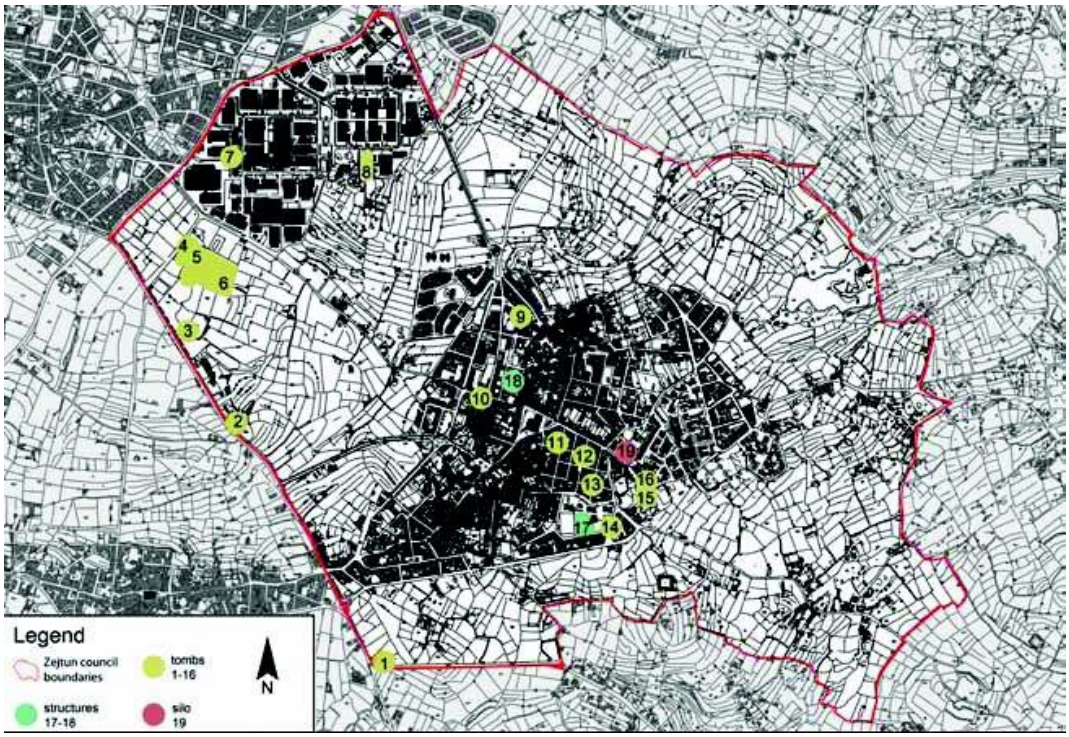


Figure 3.2: Map of Żejtun with archaeological discoveries, from Pace et al. (2012: 62). 4-6: Tal-Ħotba, 17: the villa, 2: Tal-Barrani

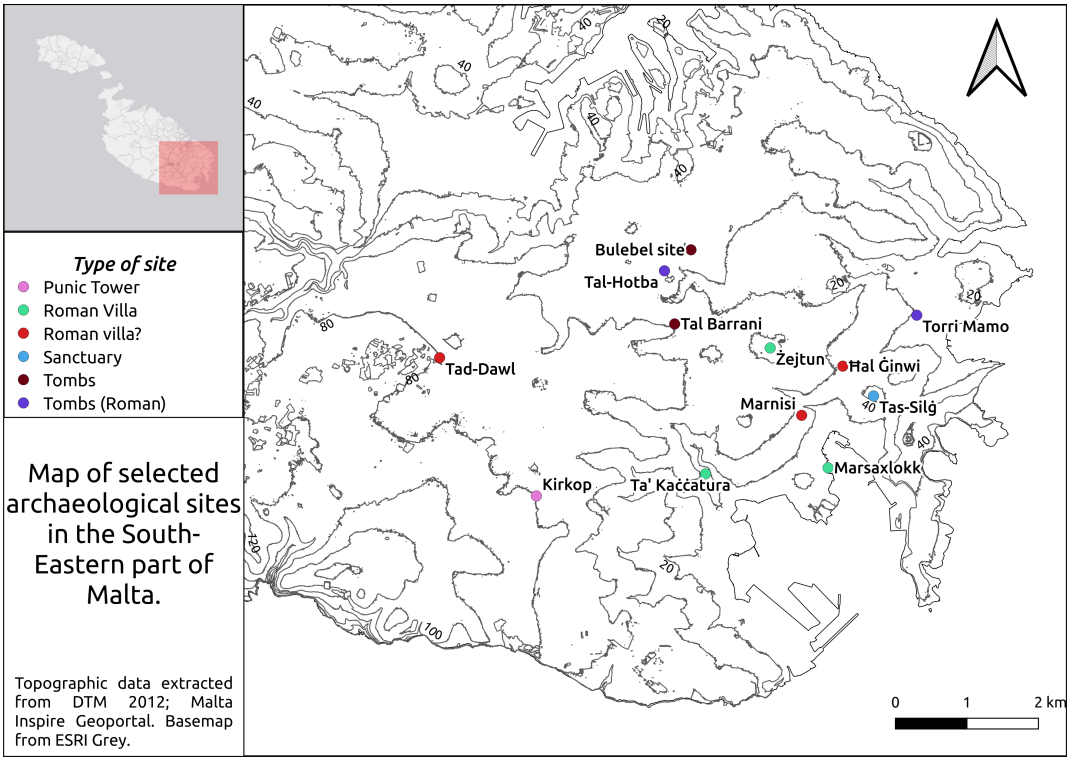


Figure 3.3: Map of selected archaeological sites in Malta. Made in collaboration with Arthur Lamolière (extraction of topographic data) and Thornton Doupnik (data collection). Some site locations are approximate as no coordinates were found (e.g. the Marsaxlokk villa)

3.2 The Tas-Silġ Sanctuary

3.2.1 The site and publications

The archaeological site of Tas-Silġ was discovered in the 1920s, although the ruins of the site were known since at least the sixteen century (Bruno 2009: 123). Figure 3.4 summarises the primary campaigns by different institutions. The site was named after the nearby chapel.

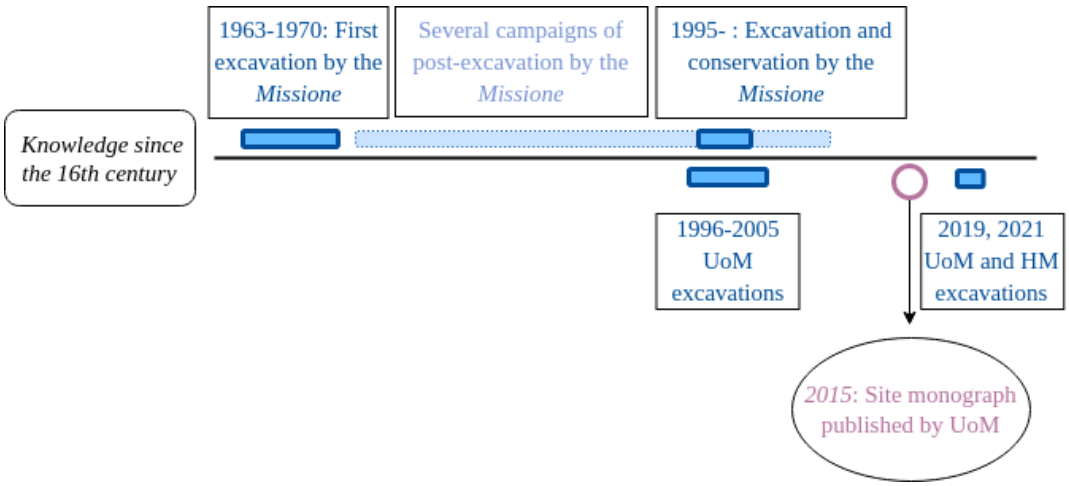


Figure 3.4: Timeline of excavation campaigns at Tas-Silġ. Dates until 2005 from Rossi (2015). Notes that the Missione campaigns continued after this date.

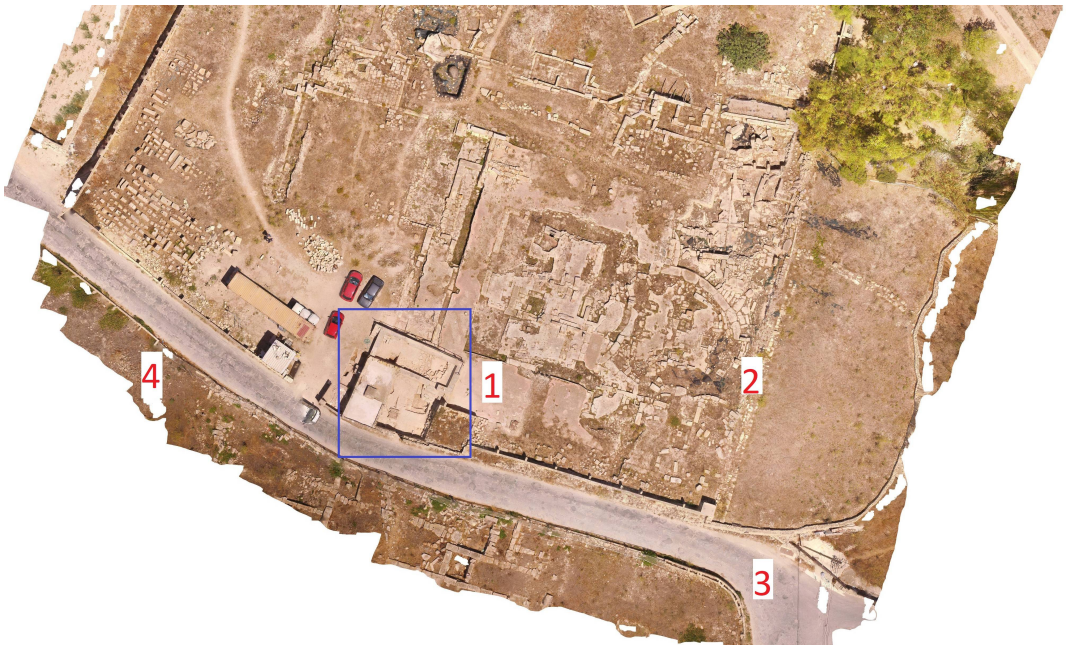


Figure 3.5: Orthophotomosaic of the Northern part of Tas-Silġ before excavation in 2019, by J.C Betts (Department of Classics and Archaeology). The dark blue square shows the area where the new excavation campaigns by UoM (2019; 2021). 1: Late Republican peristyle with *opus signinum*; 2: Temple Period megalithic apse integrated into later temple site; 3: Triq Xrobb L-Għaġin; 4: Southern part of the site. Oriented North upwards.

The site is divided into two parts by the road Triq Xrobb L-Għaġin (Figure 3.8; [3] in Figure 3.5). The first *Missione archeologica Italiana a Malta* excavated the northern part of the site, where the main temple structures are situated (Figure 3.5), and a part of the southern section ([4] in Figure 3.5). The *Missione* was established

in 1963 by Prof. Moscati at the Università "La Sapienza" of Rome following a request for assessment by the Minister for Education of the Maltese Government (Rossignani et al. 2011). The Missione published the campaigns in Italian in the *Rapporti preliminari* between 1963 and 1973. The first excavations in the 1960s did not follow a stratigraphic approach which was later adopted systematically on site (Bruno 2009: 124). The *Missione* was re-created by Prof. Ciasca after 1995 to document and expand the work of the first *Missione* (Rossi 2015: 82) as well as carry out conservation and post-excavation work (Rossi 2015: 85). An overall site monograph containing all raw data is yet to be published; however, a bibliography of the different publications is available in Rossignani et al. (2011) and several articles are available in English such as Cazzella and Recchia (2012) looking at the Neolithic part of the site.

UoM excavated the southern part of the archaeological site from 1996 to 2005. These campaigns were published in a site monograph with two volumes (Bonanno and Vella 2015b,c). Heritage Malta (HM), in collaboration with UoM, has recently started a new excavation in the northern part of the site, exploring a corner of the Roman temple (blue square in Fig. 3.8).

Prehistoric occupation

The site's first known occupation dates from the Temple Period (Trump 2002: 138-139), with megalithic structures excavated in the North by the *Missione* (Cazzella and Recchia 2007). The reconstruction of the remains is available in Vella and Anastasi (2019: Fig. 36.2). Cazzella and Recchia (2012: 19; Fig. 1; Fig. 3.6) have interpreted two main temple structures, chambers and megalithic steps. The site was then occupied during the Bronze Age, with the reuse and modification of megalithic structures from the 23rd century BCE to the 8th century BCE according to Cazzella and Recchia (2012: 18).

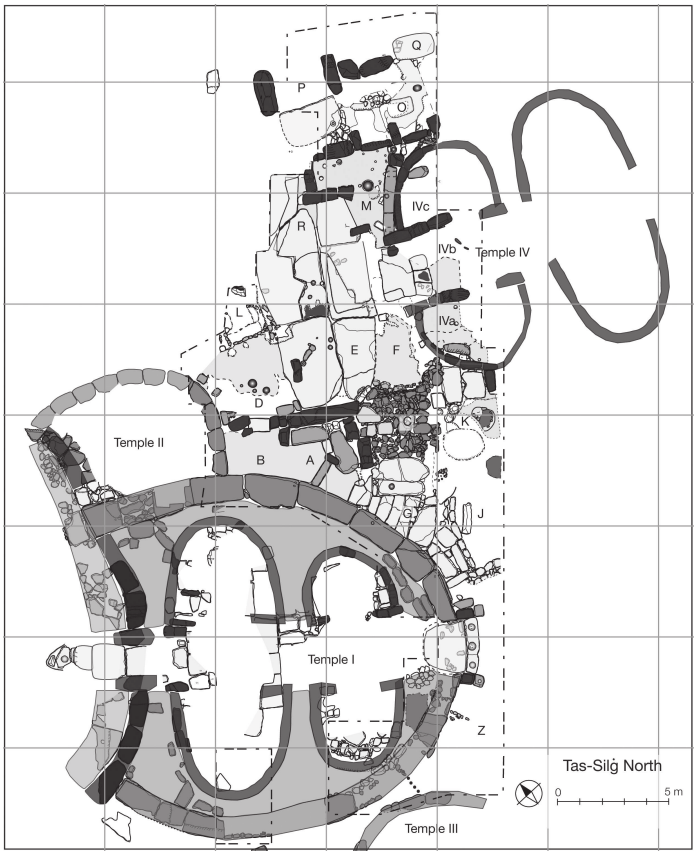


Figure 3.6: Plan of Tas-Silġ Temple Period structures from Cazzella and Recchia (2012: 19; Fig. 1)

3.2.2 Phoenician, Punic and Early Roman occupations

The evidence for the Phoenician[1] occupation includes an altar and pottery (Ciasca 1993). Archaeological evidence is more plentiful for the fourth century BCE onward, when a structural reorganisation seems to have occurred, including the building of walls around the site and pillars with possible Egyptianizing capitals (Vella and Anastasi 2019: 562). The site would have been dedicated to the goddess Astarte from at least the fourth and third century BCE, suggested by inscriptions on sherds (Frendo and Mizzi 2015: see section 2.3 for further details) as well as an altar dedicated to the goddess (Vella and Anastasi 2019: 562). Some megaliths from the Neolithic temple were incorporated into these later structures.

[1]In Malta, the Phoenician period is often described as having started sometime after the eighth century BCE (Vella and Anastasi 2019: 556)

During the 3rd-1st century BCE, Vella and Anastasi (2019: 562) mention the appearance of the additional cults to Hera and Isis, and inscriptions to Hera were found by the *Missione* (Bruno 2009: 139). Other votive objects were excavated across the site (Bonanno 2015) and Vella and Anastasi (2019: 563) have collated the evidence for feasting at the site, from the vessels, animal bones and organic residue analysis.

During the Late Republican period, named Period IV (Hellenistic/Roman) by UoM, the sanctuary was the object of several reconstruction phases. In the northern part of the site, major re-structuring works took place in the 2nd-1st centuries BCE including the erection of a "double-naved Doric porticoes paved in opus signinum" (Bruno 2009: 127; see plan in Bonzano 2017: 54; reconstruction in Figure 3.7 from Amadasi Guzzo 2011: 15). Middens likely first accumulated somewhere on site and was redeposited in the south during these restructuring works (Vella et al. 2015: 78).

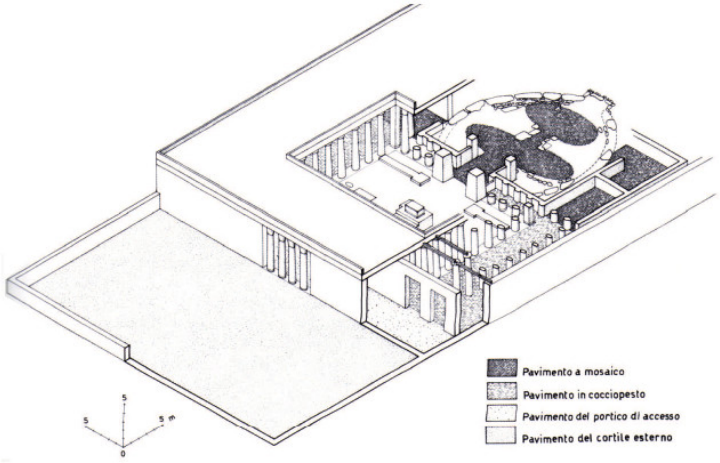


Figure 3.7: Reconstruction of the Late Republican temple at Tas-Silġ, from Amadasi Guzzo (2011: 15, Fig. 7).

During the second-century re-organisation, an ashlar structure was erected in the southern part of the site, possibly as a foundation for a podium (Vella et al. 2015: 58). Some of these ashlar walls were excavated by UoM (Area A in Figure 3.8). One stratigraphic assemblage of this dissertation (Stratigraphic Unit (SU) TSG96/352) is one fill from the numerous foundation cuts (SU TSG96/345) for the ashlars (see Table 3.1 and Figure 3.9).

In other areas of the southern part of the site, levelling deposits were laid out during this period possibly for the flooring that the *Missione* had previously identified. Some of these levelling deposits were excavated by UoM (Area C in Figure 3.8; Vella et al. 2015: 84). One stratigraphic assemblage for this dissertation comes from one of the fills (SU TSG96/2051; 3.10) of a wall erected in Area C, possibly contemporary with these levelling activities (SU TSG96/2048). The *Missione* dated the construction of the walls to the Byzantine period. Still, according to Vella et al. (2015: 85), the foundation contains pottery from the second century BCE onwards, including a few which could date from the first or second century CE.

Bruno mentions a possible shift in economic activity at the site during this period. Between the fourth and the second century, she states that the temple site was "modestly open to commerce" (Bruno 2009: 137). Closer to the first century BCE, contemporaneously with the refashioning of the temple, she notes an increase in imported amphorae.

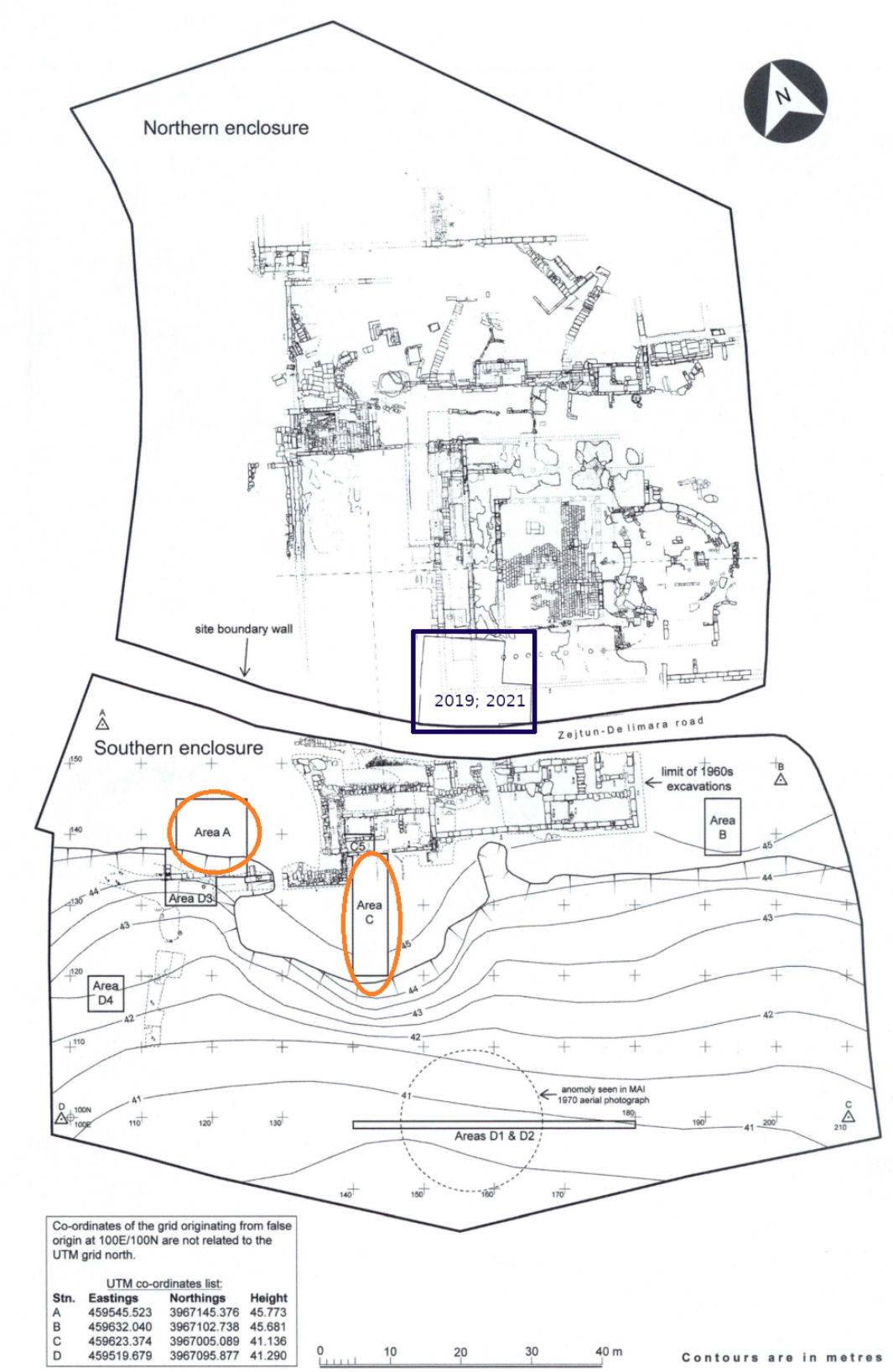


Figure 3.8: Plan of the Tas-Silġ from Bonanno and Vella (2015a: 13). The orange circles point out where the pottery studied in this dissertation comes from. The dark blue square shows the area where the new excavation campaigns by UoM (2019; 2021).

3.2.3 Tas-Silġ stratigraphic units

The two SUs (TSG96/352 and TSG96/2051) were narrowed down from the stratigraphic and pottery reports (Frendo and Mizzi 2015; Sagona 2015b; Vella et al. 2015), and a final list of over ten units. The UoM's southern trenches yielded 81,893 sherds (Sagona 2015b: 4), and a selection was therefore necessary.

Priority was given to SUs from areas C and A dated to the Late Punic to Late Republican period (Vella et al. 2015: see, for instance, note 26 for Area A, 58). Area B was avoided due to the nature of the deposits, which have been qualified as re-deposited middens. Construction fills were preferred as they are more likely to be contained and well-defined units with clear boundaries. Deposits with unclear boundaries or not fully excavated were avoided because of the lack of stratigraphic control. Thanks to the methods adopted during recent excavations, it was possible to study SUs with extensive documentation and assess how secure the contexts were. The same principles were applied to the Żejtun villa.

Stratigraphic assemblages were chosen as the first scale of study to allow the interpretation of sherds in their context and for future studies to assess changes across space and time. Hazenfratz Marks (2016: 51) argues that archaeologists often conduct fabric studies on de-contextualised material whilst samples should, as best as possible, come from secure contexts, ideally, contexts that are radiocarbon dated (Santacreu 2014: 6). However, sampling from secure contexts can conflict with the Maltese archaeological record. Later spoliation frequently disturbs sites (Sagona 2015a: 10, note 27), such as stone robbing and reuse of sites in later centuries (Bonanno 2007: 107; Bruno 2009: 122). Another limitation comes from the deposition at Tas-Silġ. The site formation processes are complex, with re-deposition occurring during the reconstruction phases in the Late Republican periods (Vella et al. 2015: 78). Residual material would therefore be expected.

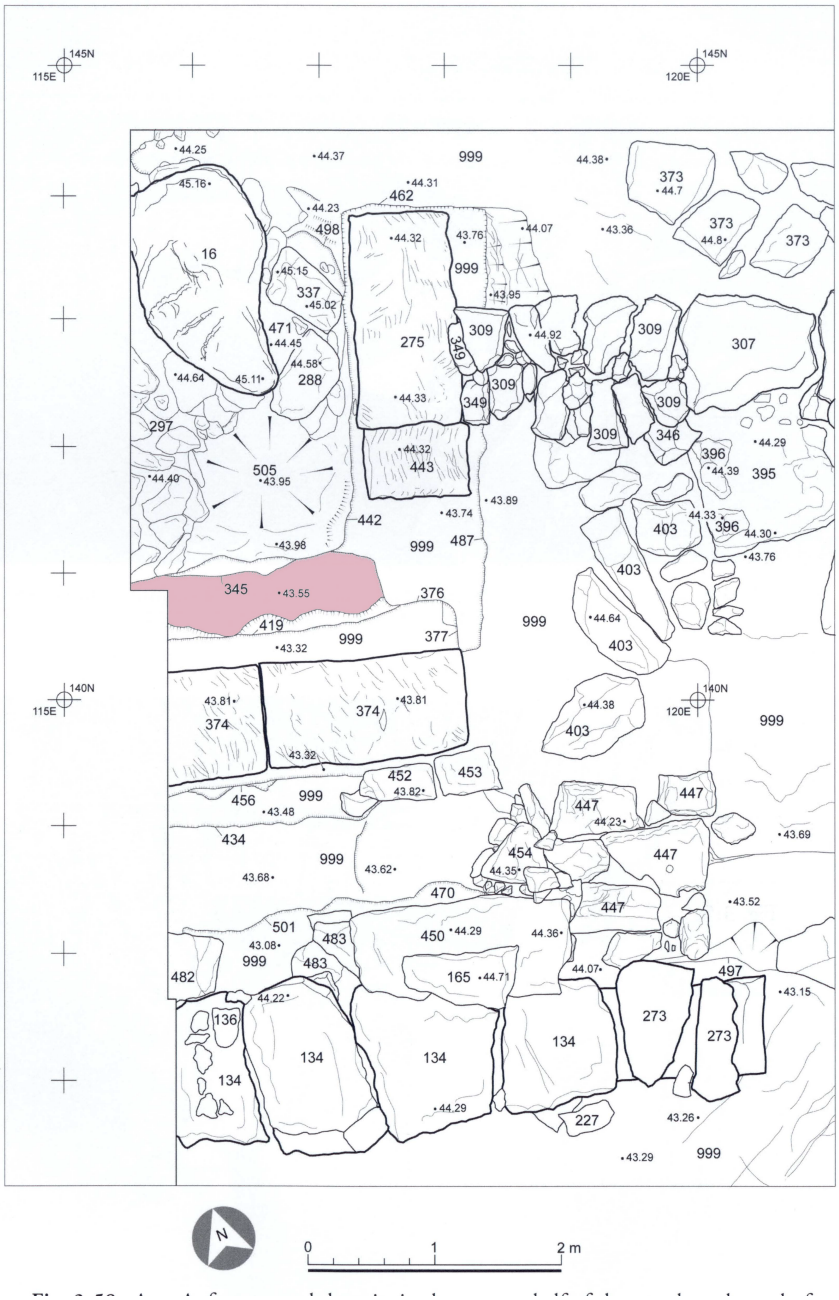


Figure 3.9: Plan of a part of Area A, Tas-Silġ after the 2005 campaign. Cut 345, fully excavated, is highlighted in pink. From Vella et al. (2015: 126)

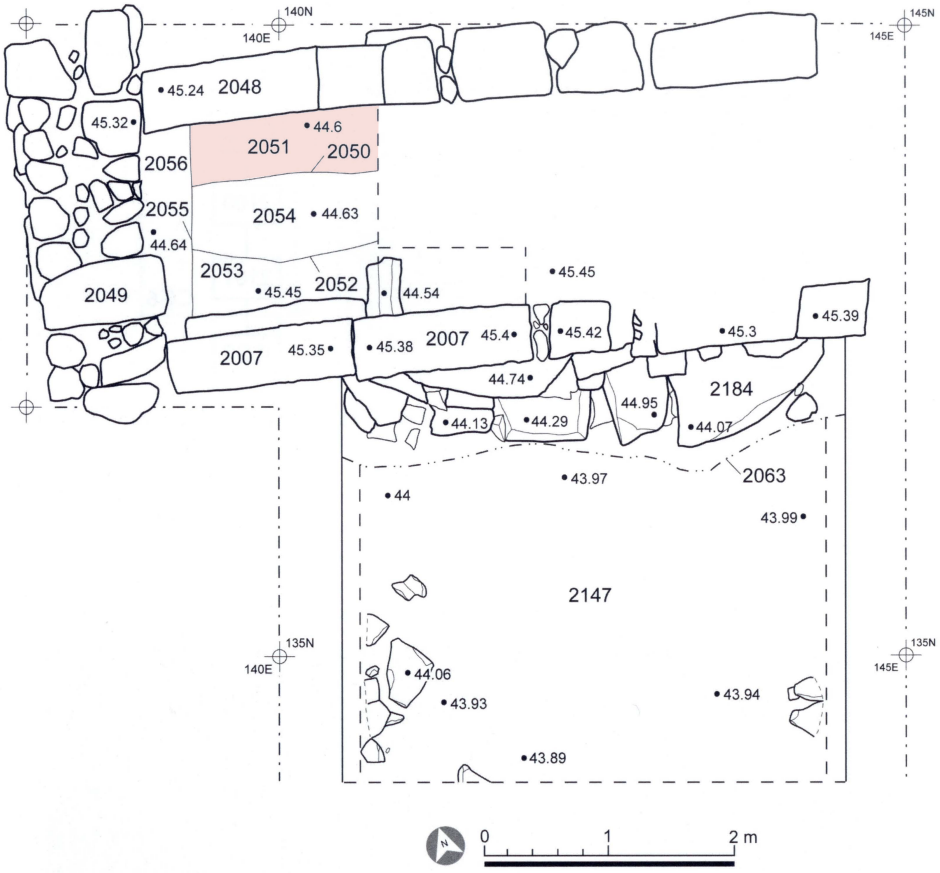


Figure 3.10: Plan of Area C, Tas-Silġ showing SU TSG96/2051, highlighted for this dissertation. From Vella et al. (2015: 198)

SU	Area	Description and formation processes	Notes from pottery report	Limitations
2051	C (CG9)	Grey brown soil. Construction fill of wall 2048. According to the Matrix (Vella et al. 2015: 209), deposited before the levelling for cocciopesto flooring in area C.	Seven sherds illustrated in publication (not found in stores), inscribed sherds on both Crisp and Red Bricky Ware. Contains sherds from earlier periods (for example, Borg in Nadur sherd). One of the sherds of Red Bricky Ware was analysed for chemical content in Mommsen et al. 2006 (not found in stores).	Residual material and could be secondary. Not precisely dated.
352	A (AG1)	Brown soil mixed with stones. Construction fills (fills cut 345) for ashlar masonry structure.	Two sherds illustrated, and ten additional inscribed sherds described. An inscription was found on Crisp Ware and Bricky ware. Contains residual material (Sagona 2015, note 59).	Wide range of data for the pottery and residual material from the foundation trench and/or fill from other parts of the site.

Table 3.1: Table presenting final SUs selected from Tas-Silġ. The descriptions can be found in Vella et al. (2015: 81,55). Pottery reports include Sagona (2015b) and Frendo and Mizzi (2015)

3.3 The Żejtun Villa

3.3.1 The site and publications

The Żejtun villa was discovered on the grounds of the Secondary School St Thomas More College in Żejtun (Bonanno and Vella 2012: 9). The first remains were uncovered in 1961, during the clearance work to build the new school (Bonanno and Vella 2012: 12). Excavations were then undertaken extensively in 1972 (Bonanno and Vella 2012: 12) and continued regularly up until 1975 (Figure 3.11). Those excavations were led using box-grid or rectangular trenches and not following the single-context recording system (Bonanno and Vella 2012: 13). This implies that information about single SUs was not recorded and stratigraphic relationships were not identified in the field (Anastasi 2010: 105). In 1976, excavations continued, of which notes survived but no report was published (Bonanno and Vella 2012: 15-16). Excavation resumed in 2006 and continued until 2018[2] led by UoM. This led to different publications such as the preliminary reports for the recent excavations (Abela 2012; Vella et al. 2017) and re-assessment of the previous excavations and pottery (Anastasi 2010). The occupation at the site can be divided into three major phases, the pre-villa phase (4th-2nd c. BCE); the villa phase (2nd c. BCE-4th c. CE) and the post-villa phase (Fort et al. 2022: 4).

[2]No excavations took place in 2010 and 2015

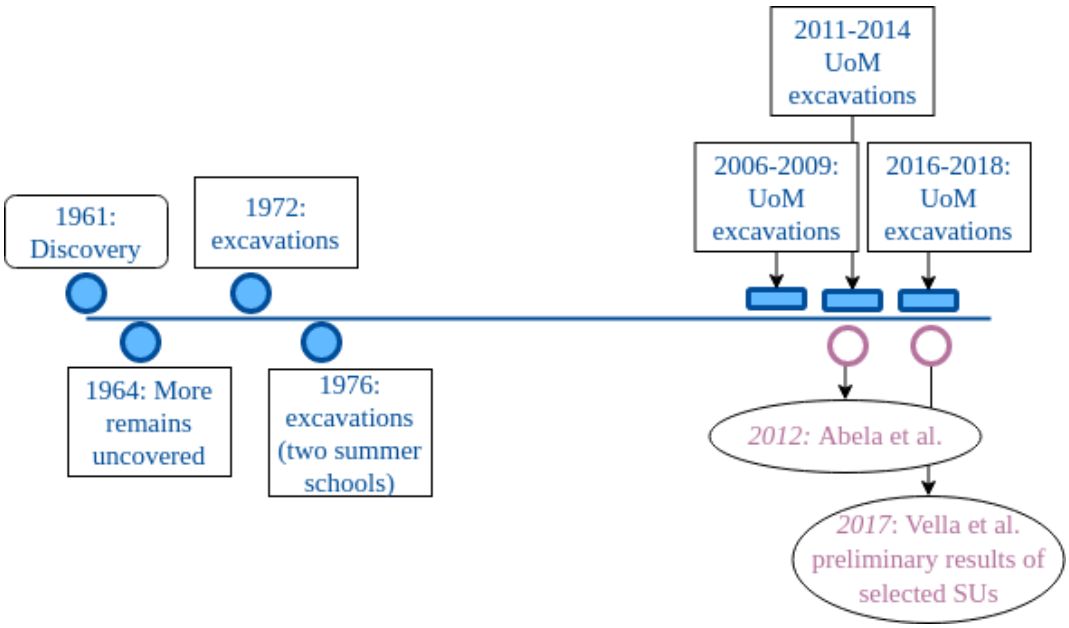


Figure 3.11: Timeline of excavation campaigns at the Żejtun villa. Dates from Abela (2012) and University of Malta (2018).

A Late Bronze Age occupation was suggested by Vella et al. (2017: 139) based on residual Bronze Age pottery. A Punic phase at the site had been suggested in the 1970s and subsequent studies (Anastasi 2012; Vella et al. 2017: 110). Walls and a cistern have been dated to the Punic period, 5th-4th century BCE, based on the ceramic finds (Vella et al. 2017: 114). Some vine trenches[3] were also dated as early as the 4th century BCE, suggesting an early existence of the vineyard (Vella et al. 2017: 119). Walls from this period ([4] in Figure 3.13) were interpreted as the foundation of a structure and were later reused and modified in the later villa complex (Bonanno and Vella 2012: 21; Vella et al. 2017: 117). One stratigraphic assemblage from this dissertation comes from one of the deposits (SU ZTN06/549) of the later reuse of one of these walls (Wall 508; see Table 3.2 and Fig. 3.12).

The main villa complex was built either at the end of the Late Republican period or early period (2nd-1st century BCE). Vella et al. (2017: 114), Anastasi (2020: 93) and Fort et al. (2022) suggest that during the second-first century BCE, the existing vineyard was abandoned. Several fills of the rock-cut trenches contain pottery dated by style to this period, and some were sealed by remains of later

[3]Vine trenches are rock-cut rectangular features associated with the growing vines as roots need depths to grow (Vella et al. 2017: 118)

structures (Vella et al. 2017: 118). The villa was built over the vineyard, and an olive press suggests a shift to the production of olive oil.

The second stratigraphic deposit from the Żejtun villa in this study comes from another area of the site (Area G), which was explored to understand the relationship between the "industrial area" (Area A; Vella et al. 2017: 111; Fig. 1; [3] in Figure 3.13), where the pressing equipment was found, and the foundation walls already mentioned. Vine trenches were excavated, and the second stratigraphic assemblage is the fill (SU ZTN06/2107) of one of these agricultural trenches (ZTN06/2116 or trench 9 in figure 3.12), which is said to have been "sealed by a later floor layer" (Vella et al. 2017: 15). The villa seems to have been maintained over centuries (Fort et al. 2022: 4). Some worked stones from earlier structures (Anastasi 2020: 92) were reused, and production might have shifted to olives rather than vines.

The Żejtun villa site is part of a broader site type: Late-Punic and Roman villae, often with continuous occupation from the Punic period (Bonanno 1977; Bruno 2009). The study of wine production and trade is becoming possible with the excavation of more sites, including vine trenches, vat and amphorae (Anastasi 2020; Bonanno 2008). Olive pressing was also an important part of the economy of Roman Malta and could have been practised at the Żejtun villa (Anastasi et al. 2022; Anastasi and Vella 2018; Bonanno 1977). Żejtun had residential quarters, fitting the category of *villa rustica* similar to San Pawl Milqi and Ta' Kaċċatura (Anastasi et al. 2022: 54).



Figure 3.12: Plan of the Żejtun villa excavations modified from the publication of Vella et al. (2017: 113). The sherds in this dissertation are from area B and area G. 549 was found where the red star is, between 508 (red), 506 and 542. SU 2107 is a fill for trench 9 (yellow).

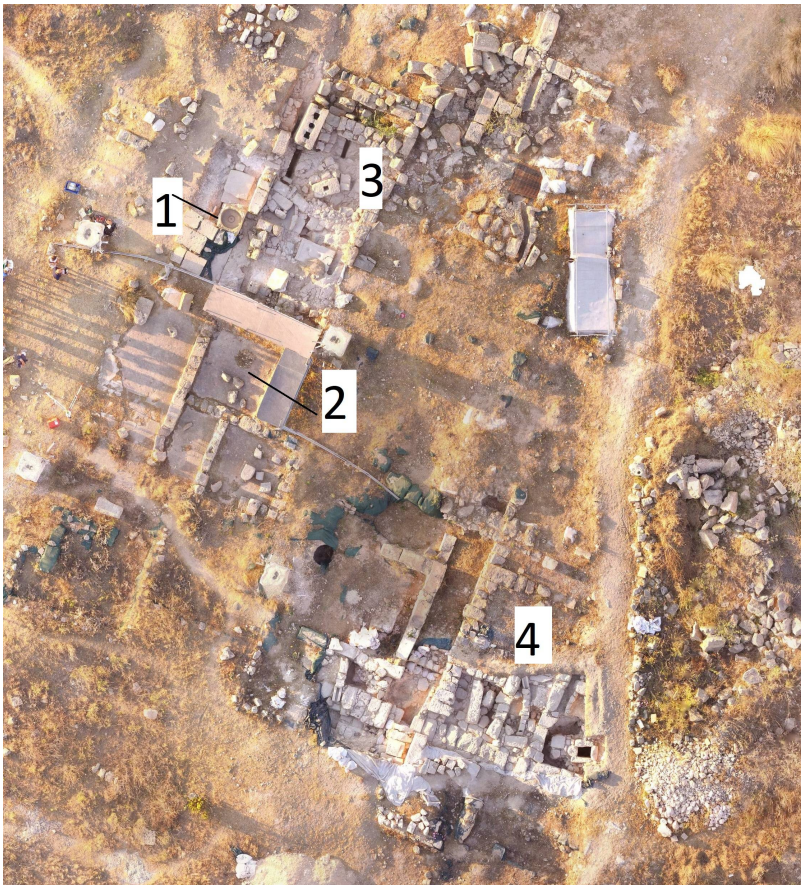


Figure 3.13: Orthophotomosaic of the Żejtun Villa, John Betts. Modified for this dissertation. [1] VAT; [2] tiled room; [3] Industrial area; [4] Foundation walls.

.

3.3.2 Selecting units from the Żejtun villa and limitations

The two SUs are summarised in Table 3.2 and photographs of the features are pictured in Figures 3.14 and 3.15.

Treating SUs as assemblages has limitations when the final site monograph is not yet available. Stratigraphic units are categories attributed by the archaeologists in the field and during post-excavation. For instance, the pottery from one of the SUs, ZTN06/549 (Żejtun Villa), is published individually as an assemblage in Vella et al. (2017). In the site documentation, however, the excavators equated SU ZTN06/549 with another unpublished SU ZTN06/551.[4] According to FACEM

[4]This information was extracted from the site documentation, SU context sheet for 549 and

(2020) and the SU register, including comments from the same pottery specialist, the pottery dating of the two assemblages is different with 551 dating from 4th/3rd BCE, whilst 549 is described as 2nd/1st BCE. A reassessment of the dating, pottery and stratigraphic relationships will be possible when the raw data is published.



Figure 3.14: Photo of areas A and G at the Żejtun villa, trench ZTN06/2116 (vine trench 9) and its fill (ZTN06/2107) after it was excavated. North-Western orientation. North-Western orientation. Labels are the same as for the orthophotomosaic.

551 as well as the excavation journal for area B (note from 30th of June 2009; p63).



Figure 3.15: Photo of areas B at the Żejtun villa. The walls are indicated, and the red square shows where the deposit ZTN06/549 was found.

SU	Area	Deposit description	Formation process and interpretation	Limitations
549	B	stony yellow brown deposit	Deposit butting wall 508, "sealing a later phase of wall 508" (Vella et al 2017:133)	Boundary with SU 551 might be not archaeologically significant
2107	G	light brown deposit	Deposit in vine trench 2116, sealed by a levelling deposit (2117) and later floor level 2028 (Area notebook 2014:70)	

Table 3.2: Table presenting stratigraphic units chosen from the site of Zejtun. Information from Vella et al. (2017: 133-5) and SU sheet for ZTN06/549.

Chapter 4

Methodology

4.1 Assemblage description and sherd sampling

This section describes how 70 sherds were sampled for analysis as part of their stratigraphic assemblages for this research. General considerations are given about the types of samples and limitations of the sampling process. Site-specific methods and challenges are provided.

4.1.1 General considerations for sampling

One aim of this work was to investigate the variations in pottery fabric using macroscopic, microscopic, petrographic and chemical analysis. According to the review of the literature, Crisp Ware/Fabric 1 (F1) is a generic local group across classifications (Section 1.2). However, it has many macroscopic variations which are not understood in terms of raw material provenance and technological processes. Bricky Red Ware/ Fabric 5 (F5) is recognised as one group, different from Anastasi F1 and across the classifications, visually and chemically (see sections 1.2 and 2.3). Its provenance has been debated and needs investigating. A refined version of Bricky Red Ware, Fabric 4 (F4), is also cited in the literature. As these fabrics/ware groups were recognised as predominant in the stratigraphic

assemblages, it was decided to focus on fabrics 1, 4 and 5 and start with a few forms. This sampling is not exhaustive as many more types and forms, as well as Anastasi fabric 7, were observed macroscopically in the assemblages. The focus on a limited amount of vessel forms allowed to sample variations in fabric, as seen in the fresh break, whilst having similar typologies.

The stratigraphic assemblages were of different sizes, reflecting the number of sherds at the two sites. For instance, ZTN06/549 contained 22 diagnostic sherds, whilst TSG96/352 contained 670 (see section B.3). The sampling strategy was, therefore, different for the two sites as less time could be dedicated to individual sherds from Tas-Silġ. In total, 70 sherds were sampled for further analysis (see the catalogue in Appendix A).

The sherds are diagnostic in terms of elucidating how fabrics relate to forms and types. Technological choices are better interpreted when combining all scales of analysis, including shape, and after a typological assessment of assemblages (Hein and Kilikoglou 2020: 180). Rims or profiles are preferred: bases or handles are more likely to be made of different pastes than the rim and body as the technical requirements might differ across the vessel (Santacreu et al. 2016: 167). Additionally, bases might not allow the differentiation between a bowl and a plate. Bases were avoided except one (Sample 59, Figures A.117) from the Żejtun villa. There was no sampling on complete vessels, such as the lid (ZTN06/549/1) found at Żejtun, but profiles were found.

Dating precisely the pottery of this period is complicated by the lack of published dated fine ware associated with shapes found in Malta, preventing dating by association (Anastasi 2010: 8, 18). In recent years, Anastasi (2019), Bechtold (2017), Quercia (2011), and Sagona (2015b) have developed the pottery chronology in Malta, enabling an estimation for the vessels in the assemblages. Shapes from the 3rd-1st century BCE were, therefore, targeted.

For Crisp Ware/ Anastasi fabric 1, plates, bowls and miniatures were selected as they have been chronologically studied (Quercia 2011). As highlighted in Anastasi (2010: 121-122), plates and bowls are also the primary forms found in Tas-Silġ

and the pottery found in the older Żejtun excavation.

Looking at Fabric 5/ Bricky Red Ware, this fabric was mostly observed on cooking vessels: casserole, olla, tegame. Bowls with similar macroscopic fabric features to these cooking vessels were also sampled (e.g. Sample 33). The main classification for dating the cooking vessel forms is the typology by Quercia (2002). Quercia's classification was also carried out on assemblage from the south of Tas-Silġ and, therefore, might present the same limitations as the assemblages sampled in this work (Quercia 2002: 407). Most of Quercia's dating for these forms relies on comparative material. The work of Sagona (2002), and Anastasi (2019) were also used to assess dates.

4.1.2 The Żejtun Villa

Bechtold (2017) studied and published the pottery from SUs ZTN06/549 and ZTN06/2107; most of the diagnostic sherds had been described and drawn. Some physical documentation was available, such as primary pottery recording sheets for Bechtold's publication. A few diagnostic sherds had not been published in 2017 and were recorded (for example, samples 59, 67). All diagnostic sherds were then described macroscopically (Appendix B.2), complementing the record by Bechtold (2017). These first observations included 17 diagnostic sherds for ZTN06/2107 and 22 for ZTN06/549. The sherds were then attributed macroscopically to a fabric group from the classification of Anastasi (2019). When variations occurred, such as in Anastasi fabric 1, they were sub-grouped according to their similarities and differences. These macroscopic variants are summarised in Section 5.1.1.

From these macroscopic groups, 12 sherds were selected for further analysis including the main macroscopic variants in Fabric 1/Crisp Ware for plate and bowl forms; all diagnostic sherds for Fabric 4 (only two). There were no diagnostic sherds of Anastasi Fabric 5 apart from an entire lid which was not sampled.

4.1.3 Tas-Silġ

SU 352

Five of the seven bags of SU TSG96/352 had been quantified and separated into wares in a preliminary unpublished report for UoM (Sagona 2005). For this dissertation, more than 650 non-diagnostic sherds were recounted but not kept for analysis (see appendix B.3).

Most of the remaining sherds had been recorded as Crisp Ware by Sagona (2005) with some Bricky Red Ware also observed. Plate, bowl and casserole forms dated to the Late Punic-Late Republican period were kept to avoid residual material (using Quercia 2002 and Quercia 2011). More than 200 sherds fitted this requirement and seemed large enough for analysis (by visual inspection). For these, quick observations were recorded on their typology and fabric (Appendix B.2).

Based on fresh breaks, they were then attributed to the macroscopic groups used for Żejtun (see section 5.1.1). As large groups of sherds remained for each macroscopic variation, the final sherds had to be picked randomly for further analysis. Figure 4.1 summarises this process.

SU 2051

The diagnostic sherds of TSG96/2051 had not been classified previously in Sagona (2005). A few sherds had been published in Sagona (2015b) but were not available to analyse. A similar but quicker approach was taken for this assemblage where sherds were described as groups (Appendix B.2). Sherds representing the different variants of Anastasi Fabric 1 and Fabric 5 were then sampled randomly. No fine sherds with no visible inclusions similar to fabric 4 were noted.

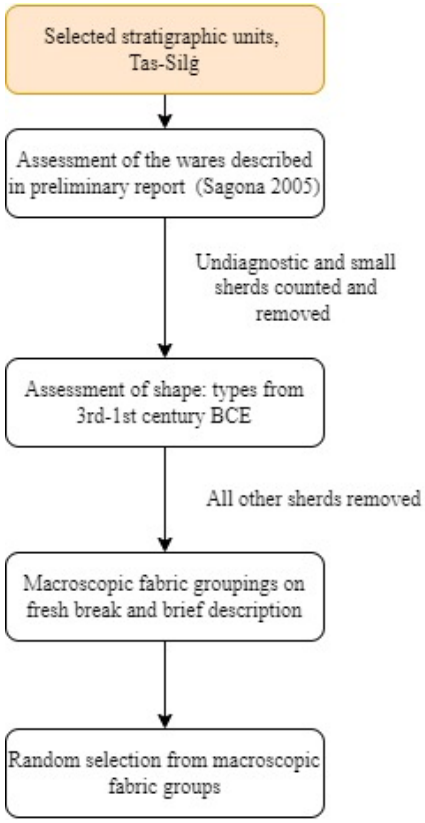


Figure 4.1: Flowchart of sampling procedure for the TSG96/352 Tas-Silġ assemblage

Limitations

SU TSG96/352 was highly fragmented, including sherds less than 1.5 mm; more than 50% of sherds were non-classified. Therefore, the fabric breakdown given in section 5.1.2 does not represent the accurate proportions. The macroscopic counts did not consider the joining of sherds, as determining the minimum number of vessels was not possible in the time frame. These counts also had to disregard sherds extracted from the assemblage before this dissertation which had not been attributed a special find number. For example, sample 70 (SU TSG06/2051) in this dissertation was located separately from the remainder with no special find number.

This dissertation aimed to assess the variations in the fabric classes in specific assemblages, focusing on the most prevalent Anastasi Fabrics 1, 4 and 5. The final sample list did not aim and could not be quantitatively representative of the fabric variations across the site at one specific period. Indeed, this would assume the existence of a prior detailed fabric classification for the site, but Sagona

(2015b) grouped most of the sherds of this period as Crisp Ware. For now, it is impossible to estimate that the fabric variations observed in the two assemblages would represent the fabric groups and variants from during this period at the sites. However, further research could build on this work to assess if these fabric variations are 1) representative of the archaeological sites under study; 2) representative of the region under study, 3) representative of the period under study; 4) found across the other forms not studied in this dissertation.

4.2 Macroscopic recording and catalogue

4.2.1 Description

The 70 sherds were attributed a sample number for this study (Samples 1-70). They were individually recorded in a spreadsheet and catalogue (Appendices A and B.1) to allow future examinations of the macroscopic features of the sherds after their partial destruction.

The data was recorded following guidelines from Orton and Hughes (2013) and other recording guidelines such as the one edited by The British Museum (2019). The information recorded is summarised in Table 4.1 and the spreadsheet in Appendix B.1.

The colour of surfaces and core/margins were recorded using a Munsell Soil Colour Chart. This information, although not necessarily indicative of differences in fabric composition (Whitbread 2016: 203), can be used to understand firing conditions (Orton and Hughes 2013: 155-157). The chart allows a standard way of describing colour and provides repeatability (Whitbread 2016: 203). "Cores" and "Margins" are described by Orton and Hughes (2013: 73) and are seen in sections in a fresh break. Cases of double-core (Orton and Hughes 2013: 154) were recorded as external margins and internal margins as in figure 4.2. The phenomenon of "Inner margins" and "Outer margins" (Orton and Hughes 2013: 73) was only observed for a few samples, for example, sample 11.

Information	References
Sherd SF number	SF list
Sample number	Randomly assigned
Number of fragments	if re-fitting possible
Sherd type	Rim/Base/Profile
Vessel form and Comparative material	Quercia (2011), Sagona (2015b), Anastasi (2019)
Diameter	Read on rim chart when possible
Production technique	From macroscopic observations and further analysis
Height, thickness and weight	
Internal surface colour	Munsell Color (2012)
External surface colour	
Internal margin colour	
External margin colour	
Core colour	
Preliminary fabric group	Anastasi (2019) classification
Surface treatment comments	Macroscopic observations and Roux (2019)
Use marks comments	As per macroscopic observations
Previous attributed group and macroscopic attribution	
Other notes	

Table 4.1: Table presenting the information recorded in the catalogue for every sherd

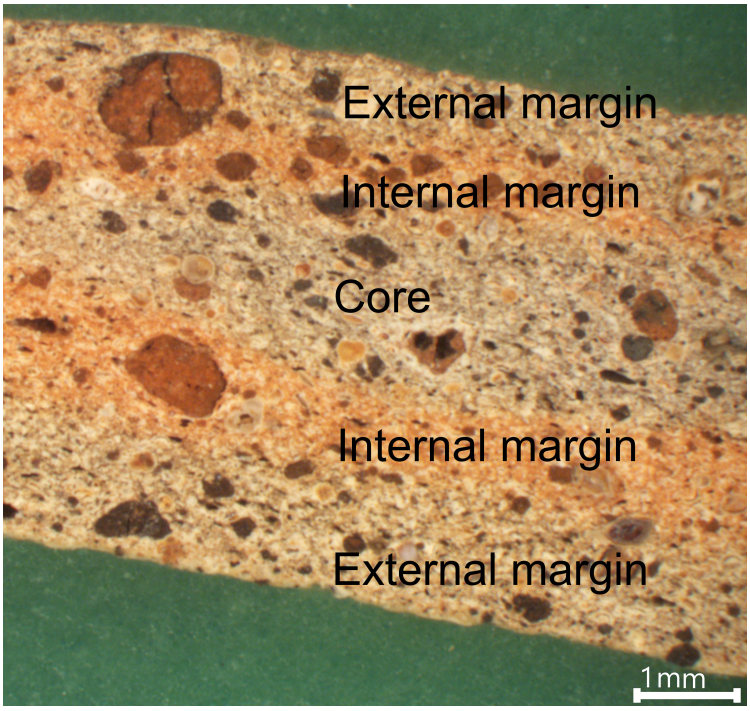


Figure 4.2: Photograph of ground sherd presenting the terminology described for the section colour when a double core was noticed

4.2.2 Photographic and drawn record

The sherds that had not been illustrated were drawn following Collett (2012) and Shirvalkar (2016). These included several sherds from the Żejtun villa (Samples 58, 59, 67) and the 58 sherds from the Tas-Silġ sanctuary (Appendix A).

All sherds were photographed using a photography stand and black background with a colour scale and a label. The white balance and colours of the photographs were then corrected using a python algorithm written by Lucas (2021).[1] Using one image previously corrected as a control, the algorithm can perform an image-to-image correction on a consecutive set of photographs (Lucas 2021: 11). The corrected photographs of both surfaces of the sherds were then combined on a digital black background using the software GIMP, ensuring that the scaling was correct (Figure 4.3). This enabled one unique image to be

[1]Iris Lucas was a student from the "Ecole Nationale des Science Géographiques" (ENSG) working toward a geoinformatics engineer degree. She was doing an internship at the Department of Classics and Archaeology, University of Malta. One aim of her internship was to find a way to batch correct the colours of photos from fieldwork taken for 3D models or orthophotomosaic. The python algorithm was then tested on artefacts photographed with similar lighting conditions.

presented in the catalogue.

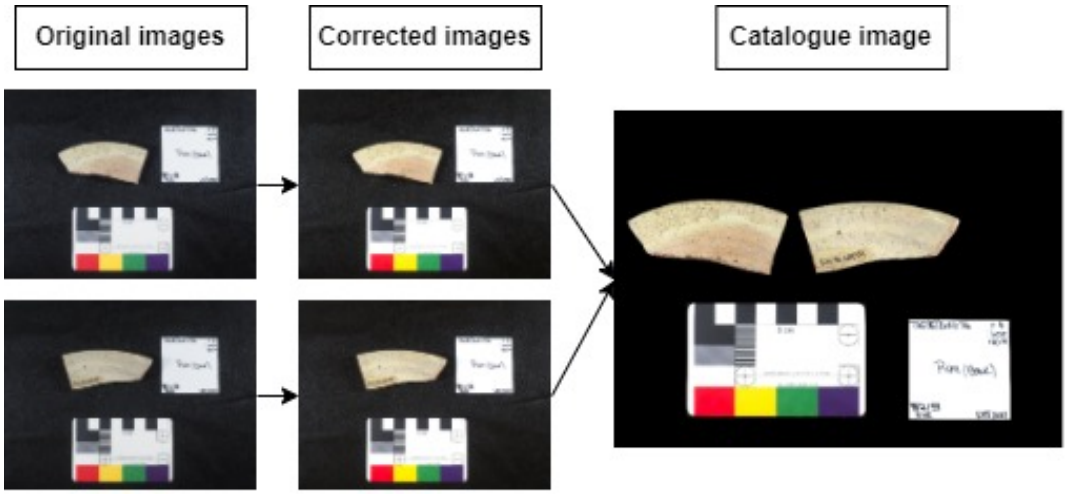


Figure 4.3: Diagram illustrating the process to correct and assemble images for the catalogue

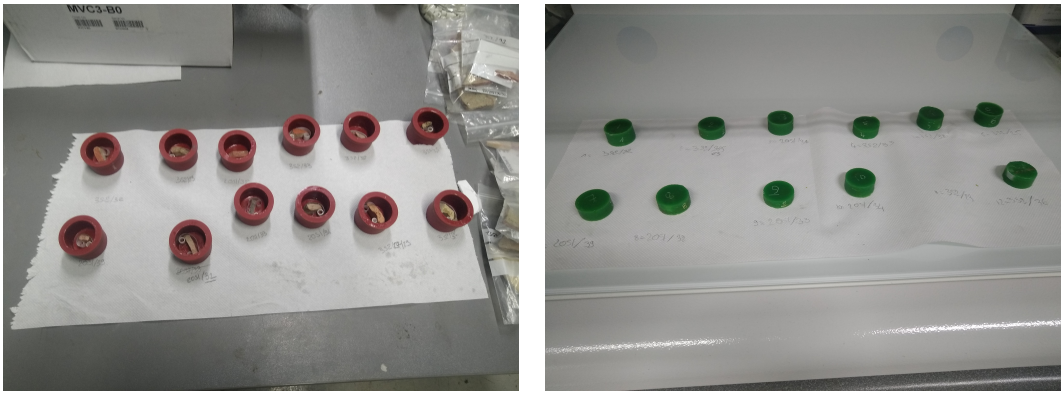
4.3 Microscopic analysis

4.3.1 Sample preparation

The sherds were embedded and ground flat for microphotography. Grounding a surface flat allows focusing on characteristics at higher magnification, such as inclusions, measuring and taking focused photographs. It also creates a permanent reference fabric collection.

A fragment of every sherd was taken using carpenter pliers. A small sample is enough; this technique is minimally destructive and fast for a large sample number. However, using the pliers, sherds with off-sets (for example, samples 54 or 61) cannot be sectioned easily perpendicular to their rim, which can have consequences on the interpretation of voids (Eramo 2020: 10).

The sherds fragments were then cold mounted in 3cm diameter moulds using either an Acrylic powder/liquid system or a 3-part powder/liquid system, according to availability. The embedding process is illustrated in Figure 4.4. This reinforced the specimens enabling processing with an automatic grinder (Struers Tegramin 25)



(a) (b)

Figure 4.4: Photographs of the mounting procedure. Sherds are placed in silicon moulds (a). The resin mix is then prepared and poured into the moulds under a fume hood. When the resin has hardened, the resin mounts can be unmolded (b) and engraved in the back with the unique sample number.

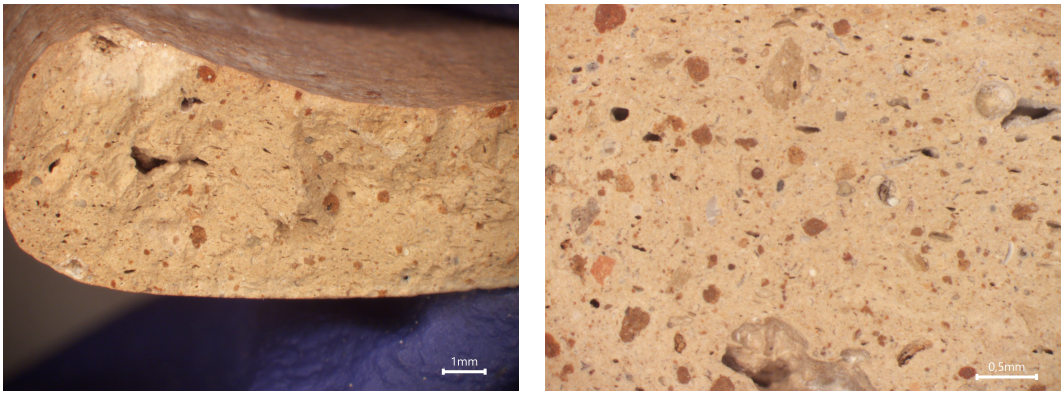
used with silicon carbide disks of grit sizes 240 (or 180), 400, 800, 1200, and 2500. Three samples were not embedded, as they had been previously ground, and there might not have been enough material for subsequent analysis.

4.3.2 Sample description and classification

The stereo-microscope used to examine the samples was a trinocular microscope (Meiji Techno RZ) mounted with a camera (Swift Cam 1803; and associated software Swift Imaging 3.0). Microphotographs were recorded at magnifications X10, X30 and higher if required to capture details of inclusions. Microphotographs from the ground resin mounts are presented in Appendix A, and fresh breaks were photographed to capture the sherd's texture (Figure 4.5).

Microscopic analysis using a stereo-microscope enables further classifying the samples, refining and/or challenging macroscopic observations. It allows the documentation and illustration of fabric classes, ensuring repeatability. The two eyepieces provide a 3D view of the samples, which helps describe voids. The stereo-microscope can enable the analysis of numerous samples before creating thin sections.

Microscopic fabric groups were created visually (similarities and differences) and



(a) (b)

Figure 4.5: Difference between the microphotographs of an unground surface and a ground surface from a resin mount (sample 65). The unground sherd microphotographs are helpful to see texture but can hinder focusing the camera on inclusions or increasing magnification.

reinforced with descriptions of individual samples based on inclusions (size and colour; available in appendix C.1). Quinn (2013: 73) argues that image recognition by the brain allows for assessing similarities and differences in visual features. Every group was given a fabric label to avoid confusion with existing classifications (Groups A to F; presented in section 5.3). Some sub-groups (e.g. D1-D3) are suggested in each section based on less significant visual differences (e.g. differences in firing conditions). These were the microscopic groups and sub-groups used to choose representative samples for assessment with other means of characterisation (PLM and XRF).

Samples and groups were described using an adapted system from Quinn (2013), designed for petrography and comparison charts (Figure 4.7). As microscopy does not allow mineral characterisation, the descriptions were limited to visual aspects. This included information about matrix, voids and inclusions (see Figure 4.6). Data included the matrix's homogeneity and colour which does not refer to the Munsell Colour chart due to the impossibility of assigning colour values to microscopic samples because of the differences in lighting.

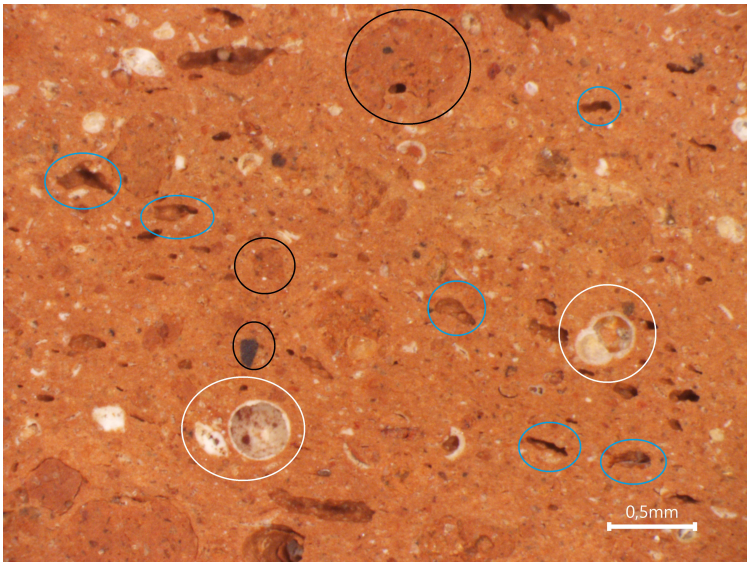


Figure 4.6: Photograph illustrating the different components described in the fabric descriptions. Black circles are examples of inclusions, and white: Foraminifera; Blue: voids. The matrix is the material surrounding all these components.

For inclusions, frequency terms are only indicative from the photos taken as no quantitative analysis had been performed. Inclusions sizes are reported from the Wentworth scale (Cuomo Di Caprio 2017a: 45) and Orton and Hughes (2013: 281) as pictured in Figure 4.7d. Visual descriptions of inclusions, including:

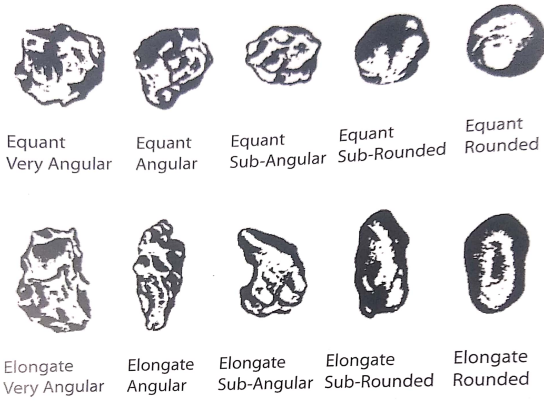
- Colour;
- Maximum size (measured thanks to Swift Imaging or ImageJ);
- Shape, described according to Quinn (2013: 84);

Predominant voids were described with the following criteria:

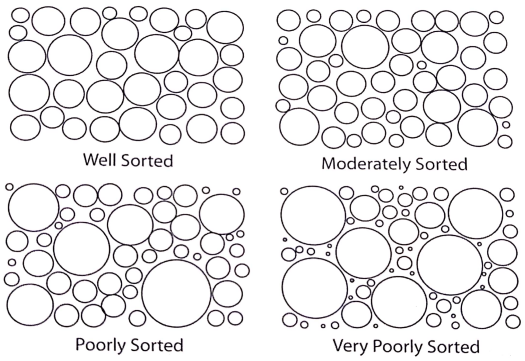
- Shape and size category, described according to Quinn (2013: 98) and measured thanks to Swift Imaging or ImageJ software;
- Presence or not of residue within the voids.

The identification of *Foraminifera* is tentative, and as argued by Wilkinson et al. (2016: 271), it is challenging to recognise *Foraminifera* in section and nearly impossible at the species level. The proposed identifications of *Foraminifera* were performed using a preliminary report on the MaltaPot project written by Dr Nicoletta Mancin (University of Pavia) on the identifiable *Foraminifera* in the

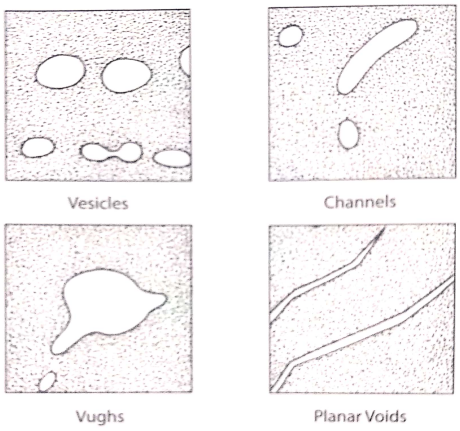
Maltese Neolithic sherds. This report is not available in print.



(a) Illustrated terminology to describe roundness, from Quinn (2013: 84)



(b) Illustrated terminology to describe inclusion sorting, from Quinn (2013: 87)



(c) Illustrated terminology to describe void shape, from Quinn (2013: 98)

very fine:	up to 0.1mm.
fine	0.1 to 0.25mm.
medium:	0.25 to 0.5mm.
coarse:	0.5 to 1mm.
very coarse	larger than 1mm.

(d) Grain-size by Orton and Hughes (2013)

Figure 4.7: Illustration of the terminology to describe inclusions and voids in fabric analysis

4.4 Petrographic recording and classification

4.4.1 Rationale and sample selection

PLM is a mineralogical technique and can be used to verify hypotheses explored with the stereomicroscope and typological analysis (Shortland and Degryse 2020: 340):

- Matrix and inclusion identification
- Fabric groups as hypothesized in section 5.3
- Production processes such as
  - Tempering
  - Forming techniques
  - Firing temperature as visible in the fabric
- Provenance

Based on the first group A-F and observations described in section 5.3, a first batch of samples were processed for thin sectioning (section 4.4.2). The samples selected for thin sections included: sherds from every group observed with the stereo-microscope (A-F) and the inscribed sherds (see sections 5.2.2 and 5.4 for the entire sample list). After the first analysis, another batch of samples was sent to clarify specific research questions or expand the typology of vessels looked at (section 5.4). In total, 34 samples were examined with PLM. Figure 4.8 illustrates the sampling and sequence of events from sampling to PLM analysis.

4.4.2 Sample preparation

Fragments of the samples were cut using either a carpenter's pincer, a hack saw for larger sherds, or cutting automatic machines (Minitom Struers and Accutom Struers) used with water. The cutting machines allowed longer and, therefore, more representative portions of sherds to be sectioned, as seen in Figure 4.9a. Samples were cut as close to a perpendicular section to the rim. This allows a comparison

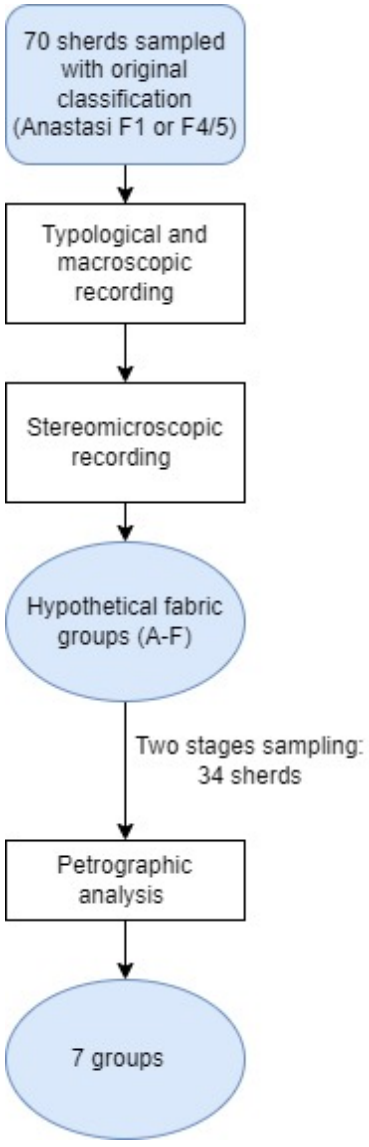
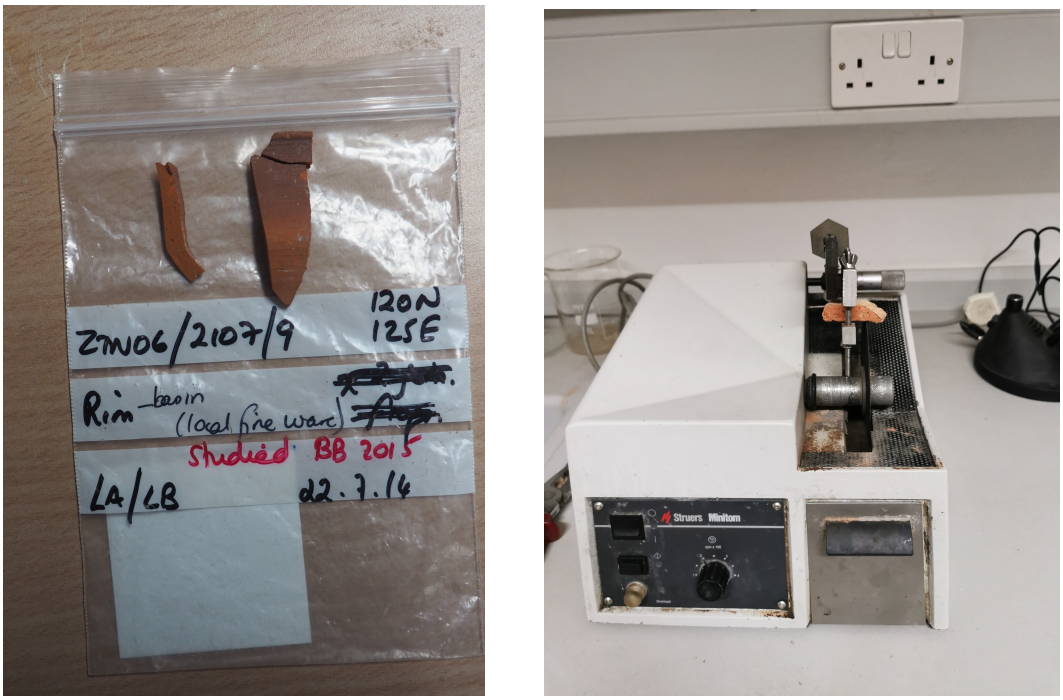


Figure 4.8: Flowchart of procedure including the microscopic analysis and the PLM analysis. Blue indicates the stages where different groups were created: macroscopic, microscopic and petrographic.

of orientations of inclusions and voids for forming technique (Thér 2020).



(a) (b)

Figure 4.9: Photographs from sample preparations: slicing the pottery sherds to send for thin sections. (a): Example of a sample 68 cut for thin sectioning; (b): Photograph of the minitom and the cutting disk with fitted pottery. The photographs were taken by Alexandra Humann.

The samples were then sent to the laboratory named *Servizi per la geologia* led by Massimo Sbrana, Italy, for the remainder of the sample preparation. Dr Claudio Capelli then performed the PLM analysis. The raw results from Capelli are in appendix C.2. Capelli created a classification based on the presence of specific inclusions (e.g. iron-rich nodules; fine quartz), their frequency and the characteristics of the groundmass. The firing temperatures and the matrix colour were so diverse that they were not taken into consideration to separate the samples into groups. Capelli was given no prior information about the typology, the macroscopic or microscopic classifications, or the sites. The groups he created were then discussed as a team, taking into consideration the knowledge of typology and the entire sample list. These groups are presented in section 5.3 and compared with the groups from the stereo-microscopy.

The data discussed with Capelli included evidence for manufacture techniques

(e.g. wheel throwing) assessing void and inclusion orientation (Eramo 2020); mineral characterisation, matrix iron/calcium ratio, surface treatment and traces of secondary deposition such as secondary calcite formation. The firing temperature was estimated by Capelli, looking at several factors. First of all, the dissociation of carbonates happens at around 850°C, although many factors might affect the dissociation rate. Therefore, carbonate inclusions, including microremains, are looked at to see any sign of dissociation. Dissociation was already noted during the microscopic assessment (appendix C.1). Secondly, the matrix is assessed for optical activity as the matrix would vitrify above 850°C (Montana 2020).

Chapter 5

Results and preliminary interpretation

Before analysing the 70 pottery sampled sherds, this chapter first describes the complete assemblages. Then, the typology and visible characteristics (e.g. surface treatment) of the 70 samples are described. The microscopic observations are combined with the petrographic analysis performed by Dr Capelli, and a fabric classification is given.

5.1 Full assemblages description

This section looks at the data produced on all the sherds of the stratigraphic assemblages before sampling. It comprises the broad visual observations/groupings made before sampling the 70 sherds and their prevalence (see section 4.1). More information can be found in Appendices B.2 and B.3.

5.1.1 Macroscopic groups

The main macroscopic groups which were sampled, looking at inclusions types and matrix colour in fresh breaks, are as follows:

- Anastasi Fabric 1/ Crisp Ware with black/brown inclusions;
  - The sherds have a great diversity in matrix colour (between and within sherds), with many having core and margins differing;
  - The primarily visible inclusions are sub-rounded brown or black;
  - Some sherds have a friable matrix;
  - One example of this group is sample 26 in Figure 5.1;
- Anastasi Fabric 1/Crisp Ware with red or orange inclusions, some white inclusions visible;
  - The sherds have an orange matrix, homogeneous throughout the section primarily;
  - It likely overlaps with the previous one, but firing conditions might be different;
  - The inclusions are hard to observe because they have the same colour as the matrix. The main inclusions are sub-rounded orange to red.
  - One example is sample 60 in Figure 5.1;
- Anastasi Fabric 1/Crisp Ware with white to greyish matrix only;
  - This group is characterized by a white and generally friable matrix;
  - Inclusions are barely visible to the naked eye, or rare sub-rounded black inclusions are visible;
  - One example is sample 67 in Figure 5.1;
- Anastasi Fabric 1/Crisp Ware with white inclusions only;
  - This group has coarse or fine predominant white inclusions throughout their sections;
  - matrix is red or orange, sometimes with a grey reduced core;
  - These sherds have the typical characteristics of the description of Crisp Ware and Anastasi Fabric 1.
  - One example is sample 64 in Figure 5.1;



Figure 5.1: Photographs of the four macroscopic Anastasi Fabric 1/ Crisp Ware variants identified, order following the text. Left to right: samples 26; 60; 67; 64. The variants were created for sampling during this study. Not to scale. Samples 67 and 64 were photographed after sampling to illustrate the chapter. For the scale of the object and full object see Figures A.51, A.119, A.133, A.127

- Anastasi Fabric 4 or Sagona Late Bricky Red Ware;
  - Fine fabric with no visible inclusions apart from rare black rounded inclusions;
  - These samples were rarely observed;
  - The matrix is red to brown;
  - One example is sample 68 in Figure 5.2.;
- Anastasi Fabric 5 or Sagona Red Bricky Ware;
  - This group has a red to a brownish matrix, red surfaces;
  - Inclusions are coarse white inclusions, often angular;
  - One example is sample 18 in Figure 5.2;



Figure 5.2: Photographs illustrating Anastasi Fabric 4 (left, sample 68) and Fabric 5 (right, sample 18). For fabric 4, no inclusions are visible in the fresh break (arrow). Not to scale, for scaled images and complete objects, see Figures A.135 and A.35.

5.1.2 Assemblages fabric overview

This section overviews the number of sherds observed for each broad macroscopic class within the assemblages to enable future research to consider each visible variation's representation and re-set the samples within their context after analysis.

Tas-Silġ sanctuary assemblages

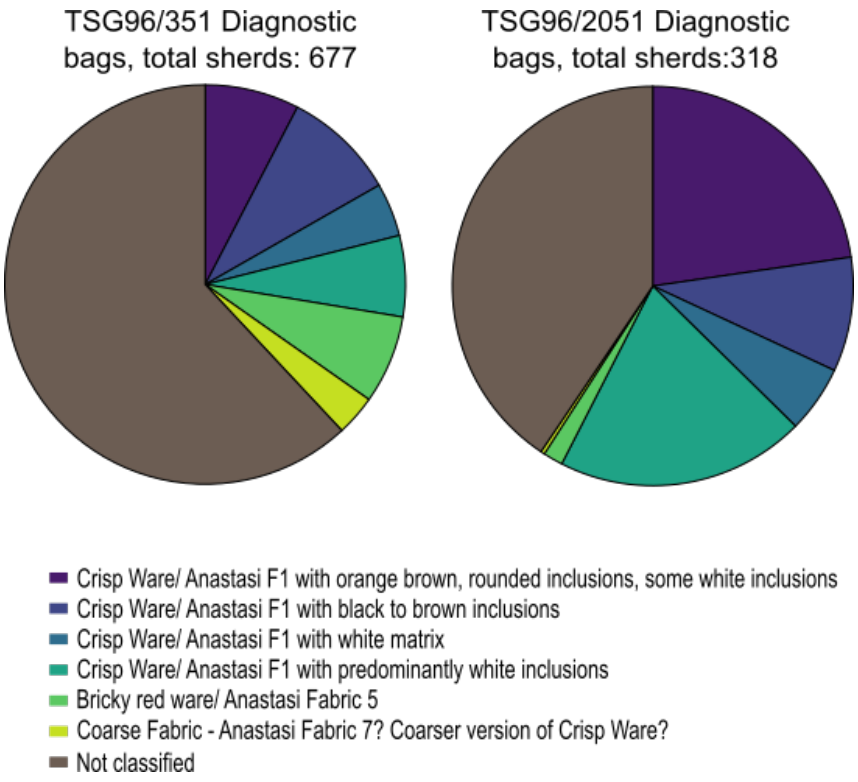
The assemblage from TSG96/352 consisted of 1505 sherds, including 677 diagnostic sherds; TSG96/2051 consisted of 703 sherds, including 318 diagnostic sherds (see appendix B.3). Figure 5.3a provides the breakdown of diagnostic sherds for each of the broad macroscopic classes described in section 5.1.1. Many of these sherds were highly fragmented and could not be classified. This is represented by the brown part of the pie chart. To clarify the breakdown of the sherds which could be classified and improve readability, figure 5.3b gives the breakdown of the classified sherds only.

The class of Anastasi F1 with white inclusions represents a higher proportion of sherds in TSG96/2051 than 352. This gap might be a chronological difference or a sampling bias. The lack of fine sherds is apparent.

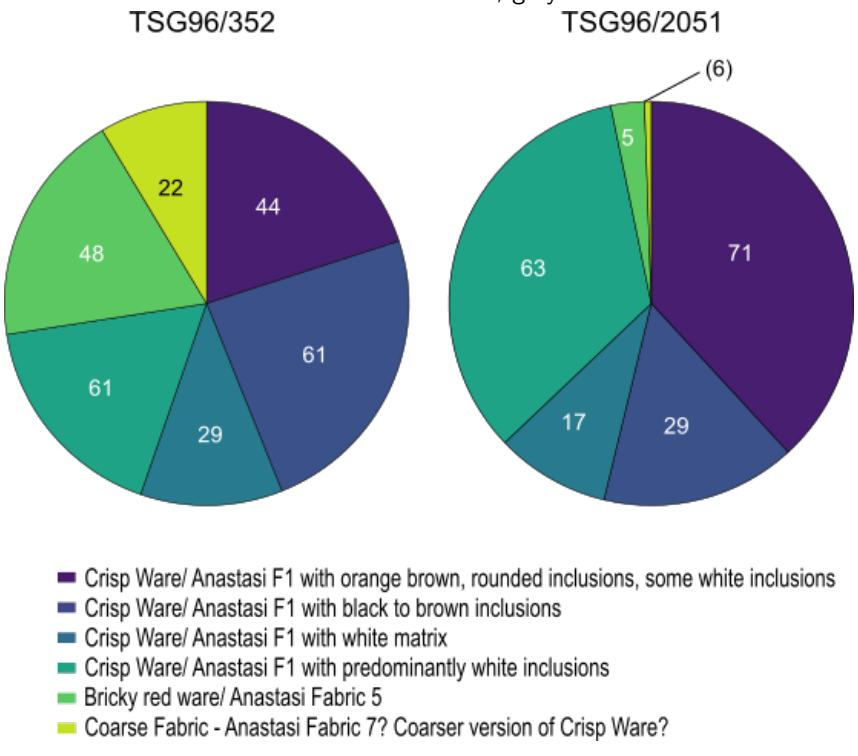
Żejtun villa assemblages

The assemblage from ZTN06/549 consisted of 88 sherds, including 21 diagnostic sherds; ZTN06/2107 consisted of 61 sherds, including 18 diagnostic sherds (see appendix B.3).

Both assemblages were combined in a graph considering the low number of diagnostic sherds. The fine ware category described by Bechtold (2017: 124) was composed of five sherds. Several profiles of coarse hand-made fabric (Anastasi Fabric 7) were found but not sampled. The boundary between Anastasi fabrics 4 and 5 is not fully established and was, therefore, not always apparent when looking at the assemblages.



(a) Pie-charts representing each broad class in Tas-Silġ units including the unclassified sherds, gray.



(b)

Figure 5.3: Representation of each broad class in Tas-Silġ stratigraphic units excluding the unclassified sherds. Summarised data in tables B.2 and B.4

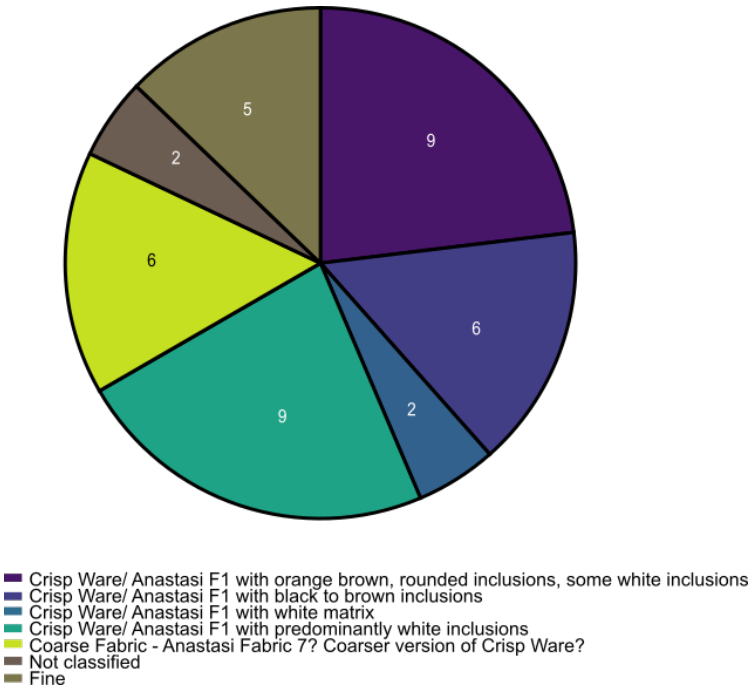


Figure 5.4: Żejtun villa, diagnostic sherds for SU ZTN06/549 and SU ZTN06/2107. Summarised data in Table B.7.

Table 5.1 summarises which categories the 70 samples classify into.

S	Macroscopic group for sampling	Type	SF number
1	F1/C.W orange-brown rounded incl., white incl.	Bowl	TSG96/352/32
2	F1/C.W black to brown incl.	Plate	TSG96/352/23
3	F1/C.W orange-brown rounded incl., white incl.	Plate	TSG96/2051/38
4	F1/C.W orange-brown rounded incl., white incl.	Bowl	TSG96/352/33
5	F5/BRW	Tegame	TSG96/352/38
6	F1/C.W white matrix	Bowl (M)	TSG96/352/25
7	F1/C.W predominantly white incl.	Bowl	TSG96/2051/39
8	F1/C.W black to brown incl.	Bowl	TSG96/2051/32
9	F1/C.W black to brown incl.	Bowl	TSG96/2051/33
10	F1/C.W orange-brown rounded incl., white incl.	Bowl	TSG96/2051/34
11	F1/C.W black to brown incl.	Bowl	TSG96/352/29;27
12	F1/C.W white matrix	Plate	TSG96/352/36
13	F5/BRW	Olla	TSG96/2051/50
14	F1/C.W orange-brown rounded incl., white incl.	Bowl	TSG96/2051/40
15	F1/C.W predominantly white incl.	Bowl	TSG96/2051/51
16	F1/C.W predominantly white incl.	Bowl	TSG96/352/48
17	F1/C.W black to brown incl.	Bowl	TSG96/352/28
18	F5/BRW	Olla	TSG96/352/50
19	F1/C.W orange-brown rounded incl., white incl.	Plate	TSG96/2051/37
20	F1/C.W predominantly white incl.	Bowl	TSG96/2051/53
21	F1/C.W black to brown incl.	Plate	TSG96/352/24

S	Macroscopic group for sampling	Type	SF number
22	F1/C.W orange-brown rounded incl., white incl.	Plate	TSG96/352/34
23	F1/C.W white matrix	Bowl	TSG96/2051/45
24	F1/C.W white matrix	Bowl	TSG96/2051/52
25	F1/C.W white matrix	Bowl	TSG96/352/20
26	F1/C.W black to brown incl.	Plate	TSG96/352/31
27	F1/C.W white matrix (yellow)	Plate	TSG96/2051/42
28	F1/C.W predominantly white incl.	Bowl	TSG96/352/47
29	F1/C.W black to brown incl.	Bowl	TSG96/352/14
30	F1/C.W predominantly white incl.	Plate	TSG96/2051/54
31	F1/C.W predominantly white incl.	Bowl	TSG96/352/49
32	F5/BRW	Olla	TSG96/2051/49
33	F5/BRW or F4?	Bowl	TSG96/2051/47
34	F5/BRW	Olla	TSG96/352/16
35	F5/BRW	Olla	TSG96/352/40
36	F5/BRW	Olla	TSG96/352/42
37	F1/C.W predominantly white incl.	Bowl	TSG96/2051/56
38	F1/C.W black to brown incl.	Bowl (M)	TSG96/352/22
39	F5/BRW	Olla	TSG96/352/44
40	F1/C.W white matrix	Bowl	TSG96/2051/44
41	F1/C.W orange-brown rounded incl., white incl.	Bowl	TSG96/2051/41
42	F1/C.W orange-brown rounded incl., white incl.	Bowl	TSG96/352/35
43	F5/BRW or F4?	Olla	TSG96/352/45
44	F1/C.W white matrix	Bowl	TSG96/2051/46
45	F1/C.W white matrix	Plate (M)	TSG96/352/37
46	F5/BRW or F4?	Olla	TSG96/352/43
47	F1/C.W predominantly white incl.	Bowl	TSG96/2051/48
48	F1/C.W black to brown incl.	Plate	TSG96/352/26
49	F1/C.W black to brown incl.	Plate	TSG96/352/30
50	F1/C.W predominantly white incl.	Bowl	TSG96/352/46
51	F1/C.W black to brown incl.	Bowl	TSG96/352/21
52	F1/C.W white matrix	Bowl (M)	TSG96/2051/43
53	F5/BRW	Tegame	TSG96/352/41
54	F5/BRW	Olla	TSG96/352/39
55	F1/C.W black to brown incl.	Plate	TSG96/2051/35
56	F1/C.W predominantly white incl.	Bowl	TSG96/2051/36
57	F1/C.W predominantly white incl.	Bowl	TSG96/2051/55
58	F1/C.W black to brown incl.	Bowl	ZTN06/2107/18
59	F1/C.W black to brown incl.	Base	ZTN06/549/19
60	F1/C.W orange-brown rounded incl., white incl.	Bowl	ZTN06/549/4
61	F4/Late Red Bricky Ware	Casserole	ZTN06/549/13
62	F1/C.W predominantly white incl.	Bowl	ZTN06/549/16
63	F1/C.W black to brown incl.	Bowl	ZTN06/549/10
64	F1/ C.W predominantly white incl. (large)	Bowl	ZTN06/2107/6
65	F1/C.W orange-brown rounded incl., white incl.	Bowl	ZTN06/2107/7
66	F1/ C.W predominantly white incl. (large)	Plate	ZTN06/2107/4

S	Macroscopic group for sampling	Type	SF number
67	F1/C.W white matrix	Bowl	ZTN06/2107/17
68	F4/Late Red Bricky Ware	Bowl	ZTN06/2107/9
69	F1/C.W predominantly white incl.	Bowl?	ZTN06/549/6
70	F5/BRW or F4?	Olla	TSG96/2051/61

Table 5.1: List of samples selected and their macroscopic group. S: sample number; (M): miniature; CW: Crisp Ware; BRW: Bricky Red Ware. Highlighted sherds are inscribed.

5.2 Macroscopic observations for the 70 sherds

5.2.1 Typology of the samples

This section presents general observations of the 70 sherds selected for further analysis. Drawings, photographs and comparative material are presented in the pottery catalogue in Appendix A. A few drawings are presented in this section.[1] Table 5.2 summarises the comparative material.

S	Form	Type	S	Form	Type
1	Bowl	Anastasi D6	36	Olla	Anastasi C3.2
2	Plate	Anastasi D27.2	37	Bowl	Anastasi D6
3	Plate (Bowl?)	Anastasi D26.2	38	Bowl (M)	Sagona 1:61:14.
4	Bowl	Anastasi D6.2	39	Olla	Quercia B8?
5	Tegame	Quercia C3	40	Bowl	Sagona 1:68:4-5
6	Bowl (M)	Sagona 1:61:14,	41	Bowl	Anastasi D6.3
7	Bowl	Anastasi D6.6	42	Bowl	Anastasi D6.2
8	Bowl	Anastasi D8.2	43	Olla	Quercia B
9	Bowl	Sagona 1:66	44	Bowl	Anastasi D6
10	Bowl	Anastasi D6.5	45	Plate (M)	Sagona 1:65:13
11	Bowl	Anastasi D6	46	Olla	Quercia B3

[1] Considering the PLM analysis and the questions around the method of manufacture, these drawings would have to be amended not to give the impression that they are wheel-thrown.

S	Form	Type	S	Form	Type
12	Plate (Deep plate?)	Sagona 1:98:2-3	47	Bowl	Anastasi D6
13	Olla	Quercia A1	48	Plate	Anastasi D27
14	Bowl	Anastasi D6.4	49	Plate	Anastasi D27
15	Bowl	Anastasi D6.5	50	Bowl	Sagona 1:70:5-6.
16	Bowl	Anastasi D7	51	Bowl	Anastasi D6
17	Bowl	Sagona 1:71:1-2	52	Bowl (M)	Sagona 1:62:3,5,7
18	Olla	Quercia B1	53	Tegame	Quercia C
19	Plate	Anastasi D26	54	Olla	Quercia B2
20	Bowl	Sagona 1:68:4-5	55	Plate	Anastasi D27
21	Plate	Anastasi D26	56	Bowl	Sagona 1:70:6
22	Plate	Anastasi D27	57	Bowl	Anastasi D6
23	Bowl	Sagona 1:68:4-5	58	Bowl	Anastasi D6.6
24	Bowl	Sagona 1:66	59	Base	Bowl or plate eg. Quercia (2011) 2:5
25	Bowl	Anastasi D6.6	60	Bowl	Uncertain
26	Plate	Anastasi D26.2	61	Olla	Quercia B5
27	Plate	Anastasi D26.3-27.1	62	Bowl	Quercia (2011) 2.3
28	Bowl	Anastasi D6.6	63	Bowl	Quercia (2011) 2.7
29	Bowl	Sagona 1:67:2	64	Bowl	Anastasi D6
30	Plate	Anastasi D26	65	Bowl	Anastasi D8
31	Bowl	Anastasi D6.3	66	Plate	Quercia (2011) 1.6
32	Olla	Anastasi C3?	67	Bowl	Anastasi D6
33	Bowl	Sagona 1:65-1:66?	68	Bowl	Anastasi D11?
34	Olla	Quercia B2-3	69	Bowl (or Basin?)	Uncertain
35	Olla	Quercia B1	70	Olla	Anastasi C3

Table 5.2: Table of samples with their shape and typology. S: Sample number; Anastasi (2019) and Quercia (2002; 2011); Quercia refers to the 2002 classification except specified otherwise; (M): miniature vessel.

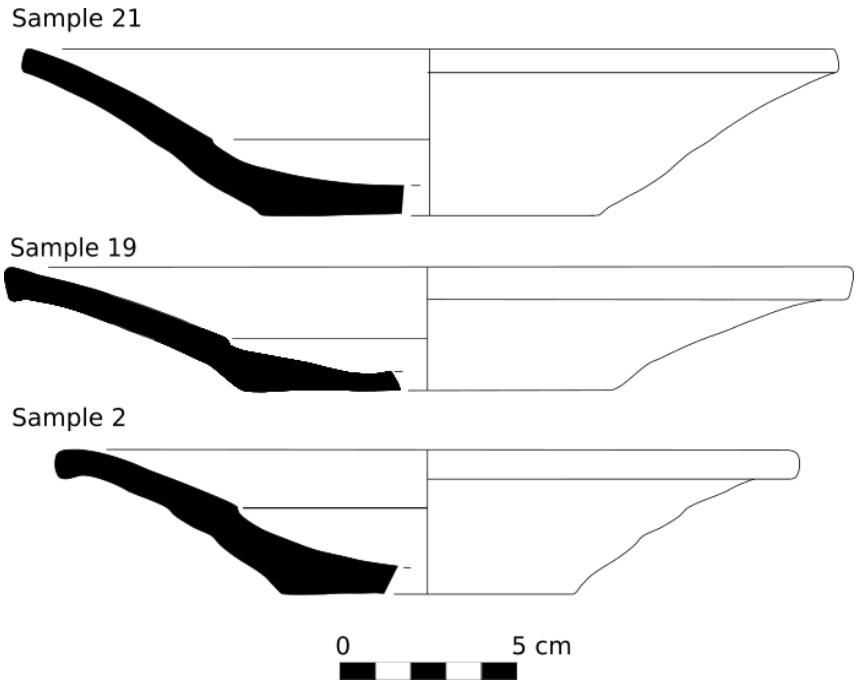


Figure 5.5: Examples of profiles of plates found in the assemblages, Samples 21, 19 and 2.

The plates are similar to Anastasi (2019) form D26 (see sample 21 in Figure 5.5), and some have the characteristics of later D27 (see sample 2 in Figure 5.5). Forms D26-D27 are typical of the Late Punic-Early Roman period at Tas-Silġ (Quercia 2011) and are standard at other sites in Malta (Anastasi 2019). The thicker and shallower plates were more common in the 3rd-2nd century BCE Quercia (2011: 437; type 1:4). Thinner and deeper plates with flaring rims (e.g. Sample 19) are introduced in the 2nd-1st century BCE century at the site of Tas-Silġ (Quercia 2011: 437).

The selected bowls are mainly Anastasi type D6 (Anastasi 2019), close to Quercia types 2.6-2.8 (Quercia 2011). According to both typologies, these bowls are common in the 3rd-1st century at Tas-Silġ and the Żejtun villa. Lip variations are common, more or less flaring. The walls of the body are sometimes ribbed. The depth and roundness of these bowls vary. Some bowl shapes are illustrated in Figure 5.6. Some samples have relatively straight walls and are closer in shape to D8, although, in Anastasi (2019: 106), this form was more associated with funerary assemblages.

Some bowls have only parallels illustrated in figures from 1:65-1:71 Sagona (2015b). For instance, sample 20 (Fig. A.39) has a rolled rim similar to figure 1:68:5. Other bowls are deep shapes with rounded everted rims and ribbed walls (e.g. 50 and 56: Figs. A.99 and A.111) close to Sagona (2015b) 1:70:6. These shapes are primarily found in contexts dated to Tas-Silġ Period IV. However, some are found in redeposited contexts (Area B) and might be residual.

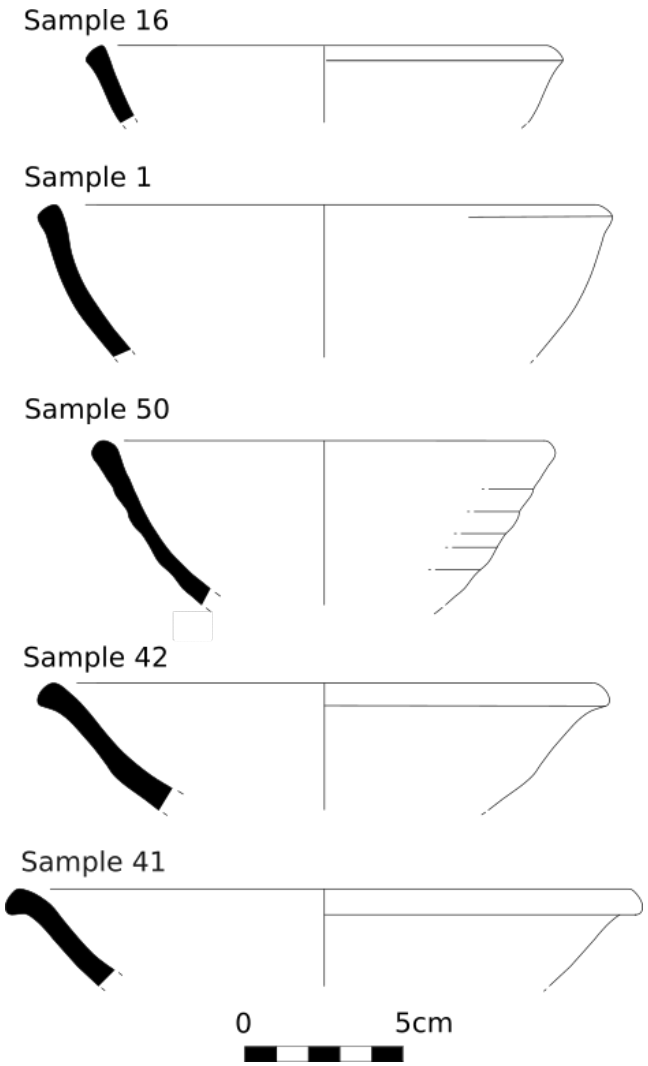


Figure 5.6: Examples of bowl shapes: : Samples 16, 1, 50, 42, 41

Miniature vessels have been broadly classified by Quercia (2011: 444); however, variations are not described. Parallels are found in illustrations of Sagona (2015b), such as 1:61:14 or 1:62 (bowl form) and 1:65:13 for the plate form (illustrated in Figure 5.7). These small miniature vessels have been interpreted as used for offerings in this temple context (Anastasi 2010: 102).

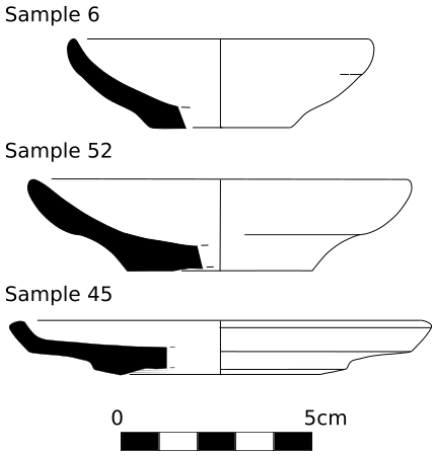


Figure 5.7: Examples of profiles of miniatures found in the assemblages, Samples 6, 52 and 45.

The last category of vessels is cooking vessels. All cooking vessels fit within the category *olla* of Anastasi (2019) and are close to forms A and B in Quercia (2011). A few are illustrated in Figure 5.8. In terms of comparative material, sample 13 (Fig. A.25) compares with Quercia (2011) A1, which has a flat rim and is typical during the 4th to the 2nd century BCE. Several samples are comparable to Quercia type B, with some variations observed. For example, sample 18 (Fig. A.35) compares with B1, with thicker walls and rounded rim, whilst some other vessels, such as sample 70 (Fig. A.139), have thinner walls and flatter tops. According to Anastasi (2019: 77-78), these thinner vessels are more common in later periods, although they are known in Late Punic/Early Roman contexts. The only fine olla (no visible inclusions with the naked eye), sample 61 (Fig. A.121), also has a flat top. All these cooking vessels, except sample 13, have a lid locator.

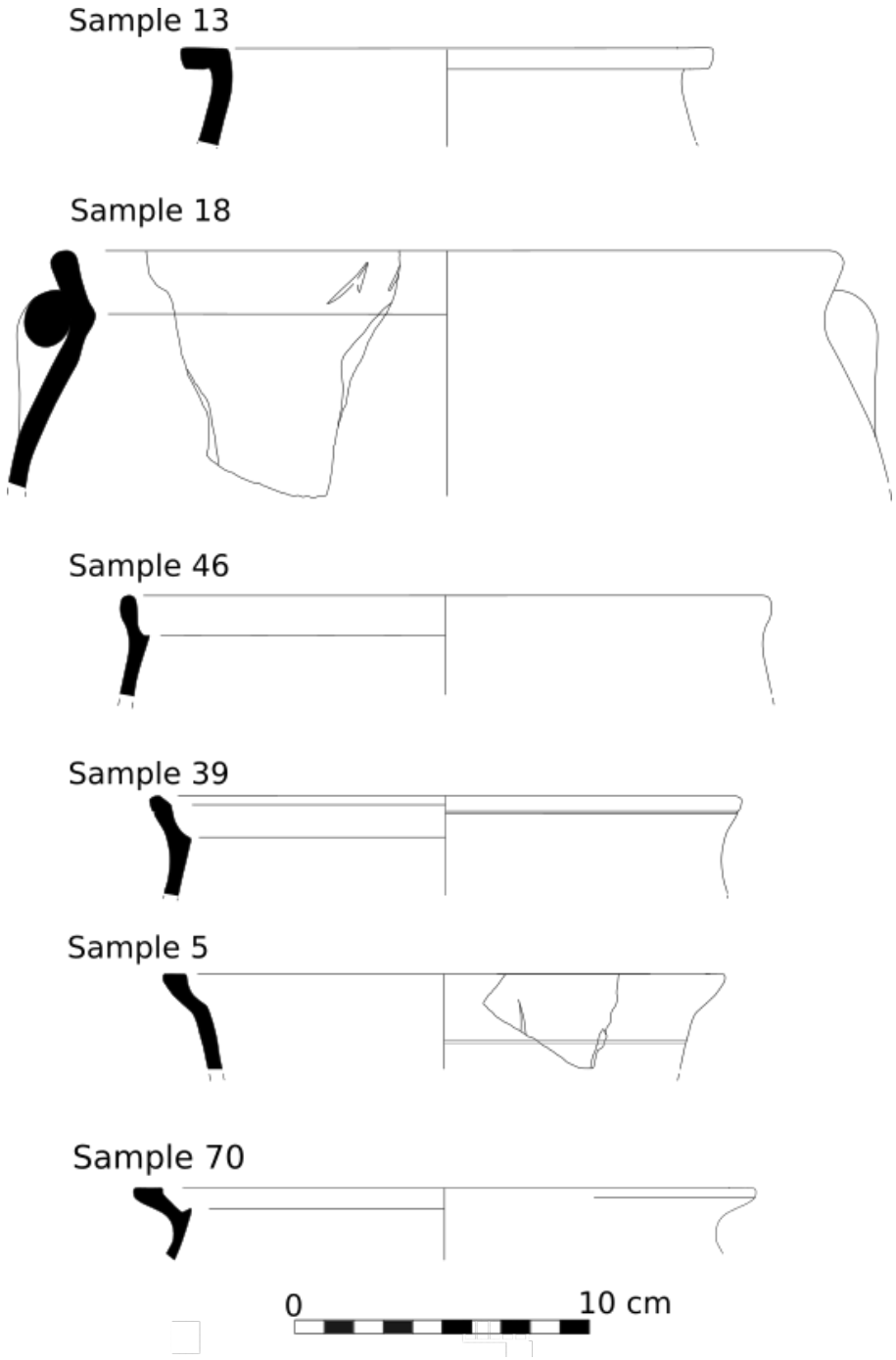


Figure 5.8: Examples of casserole and olla shapes, samples 13, 18, 46, 39, 5, 70

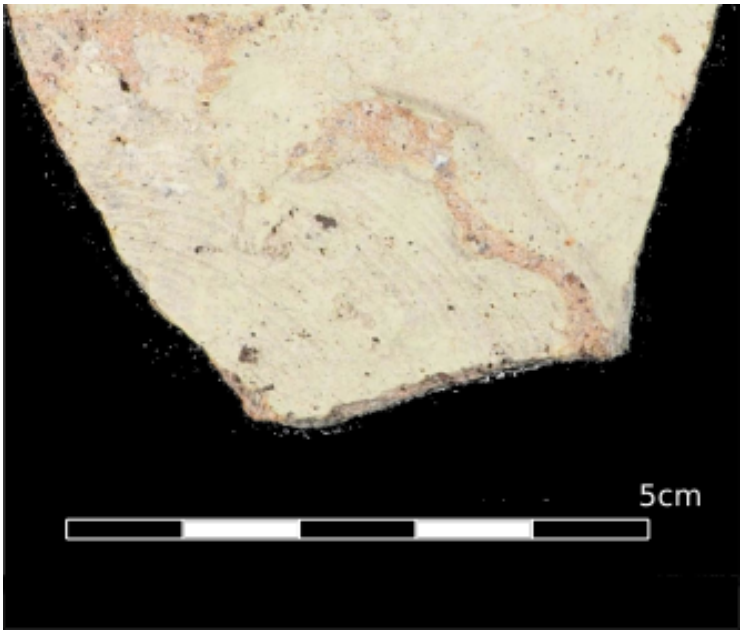
5.2.2 Colour, surface finish and forming methods

The surface finish marks and surface colours of individual samples are presented in the catalogue in appendix A.

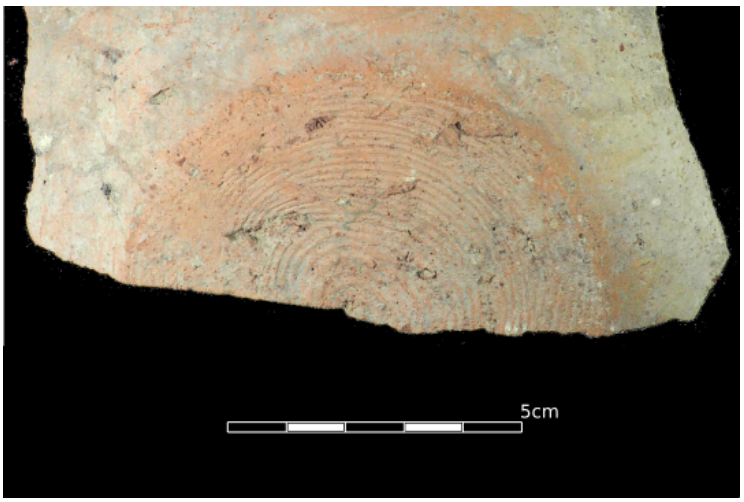
Plates, bowls and miniatures

Many vessels have visible striations on their surface, parallel or not, but mostly sub-parallel. These striations could have been caused by wiping/smoothing the vessel when it was still wet (Anastasi 2019: 35) and could be evidence of a quick surface finish.

Some of the bases are irregular, not smoothed (e.g. sample 2 - see Figure 5.9a, samples 19, 52) and have concentric striations (e.g. 19, 21 - see Figure 5.9b, samples 22, 38, 45). These can be the traces of using a string to remove a vessel whilst turning a device, such as a wheel. The use of the wheel is discussed in light of the petrographic results in section 9.1.2.



(a)



(b)

Figure 5.9: Close-up photographs of irregular vessel bases: sample 2 (for full images see Fig. A.3) where the base was not smoothed (a); sample 21 (for full images see Fig. A) where the base has string-marks (b)



(a) Sample 21



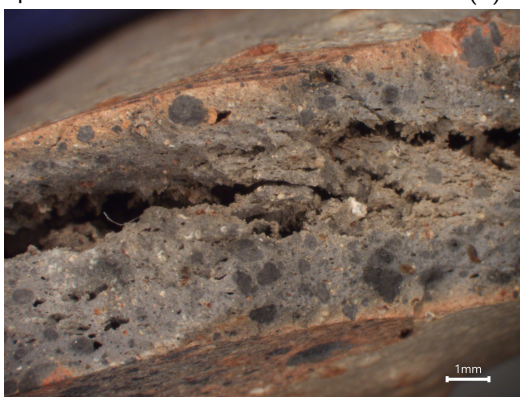
(b) Sample 31



(c) Sample 7



(d) Sample 9



(e) Sample 9

Figure 5.10: Photographs of sherds with surface treatments, irregular surface colours and firing defects. (a-b) Samples 21 and 31 have irregular surface colours; (c) Sample 7 has a homogenous white surface; (d-e) Sample 9: macroscale photograph and microphotograph of the air bubble.

Some samples, such as plate sample 2, have visible inclusions on the outer surface but not on the inner surface. Therefore, there was probably some effort to smooth the inner surface and visible part. The rims are often irregular. For example, sample 50 (Fig. A.99) is a bowl with an irregular rim (Fig. A.100).

Many samples have heterogeneous surface colours (e.g., samples 1, 4, 9-11, 21-22, and 31, among others). Sample 31 (Fig. A.61 and Fig. 5.10b) has two different colours on the outer surface, pale brown close to the rim (2.5Y 8/2) and predominantly light red (2.5YR 6/6) on the rest of the surface. Sample 21 (Fig. A and Fig. 5.10a) has mottled surfaces with pink (5YR 7/4) and light brown (7.5YR 6/3) hues.

Some sherds have homogeneous white surfaces, which were believed to be slipped at the start of the study, as mentioned in the literature (Sagona, 2015b: e.g. 51,

Quercia, 2011: 442). This is the case for sample 7 (Figs. 5.10c andA.13). The lack of homogeneity on most sherds, however, such as sample 31 (Fig. 5.10b, Fig. A.61), suggest that this colouring was not entirely intentional. These surfaces are revisited in light of the petrographic results are discussed in section 9.1.3.

Defects such as air bubbles were observed, with the most dramatic being sample 9 (Fig. A.57 and Fig. 5.10e). A defect does not necessarily mean that the vessel failed and was not used and could result from a lack of homogenisation of the paste (Cuomo Di Caprio 2017b: 108), or an inadequate firing regime. Sample 22 (Fig. A.43) has a prominent inclusion that broke the surface, possibly from lime spalling (rehydration of lime after firing). This could also be a secondary alteration. Some vessels had highly brittle fabrics, particularly in vessels with a white/yellow fabric such as samples 6 (Fig. A.11), 23 (Fig. A.45), 26 (Fig. A.51), 27 (Fig. A.53), 44 (Fig. A.87), 67 (Fig. A.133).

Vessel brittleness

Light-coloured vessels with white and yellow matrices (Munsell colours Pale brown or very pale brown) were, for most, easily breakable. Some brittle sherds could be broken off by hand pressure only. Nine vessels have a white-yellow to green fabric with no black inclusions (23, 24, 27, 40, 44, 45, 52 and 12), although sample 12 was not brittle. Other sherds, samples 6, 25 and 67, have a yellow-whitish fabric with dark inclusions. A few other pale sherds, such as sample 20, were similarly brittle. Among all these sherds, three are miniature vessels, and three have a similar typology (samples 20, 23, 40) with similar rims (rounded, slightly flaring) and relatively small diameters (12-13cm for the three). This brittleness could be caused by factors such as post-depositional processes or differences in raw materials.

Greenish/white clay matrix is broadly mentioned in the literature, including by Blagg et al. (1990). A similar matrix colour and texture is attributed to the fabric MALTA-A-5 described in Bechtold et al. (2020) for a Punic transport amphora. This fabric is described as soft and granular and assumed to be produced locally.

Cooking vessels

The surfaces of the cooking vessels could have been wet-smoothed, possibly wiped, as suggested by the sub-parallel and irregular marks on the outer surfaces (see parallels in Roux, 2019: 197). Some might have been finished using a rotary force (e.g. using a turntable) as parallel striations are visible on the surfaces of some of these vessels (e.g. Sample 39 in Fig. 5.11a). Others, such as sample 13, have fewer regular marks.

Many of the inner surfaces of the cooking vessels were smooth and slightly reflective (e.g. 18, 36, 43, 46, 54, 70), while the outer surfaces were not. These features could indicate burnishing (Roux 2019: 201). Sagona (2015b: 74) argues that these vessels are wheel-made, possibly based on the wall's parallel striations.

In terms of surface colour, this group is homogeneous except for sample 5 (Fig. A.9), which has darker surfaces (10YR 4/2 dark greyish brown). Most samples, however, have red or reddish brown surfaces (see, for example, Figs. A.35, A.91), sometimes with a darker outer surface (e.g. Sample 70 in figure A.139).

Sample 61 (Fig. 5.11b, Fig. A.121) and sample 34 have black deposition on the outer surface, which is probably soot due to use on fire (Rice 2015: 415). However, other hypotheses should be considered to explain this blackened surface. Bonifay (2004: 71), for instance, mentions the "*orlo annerito et patina cenerognola*" where cooking vessels in Tunisia were fired in direct contact with the flames with no chamber no protect them. This would cause part of the outer surface to be black.

Inscribed vessels

Samples 29 and 34 are inscribed vessels published by Frendo and Mizzi (2015: 598), whilst sample Sample 18 is unpublished (Figure **??**). Two inscriptions are on cooking vessel shapes, and one is a bowl. The published inscriptions were analysed as "LT" (sample 29) and [L']ST[RT] (sample 34) and were both inscribed on the vessel before firing. [L']ST[RT] was interpreted specifically as dedicatory to the



(a) Sample 39 (b) Sample 61

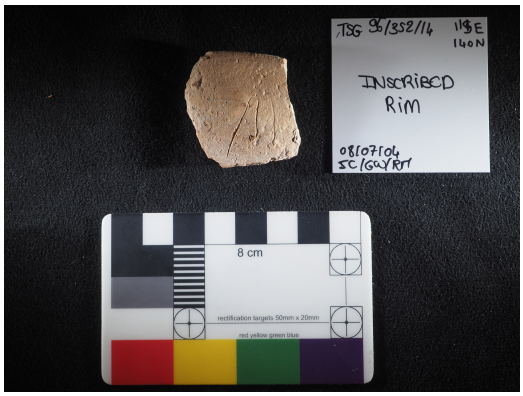
Figure 5.11: Photographs of cooking vessels; (a) shows parallel striations on the vessel surfaces on sample 39; (b) Sample 61 (fine olla) has an outer surface with soot (arrow)

goddess Astarte (Frendo and Mizzi 2015: 550). Sample 18 read as T, possibly followed by an L for "LT" (pers. comm. Prof. A Frendo 24th November 2021).

The *Missione* had interpreted this inscription as *To Astarte*, with T being an abbreviation of the name of the goddess and has reiterated this claim recently (De Bonis et al. 2019: 1631). This followed the argument made by Amadasi Guzzo (1993) from the *Missione*. These papers have not considered the transliteration work and comparative material brought forward by Frendo and Mizzi (2015), who argue that "LT" was interpreted by previous literature as a general dedicatory inscription understood as an abbreviation of *for the offering* (Frendo and Mizzi 2015: 546-547).



(a) Sample 34



(b) Sample 29



(c) Sample 18

Figure 5.12: Photographs of inscribed sherds; razing light; (a): cooking vessel with [L']ST[RT]; (b-c) bowl and cooking vessel with "LT"

5.3 Microscopy and petrography

This section presents the results of the microscopy (stereomicroscope; OM) and polarised light microscopy (PLM).

5.3.1 Groupings summary and section structure

The six groups (A-F) created using the stereomicroscope (section 4.3) are presented in tables 5.6, 5.11, and 5.17 for the three main groups identified, and a summary is available in table 6.1. The tables for each group, including descriptions of each sample (with measurements) are given in Appendix C.1. The main characteristics of these 6 groups (A-F) are summarised in table 5.3.

The analysis of the thin sections using polarised light microscopy of selected sub-samples by Capelli generated 7 groups (groups 1-7). The equivalences between the groups (macroscopic, OM and PLM) are summarised in table 5.5. The list of samples sent for petrographic analysis is presented in table 5.4, which also tabulates their microscopic group.

To avoid repetition, and since the different classifications had a good agreement, the following sections present the groups combining observations made by stereomicroscope (OM groups A-F) and the groups made using polarised light microscopy (PLM groups 1-7). The structure followed is the group structure from the PLM (Groups 1-7), but the descriptions integrate comments from both techniques. The main reason for choosing the PLM structure is that Capelli's groups include observations of fine quartz which can not be detected with the stereo-microscope or the naked eye.

The differences and similarities between the groups generated using the two techniques are stated in each section. The agreement of the groups between techniques means that, to some extent, the fabric groups can be assessed microscopically, although some differences are not visible except with PLM.

Group	Sub-group	Main inclusions	Main voids	Colour matrix	Preliminary classification: number of samples	Confirmed by PLM?
A		Fine fabric , <0.211mm black/brown rounded inclusions. Angular light reflective inclusions, <0.07mm.	elongated and sub-parallel, meso	Orange to brown matrix, homogeneous in colour.	2	Yes (group 7)
B	B1	the pinkish-white to yellowish-white inclusions, irregular in shape but mostly angular (<1.6mm). Angular light reflective inclusions (<0.15mm). Others include rare brown inclusions and rare foraminifera.	Macro channels and vesicles	Brownish orange to dark brown.	5 certain, 5 uncertain	Yes but some misclassifications (group 5)
	B2	Presence of green inclusions set them aside			3	No
C		Carbonate inclusions have dissociated, rare other inclusions (sub-angular to subrounded white and slight rounded red inclusions <0.8mm)	elongated meso-voids sub-parallel to wall	from greenish white, light grey to cream white	8	Merged with group 1
D	General	Large irregular red, brown or black colour (max 1.27mm but most 0.7-0.8mm) and foraminifera	Meso vughs and vesicles as well as meso and elongated macro voids			Group 2, group confirmed but some misclassifications. Sub-groups dropped
	D1	The large inclusions: reddish brown to brown inclusions		orange, pink, light greyish brown to greenish	3 and 1 uncertain	
	D2	The large inclusions: black inclusions		Grey, yellow, brownish, pink, light brown and brownish orange.	11 and 4 uncertain	
	D3	Subgroup set aside because of red inclusions but also oxidised matrix throughout		light orange-brown to orange.	8 and 2 uncertain	
E		Predominant: bright white inclusions and translucent inclusions. Rare angular brown inclusions. Micro-fossils.		Light pink to orange.	10	Merged with group 1
F?		Sub-angular white/cream inclusions and light pink, foraminifera	Elongated voids and meso vesicles	light orange/light pink-orange.	3	Merged with group 1
Unclassified: 3						

Table 5.3: Tables summarising the description of the microscopic analysis and the groups observed

Sample number	Analysis Batch	Microscopic grouping	Reason for adding
4	First batch	D3	
7	First batch	E	
10	First batch	D1	
12	First batch	C	
15	First batch	E	
18	First batch	B1	Inscribed sherd
21	First batch	D2	
25	First batch	D?	
27	First batch	C	
29	First batch	D2	Inscribed sherd
30	First batch	E?	
33	First batch	B2	
34	First batch	B1	Inscribed sherd
35	First batch	B?	
37	First batch	E	
46	First batch	B1	
48	First batch	D2?	
58	First batch	D2	
60	First batch	D3	
61	First batch	A	
64	First batch	F?	
65	First batch	D3?	
66	First batch	?	
68	First batch	A	
69	First batch	?	
36	Second Batch	B	Typology
9	Second Batch	D2	Firing failure
13	Second Batch	B1?	Typology
22	Second Batch	F?	Close to sample 64?
40	Second Batch	C	White matrix clarification
52	Second Batch	C	White matrix clarification
54	Second Batch	?	Typology
62	Second Batch	B1?	Typology
70	Second Batch	B	Typology

Table 5.4: Sample list sent for thin-sectioning and reason to add to the randomly selected samples.

PLM grouping	OM grouping	Macroscopy
1	C, E, F	Anastasi F1 with white inclusions; Anastasi F1 with white matrix
2	D	Anastasi F1 with orange-brown rounded inclusions, some white inclusions and Anastasi F1 with black to brown inclusions
3	(one sample only)	
4	(one sample only)	
5	B	Anastasi F5
6	(one sample only)	
7	A	Anastasi F4

Table 5.5: Table of equivalence in the different scales of study: macroscopy, stereomicroscopy and PLM. These equivalencies are loose, as a few samples were misclassified.

5.3.2 Fabric 1

Samples identified by PLM	15, 37, 30, 69, 7, 22, 66, 27, 40, 52, 29 (1.2), and 64 (1.3?) and 12 (1.4?)
Other samples based on OM (in groups E, F and C):	23, 24, 45, 44, 20, 16, 31, 28, 57, 47

Table 5.6: Sample list for Fabric 1 based on the PLM and OM analysis.

Fabric 1 (Table 5.6) loosely corresponds to the macroscopic groups Anastasi Fabric 1/Crisp Ware with prevalent white inclusions and Anastasi Fabric 1/Crisp Ware with a white matrix. Fabric 1 also incorporates the OM groups C, E and F. Indeed, their predominant inclusions were the same despite the different colours in matrices.

OM summary

The samples had been divided into three groups: C, E and F. For each group, a microphotograph is given from a ground-embedded sample as well as the characteristics of the whole group (see appendix C.1 for individual samples). All types of voids are observed across the samples. Voids are mostly meso-elongated for all three groups, although there are frequent meso-vesicles. A few samples, for example, sample 30, have elongated voids sub-parallel to the wall of the sherds, which could indicate forming methods with rotary force (i.e. wheel).

The main differences between these three groups were the matrix colour and inclusion size. Group C had this white matrix, with inclusions challenging to see with the naked eye (Table 5.7; Figure 5.12; 5.14). Groups E and F have predominantly white inclusions, including microfossils (Table 5.8; Figures 5.15; 5.16; 5.17). Group F included three samples (22, 47, 64), and the main difference with group E was the coarse angular cream inclusions ($<$1.74 mm in sample 22) and coarse pink inclusions ($<$1.54 mm in 64).

Some samples have a core colour differing from the rest of the matrix (see catalogue Appendix A). An example is sample 30, where the core colour is brown, and the margin colour is red. This is caused by the firing regime and is discussed in section

9.1.4. The dissociated *foraminifera* gives the matrix a heterogeneous appearance. Some micro-fossils have red patches around them.

	Description
Matrix	white to yellow matrix
Predominant	*foraminifera* including dissociated tests
Few	white inclusions, including some larger angular white inclusions (e.g. sample 23 <0.9 mm)
Rare	rounded red or brown inclusions, with sample 45 having the largest (up to 0.9 mm), but most are below 0.2 mm

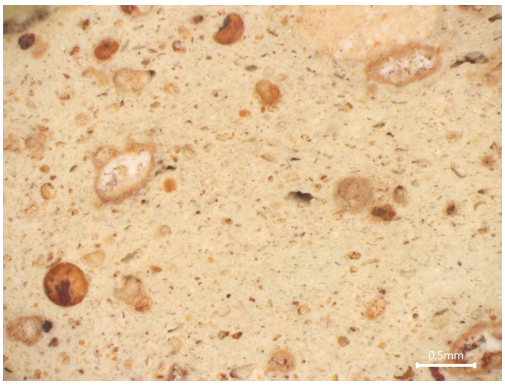
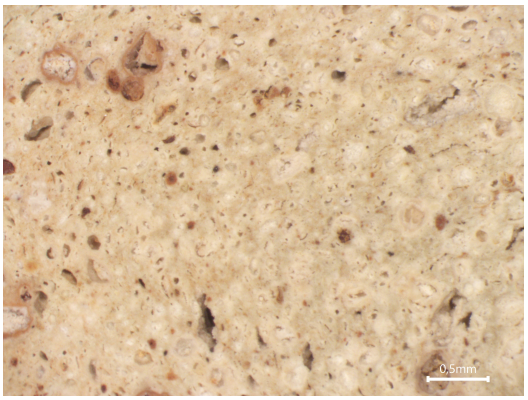
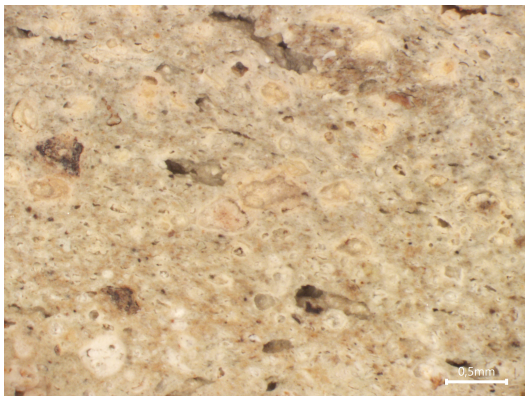


Table 5.7 & Figure 5.13 : Group C characteristics & Sample 52 microphotograph



(a) Sample 40



(b) Sample 12

Figure 5.14: Microphotographs of group C members

	Description
Matrix	varied matrix colour from light pink to orange.
Dominant	micro-fossils, with a majority appearing dissociated (creating voids rather than inclusions).
Frequent	bright white inclusions and greyish inclusions (including nearly translucent inclusions), up to 1.05 mm in sample 15

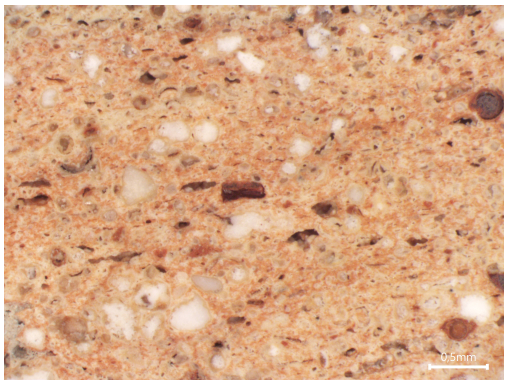
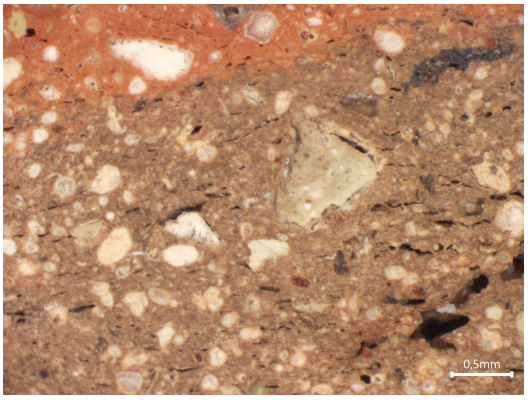
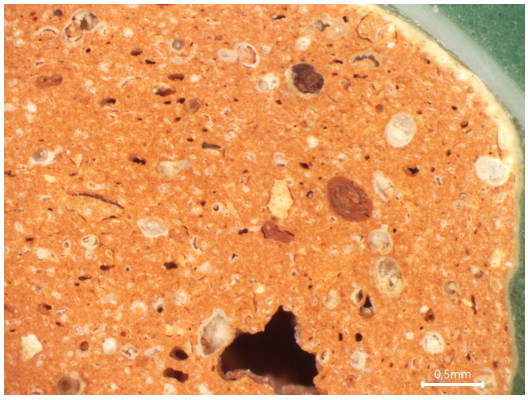


Table 5.8 & Figure 5.15 : Table of Group E characteristics & Microphotograph of sample 15

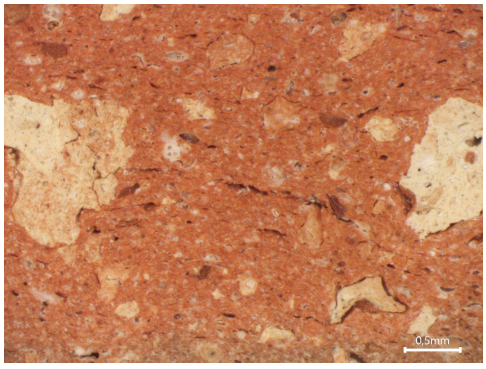


(a) Sample 30

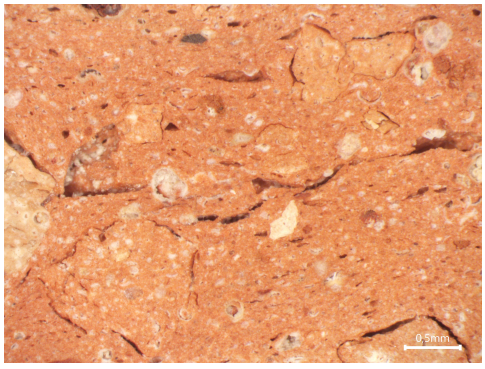


(b) Sample 7

Figure 5.16: Microphotographs of group E members



(a) Sample 64



(b) Sample 22

Figure 5.17: Microphotographs of group F members

PLM summary: inclusion identification

These groups were merged thanks to PLM analysis as these visible variations could have been caused by natural variations expected in Blue Clays. The characteristics of Fabric 1 are summarised in table 5.9 and illustrated in Figures 5.18; 5.19; 5.21. For the subgroups, the differing characteristics from group 1.1 are stated. Some examples are illustrated with PPL and XPL photographs in Figs. **??**, 5.18, 5.21.

Variant	Frequency interpretation	Inclusion description	Notes
1.1	Predominant - Dominant	Fossils (microfossils)	
	Common to Few	Limestone fragments. These correspond to the white inclusions with varied shapes and sizes noted visually.	Common in samples 15, 37 and 30
	Very rare to rare	Possible Chamotte or biomicrite?	Only a few samples, for example, 22 (group F) and 30
	Very rare to rare	iron-rich inclusions with quartz inside (Limonite? Terra Rossa?)	Only a few samples, for example, 37, 66
1.2	Few	Fine quartz in matrix and iron rich inclusions	Sample 29 only
1.3	Common	Fine quartz inclusions and biomicrite	Sample 64 only
1.4	Common	Fine quartz	Sample 12 only

Table 5.9: Characteristics of PLM Fabric 1

There are several subgroups for Fabric group 1. Group 1.1 is the primary group, and within, there are variations in the matrix, inclusion frequency and firing temperature. The other subgroups proposed are one sample each. 1.2 is sample 29, 1.3? is sample 64, and 1.4? is sample 12. The subgroups are as tentative subgroups, which should be confirmed or rejected by further sampling. Compared to the main bulk of the samples, they have differences which could be caused by a different material source.

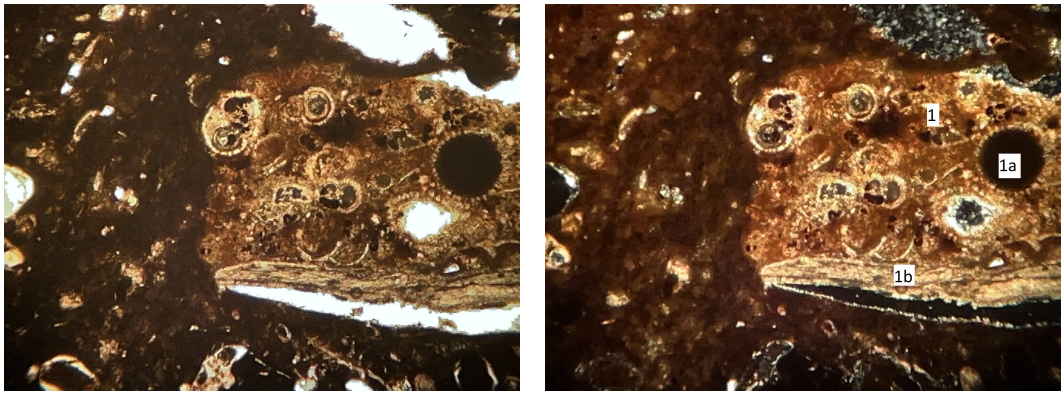
Looking at the subgroups, sample 29 has some fine quartz and more prevalent iron-rich inclusions (but not as many as Fabric 2) than the bulk of the group.

Sample 64 and 12 have common fine quartz (Fig. 5.19a[4]) in their matrix, and this set them apart from the bulk of the samples. Sample 64 also has frequent chamotte/biomicrite, which was noted visually in the OM (Group F).

Matrix colour varies in this group due to the assumed content of calcium and the firing regimes (e.g. atmosphere). For instance, samples 27 or 40 (formerly classified as group C) have white/ yellow matrices due to their composition (probably high calcium).

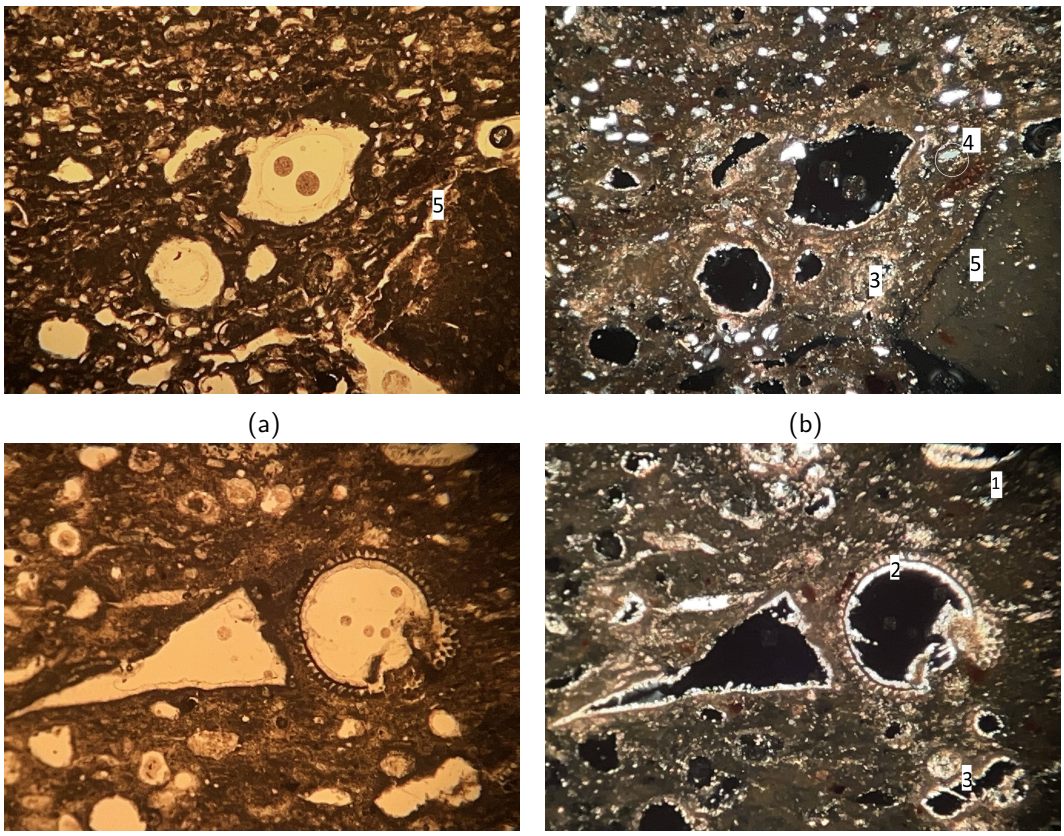
Other comments from the PLM on inclusions include the following:

- Rare glauconite was observed, for example, in sample 30.
- Other rare minerals, such as biotite (mica - sample 37), were observed.
- Sample 69 has a marl fragment with mollusc remains ([1b] in figure 5.18).



(a) (b)

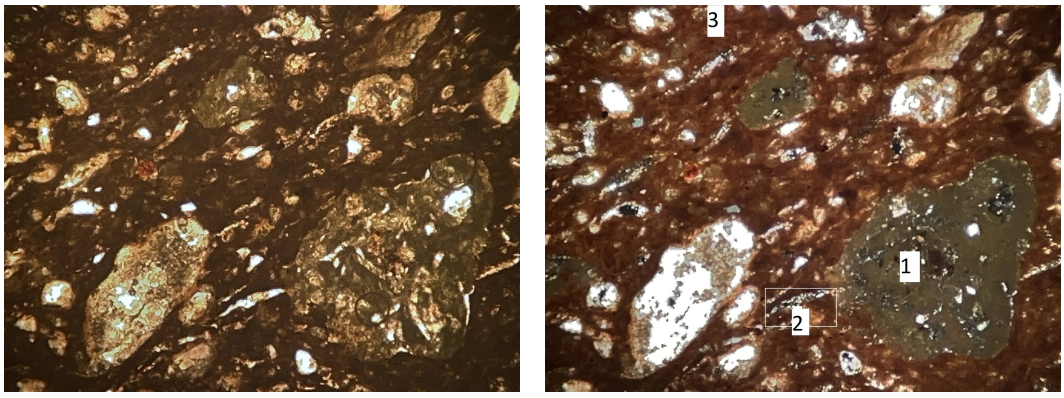
Figure 5.18: Samples 69 (Fabric 1.1), PPL (a), XPL (b). FOV: 1.3 x 1 mm. 1: biomicritic limestone with 1a: microfossils and 1b: fossilised shell fragment.



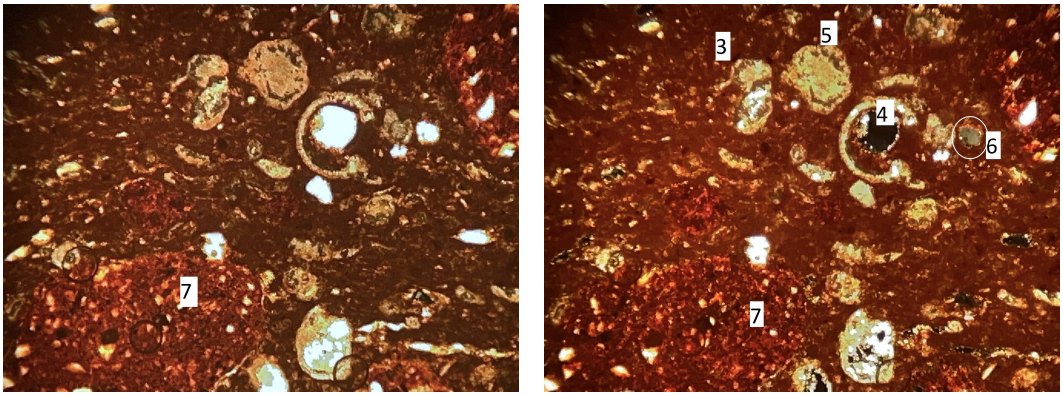
(a) (b)

(c) (d)

Figure 5.19: Samples 12 (Fabric 1.4) and 40 (Fabric 1.1), PPL (a,c), XPL (b,d). FOV: 1.3 x 1 mm. 1: Calcareous matrix; 2: micro-fossils, shape preserved; 3:dissociated carbonate inclusions, suggesting a high firing temperature (above 850°C); 4: quartz; 5: limestone/marl/chamotte? rock fragment; 6: void from the matrix and inclusion shrinking during the firing process. Note that sample 12 also had post-depositional carbonates, most probably from water infiltration. The difference between the two is the more prevalent fine quartz in Sample 12.



(a) (b)



(c) (d)

Figure 5.20: Samples 30 and 37 (Fabric 1.1), PPL (a,c), XPL (b,d). FOV: 1.3 x 1 mm. 1: Fossiliferous marl fragment; 2: Void more or less parallel to the walls; 3: iron-rich matrix; 4: microfossil; 5: dissociated carbonate; 6: example of fine quartz; 7: iron-rich nodule (terra rossa?). Sample 37 also shares similarities with Fabric 2 but has more carbonate inclusions.

Typology and surface treatment

The samples belong to bowl and plate forms. Some samples (e.g. sample 7) have a whitened surface which, based on the PLM analysis, was not interpreted as a slip but caused by the firing process. This phenomenon is discussed in section 9.1.3. Other samples 69, 22, and 66 also have white surfaces (PLM) caused by firing, although they are less thick in section and do not cover the whole vessels.

Estimated firing regimes

Table 5.10 presents the temperatures estimated for the samples sent to PLM analysis.

Firing temperature	Samples (PLM)
Less than 850°C	15, 37
Around 850°C	30, 69, 7, 22, 12
Beyond 850-900°C	66, 27, 40, 52, 29, 64

Table 5.10: Estimated firing temperature for samples sent to PLM analysis

The firing temperatures were not used to define subgroups, as this was unlikely a factor intentionally controlled for this assemblage considering the variation of

colours, differing oxidation (core colour) and non-homogeneous surface whitening. This is explored in section 9.1.4 and 9.1.3.

Discussion on group-specific characteristics

There were a few disagreements between the classification by OM and PLM, including sample 29, which had been classified as group D (Fabric 2) because of the numerous iron-rich inclusions. Sample 69 had been classified as "uncertain" during the microscopy and identified as Fabric 1 by PLM.

Fabric 1 has the characteristics often described for locally made pottery with numerous micro-fossils and limestone fragments (Sagona, 2015b: Crisp Ware, Anastasi, 2019: Fabric 1). The matrix has a varying Fe/Ca ratio observed with PLM (not quantified), meaning that the raw material is more or less calcareous. This could result from the differing amount of $CaCO_3$ in Blue Clay formations (see section 2.1) as mentioned by Pedley and Clarke (2002: 41) and Scerri (2019: 40). Variations within the fabric group are probably representing variations within the material itself. The provenance hypothesis for Fabric 1 is explored in section 8.1.

Chamotte is a term used to describe the use of crushed pottery vessels as a temper (Eramo 2020: 6).[2] The identification of chamotte, as opposed to natural clay pellets or other argillaceous rocks, has long been discussed in petrography (Whitbread 1986). Identifying inclusions as *chamotte* in these samples is not straightforward. To change the physical properties of a paste, the temper needs to be in sufficient quantities (Cuomo Di Caprio 2017a: 63), although experimental studies have not been carried out on Maltese clays. Based on the discussion around the PLM results, the inclusions that look like chamotte are rare (present in samples 30, 29, 66, 27) in 1.1, so they are unlikely a temper. In 64, these are more frequent, but their identification as chamotte is not entirely certain.

[2]Some authors have attempted to give a different definition to grog and chamotte, such as Eramo, 2020. In practice, they have been used interchangeably.

Biotite (one type of mica) was noticed in sample 37. This sample has the characteristics of being a local shape and is associated with fossils, rare glauconite and limestone fragments. Biotite is common in igneous rocks (Lutgens et al. 2016: 85) or metamorphic rather than in sedimentary geology. However, no other rock fragments were inconsistent with sedimentary geology. These biotite minerals are small and rare volcanic minerals. They could have resulted from an eruption event in the Mediterranean, and the minerals could have been transported by the wind (Capelli, *pers. comm.*).

Subgroups 1.3-1.4 have frequent fine quartz. Since the presence of quartz in local material is a recurring question through the fabric groups, it is discussed more generically in section 8.1.

5.3.3 Fabric 2

Samples identified by PLM	60, 4, 10, 21, 25, 9, 58 (2.2), 48 (2.2)
Other samples based on OM (in group D):	51, 8, 11, 49, 2, 38, 55, 17, 63, 26, 6, 59, 3, 14, 19, 41, 42, 56, 1, 67

Table 5.11: Sample list for Fabric 2 based on the PLM and OM analysis.

Fabric 2 (Table 5.11) had the macroscopic characteristics of Anastasi F1 (Anastasi 2019) with orange-brown or black-to-brown inclusions (see Table 5.5). Using the stereomicroscope, it was then identified microscopically as Group D. All the samples from Fabric 2 had been classified as D. However, some samples previously classified as D because of their iron-rich inclusions have a different fabric classification: samples 29 (Fabric 1), 62 (Fabric 4), 65 (fabric 3). Some mineral characteristics which make them different were not visible with the stereomicroscope.

OM summary

Group D consisted of three subgroups, D1-3, based on their matrix colour (from yellow to grey to homogeneous orange) and inclusion colour (see table 5.12 for descriptions of D1-3; Figure 5.12). Some samples were heterogeneous in colour within the sherds. Sample 21 (section A) has, for instance, a pale brown core colour matrix (10YR 6/3 pale brown), sample 60 (section A.119) light red (2.5YR 6/8 Light red) and sample 25 (section A.49) dark grey (5Y3/1 very dark grey).

Some samples, like 25 or 58, have a more calcareous raw material, which would explain variation. The colour variation would also be due to the firing regime (oxidation or lack of firing time and temperature). Samples 9, 17, 63, 25 and 29 have a grey core (reduced) and orange margins (oxidised). Sample 17 has the least pronounced difference.

The hypothesis was that the dominant inclusion type visible in this group was the same across the subgroups, and the oxidation of the iron content could explain the colour variations. This inclusion type spans size ranges from coarse to fine. For instance, in sample 8, the largest is 1.27mm, but plenty of these inclusions are

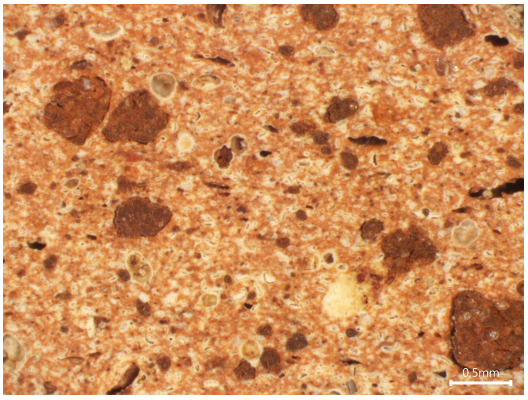
between 0.7-0.8mm, and others range from 0.2 to 0.4mm. This distribution is not bimodal, as expected with tempering action. Some of these inclusions have finer particles within, reflective, different from the ones observed in the sample.At first, it was hypothesized that these orange-to-black inclusions could be grog.

The dissociation of micro-fossils and carbonate inclusions is causing pores. All types of voids are visible in this group, including meso vughs and vesicles, and meso and macro-elongated voids (sub-parallel to margins) were noted sporadically. Shapes of *foraminifera* include:

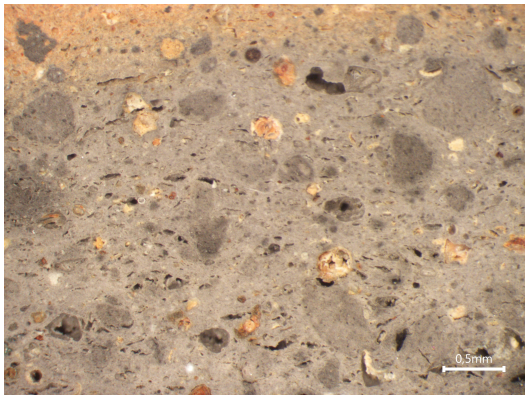
- most frequently linear segmented bodies: shape close to *nodosariid*? (see an example of species of *nodosariida* in Cilia, 2022b)
- elliptical and segmented body (see group C description). They could also be fragments of *foraminifera*/shell/micro-remains.
- bilobed or trefoil shapes: *globigerinoides*? *orbulina*? (see examples of species of *globigerinida* at Cilia, 2022a and photograph of *orbulina* specie at Cilia, 2022c)
- Possible pieces of shells?

Component	Subgroup	Description
Matrix	D1	Orange to brown matrix but heterogeneous in colour because of the dissociated *foraminifera*
	D2	Mixed, brown to grey to yellowish, heterogeneous in colour because of the dissociated *foraminifera*
	D3	Orange matrix but homogeneous in colour
Frequent to Dominant		Irregularly shaped inclusions, mostly sub-rounded but vary to equant and sub-angular
	D1	Brown to orange inclusions
	D2	Black inclusions, some orange to brown inclusions
	D3	Orange inclusions
Frequent	D1 and D2	small white inclusions (including smaller than 0.05mm), which are voids with a white "deposit" inside (dissociation of $CaCO_3$). Some of those have a crescent-like shape and lobes and are most likely dissociated microfossils and *foraminifera*.
Common	D3	*Foraminifera* but not dissociated

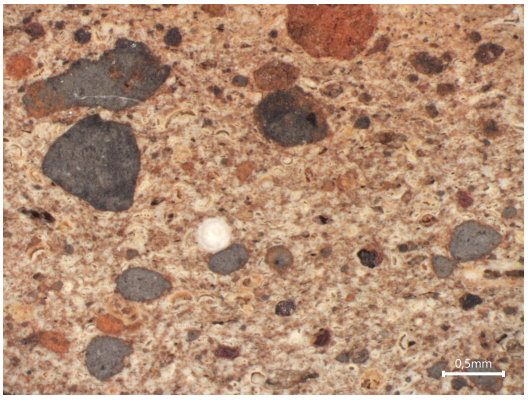
Table 5.12: Characteristics of Group D and hypothetical subgroups



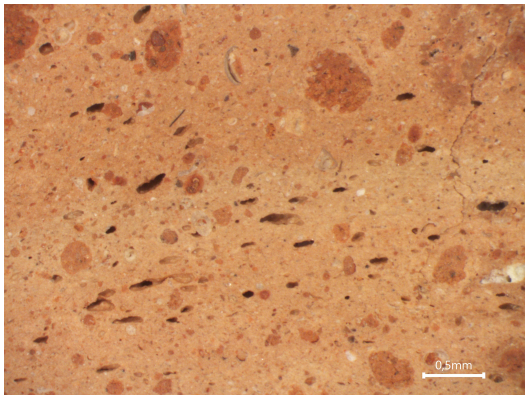
(a) Sample 10, D1



(b) Sample 9, D2



(c) Sample 21, D2



(d) Sample 60, D3

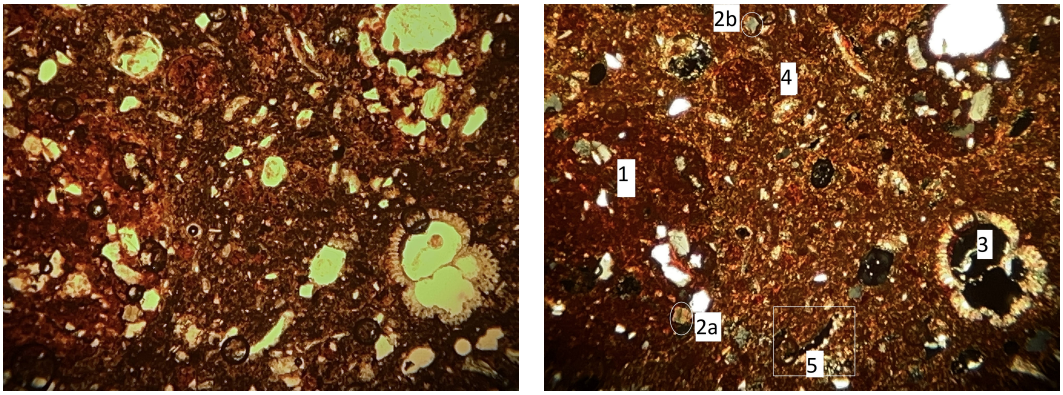
Figure 5.21: Micorophographs of examples of members of group D

PLM summary: inclusion identification

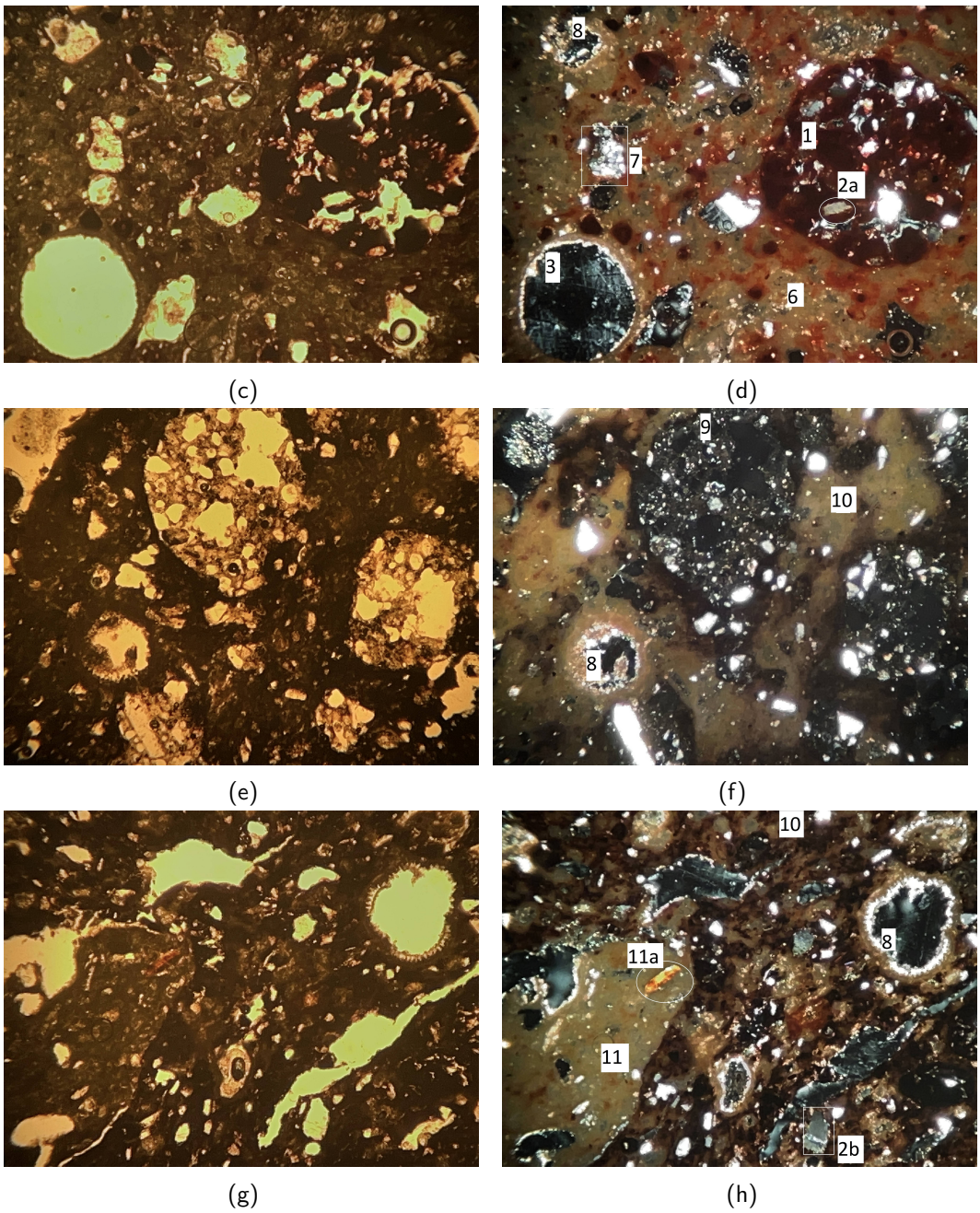
During PLM the subgroups were, as the analysis confirmed the hypothesis that these inclusions were the same but were fired differently. The variant is 2.2, composed of samples 48 and 58 (see table 5.13 for descriptions of 2.1 and 2.2). These samples are aside because their matrix contained more fine quartz than 2.1. Sample 48 also contained a few limestone fragments. Some PLM photographs are given in Figure 5.22.

Variant	Frequency interpretation	Inclusion description	Notes
2.1	Dominant (group marker)	iron nodules rich in quartz. These could be limonite or Terra Rossa nodules.	
	Frequent to common	Fossils	
	Few	Fine quartz systematically present	Only a few samples, for example, 22 (group F) and 30
	Very Rare	Biotite	samples 21 and 25
2.2	common	Fine quartz in matrix	
	Few	Limestone fragments	in sample 48
	One	Trachyte fragment ? (volcanic rock fragment)	in sample 58

Table 5.13: Characteristics of PLM Fabric 2



(a) (b)



(c) (d)

(e) (f)

(g) (h)

Figure 5.22: Samples 4, 10, 25 (Fabric 2.1), 48 (Fabric 2.2), PPL (a,c,e,g), XPL (b,d,f,h). FOV: 1.3 x 1 mm. 1 and 9: Iron-rich nodules (limonite or terra rossa) but 9 are reduced and highly fired; 2: fine quartz in nodules (2a) and in matrix (2b); 3: microfossils; 4: low or mid-fired matrix (non-vitrified); 5: microfissil fragment; 6 and 10: high-fired matrix (non-active and vitrified); 7: polycrystalline quartz?; 8: dissociated carbonates possibly microfssils; 11b: mica in marl (?) fragment

Typological discussion for this group

These vessels are plates, bowls and one miniature. There are no main typological differences compared to Fabric 1. Samples 10 and 48 have a white surface visible

in the section caused by firing (assessed by PLM), similar to Fabric 1, despite that it was believed that sample 48 had a white slip.

Estimated firing regimes

The samples predominantly had a high firing temperature (Table 5.14). The dissociation of the micro-remains was also visible in microscopy (OM). Sample 60 was low-fired, and samples 4 and 48 had medium firing temperatures.

Firing temperature	Samples (PLM)
Below 850°C	60
Around 850°C	4, 48
Beyond 850-900°C	21, 25, 9, 58

Table 5.14: Estimated firing temperatures of the samples sent for PLM analysis

Discussion on group-specific characteristics

This fabric shares some similarities with Fabric 1 with the common fossils. However, Fabric 2 has fine quartz inclusions in the matrix, which sets it apart from Fabric 1. The presence of quartz in Blue Clays is addressed in section 8.1.

The groundmasses are not homogenous, and this is particularly clear in Figure 5.22h(d)[6] where both greyish-yellow and red are mixed within the matrix. This could be because different soils/ clays were mixed intentionally or non-intentionally. This is discussed further in section 9.1.1.

The hypothesis that the main inclusions, the red iron-rich inclusions, were chamotte/ grog came from the literature. For example, in Sagona (2015b: 50), Crisp Ware has red inclusions, which are "ochre particles and grog". PLM analysis challenged this hypothesis as the inclusions were unlikely fired before the vessels themselves. Indeed, there are no voids around these inclusions; their boundaries with the matrix are not sharp (see Whitbread 1986 for characteristics). Chamotte is usually more inert than the surrounding matrix as it was part of a fired object. Therefore, chamotte inclusions would not shrink when fired in a

newly made artefact. The shrinkage of both the inclusions and the matrix creates a void around the inclusion. The oxidation of chamotte would also not necessarily match the oxidation state of the surrounding vessel matrix, as is the case for these inclusions. In sample 9, for example, inclusions are darker in the core and lighter in the margins, suggesting the inclusions were not fired prior to the vessel.

Sample 58 contains one unique volcanic rock fragment (igneous extrusive) incompatible with Malta's sedimentary geology.

5.3.4 Fabrics 3-4

Fabrics 3 and 4 comprise one sample each that could not fit in any other fabrics.

Fabric 3: Sample 65

Microscopically, this sample was classified with group D as the brown/red rounded irregular inclusions were similar to other sherds (Figure 5.23). This sample has characteristics of both Fabric 1 - the biomicrite - and Fabric 2 - the quartz and dominant iron-rich nodules (Table 5.15). The metamorphic quartz or large quartz grains are unexpected in Maltese geology (Figure 5.24). This sherd was therefore set aside for both these differences.

	Description
Matrix	Calcium rich
Dominant	iron nodules rich in quartz similar to Fabric 2
Common	Fossils
Common	Biomicrite or chamotte
Few	Fine quartz
One	Metamorphic quartz?
Firing	Firing temperature: below 850°C (matrix optically active)

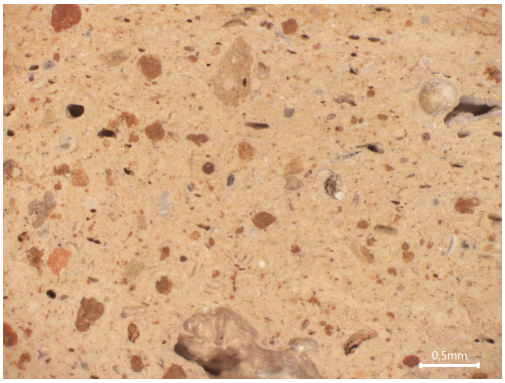
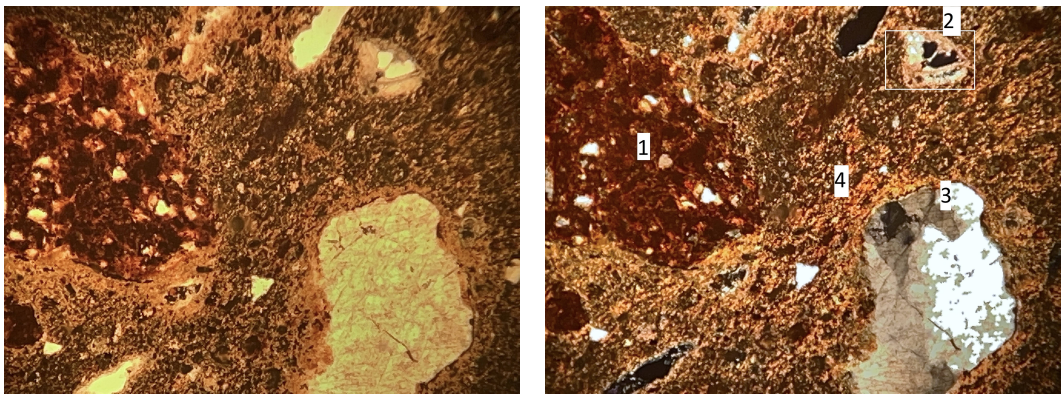


Table 5.15 & Figure 5.23 : Table of characteristics of Sample 65 & Sample 65 microphotograph



(a) (b)

Figure 5.24: Sample 65, PPL (a), XPL (b). FOV: 1.3 x 1 mm. 1: Iron-rich nodule; 2: Secondary deposition of calcium carbonate; 3: large quartz grain; 4: iron-rich optically active matrix

Fabric 4: Sample 62

This bowl from Żejtun had macroscopic and microscopic characteristics, which made it hard to classify (Figure 5.25). The OM analysis classified it with the cooking vessels of Group B (Fabric 5). The dominant biomicrite combined with the frequent fine quartz and common microfossils make it, for now, a unique combination of inclusions (Table 5.16 and Figure 5.26).

	Description
Matrix	Iron rich
Dominant	chamotte OR biomicrite (limestone) which is itself finer grained than other samples
Common	Fossils
Common	Fine quartz
Firing	Firing temperature: around 850°C

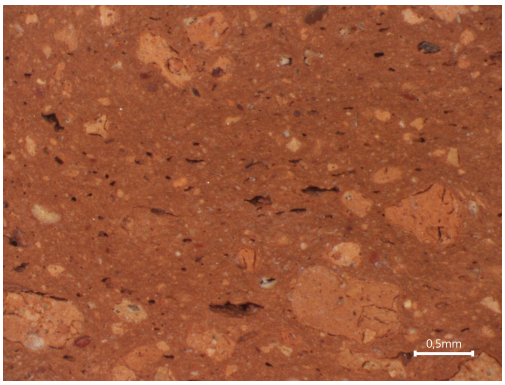
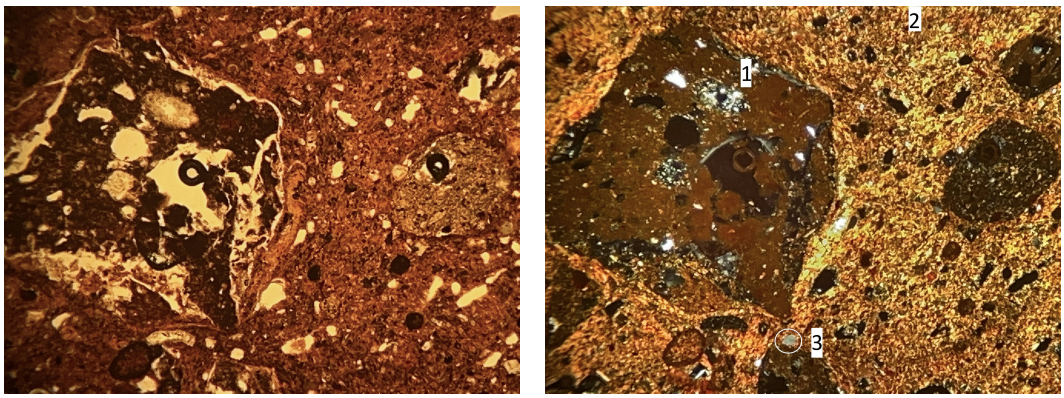


Table 5.16 & Figure 5.25 : Table of characteristics of Sample 62 & Sample 62 microphotograph



(a) (b)

Figure 5.26: Sample 62, PPL (a), XPL (b). FOV: 1.3 x 1 mm. 1: Chamotte; 2: Iron-rich matrix, optically active; 3: example of fine quartz

5.3.5 Fabric 5

This group was identified consistently through visual observation (Anastasi Fabric 5), microscopic analysis (Group B) and PLM (Fabric 5, Table 5.17). Samples 62 (see section 5.3.4) and 33 (see section 5.3.6) were microscopically classified as B on visual characteristics but the PLM revealed that the inclusions were different. These two sherds are also typologically different as they are not cooking vessels. Fabric 5 has been found only in cooking vessels.

Samples identified by PLM	46, 34, 70, 35, 18, 36, 13, 54
Other samples based on OM (in group B):	5, 53, 39, 32

Table 5.17: Sample list for Fabric 5 based on the PLM and OM analysis.

OM summary

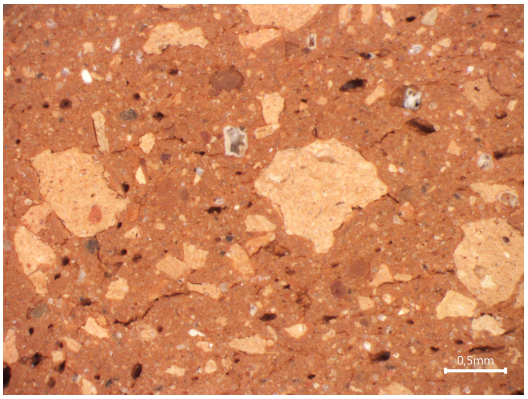
These sherds group together (Group B, Figure 5.27) using the stereo-microscope thanks to their similar matrix, texture and predominant inclusions. The matrix was visually darker and more homogeneous in colour than Fabrics 1-3. In this way, the matrix shared more visual similarities with Fabrics 4 and 7.

These sherds have inclusions with a bimodal distribution; visually, it seems that there are two size fractions: fine and coarse. As such, table 5.18 presents them separately. One of the angular light pinkish inclusions in Sample 34 was tested with the Mohs hardness kit. The inclusion was deeply scratched by point 4 and slightly scratched by point 3, which supported the calcite or crushed limestone hypothesis.

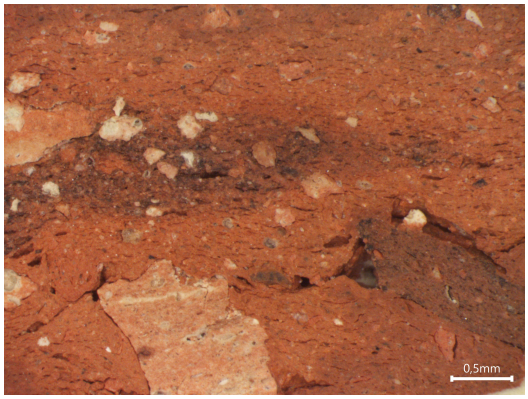
Meso and macro channels are the most common voids in the photograph, although there are also vesicles. Visually, this group appears less porous (fewer voids) than other groups. However, voids differ between samples, such as channels for sample 70 and meso vesicles and cracks for sample 35 (Figure 5.28b). These differences are explored in section 9.1.2 on manufacturing techniques.

	Component	Description
	Matrix	Red (mostly 2.5YR 4/8 or 5/8 or 6/8)
Coarse fraction	Dominant	Medium to very coarse pinkish-white to yellowish-white inclusions, irregular in shape but mostly sub-angular to angular (<1.6mm). Size varies across samples. Samples 5 and 34 contain very coarse inclusions (>1mm), whilst samples 43 and 53 do not.
	Few	angular bright white or light grey angular inclusions. Same as the one above?
	Rare	brown inclusions are also visible in the coarse fraction (claystone?). They vary in shape, and the largest recorded is 0.97mm.
Fine fraction	Dominant	very fine to fine white and grey and angular reflective/grey inclusions are frequently visible across the matrix (<0.15mm).
	Very rare	Very fine to fine dark red/brown homogeneous inclusions, sometimes reflective after grinding, are visible but rare
	Rare	Microfossils

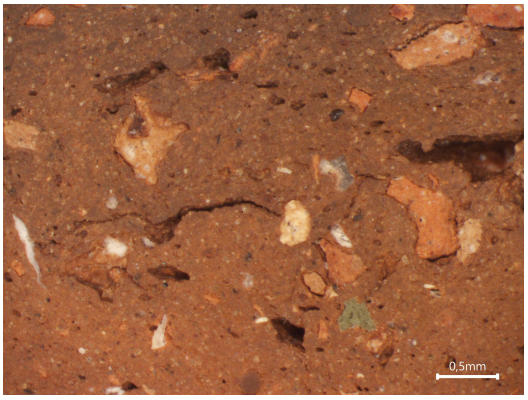
Table 5.18: Characteristics of group B



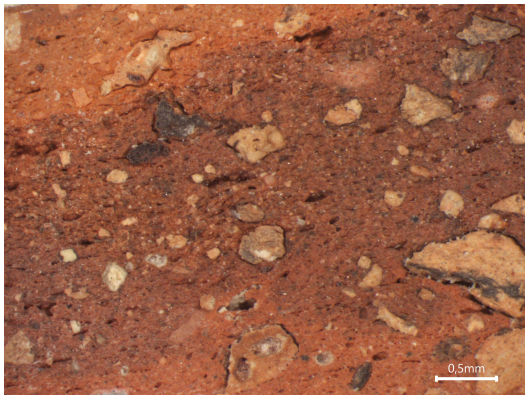
(a) Sample 18



(b) Sample 34

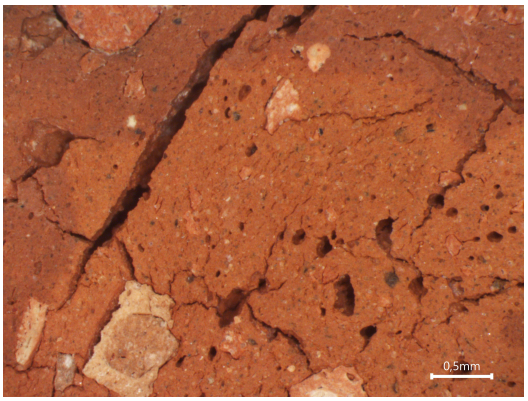


(c) Sample 36



(d) Sample 53

Figure 5.27: Microphographs of examples of group B members



(a) Sample 35 ground



(b) Sample 35 fresh break

Figure 5.28: Microphotographs of sample 35, ground and unground

Sample 18 appeared different because of the colour of its inclusion, the inclusions' size range and prevalence. The primary type of inclusion of sample 18 was tested using a Mohs kit, and the point of hardness three scratched the inclusion while two did not, which supports the hypothesis that these inclusions are calcite or have a similar hardness.

Sample 35 had been set aside during the macro and microscopic observations due to its texture. The matrix is similar to the samples in group B. Inclusions are similar with more prominent pink irregularly shaped inclusions (< 1.2mm) and angular white inclusions (< 1mm). The voids (mostly vesicles) and texture suggest, however, that the vessel was not wheel-made. Cuomo Di Caprio (2017a: 87) and Roux (2016: 183) highlight that wheel-thrown vessels tend to have elongated voids parallel or sub-parallel to the vessel wall because of pressure applied by and

in between the fingers.

PLM summary: inclusion identifiction

Table 5.19 summarises the characteristics and minerals as analysed by PLM. There are differences between this group and Fabric 1-4, including the matrix, which is systematically iron-rich and contains frequent fine quartz (Figure 5.29).

Variant	Frequency interpretation	Description	Notes
Matrix		Iron rich	Share similarities with matrix of group 7
5.1	Very frequent	fine quartz in matrix	
	Few	Fossils	
	Few	Limestone rock fragments	
	Dominant	chamotte/Biomicrite or claystone	
	Few	Rounded red clay nodules	Samples 18, 34-35 and 46
5.2?	Frequent	Carbonate inclusions	Sample 54

Table 5.19: Table of PLM Fabric 5 characteristics

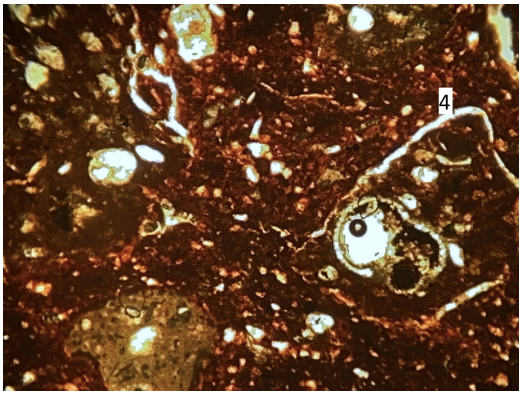
Rare inclusions include a clinopyroxene in sample 36 (5.1), a trachyte fragment, 1 biotite, and 1 plagioclase in sample 54. Sample 54 is classified as a possible subgroup because it has more carbonate and volcanic inclusions.

Other subgroups are not suggested. However, some differences were observed in the coarseness of the material; for instance, sample 46 is finer; or the manufacturing technique with the coarse sample 35 handmade and sample 70 could have been wheel made. This classification could later be refined by adding more samples of the different forms to see if there are patterns in the variations.

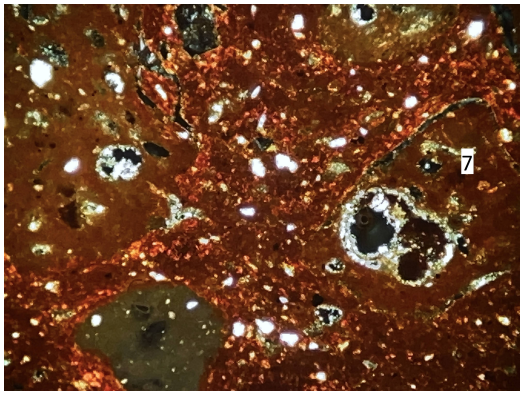
Typological discussion for this group

The samples from this fabric belong to olla forms and other vessels interpreted as cooking vessels (Anastasi 2019; Quercia 2002; Sagona 2015b). The link between

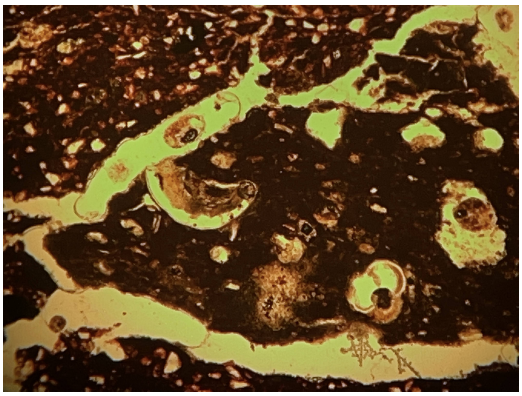
these specific forms and the choice of raw material is explored in section 9.2. There are three primary forms: Quercia type B (B1-3) with more or less thick walls, Quercia type A and Anastasi type C. There are, for now, no patterns in the fabric according to form, but this could be caused by the small sample size that this study allows for.



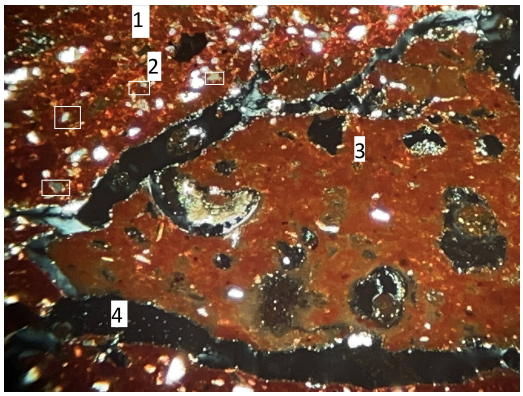
(a)



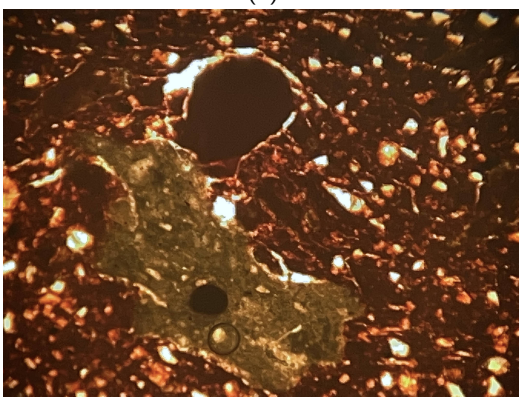
(b)



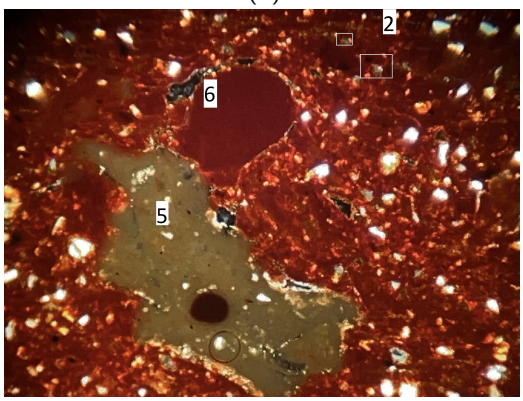
(c)



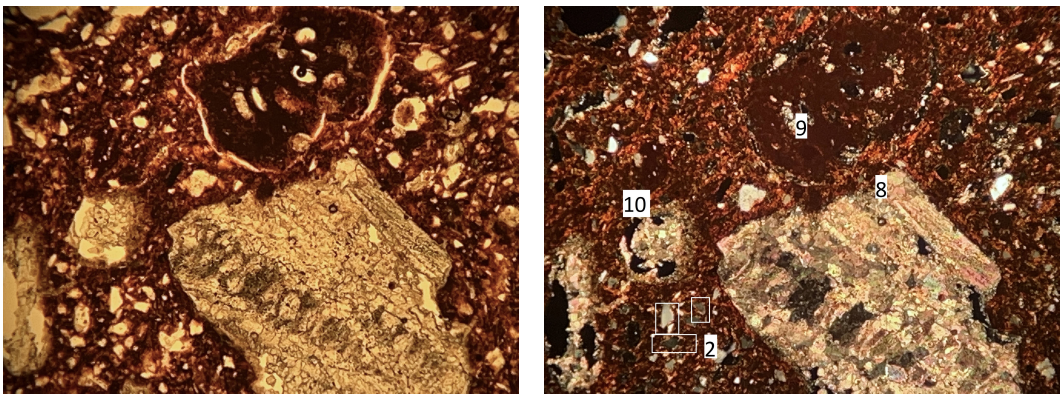
(d)



(e)



(f)



(g) (h)

Figure 5.29: Samples 13, 35, 46 (Fabric 5.1) and 54 (Fabric 5.2?). PPL (a,c,e,g), XPL (b,d,f,h). FOV: 1.3 x 1 mm. 1: iron-rich matrix; 2: examples of fine quartz; 3: highly fired rock fragment (claystone or marl?); 4: large voids around inclusion from the firing process or thin section preparation; 5: marl fragment; 6: Pure iron-rich clay nodule; 7: biomicrite with microfossil; 8: Biosparitic limestone with visible calcite minerals; 9: iron-rich limonitic nodule (terra rossa?); 10: possible microfossil?

Estimated firing regimes (PLM)

Table 5.20 presents the firing regimes assessed by PLM.

Firing temperature	Samples (PLM)
Below 850°C	18, 36, 54
Around 850°C	12, 46
Beyond 850-900°C	34, 70, 35

Table 5.20: Estimated firing temperatures of the samples sent for PLM analysis; Fabric 5

Discussion on group-specific characteristics

Sedimentary rock fragments (including limestone) are the predominant inclusions. Bimodal distributions are often associated with tempering (Eramo 2020: 17). The angularity of some white inclusions suggests crushed material such as limestone pieces or claystone (Cuomo Di Caprio 2017a: 103; Eramo 2020: 16). However, to conclude that this is a case of adding temper, one would first have to assert that the raw source material does not naturally have this type of inclusion (see section 7.4).

The inscribed sherds (34 and 18, figure A.67 and A.35; section 5.2.2) did not have any specific fabric markers compared to the rest of the group.

Black rounded inclusions in pottery from Malta have been described as either glauconite (Anastasi 2019), magnetite, wustite, or hematite (Asciak 2019; Grech 2019: for Anastasi Fabric 2) for other fabric groups. The black rounded inclusions in this analysis are not glauconite but iron-rich nodules. However, that does not rule out that other sherds could have glauconite.

Although some foraminifera were observed, such as shapes close to *Heterolepia bellincioni*, they are rare in these samples compared to other groups, such as Fabrics 1-2. The lack of foraminifera implies that the raw material was either naturally depleted of micro-fossils or was processed to be finer.

5.3.6 Fabric 6

This group is only made of one sample, sample 33, which could not be classified into other categories. This bowl had macroscopic and microscopic characteristics (Figure 5.30), making it hard to classify, and it was first classified with the cooking vessels in Group B due to its colour and texture. However, there is only rare fine quartz in the matrix. One inclusion ([1] in Fig. 5.31; Figure 5.30; Table 5.21) is vitrified, unlike the matrix, which could indicate the use of chamotte or material fired before the vessel's manufacture.

	Description
Matrix	Iron rich
Dominant	biomicrite or chamotte
Rare	fine quartz
Rare	fossils
Rare	iron nodules rich in quartz
Rare	limestone fragments
Firing	Firing temperature: around 850°C

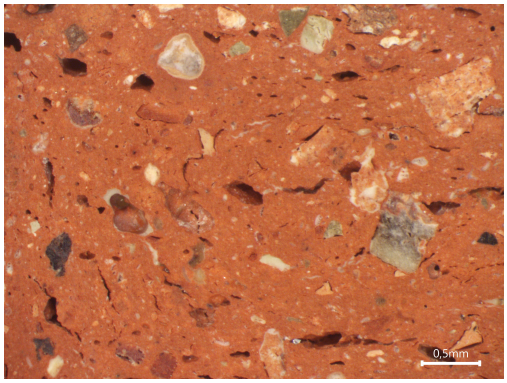
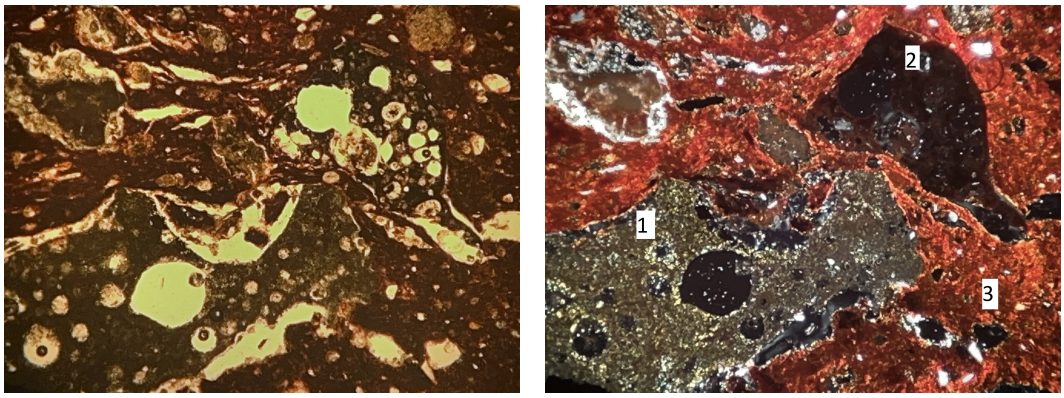


Table 5.21 & Figure 5.30 : Table of characteristics of Sample 33 & Sample 33 microphotograph



(a) (b)

Figure 5.31: Sample 33, PPL (a), XPL (b). FOV: 1.3 x 1 mm. 1: Vitrified chamotte; 2: stone fragment or chamotte; 3: iron rich matrix.

5.3.7 Fabric 7

This group was identified consistently through visual observation (Anastasi fabric 4), microscopic analysis (Group A) and the PLM (Group 7). Two samples belong to this group: 61 and 68, both from the Żejtun villa. Samples 61 and 68 were described as very fine with little impurities by all methods.

OM summary

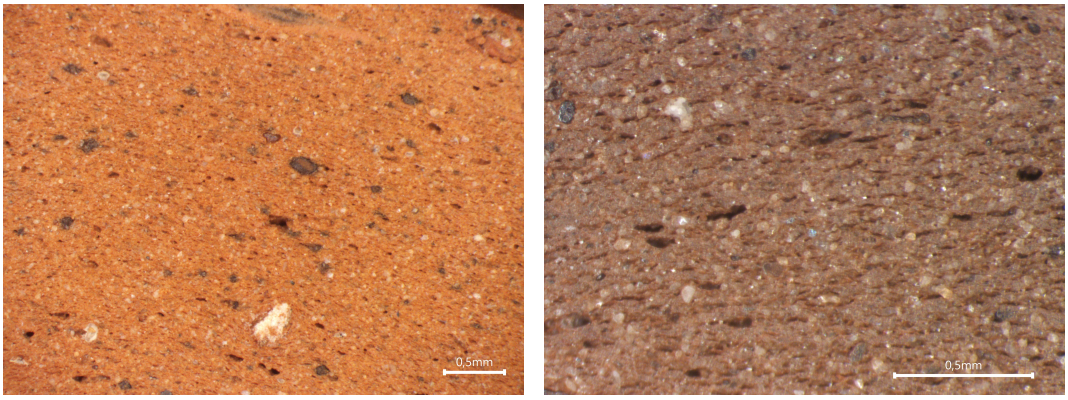
The colours of the sample matrix differ across samples (Figure 5.32). This could be attributed to use or firing conditions. Most voids are visible at high magnification and are elongated, parallel to the wall of the sherd. Rare macro elongated voids are also visible (Table 5.22). The elongated voids are a feature of wheel throwing (Cuomo Di Caprio 2017a: 87).

Component	Description
Matrix	Orange to brown matrix, homogeneous in colour. Dense/compact matrix.
Dominant (relative to total inclusion)	Very fine to medium black/brown rounded to sub-rounded inclusions (<0.211mm)
Very rare	Very rare medium inclusions of matrix colour.
Frequent to Dominant	Irregularly shaped inclusions, mostly sub-rounded but vary to equant and sub-angular
Rare	Very fine dissociated white inclusions
Frequent	At high magnification, very fine inclusions <0.07mm including angular light reflective inclusions and angular white inclusions

Table 5.22: Characteristics of group A

PLM summary: inclusion identification

Dominant fine quartz inclusions were observed in the matrix (Figure 5.33). Iron-rich nodules are the only inclusions apart from the quartz. These observations are coherent with the microscopic analysis, with the iron-rich nodules probably being the rounded inclusions.



(a) Sample 68 (b) Sample 61

Figure 5.32: Microphotographs of members of group A

The voids observations were confirmed by Capelli, who highlighted that these samples had unequivocal evidence of fast-wheel throwing: the elongated voids parallel to the wall of the vessel. Finally, the matrix is rich in iron compared to the other groups. The matrix shares similarities with group 5, the cooking vessel.

Typology and samples

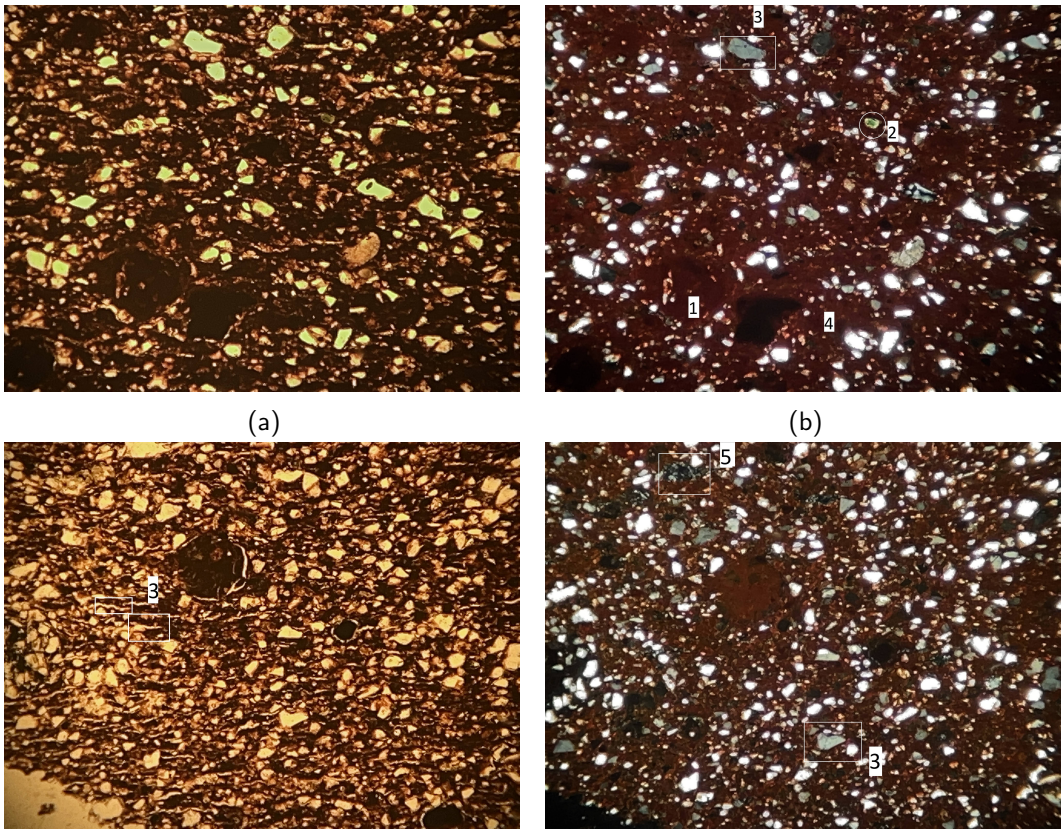
Only two samples classify in this fabric, one cooking vessel and one carinated bowl. Sample 61 had blackening on the outer surface, which could be soot (section 5.2.2), supporting its use as a cooking vessel. This can not, however, be confirmed with this analysis.

Estimated firing regimes

Both samples have high firing temperatures beyond 850-900°C as the matrix of both samples is vitrified (PLM).

Discussion on group-specific characteristics

Capelli suggested that considering how fine the fabric is, the clay could be an alluvial clay transported across long distances, causing a natural sorting of the raw material. The hypothesis that the raw material could be similar to Fabric 5 but



(a) (b)

(c) (d)

Figure 5.33: Samples 61, 68, PPL (a,c), XPL (b,d). FOV: 1.3 x 1 mm. 1: pure iron-rich nodule; 2: heavy mineral, rare in Malta; 3: Quartz; 4: iron-rich matrix; 5: polycrystalline quartz?; 6: elongated voids parallel to the sample wall

levigated (Anastasi 2019: 37) cannot be disproved at this stage (section 9.1.1).

Vessels with no coarse inclusions, also called *fine ware*, lack rock fragments which can be diagnostic of specific geology (Quinn 2013: 10). There are no rock fragments which contradict a Maltese origin. However, the source of the raw material is still not identified.

Part III

X-Ray Fluorescence and data analysis

Chapter 6

Methodology

This chapter presents the methodology used for the XRF investigation, from sample selection to data analysis.

6.1 X-Ray Fluorescence

6.1.1 Sample selection for XRF

Sherds

Only a selection of sherds could be analysed with the XRF within the time allocated. The samples were picked according to the microscopic groupings presented in section 5.3 (groups A-F). Since no local reference groups exist with known composition, which would be an ideal scenario (Hein and Kilikoglou 2020: 180), or previous chemical analysis, the microscopic groupings were the only systematic groups available to visualise the data. The groups studied in this chapter are the OM groups established before the PLM analysis, which are the groups A-F (see the second column in Table 6.1). Several reasons underlie this choice:

- The chemical analysis might have revealed another group structure than the

PLM.

- Not all sherds analysed by XRF had been sent for PLM analysis. Therefore, the classification of some sherds would not have been specific.
- The PLM results were still being discussed when the XRF analysis was conducted, and the group structure was not fully established.

The samples sent for petrographic analysis were processed for XRF, and the groups were inflated with randomly selected samples from the various groups (see Table 6.1 for a complete sample list). Although the SCH had granted permission to destroy the inscribed sherds partially, it was decided not to destroy further two of them (samples 34 and 29) for this study. Indeed, the sample preparation for XRF was destructive, and it was deemed that the petrographic results would suffice to see if the sherds were made of the same fabric as the ones tested with the XRF. As such, their destruction was no longer justified. Sample 18 could be sampled without damaging the inscription.

Raw materials

Raw materials (i.e. clays) were analysed, comparing possible sources to the vessels. The geological samples were selected from a wider collection built by the CoFIPoMS project carried out at UoM (University of Malta 2021). Older samples from the MaltaPot Project (University of Malta 2020) and Asciak (2019) were additionally analysed. These samples are listed in Table 6.2 and further described in Appendix B.4. Their locations are represented in Figure 6.1.

The list includes soils derived from Blue Clay (or assumed) both collected on the surface (opportunistic collection) and a few samples following a systematic procedure using a hand auger as detailed in the documentation produced by Vella and Richard-Trémeau (2021b). The list further includes marl samples from the Globigerina layers as well as Red soils from the Globigerina Limestone layer (DLA.A1) and Terra Rossa from the erosion of the Upper Coralline Limestone layers (LP.A1 and LP.E1).

S	OM	PLM	XRF	S	OM	PLM	XRF
1	D3		x	36	B	5	x
2	D2		x	37	E	1.1	x
3	D3			38	D2		
4	D3	2.1	x	39	B?		x
5	B		x	40	C	1.1	x
6	D2?			41	D3		
7	E		x	42	D3		x
8	D1		x	43	B		x
9	D2	2.1	x	44	C		
10	D1	2.1	x	45	C		
11	D1		x	46	B	5	x
12	C	1.2	x	47	F?		x
13	B	5	x	48	D2?	2.2	x
14	D3			49	D2		
15	E	1.1	x	50	E		x
16	E			51	D1		
17	D2		x	52	C	1.1	x
18	B?	5	x	53	B		x
19	D3		x	54	B?	5	x
20	E			55	D2		
21	D2	2.1	x	56	D3		
22	F?	1.1	x	57	E?		
23	C		x	58	D2	2.2	x
24	C			59	D2?		
25	D?	2.1	x	60	D3	2.1	x
26	D2		x	61	A	7	x
27	C	1.1	x	62	B?	4	x
28	E		x	63	D2		
29	D2	1.2		64	F?	1.3	x
30	E?	1.1	x	65	D3?	3	x
31	E			66	?	1.1	x
32	B		x	67	D?	1.1	
33	B	6	x	68	A	7	x
34	B	5		69	?	1.1	x
35	B?	5	x	70	B	5	x
				Total	70	34	49

Table 6.1: List of sherd samples analysed by XRF (marked with a x) and summary of OM and PLM analysis

Most locations were sampled multiple times, for instance, at different elevations or, when possible stratigraphic layers. There is an over-representation of the Għajn Tuffieħa, Ġenjna, Ta'Lippija and Il-Qarraba area as many layers were observed and the clay layers are easily accessible.

The samples are named following the convention *AAA.BX*, explained as:

- AAA: two or three letters for sample location (e.g. GH: Gelmus Hill)
- B: sub-sample location (eg. GH.A1 and GH.B1 represent different elevation on Gelmus)
- X: number of the sample if several samples were taken at the same elevation in the location

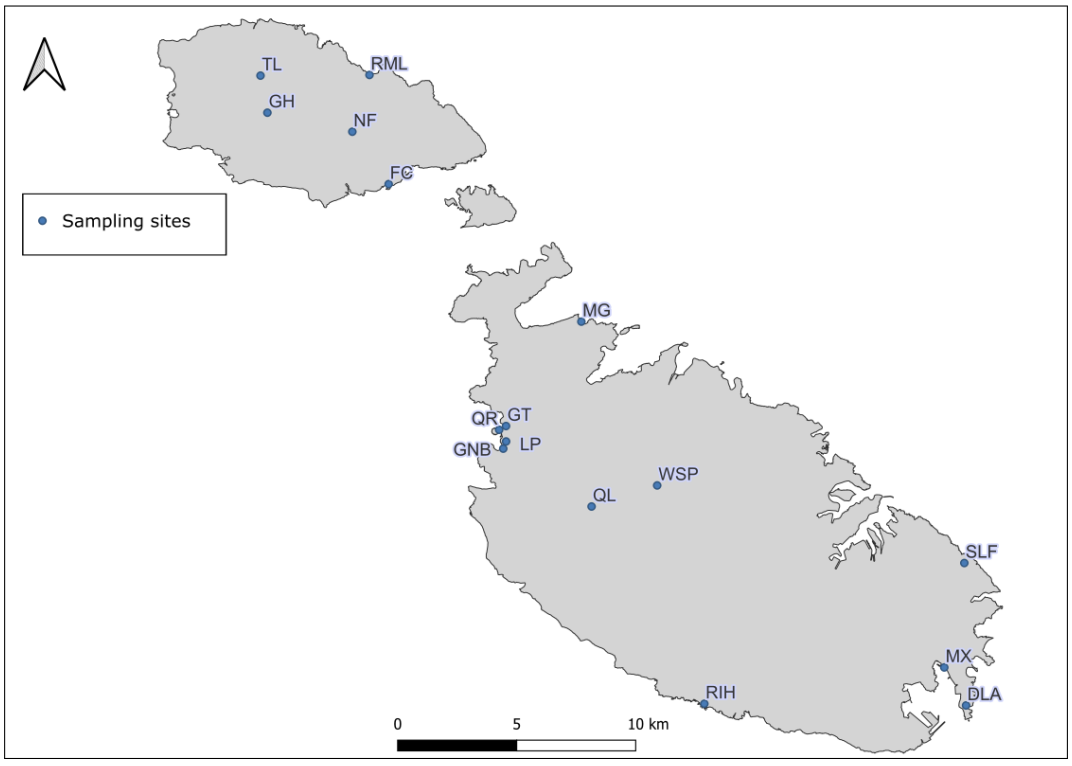


Figure 6.1: Map of the Maltese Islands with the main sample locations (geological samples)

Sample name	Location	Island	Type of raw material
DLA.A1	Delimara (Kalanka Bay)	Malta	Terra Rossa?
FC.A1	Fort Chambray	Gozo	Uncertain
GH.A1	Gelmus Hill	Gozo	Blue Clay
GH.B1	Gelmus Hill	Gozo	Blue Clay
GH.C1	Gelmus Hill	Gozo	Blue Clay
GNB.A1	Ġnejna Bay	Malta	Blue Clay
GNB.B1	Ġnejna Bay	Malta	Blue Clay
GNB.D1	Ġnejna Bay	Malta	Blue Clay
GNB.E1	Ġnejna Bay	Malta	Blue Clay
GNB.F1	Ġnejna Bay	Malta	Blue Clay
GT.A1	Għajn Tuffieħa	Malta	Blue Clay
GT.B1	Għajn Tuffieħa	Malta	Blue Clay
LP.A1	Ta'Lippija	Malta	Terra Rossa
LP.E1	Ta'Lippija	Malta	Terra Rossa
MG.A1	Imġiebaħ	Malta	Uncertain
MG.B1	Imġiebaħ	Malta	Uncertain
MX.A1	Marsaxlokk	Malta	Globigerina marl
MX.D1	Marsaxlokk	Malta	Globigerina marl
NF.A1	In-Nuffara	Gozo	Blue Clay
NF.B1	In-Nuffara	Gozo	Blue Clay
QL.A1	Il-Qolla	Malta	Blue Clay
QL.B1	Il-Qolla	Malta	Blue Clay
QR.A1	Il-Qarraba	Malta	Blue Clay
QR.C1	Il-Qarraba	Malta	Blue Clay
QR.D1	Il-Qarraba	Malta	Blue Clay
RIH.A1	Ras Il-Ħamrija	Malta	Uncertain
RIH.B1	Ras Il-Ħamrija	Malta	Uncertain
RIH.D1	Ras Il-Ħamrija	Malta	Uncertain
RML.B1	Ramla Bay	Gozo	Blue Clay
RML.D1	Ramla Bay	Gozo	Blue Clay
RML.E1	Ramla Bay	Gozo	Blue Clay
SLF.A1	San Leonardo area	Malta	Uncertain
SLF.B1	San Leonardo area	Malta	Uncertain
TL.A1	Ta' Leveċa	Gozo	Blue Clay
TL.B1	Ta' Leveċa	Gozo	Blue Clay
WSP.B1	Wied tal-Isperanza	Malta	Uncertain

Table 6.2: List of geological samples used in the analysis

6.1.2 Sample preparation and analysis

X-Ray Fluorescence Energy Dispersive Spectroscopy (XRF-EDS) is a qualitative and quantitative analysis of the elements of which a sample is made of (Cuomo

Di Caprio 2017b: 587). It is used to measure major, minor and trace elements in samples for grouping sherds and provenance studies (Hein and Kilikoglou 2020). The pool of XRF characterisation instruments in Malta is limited, and the XRF from the Department of Chemistry (Figure 6.2f, Bruker S2 Ranger), University of Malta, had to be used. Until the analysis itself, it was unsure which instrument would be available for the analysis; the samples were prepared in a generic way to suit all possibilities.

The protocol for sample preparation for this dissertation was designed for semi-quantitative analysis with an XRF or a pXRF, considering the vast literature on the limitations of semi-quantitative studies (Hunt and Speakman 2015; Speakman et al. 2011). The sherds' surfaces were removed using a Dremel 3000 rotary tool with a sanding accessory (Ref. Dremel 408). Figure 6.2a illustrates how sample 21 (TSG96/352/24) looks after surface removal. All surface treatments, such as slip, and surface contamination, are removed, avoiding any contribution of these to the analysis. Figure 6.2b features two samples after surface removal. For instance, sample 27 had a concretion on the outer surface, which could not be removed during washing (Figure A.53).

When possible, five grams of sample were then crushed to a fine powder using a pestle and mortar. Geological samples were crushed without any other treatment (Figure 6.2c). Ideally, samples would have either been prepared pressed pellets or fused beads, making them perfectly homogeneous and flat. This sample preparation eliminates variation within grain size, for example, and the analysis is optimised (Hunt and Speakman 2015). However, it was not possible to use these methods for this study. The presence of organic material, particularly in the raw materials, could have introduced additional variation which can not be controlled. Loss of Ignition could not be carried out for this dissertation. One reason was that it required the sample to be heated at 1050°C; the same sample cannot be reused for XRD.

The powdered samples (sherds and geological materials) were dried at 110°C for 24 hours (Figure 6.2d). The samples were then analysed using XRF cups with

Mylar membrane (Figure 6.2e). The XRF was calibrated with internal standards, as no calibration was possible with geological or pottery samples. The chamber was flushed with Helium before analysis.



(a) sample 21 (TSG96/352/24) with surface removed (right-hand side of the sherd). Note the differences in colour before and after surface removal.



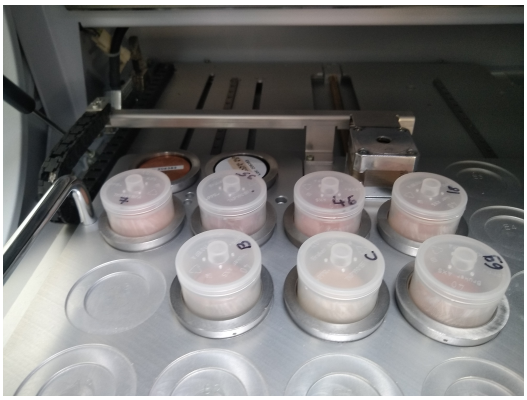
(b) Sherds TSG96/2041/42 and TSG96/352/39 with parts of their surface removed.



(c) Sherd after cutting and before being crushed



(d) Photograph of crushed samples in the drying oven



(e) Prepared sample cups in the XRF



(f) Photograph of XRF Bruker S2 Ranger

Figure 6.2: Photographs of XRF sample preparations and analysis

6.1.3 Control samples: XRF analysis from CRB laboratory

Five samples (Table 6.3) were sent to Germany for quantitative analysis with XRF at the laboratory CRB GmbH. Forty elements/oxides were quantified after the laboratory carried out its own sample preparation, including crushing, drying and determination of Loss of Ignition (LOI). Parts of the samples were then prepared as fused beads. The raw results, as provided by the laboratory, are found in Appendix D. The leftover powdered samples were used as a control for this dissertation to assess the precision and accuracy of the Bruker as it could not be calibrated to geomaterials. Sample preparation is not the same as for the fused beads, and, therefore, readings cannot be fully compared. However, this permitted a broad assessment of the precision and accuracy of the methodology.

Sample name	Sample type	Laboratory	Laboratory sample number	Method
TL.B1.S0.CR	clay sample	CRB	35790	XRF
SPP.A1.S0.CR	marl sample	CRB	35791	XRF
QL.B1.S0.CR	clay sample	CRB	35792	XRF
G2005	Għar Dalam pottery sherd	CRB	35793	XRF
TSG96/352/24 (Sample 21)	Late Republican pottery sherd	CRB	35794	XRF

Table 6.3: Samples sent for analysis to CRB laboratory, Germany

6.1.4 Lack of calibration and implications

It was impossible to calibrate the XRF instrument with material-specific calibration and compensate for matrix effects. Matrix effects result in the fluorescence of some elements being absorbed whilst others are enhanced (Schramm 2015: 41). The calibration of an instrument with samples that have known true quantities and similar matrices to the unknown sample compensates for these effects. When an instrument can be calibrated using a few samples of known compositions, it allows the instrument to associate the numbers of counts with the actual concentration and, therefore, correct for matrix effects, assuming matrices are similar. However, the Bruker XRF did not permit this calibration resulting in the data being semi-

quantitative.

Several tests were conducted to assess how to maximize the analysis whilst being realistic about its limitations. During the first test, it was noticed that more Calcium oxide (CaO) was detected than Silicon dioxide (SiO_2), looking solely at X-Ray counts. However, when looking at the quantification led by CRB, SiO_2 is the predominant oxide. This is most likely due to matrix effects, and, although it was not possible to calibrate the XRF, the instrument had the option to stipulate a matrix for the sample. During preliminary tests on known samples, it was observed that the values for major elements were closer to the values given by CRB laboratory, so it was decided to use SiO_2 as a matrix.

Accuracy and precision of methodology

It was necessary to get an estimation of how accurate and precise the method would be for the readers to assess how reliable the analysis is. Building on the metaphor of the dartboard illustrated in Figure 6.3, accuracy is the ability to hit the centre of the board or "the closeness of the determined concentration to the true concentration" (Hein and Kilikoglou 2020: 3). Precision, on the other hand, is the ability to hit the same point on the board over and over again or "the reproducibility of analytical results"(Hein and Kilikoglou 2020: 3).

Precision Four samples were analysed on the same day three times to test the repeatability of the readings. Additionally, samples 21 (sherd) and QL.B1 (clay) were run with every batch of analysis and sample 21 was run regularly between samples during the analysis. In total, sample 21 was run 14 times and QL.B1, 12 times. The mean, standard deviation and relative standard deviation for these readings are presented for the variables retained for analysis in table 6.4. Some elements still have a high standard deviation, such as Copper and Chromium. This will have to be kept in mind when analyzing the loadings for the statistical analysis. The data for these descriptive statistics and the transformations can be found in Appendix D.2.6 (Digital).

	QL.B1, n=12			Sample 21, n=14		
	Mean	σ	Relative σ	Mean	σ	Relativeσ
Al2O3	13.3	0.9	6.5	14.9	0.7	5.03
CaO	15.2	0.2	1.3	13.7	0.2	1.11
Cr2O3	0.0119	0.0132	111.37	0.0151	0.0108	71.47
CuO	0.0016	0.0013	85.00	0.0024	0.0006	27.09
Fe2O3	6.75	0.09	1.31	7.30	0.09	1.23
Ga2O3	0.0032	0.0004	13.14	0.0029	0.0003	10.75
K2O	2.39	0.06	2.60	2.64	0.04	1.63
MgO	3.52	0.43	12.32	2.85	0.90	31.76
MnO	0.0431	0.0043	9.90	0.0748	0.0038	5.03
Nb2O5	0.0030	0.0009	28.85	0.0033	0.0003	7.58
NiO	0.0035	0.0011	32.98	0.0049	0.0009	18.82
P2O5	0.671	0.047	6.94	0.778	0.032	4.14
Rb2O	0.0156	0.0007	4.77	0.0175	0.0004	2.16
SiO2	45.01	1.29	2.87	47.05	3.34	7.10
SO3	0.92	0.04	4.08	0.38	0.02	4.32
SrO	0.0578	0.0008	1.41	0.0572	0.0010	1.69
TiO2	0.82	0.02	2.62	0.88	0.02	2.24
Y2O3	0.0031	0.0008	24.20	0.0050	0.0003	5.47
ZnO	0.0129	0.0005	4.14	0.0134	0.0005	3.51
ZrO2	0.0319	0.0061	19.14	0.0486	0.0016	3.30

Table 6.4: Means, standard deviation and relative standard deviation (in %) for the readings (n = number of readings) of Sample 21 and QL.B1.

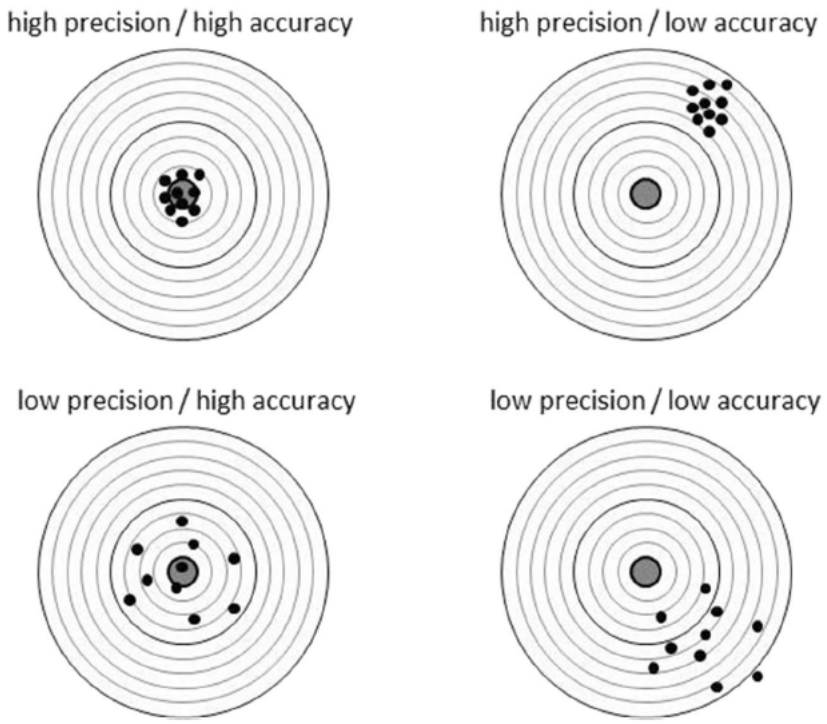


Figure 6.3: Precision and accuracy as illustrated by Hein and Kilikoglou (2020: 5, Fig. 2)

Accuracy Accuracy was assessed by comparing the Bruker XRF readings and the laboratory CRB readings for QL.B1 and Sample 21. The CRB readings were normalised without LOI. The mean of the readings used for precision (section 6.1.4) was used to compare the instruments. The CRB and the local readings (in %) were converted from oxides to elements and renormalised to 100%. The results are not entirely comparable as a different list of elements was analysed with the two methods, and the sample preparation was different. The relative difference as a percentage is expressed for the variables analysed by both instruments in Table 6.5. There seems to be a problem with the sodium (Na) value, and the data will have to be normalised without this variable. Several trace elements of interest, such as Zinc (Zn), Strontium (Sr), and Niobium (Nb), seem to be read with less than 15%. Major elements, such as Calcium (Ca) and Silicon (Si), are also read with less than 20% difference. Therefore, the methodology can not be quantitative, as the readings need to be more accurate. The methodology will therefore be referred to as semi-quantitative. The data for can be found in Appendix D.2.7 (Digital).

	CRB	S21 home	Diff in %	QLB1 CRB	QL.B1 home	Diff in %
Al	17.8139	13.8439	22.2858	17.2300	12.2234	29.0576
Ba	0.0536	0.0153	71.5430	0.0269	0.0109	59.5521
Ca	17.6901	17.2057	2.7382	23.4900	18.8646	19.6910
Cr	0.0298	0.0182	39.1082	0.0269	0.0141	47.4540
Fe	9.2725	8.9730	3.2300	8.7877	8.1984	6.7067
Ga	0.0045	0.0038	15.7567	0.0036	0.0041	16.1925
K	4.2030	3.8532	8.3218	3.8583	3.4454	10.7010
Mg	2.1035	3.0158	43.3745	2.3872	3.6865	54.4250
Mn	0.0960	0.1018	6.0294	0.0543	0.0580	6.8271
Na	0.7790	11.5966	1388.6332	0.2969	13.9711	4604.9183
Nb	0.0038	0.0041	8.0890	0.0036	0.0036	2.3525
Nd	0.0054	0.0069	27.4423	0.0000	0.0000	
Ni	0.0129	0.0068	47.7030	0.0096	0.0041	57.1864
P	0.2430	0.5965	145.4184	0.1931	0.5085	163.3083
Pb	0.0047	0.0092	96.9771	0.0042	0.0081	91.9769
Rb	0.0225	0.0281	24.9666	0.0213	0.0248	16.0352
S	0.0939	0.3359	257.8865	0.8570	0.7688	10.2919
Si	41.6202	43.5134	4.5488	46.3150	38.6469	16.5565
Sr	0.0904	0.0850	5.9618	0.0961	0.0853	11.1678
Ti	1.0488	0.9222	12.0734	0.9532	0.8355	12.3469
Y	0.0086	0.0069	19.7906	0.0047	0.0039	15.9636
Zn	0.0191	0.0189	1.0955	0.0191	0.0206	7.6691
Zr	0.0482	0.0632	31.1935	0.0300	0.0366	22.0214
	100	100		100	100	

Table 6.5: Readings by the laboratory CRB XRF and the XRF used in this study using Sample 21 (S21) and QL.B1 which were analysed multiple times (see section 6.1.4). The difference is expressed in % (Diff in %).

Six samples test

Six unknown samples were analysed for a final test. The aim was to choose samples from two very distinct groups to assess if, despite the semi-quantitative nature of the analysis, there was a potential to observe differences and patterns in the sherds' compositions. The hypothesis was that the sherds from the same group would cluster together and separately from the other group.

The six samples were from confirmed groups. Three samples were selected from group E (Part of Fabric 1 PLM; *Crisp Ware*) and three from group B (Fabric 5 PLM; *Bricky Red Ware*). Raw percentages (with SiO_2 matrix), not normalized, of varied elements, were plotted in scatter plots. This permitted to get a first visual

representation of the data. The pairs of oxides were: FeO_3/CaO, SiO_2/CaO, Rb_2O/Nb_2O_5, Rb_2O/Nb_2O_5, SrO/ZrO_2. Four were chosen from Pirone and Tykot (2017) for the trace elements. Examples of these scatterplots are given in Figure 6.4.

The samples seem to cluster according to groups, although sample 15 plots slightly apart from the others in group E. This suggests a potential for the semi-quantitative analysis to cluster samples according to their fabric. Note that this is based on visual inspection and not a statistical test. The data can be found in Appendix D.2.2.

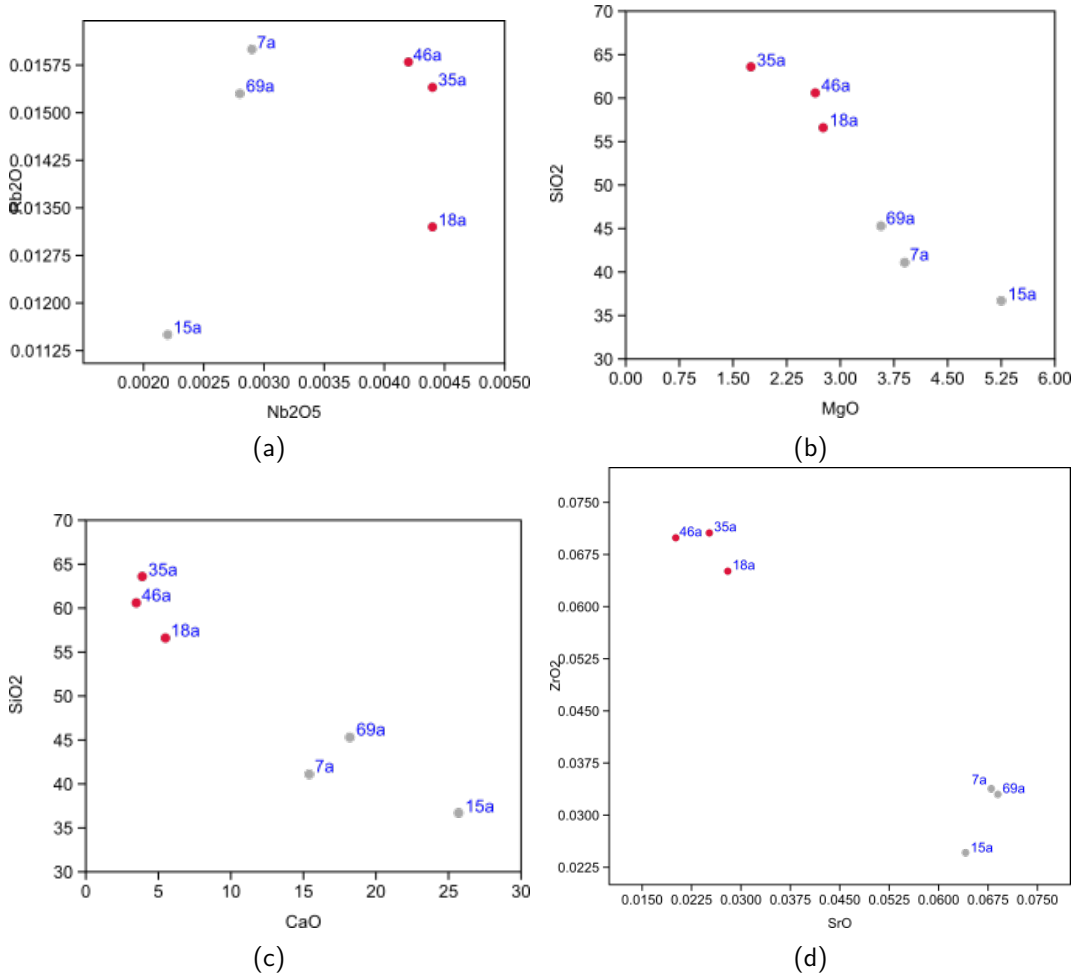


Figure 6.4: Scatterplots for the trial with six samples of untransformed and non-normalized percentages. (a):Nb_2O_5/Rb_2O; (b): $MgO/SiO2$; (c): SiO_2/CaO ; (d): SrO/ZrO_2. The red data points are group B and the gray data, group E. The readings were called "xa", x for the sample number and a signifying the first reading.

6.1.5 Choosing variables

The XRF instrument provided 44 oxides to analyse. The first step was, therefore, to remove variables which could be problematic. A preliminary list of variables was chosen not to be included in the analysis based on reasons summarised in Table 6.7. Most of these variables are trace elements. The CRB analysis results and knowledge from four references which are Barone et al. (2010; 2015), Mommsen et al. (2006), and Pirone and Tykot (2017), were used to narrow down the list of variables.The variables which were not included in the CRB analysis or any references were excluded. This also applies to variables only reported as being detected by NAA (Neutron Activation Analysis) in quantities of very low ppm and are, therefore, likely not to be detected or not correctly by XRF. Similarly, variables with more than half the data points being 0. This is most likely because of the LoD (Limit of Detection).[1]

As an example, Cobalt was analysed by Barone et al. (2010; 2015) and Mommsen et al. (2006). However, the values are very low, as seen in table 6.6. No values under 17ppm were detected for cobalt in the data set for this dissertation, and the values from the CRB laboratory were below 20ppm. Therefore, it is likely that Cobalt is not being detected in a similar situation to the CRB data because the quantities present, if at all, are below the detection limits of the instrument.

BaO and V_2O_5 were removed at a later stage, considering that the datasets contained many zero values. PbO was removed due to its inconsistency with CRB laboratory readings and its weight on the analysis.

	CRB	Mommsen et al. (2006: 85) SILA	Barone et al. (2015: 107) Maltese material
$\overline{x}$	NA - <20ppm	13.7	5.5
s		1	3.3

Table 6.6: Comparison of values for Cobalt in different dataset

[1]Ideally, the LOD is reported, as they allow assessment of the data (Hall 2016: 352). However, the LOD for elements could not be provided by the laboratory where the XRF was used, which is a limitation of this analysis.

Variables	Possible problems with the readings	No reference values in Maltese literature	No reference values in CRB or below CRB LOD	Likely below LOD	Contains more than 50% 0s	Only 0s
As_2O_3		Only NAA reference	✓	✓	✓	
Bi_2O_3		✓	✓	✓		
Br		✓	✓			
CdO		✓	✓			
CeO_2				✓		✓
CoO				✓	✓	
Cu				✓		✓
$Cs2O$						✓
O						✓
GeO_2		✓	✓		✓	
I		✓	✓		✓	
La_2O_3						
MoO_3		✓	✓			
Nd_2O_3	✓	Only NAA reference	✓			
Pr_6O_11						
Sb_2O_3	✓	Only NAA				
SeO_2		✓	✓			
SnO_2	✓	✓	✓			
Ta_2O_5				✓	✓(only two readings)	
Te				✓		
WO_3				✓		✓

Table 6.7: Variables excluded from analysis

6.2 Elemental composition: Data analysis

Data transformation, cleaning and descriptive statistics were performed using spreadsheets. The correlation analysis, scatterplots and Principle Component Analysis were carried out with the software Past 4.10 (Hammer et al. 2001) and the cluster analysis with RStudio.

6.2.1 Data transformation

The data were first normalized, with normalization defined by Baxter (2016: 30): the data was scaled to 100%. Oxides are given in percentages when extracting the data from the instrument; however, because of uncertainties, measurement mistakes, or rounding up, the sums are rarely 100%. For example, the sum of all variables for sample 1 is 99.960%. To ensure that the data is scaled exactly on the same constant, they were normalized to 100%. The formula applied for normalization is:

$$y_{ij} = \frac{x_{ij}}{\sum_i} \times 100$$

During normalization, the variable Na_2O (Sodium Oxide) was removed, and the data was re-normalized without it. Na_2O (Sodium Oxide) is the lightest element that the XRF can detect and is prone to error, especially when sample preparation is not optimal. Na_2O caused variations in the major elements of the dataset and was therefore removed before normalization.

Data transformation rationale

XRF datasets are compositional datasets expressed in weight percentages and, by convention, in part per million for trace elements. This means that the variables, here the oxides, are "expressed as part of a whole" (Rollinson and Pease 2021: 20), which is here 100%. This creates the *constant sum* problem and means that the

data is always expressed in relation to this constant (100%). This can affect the data analysis, including imposed correlations on the dataset (Rollinson and Pease 2021: 23). This also causes the dataset to be closed, meaning that the variables are not free to vary within an unlimited range of values.

Statistical analysis of XRF data often involves sub-compositional datasets. Studies rarely include all the measured variables, as some might be prone to analytical error because of instrumentation or contamination. This sub-compositional dataset in only a portion of the data and does not add up to 100% (López-García et al. 2018: 105), which is the case in this study where only 20 variables out of 44 were analysed. Aitchison et al. (2002: 297) have reviewed at length the theoretical and practical considerations of dealing with sub-compositional datasets and state that classical data analysis could be misleading if the data is not being transformed. They take the example of the lack of "sub-compositional coherence" (Aitchison et al. 2002: 296), highlighting that with closed data, statistical analysis of a selected set of variables can lead to drastically different conclusions than when carried out with all variables.[2] Different techniques have been used to open the dataset, and these are reviewed by López-García et al. (2018) where they discuss standardization, logarithmic transformation, and log-ratios. Mathematically, it is argued that log-transformed ratios (additive, centred or isometric) are one correct way to transform the data to keep them coherent sub-compositionally (Greenacre 2018). Other researchers have used log-transformations to base 10 (Glascock 1992), which has been deemed by Aitchison et al. (2002: 302) as correct for trace elements.

Baxter and Freestone (2006) and Baxter (1995) have been proponents of data standardization to explore patterns rather than more complicated transformations. They highlight the practical use of this data transformation method to visualise data structure using PCA. In their paper, Baxter and Freestone (2006) use datasets of glass compositions to demonstrate that taking absolute standardized data is often enough to uncover data structure and answer archaeometric research questions. Another problem is that log-ratio transformed data are complex (Greenacre 2018: 19), and researchers might struggle to understand the ramifications and impact of

[2]Sub-compositional coherence is explained and illustrated in detail by Greenacre (2018: 5-6).

the data transformation. Baxter's practical approach is to state that, despite the limitations of these non-logged data, they can still be used to answer archaeological questions.

Standardization follows the formula by Baxter and Freestone (2006: 514):

$$y_{ij} = \frac{x_{ij} - \overline{x}_j}{s_j}$$

where $\overline{x}$ is the mean of variable j and s_i is the standard deviation of variable j. x_{ij} denotes one observation for case i and variable j. This allows all variables to have a similar scale or magnitude and, thus, a similar impact on the PCA analysis.

Data transformation in this study

To tackle the research aims on fabric classifications and provenance, different questions were investigated during the data analysis:

- Can the microscopic/macroscopic observations and groups (i.e. fabric classification) be corroborated by elemental analysis?
- Can these sherds be compared to local raw materials, and can this analysis provide indications about their potential provenance?

Based on these questions, two sets of analyses were performed. Two datasets were analysed subsequently. The first dataset contained the readings for the pottery sherds composition (Dataset 1) to analyse fabric classification. The second dataset contained readings for pottery sherds and the compositions of the raw materials (Dataset 2). To simplify intext, the raw materials will be termed *clays*.

The data was standardized following the formula Baxter and Freestone (2006: 513). Since the analyses were performed on two different datasets (datasets 1 and 2) and the standardization formula includes the standard deviation for all cases, this produces two standardized datasets. The final datasets used for analysis are in Appendix D.2.4. The raw data and transformation steps are given in the appendices

D.2.5 and D.2.8 (Digital).

6.2.2 Analyses

Descriptive statistics

The mean ($\overline{x}$), sample standard deviation (s) and coefficient of variation (CV) are given for the final variables for both the pottery and the raw material groups. These were computed on the normalized but not standardized data (see digital appendix D.2.5). The CV allows variation to be comparable even between trace and major elements. To follow conventions and allow comparison with literature, the data is presented in % for the major and minor oxides and ppm for minor elements (converted from oxides) for the descriptive statistics.

In further analyses, however, all data are in the same units (%) as advised by Hall (2016: 352). Scatterplots of selected pairs of oxides are then presented to highlight the potential of a few variables to discriminate between groups but also the complexity of the dataset and the need for multivariate analysis.

Correlation

Correlation between variables was tested for Dataset 1. A correlation matrix was produced with the selected variables. The PAST software tests for the Spearman correlation for each pair of variables and is used here as a non-parametric equivalent for Pearson correlation. In correlation analysis, a correlation coefficient (ρ), here, Spearman's rho, is calculated and then tested for statistical significance. The coefficient varies between -1 and 1, with -1 indicating a negative correlation and 1 a positive correlation, whilst 0 indicates there is no correlation.[3] The software then tests for the following (simplified) hypotheses:

[3] A positive correlation means that when one variable increases, the other increases. A negative correlation means that when one variable increases, the other decreases.

H_0: The two selected variables are independent.

H_1: The two selected variables are not independent (and therefore correlated).

This is tested with a 0.05 level of significance, meaning that for H_0 to be rejected, the *p*-value should be less than 0.05. This test is carried out to begin understanding relationships between variables. Highly correlated variables will likely have strong loadings on the same components in PCA. Strong positive correlations could also indicate that two variables are part of similar components (e.g. specific minerals) in the pottery sherds.

Principle component analysis (PCA)

PCA is a technique of data reduction which allows visualising a dataset with a high number of variables into a reduced number of dimensions. Every sample has 20 dimensions corresponding to the 20 oxides selected for analysis. Looking for patterns of similarities and differences using these many variables as such is not possible.

PCA transforms these dimensions into 20 Principal Components (PCs). These components are worked from the correlation matrices between variables. The first components carry most of the variations in the data, meaning that most of the dataset can be explained with the first few PCs (instead of 20 variables). The first components aim to explain as much variability of the dataset possible (Drennan 2009: 300-301), which allows visualising most of the variation in the data in two or three dimensions. Detailed explanations on PCA can be found in Baxter (2016) and Rollinson and Pease (2021).

PCA was carried out for Dataset 1 and twice for Dataset 2, as some outliers had to be removed. The methodology is illustrated in Figure 6.5. Scatterplots of the two first PCs were produced for visualisation.

Hierachical cluster analysis (HCA) on PC scores for Dataset 2

HCA had been performed on Dataset 2. However, no solid new patterns emerged from these analyses. Clustering methods were then used on the PCA results of Dataset 2. HCA was carried out on the Principle Component scores from the final PCA of Dataset 2. The *scores* are the new coordinates for each sample generated during the PCA and can be treated as a new dataset. These scores are given in appendices D.2.8 (digital) and in table D.8.

This analysis aimed to classify the samples systematically and as objectively as possible, using the PCA results rather than drawing ellipses with tentative groupings on the PCA scatterplots, as is often done in the archaeological literature.[4]

HCA is explained by Baxter (2016) and Baxter (2008: 63), Drennan (2009: 308) and Papageorgiou (2020: 7-8) who detail the different clustering methods. There are many methods available, and to choose between them, the agglomerative coefficient (AC) for each method was calculated using RStudio (Table 6.8). Generally speaking, when the AC is close to 1, a clustering structure is identified (Kaufman and Rousseeuw 2009: 213).

Since both the Average, Complete and Ward methods had values close to 1, the Average and Complete link methods were used because they are often cited in the archaeometric literature. Baxter (2016) mentions that the average link method is one of the most used in the literature, whilst Drennan (2009: 315) argues that for sourcing raw material, the complete link method is most likely used used. Average-link clustering re-calculates a matrix after each pairing and treats the newly created cluster as any other case (Drennan 2009: 313, see 308-305 for complete case studies comparing the methods); whilst complete-link clusters use the "largest distance between two cases" (Baxter 2016: 65). Baxter (2016: 65) advises running different clustering methods and comparing the results to assess the limitations of the methods.

HCA was run using the complete and average link methods and plotted in two

[4] see section 2.2.2 with the Bronze Age case study, where the graph ellipses are suggestions from the authors

Method	average	single	complete	ward
Agglomeration coefficient	0.9132891	0.7603442	0.9519531	0.9803138

Table 6.8: Agglomerative coefficient (AC) calculated using the Agnes R package for each clustering method.

dendrograms. Clustering methods work with similarity matrices; the output is often a dendrogram representing distances between points. One major challenge of HCA is to assess the correct number of clusters to keep as the dendrogram can be cut at any level.

One method to assess the number of groups is the silhouette method. Silhouette coefficients are calculated to know how well one point fits into a cluster. Calculating these coefficients for a different number of clusters (k), the results can be plotted into a silhouette average plot (Kaufman and Rousseeuw 2009: 41). The dendrograms and the silhouette graph are presented and interpreted in section 7.3.3.

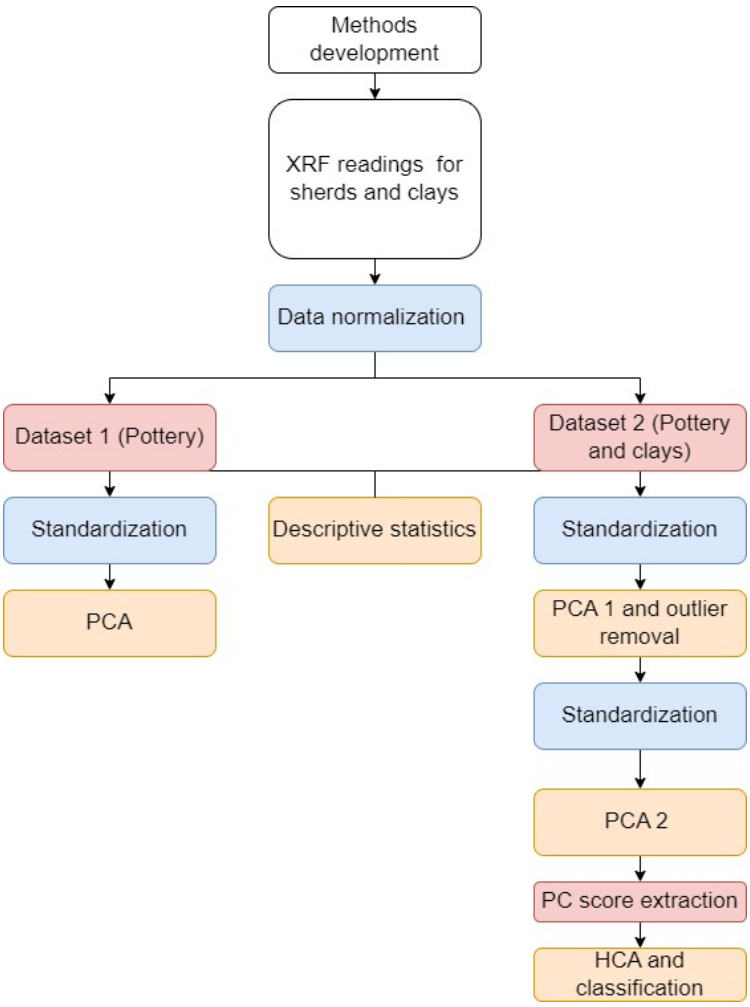


Figure 6.5: Flowchart, presenting the sequence of data treatment statistical analysis. orange: Analysis; Blue: data transformation; Red: Dataset used.

6.3 Experimental archaeology

One hypothesis developed throughout the PCA and HCA that Terra Rossa could have compositional similarities with group B, the cooking vessels (see section 7.3.2). To test this hypothesis further, experimental briquettes with the raw materials LP.A1 and LP.A2 were manufactured (Figure 6.6). The methodology followed the Standard Operating Procedure established by Vella and Richard-Trémeau (2021b). The experimental briquettes were fired at 500°C and were sent to PLM analysis, where they were prepared and analysed using the same methodology described in section 4.4.

In discussing this research in sections 9.1.1 and 8.3, unpublished results of experimental archaeology carried out at the Department of Classics and Archaeology project CoFIPoMS (University of Malta 2021) are mentioned. The manufacture of these briquettes is not described here, as these experiments were carried out outside the scope of this dissertation. Two sub-projects were led: an undergraduate engineering dissertation by Xuereb (2021), accessible online, and an internship project led by Kellian Coste (Results are not accessible). During the internship, briquettes were manufactured, and the results have yet to be thoroughly analysed. The briquettes were made of Globigerina marls, Blue Clay with grog, Blue Clay mixed with Globigerina red soils, Blue Clay mixed with Globigerina marl and Blue Clay briquettes manufactured with seawater. The Blue Clay used was similar to the Bue Clay used in Xuereb (2021: QL.B1), which had been earlier sieved.



Figure 6.6: Photograph of Terra Rossa briquettes during drying. Slabs are made of four briquettes to allow measuring shrinkage

Chapter 7

Results and preliminary interpretation

7.1 Descriptive statistics

The mean ($\overline{x}$), sample standard deviation (s) and coefficient of variation (CV, expressed in %) are given in Table 7.1. First, the CV of pottery and clays for each oxide/element differ, although they are similar for CaO, Cr, Nb, Rb, Sr, Zn. The composition of the sherds, as a group, seems to be more homogeneous than the clays for the major elements: Al_2O_3, Fe_2O_3, SiO_2. These elements make up the bulk of the composition of these samples, Al_2O_3 and SiO_2 are the major components of clay minerals. The highest CVs and, therefore, the highest variations for the trace elements are Ni, Sr, Zr, Cr and Cu for the pottery sherds. However, Cr and Cu variations might be caused by the instrument (see section 6.1 on precision and accuracy). This pattern is similar for the clays, except for Zr and Y. These elements are possibly the elements that could help discriminate between groups of samples.

The same measures of location and dispersion are provided for each microscopic group (A-F, section 5.3) in Table 7.2. Putting aside groups A and F, which only had two samples, groups B and C have less variation in CaO than groups D and

E. It was mentioned in sections 5.3.2 and 5.3.3 that groups D and E had a wide range of matrix colours and differing amounts of calcareous components in the matrix. The CVs for SiO_2 are low, except for group C. Groups A and B have a high SiO_2 content, possibly because of the fine quartz in the matrix (sections 5.3.7 and 5.3.5). The CV for Fe_2O_3, iron(III) oxide, is similar across groups.

	Pottery			Clays		
	$\overline{x}$	s	CV	$\overline{x}$	s	CV
Al2O3	14.23	1.41	9.94	11.92	2.92	24.46
CaO	14.13	7.76	54.96	23.89	13.76	57.63
Fe2O3	7.66	0.64	8.30	6.49	1.70	26.16
K2O	2.59	0.67	26.03	2.48	0.45	18.04
MgO	3.10	1.28	41.29	3.30	1.01	30.53
MnO	0.10	0.07	71.94	0.05	0.02	37.87
P2O5	0.86	0.19	21.98	0.75	0.06	7.81
SiO2	55.19	8.10	14.69	47.98	10.14	21.13
SO3	0.54	0.15	27.37	1.30	0.76	58.15
TiO2	0.98	0.16	16.78	0.79	0.19	23.79
Cr	130	72	55.5	135	76	56
Cu	25	15	59.0	28	31	113
Ga	25	7	26.7	27	11	42
Nb	26	5	20.4	21	5	23
Ni	38	19	48.8	32	29	89
Rb	148	35	23.9	143	29	21
Sr	472	211	44.8	615	289	47
Y	38	6	17.0	30	11	38
Zn	120	18	14.8	108	19	17
Zr	420	181	43.1	274	78	28

Table 7.1: Descriptive statistics for the pottery sherds and Clays. These were carried out before the transformation of the data. Major and minor elements are expressed respectively as oxides in weight per cent and trace elements as elements in ppm to allow comparison with the literature. These are carried out on the data before data standardization.

	Group A, n=2			Group B, n=14			Group C, n=6			Group D, n=8			Group E, n=6			Group F, n=2		
	$\overline{x}$	s	CV	$\overline{x}$	s	CV	$\overline{x}$	s	CV	$\overline{x}$	s	CV	$\overline{x}$	s	CV	$\overline{x}$	s	CV
Al2O3	14.20	1.70	11.96	14.52	1.00	6.91	13.39	1.13	8.41	14.78	1.30	8.79	12.54	1.95	15.59	14.20	0.40	2.83
CaO	14.78	2.75	18.61	13.63	5.19	38.07	21.08	6.27	29.73	13.00	9.17	70.52	12.19	6.44	52.82	21.81	3.68	16.89
Fe2O3	7.52	1.24	16.48	8.19	0.53	6.47	7.18	0.54	7.46	7.64	0.56	7.29	7.33	0.42	5.77	7.05	0.28	3.99
K2O	1.48	0.17	11.48	2.67	0.59	22.05	1.67	0.49	29.33	2.98	0.33	11.07	2.78	0.12	4.32	2.81	0.04	1.47
MgO	1.59	0.24	15.13	2.31	0.85	36.68	4.20	1.94	46.24	3.15	0.83	26.41	3.23	1.67	51.69	4.10	0.29	7.04
MnO	0.28	0.01	4.37	0.17	0.09	51.21	0.05	0.01	10.98	0.08	0.01	13.86	0.07	0.03	45.40	0.05	0.01	14.86
P2O5	0.48	0.01	3.10	0.71	0.06	8.56	1.14	0.14	12.35	0.84	0.08	9.91	0.96	0.07	7.08	1.06	0.16	14.65
SiO2	71.11	3.67	5.16	63.81	3.85	6.04	44.48	4.99	11.22	53.63	3.96	7.39	50.43	2.54	5.03	50.88	1.59	3.13
SO3	0.32	0.02	5.51	0.45	0.09	19.51	0.69	0.11	15.96	0.55	0.17	30.94	0.62	0.08	12.96	0.61	0.05	7.55
TiO2	1.31	0.01	1.07	1.17	0.13	10.70	0.81	0.05	6.74	0.93	0.03	2.88	0.87	0.08	8.89	0.87	0.05	5.93
Cr	115	88	76	140	84	60	100	36	35	142	69	49	107	89	84	163	43	26
Cu	12	6	47	29	11	39	21	18	113	31	16	52	24	11	46	5	7	141
Ga	18	0	0	25	4	17	21	3	16	28	8	30	23	5	21	19	0	0
Nb	33	2	6	30	4	14	21	4	18	27	5	17	21	2	10	23	1	7
Ni	16	4	24	39	13	34	28	13	52	48	22	45	36	12	33	22	1	3
Rb	130	12	9	154	21	13	80	14	17	168	19	11	154	17	11	164	4	2
Sr	90	10	11	230	75	33	706	101	14	542	120	22	560	78	14	576	8	1
Y	46	1	2	40	6	16	37	4	11	41	5	12	32	4	12	30	3	9
Zn	94	11	11	111	19	17	133	21	16	125	15	12	124	14	11	109	3	3
Zr	959	99	10	555	164	30	272	60	23	387	42	11	277	76	28	322	52	16

Table 7.2: Descriptive statistics for each microscopic group of sherds (A-F). n= number of samples in the group.

7.2 Bivariate analysis

7.2.1 Correlation analysis

Figure 7.1 presents the Spearman correlation matrix for Dataset 1. The full results are available in Appendix D.2.3. In the matrix, all the non-statistically significant correlations were omitted. Red ellipses represent negative correlations and blue ellipses positive correlations. The thinner the ellipse and the stronger the colour, the stronger the correlation coefficient.

There are strong relationships between most major elements. Aluminium oxide and iron oxide have different patterns from the other major elements; the correlation coefficients are not as strong as other correlations. For instance the ρ between Al_2O_3 and Fe_2O_3 is 0.64 whilst ρ between CaO and SiO_2 is -0.94 (see Appendix D.2.3). This last correlation shows that the more CaO (mostly from carbonate materials such as calcite) in a pottery sherd, the less SiO_2 (from clay minerals and quartz).

Since the XRF was not calibrated for matrix effects, correlations might be obscured by matrix effects or forced upon by the instrument's calculation algorithm. However, when looking at trace elements, for instance, SrO has a strong positive relationship with CaO. Pirone and Tykot (2017: 214) observed that the clays collected close to limestone had higher content in strontium. This can be explained, at least to some extent, by a substitution phenomenon in calcite minerals where *Sr* sometimes replace *Ca* in calcium carbonate (Finch and Allison 2007; Turi et al. 1990).[1]

Other relationships with trace elements need to be better understood. However, this is beyond the scope of this dissertation as this requires expert knowledge in geochemistry. One example is the strong positive correlation between SiO_2, TiO_2 and ZrO_2.

[1]Other substitutions in calcite are known such as Fe, Mg, Mn, Ba, Co, Zn (Alderton 2020: 385)

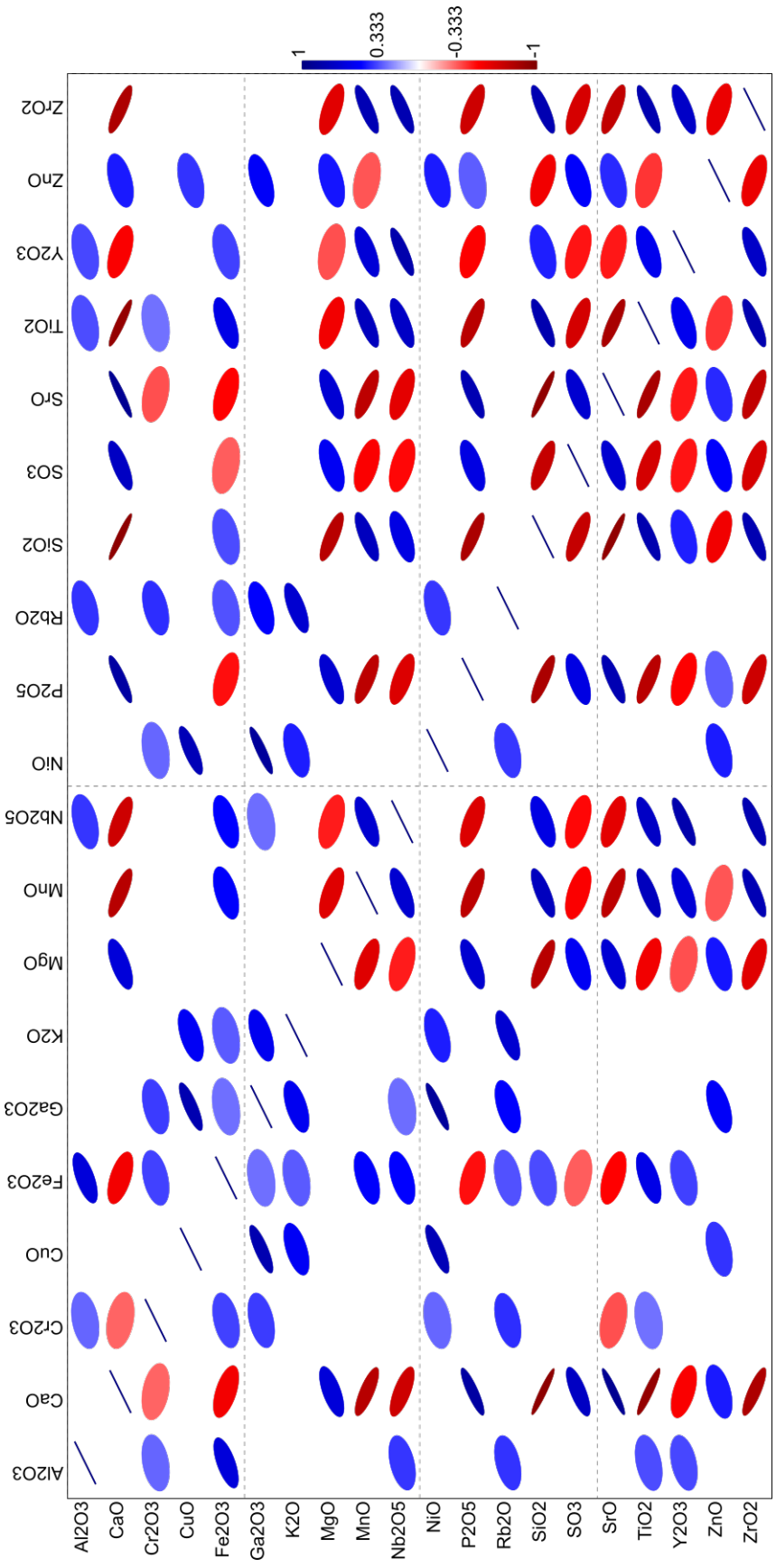
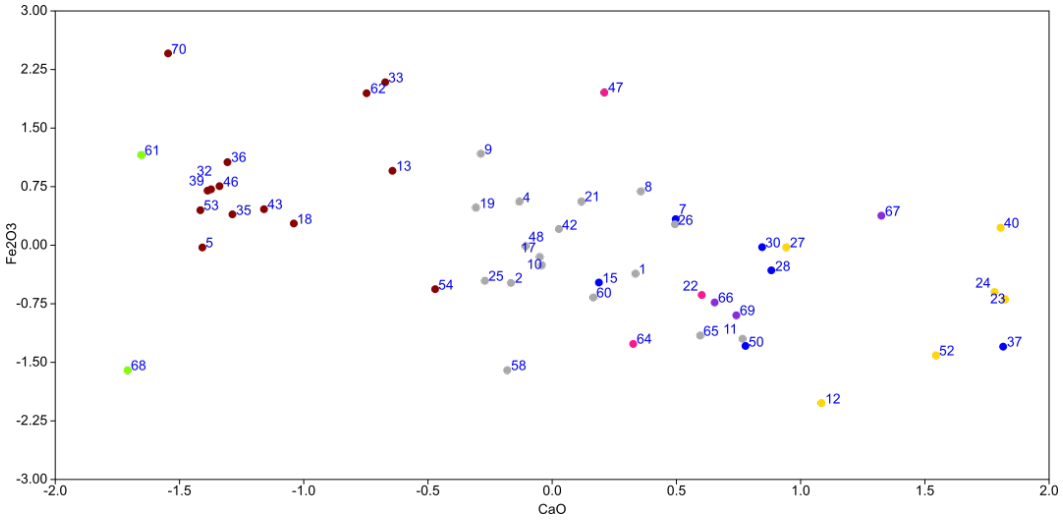


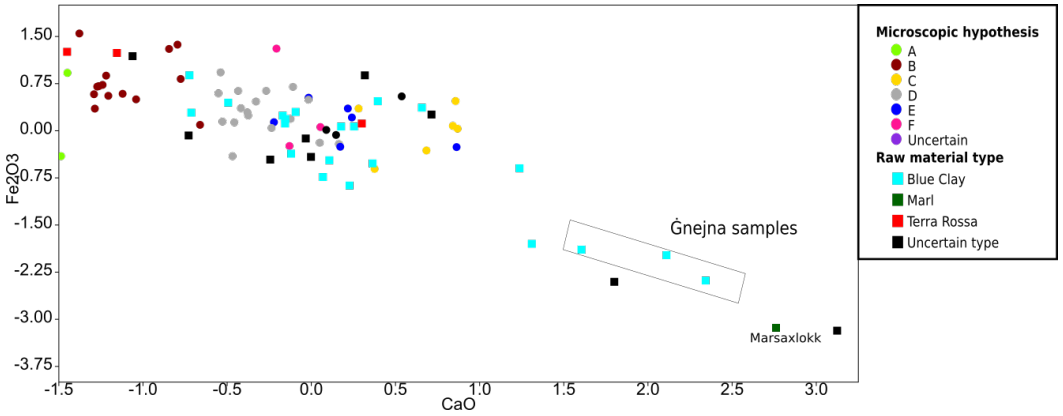
Figure 7.1: Correlation matrix, Spearman correlation, for all variables

7.2.2 Bivariate scatterplots

A few scatterplots of pairs of variables are presented to assess the potential of some variables in discriminating between sherd groups and clays. Both datasets 1 and 2 are used in the scatterplots.



(a) Scatterplot of CaO and Fe_2O_3 for dataset 1. Caption is the same as below.



(b) Scatterplot of CaO and Fe_2O_3 for dataset 2 (with outliers). Squares are the clays, and dots are the pottery sherds.

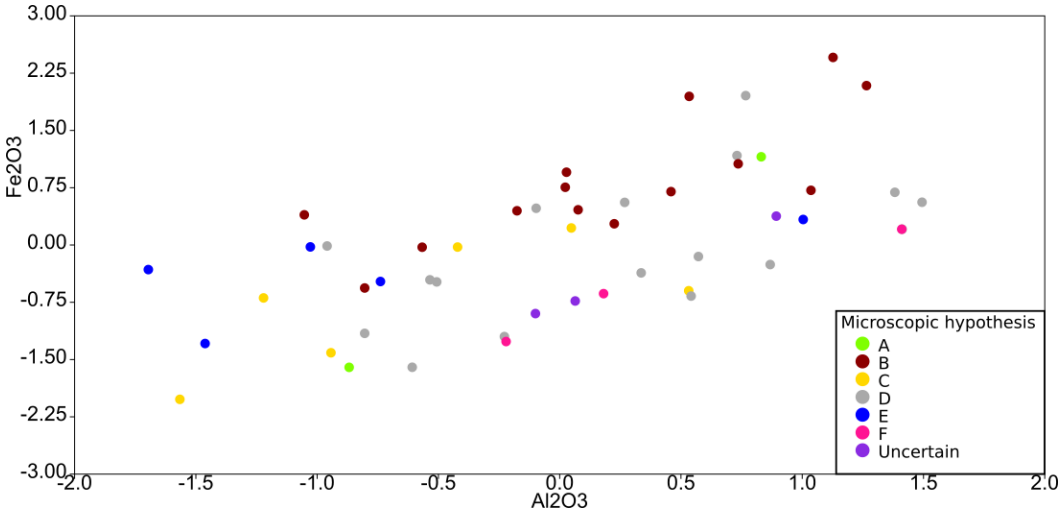
Figure 7.2: Scatterplot of CaO and Fe_2O_3 for both datasets

The graphs in Figure 7.2a and Figure 7.2b plot CaO against Fe_2O_3. For Dataset 1, as expected, CaO discriminates between some of the groups with group B, the red vessels, being depleted in CaO and Group C, the yellow or white, friable vessels, being rich in CaO. However, iron is not as discriminating for the pottery groups. Sample 68, the fine carinated bowl from Żejtun, has an unexpected result as it is depleted in iron despite its colour (orange).[2]

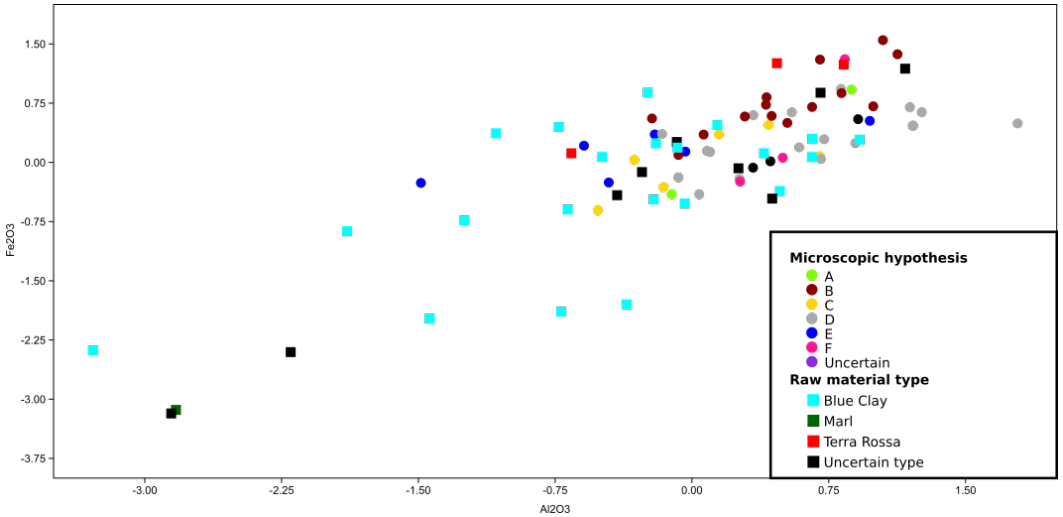
[2]This would have to be confirmed with additional reading.

For Dataset 2 (Figure 7.2b), the Blue Clay samples group well with groups E, F and, to some extent, C and D. The Globigerina marl sample from Marsaxlokk, MX.A1, and other calcium-rich samples (mainly from Ġnejna Bay) group in the bottom right of the plot. It might indicate that the Ġnejna samples (GNB.A1-F1-E1) are closer in composition to the Limestone marl than Blue Clay.

Aluminium and iron oxides are plotted in Figures 7.3a and 7.3b. There seem to be variations in the data, but these are not related to microscopically observed fabric. In Figure 7.3b, the variations in values are obscured by the low content of iron and aluminium in the same clays.

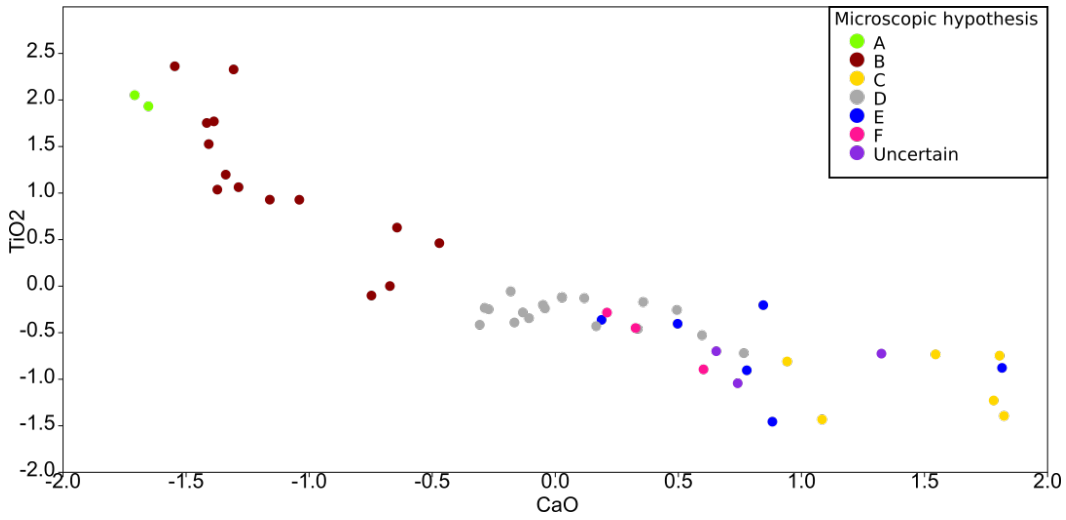


(a) Scatterplot of Al_2O_3 and Fe_2O_3 for the Dataset 1. Cases 26 and 37 were excluded of the graphs because they were outliers

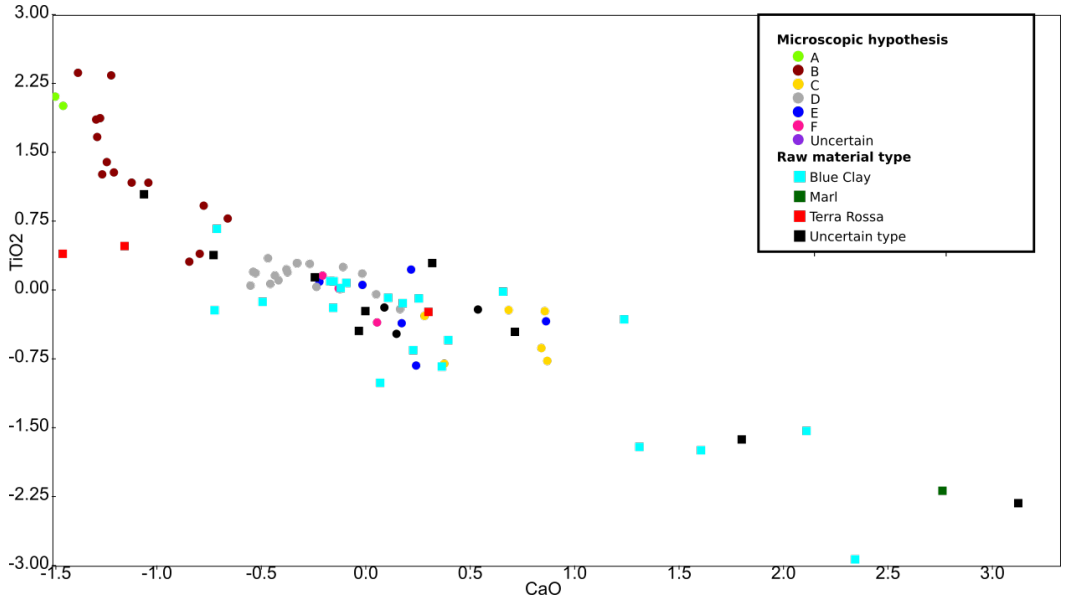


(b) Scatterplot of Al_2O_3 and Fe_2O_3 for Dataset 2. No cases were removed

Figure 7.3: Scatterplots of Al_2O_3 and Fe_2O_3 for both datasets



(a) Scatterplot of TiO_2 and CaO for Dataset 1.



(b) Scatterplot of TiO_2 and CaO for Dataset 2. No cases were removed

Figure 7.4: Scatterplots of TiO_2 and CaO for both datasets

Plotting titanium and calcium oxides in Figure 7.4a, there is discrimination between the groups by both variables. The fabric group B is rich in titanium and depleted in calcium, and group D appears to sit in the middle. The clays' TiO_2 content is strongly correlated with SiO_2 (Figure 7.1), so the patterns would be expected to be similar. For trace elements, in figure 7.5, ZrO_2 seem to set groups A and B on top of the graph. However, group B does overlap with group D. Rubidium, on the contrary, appears to be a good discriminator for Group C.

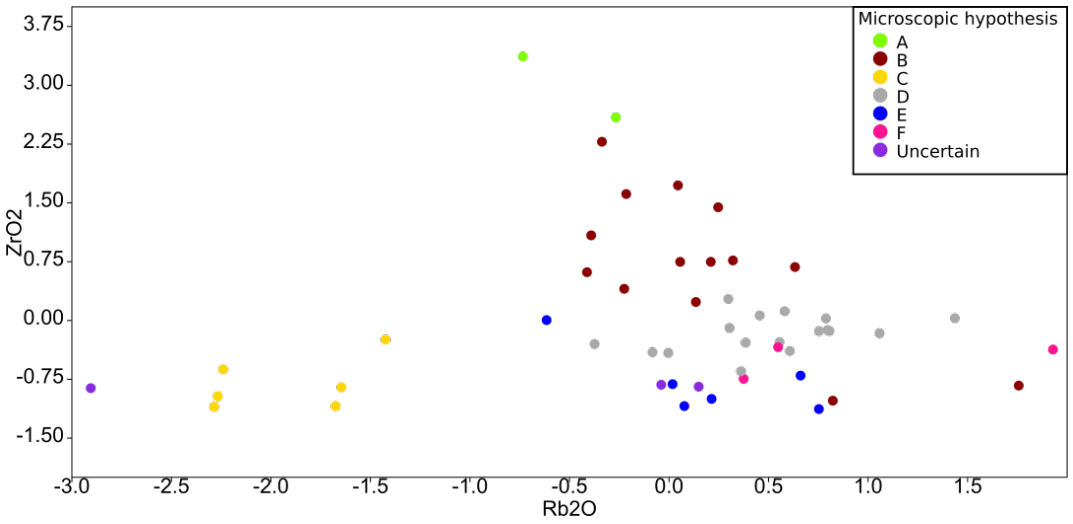
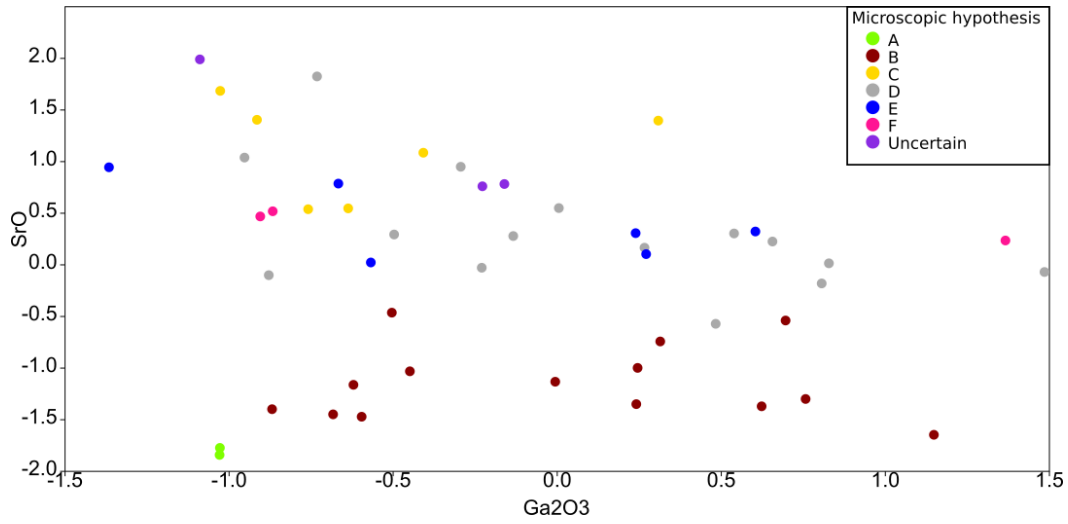
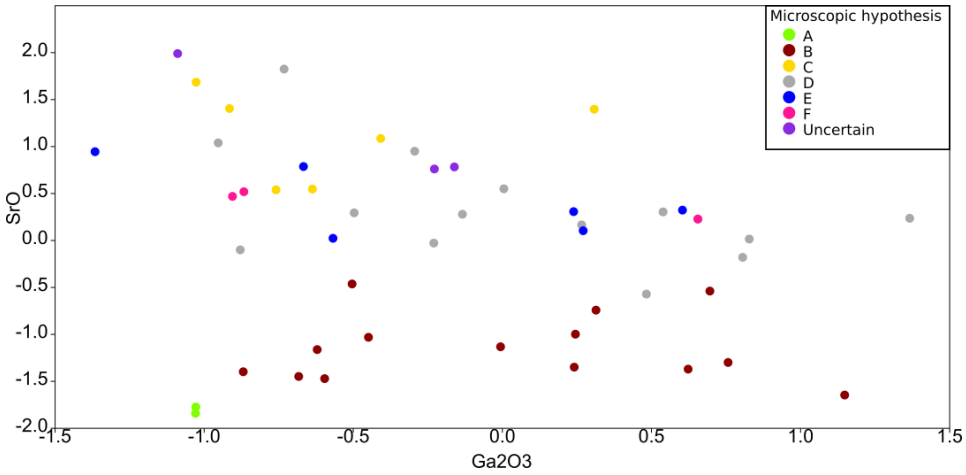


Figure 7.5: Scatterplot of ZrO_2 and Rb_2O for the Dataset 1.



(a) Scatterplot of SrO and Ga_2O_3 for the Dataset 1. The outliers for gallium were removed (60, 1, and 9)



(b) Scatterplot of SrO and Ga_2O_3 for the Dataset 2. One outlier of Ga removed (GNB.E1)

Figure 7.6: Scatterplots of SrO and Ga_2O_3 for both datasets

In Figure 7.6b, the Ga_2O_3 content varies, but it does not seem related to fabric groups. SrO seems to discriminate between the groups of sherds. This discrimination could be explained by its correlation with CaO as depicted in Figure 7.1. Some samples of marl material and a few samples of pottery and marl seem to have high strontium and high gallium values. This is interesting because if the gallium variations do not represent fabric, they could be associated with diversity in the clays and possibly be associated with provenancing.

To summarise, there is potential for some variables to discriminate between fabric groups and group sherds with clay samples. However, some variations observed in the graphs do not seem related to the fabric groups of the sherds. These patterns should be explored with multi-variate techniques.

7.3 Multivariate analysis

7.3.1 PCA for Dataset 1

The first analysis presented is a Principle Component Analysis (see Section 6.2) on Dataset 1.

Describing the Principle Components (PCs)

After running the PCA, based on the correlation matrix, table 7.3 shows that the cumulative sum in table 7.3 shows that the first 3 PCs explain 72.1% of the variation in the data. Four Principle Components (PCs, see section 6.2) have Eigenvalues higher than 1, which is one accepted threshold to assess how many PCs could be investigated furher (Sheytanova 2015; Zwick and Velicer 1986).[3] The scree-plot (blue line), in Figure 7.7, tends to indicate that the first three PCs could be explored further, being located before the scree plot elbow (Sheytanova 2015; Zwick and Velicer 1986) and the broken stick (red line) that two PCs explain most of the variations in the data.

The loadings for each PC are in Appendix D.2.4. As the loadings can be challenging to interpret, a loading plot with four PCs is shown in Figure 7.8. For each PC, the loading of each variable is represented.[4] The longer the negative or positive bar, the stronger the loading. For instance, PC 1 is highly correlated with 10 variables with $CaO, SiO_2, SrO, ZrO_2, TiO_2, P_2O_5$ having the highest loadings, which were correlated with the Spearman test already (section 7.2.1). Trace elements such as Ga_2O_3, NiO and CuO dominate PC 2. Most variables correlate with the two first PCs, with Al_2O_3 having a high loading in PC 3. Since a PCA scatterplot can only represent 2 PCs at any time, variables that have a high loading in the other PCs, such as aluminium oxide in PC 3, might be under-represented in the scatterplot.

[3] See Drennan 2009: 302-303 for an explanation of PC and Eigenvalue.

[4] Loading represents how correlated one variable is to the PC, see Drennan 2009: 303 for examples.

PC	Eigenvalue	% variance	Cumulative sum for variance %
1	8.39679	42	42
2	4.06352	20.3	62.3
3	1.95478	9.8	72.1
4	1.71572	8.6	80.7
5	0.939896	4.5	85.4
6	0.706007	3.5	88.9
7	0.530461	2.7	91.5
8	0.501953	2.5	94.0
9	0.291681	1.5	95.5
10	0.221785	1.1	96.6

Table 7.3: Eigenvalues for the 10 first PCs (out of 20) as well as variance and cumululative variance (in %)

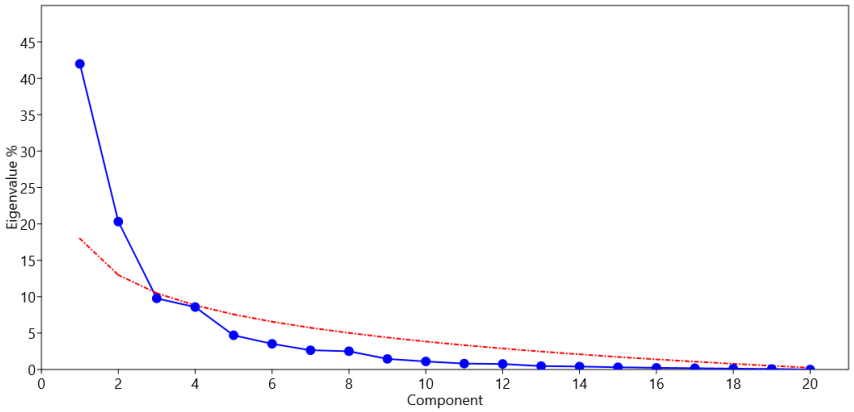


Figure 7.7: Screeplot (Blue line) and broken stick (red line) for the PCA of dataset 1. This method is based on ordering the Eigenvalues of each PC in decreasing order to assess which PCs are to be retained for analysis. The elbow of the curve (here at PC 3) is often used as a threshold(Sheytanova 2015; Zwick and Velicer 1986)

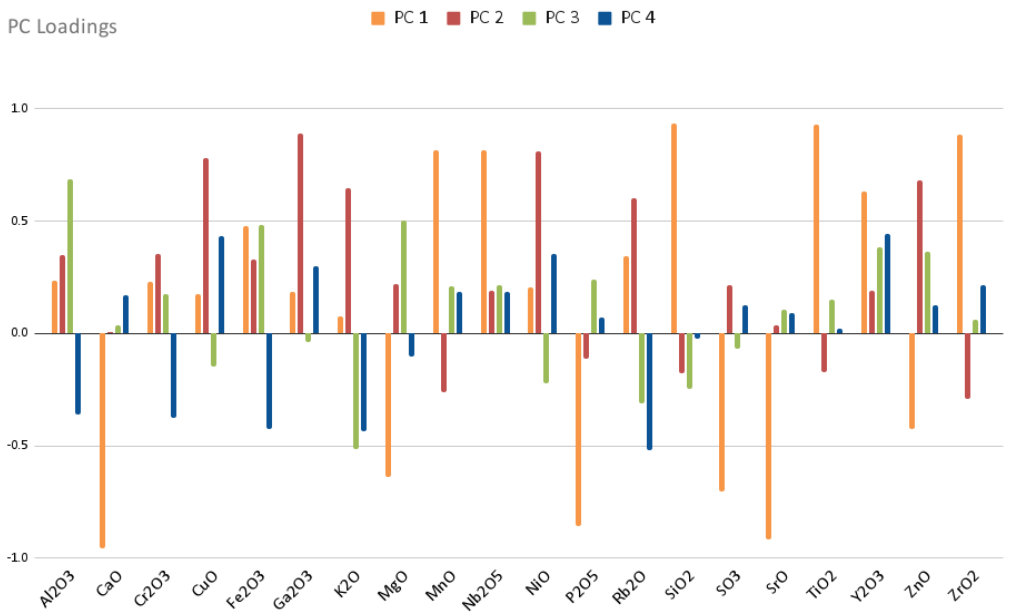


Figure 7.8: Bar chart of the loadings for each variable for the four first PCs. Data in Table D.4, Appendix D.2.4

Scatterplot

The scatterplot of the two first PCs is shown in Figure 7.9. Similarly to the scatterplots in section 7.2.2, it was decided to colour the cases (samples) according to the groups created during microscopy. Two things are necessary to keep in mind when reading this graph. Firstly, although the dots were coloured according to their group; it does not play an active role in the analysis. Secondly, the patterns observed in PCA are always subjective to some extent (Hall 2016). PCA allows visualisation but does not test the groups themselves.

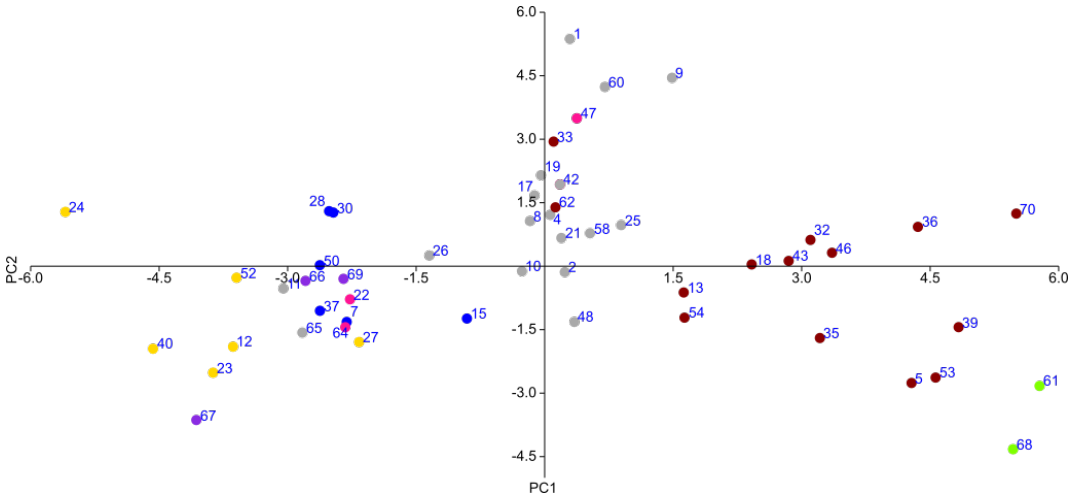


Figure 7.9: Scatterplot of PCs scores for PC1 and PC2

First observations and discussion of PCA

For groups A, B and D, some patterns are visible.

Group B (≈ Fabric 5; cooking fabric): Group B displays variation within the group itself. Different raw materials, provenances or inclusions/tempers could cause the variations. However, the samples cluster in the same part of the plot. Variations in coarse vessels would be expected, even within one vessel, due to the heterogeneity of samples. The PCA plots seem to confirm that the cooking vessels can be considered, for now, as one fabric group. Samples 33 and 62 are not cooking vessels (sections 5.3.4 and 5.3.6), and the XRF analysis confirms the petrographic analysis stating that these two samples have a different fabric than the cooking vessels. Compositionally, they are closer to group D rather than B. Typologically, macroscopically and microscopically, they are different from both B and D.

When looking at the different forms in group B, it is notable that Anastasi form C3; Quercia form C, and to some extent Quercia B1-3, seem to group more or less by form; with the exception of sample 35 and 54. Sample 13 is Quercia type A. This display is only exploratory, however, the link between specific forms and composition could be investigated in future research.

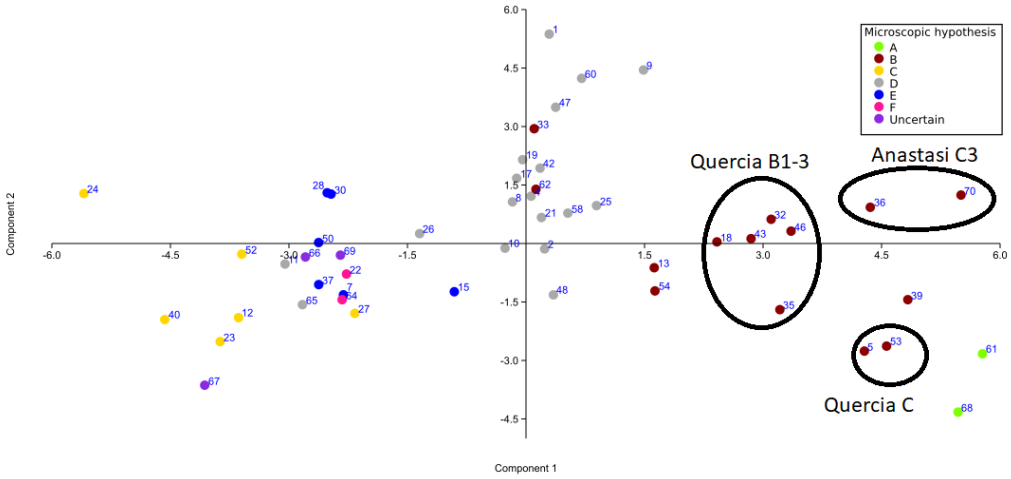


Figure 7.10: Scatterplot of PCs scores for PC1 and PC2, ellipses are not statistically determined and are only here to improve readability.

Group A (= Fabric 7, fine vessels): The results are consistent with the PLM and microscopic analyses where the two samples group together but display differences. Group A (green dots) is closer to group B than groups C-F on the PCA plot. It was expected as their matrix is similarly iron-rich and contain fine quartz (sections 5.3.5 and 5.3.7). The distance between samples 61 and 68 is also consistent with what was observed in the bivariate analysis (section 7.2.2). Their elemental composition, for instance, iron(III) oxide, differs, but this would need to be confirmed by additional readings.

Group D ($\approx$ Fabric 2): Group D (grey dots) seems to have internal variation. However, most samples cluster together in the graph. Therefore, there seems to be a good consistency with the other analyses where it was described as one group with many variations in the matrix and components frequency (section 5.3.3).

Samples 11 and 26 do not classify well with group D. Since they had similar inclusions to the other samples, they had not been selected for thin sections. Their odd grouping is probably because of a higher content of CaO, with 26 being particularly rich in the remnants of microfossils (see Figure A.51).

Sample 65, which does not group well either, was an uncertain classification

during microscopic analysis because of the lower frequency (and finer) of iron-rich inclusions (Appendix C.1). During PLM analysis, sample 65 was classified as Fabric 3 (section 5.3.4). This sample contained common biomicrite or chamotte.

Groups C, E and F ($\approx$ Fabric 1): Looking at C, E and F, these groups tend to cluster together with internal variations and represent one large compositional group. These samples are rich in CaO and associated elements. The PCA is more consistent with the PLM analysis than the microscopy as the sherds from groups C, E-F were merged into Fabric 1 during PLM (see section 5.3.2).

Sample 24 is the main outlier of this analysis but can not be interpreted independently, as it could be a problem with the reading. This sample had not been sent for petrographic analysis. Sample 47 (Figure A.83) is an unexpected classification considering the microscopic analysis (Group F?). This sample was not analysed with PLM and will be considered as an outlier for now.

7.3.2 PCA for Dataset 2

This section presents the PCAs run on Dataset 2 (Pottery and clays). The direct comparison between pottery and clays is limited because these raw materials were not fired and are possibly high in organic material (see section 6.1). GNB.B1 and MX.D1 were removed from the analysis because of problems with the readings and mislabelling.

Describing the Principle Components (PCs)

A first PCA was run with Dataset 2; however, the scatterplot was not readable due to outliers (see Figure D.2 in Appendix D.2.4). Some outliers were visually noted: GNB.E1 (possible analysis problem), MG.B1 and MG.A1, MX.A1 (marl), MX.D1 (marl), GNB.F1 but then also RML.D1 and GNB.A1. These readings indicate that the Ġnejna samples could be the marly layers accessible from the beach or calcium carbonate-rich layers within the Blue Clays. Since the Gnejna sampling

was performed before this dissertation's time, it is possible that they were sampled from marly layers, not from Blue Clays. Indeed at Ġnejna Bay, the marly layers of Globigerina are exposed close to the beach and easy to access. Since these raw materials obscured the scatterplots, it was decided to remove these samples from the analysis.

A second PCA was then conducted, removing these outliers and samples 24 and 67 and after re-standardising the dataset (section 6.2). The loading plots and scree-plot can be found in Appendix D.2.4. Four PCs have Eigenvalues higher than 1 (Table D.6 in appendix D.2.4). The first two PCs are presented in a scatterplot (Fig. 7.11).

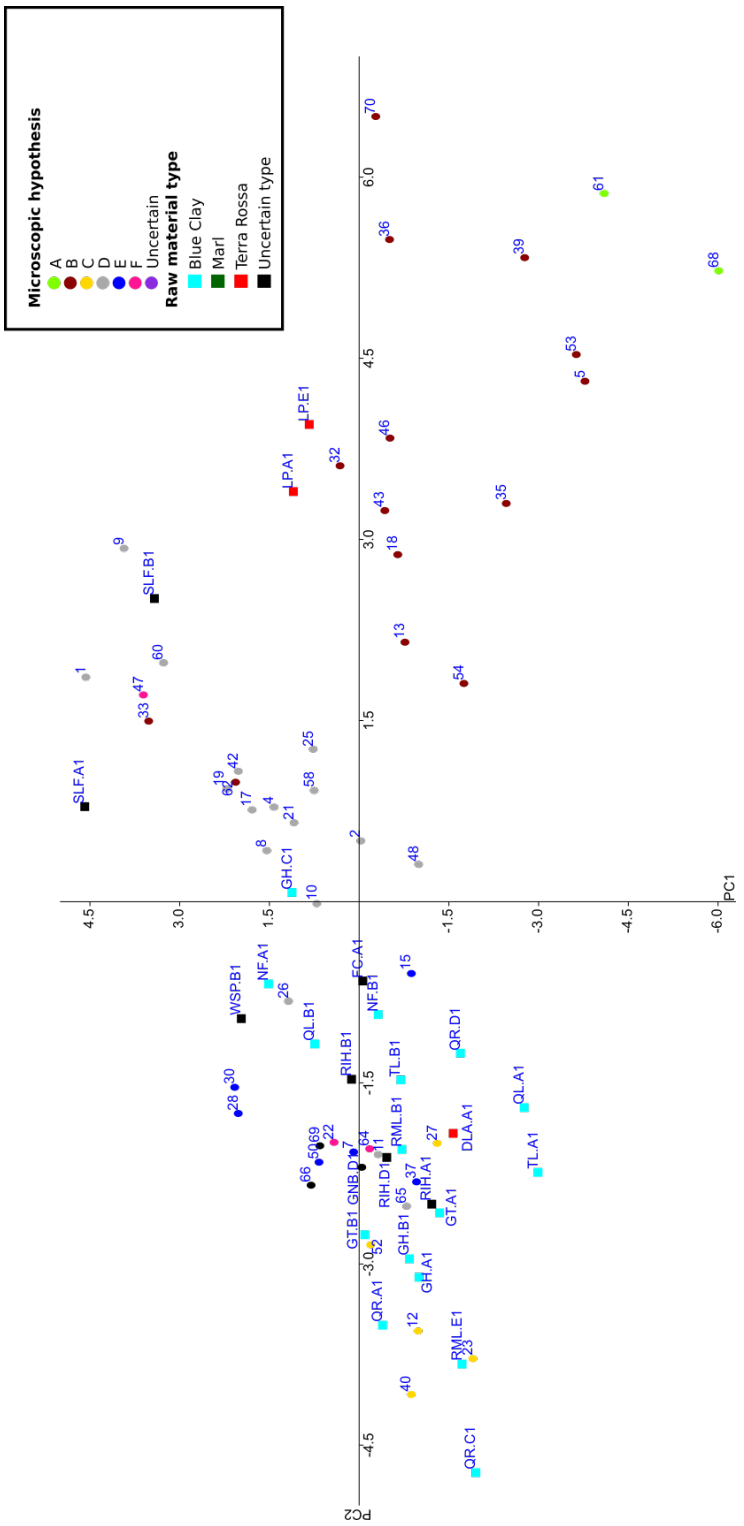


Figure 7.11: Scatterplot of PCA 2 for dataset 2.

First observations and discussion of scatterplot

Based on the two first PCs, the Blue Clay samples are close to the composition of pottery groups C, E, and F.

With this dataset, possible subgroups in pottery group D are visible. Samples 1, 9, 33, and 60 groupings one end; sample 48 is alone or close to sample 2, and the rest of the samples for D clustering together. Group D does not group with the bulk of the Blue Clay samples. Some samples from group D are close to GH.C1 from the top part of Gelmus Hill (Rabat, Gozo). Two other samples are close to group D, clays from San Leonardo Fort.

Some members of group B cluster close to the Terra Rossa samples from Ta'Lippija (LP.A1, LP.E1). There are different kinds of soils which are red in this dissertation. One sample is from Delimara (DLA.A1) and is formed by the erosion of Globigerina limestone, whilst the Lippija samples are from the Coraline limestone erosion. According to Lang (1960: 44), the soils developed on Globigerina limestone are Xerorendzinas rather than Terra Rossa, whereas Terra Rossa is constrained to Upper Coraline limestone (Lang 1960: 59). Terra Rossa and the implications of its use as a potential Maltese raw material is discussed in section 8.2.1.

A limitation of visualising the PCA as a scatterplot is that only two data dimensions are explored. However, some oxides have strong loadings in PC 3 (Fig. D.3), and this can change the groupings. The groupings become more complicated when looking at the data in 3D (Fig. 7.12). Indeed, group C (yellow dots) does not group as well with the Blue Clay samples (light blue square) anymore. This could be explained as the first PC being dominated by main elements such as CaO. This should be kept in mind when interpreting the PCA results.

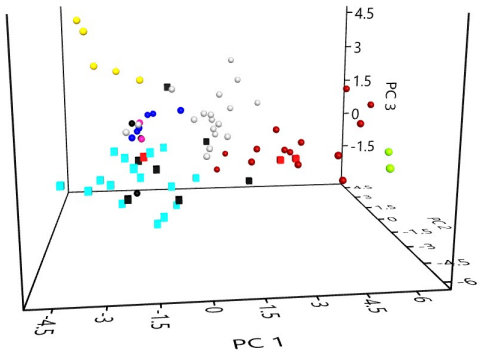


Figure 7.12: 3D plot of the PC1, PC2 and PC3

7.3.3 Hierarchical clustering on PCs

The rationale behind performing hierarchical clustering on Principle Components was detailed in section 6.2.

Once the hierarchical clustering was run on the PC scores using the complete and average methods, dendrograms were produced (see section 6.2). To decide where to cut the dendrograms (ie. how many groups to form), the silhouette plot produced by RStudio (Fig. 7.13) indicates that the best fit for the dataset is to create three clusters of samples. The trees were, therefore, automatically cut to form three groups of samples.

Classification and interpretation

The sherds and raw materials were attributed to three groups as represented in table 7.4 with both methods. These are given a number (1-3) independent of the fabric classification. The two clustering methods differ in classifying a few sherds: samples 2, 15 and 48 are attributed differently according to the methods. Looking at the PCA results in section 7.3.2, these samples could not be attributed to a

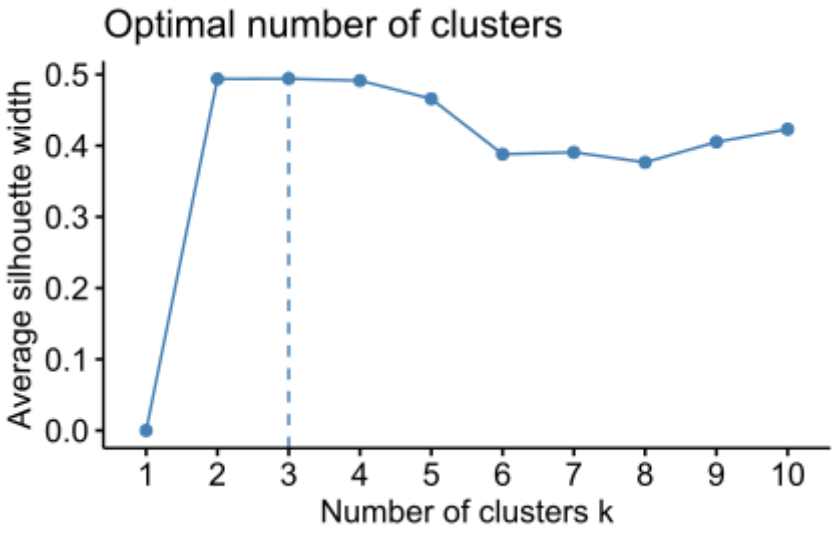


Figure 7.13: Plot of the average silhouette for different k values (number of clusters chosen); here, three clusters.

group based on the scatterplot. Some clays classify differently according to the method used: NF.B1, FC.A1, RIH.B1, QL.B1.

Comparing with the microscopic groups (second column in table 7.4), the following remarks can be made. Samples from Groups C, E and F cluster together (1 in columns A and C in table 7.4) with some sherds from Group D: samples 2, 11, 48 and 65. Samples 2 and 48 were discussed in section 7.3.2 as grouping separately in the scatterplot from the rest of group D. Samples 65 and 11 were spotted in the scatterplot as being closer to group E (section 7.3.1).

Group D sherds mostly cluster together using both methods (2 in columns A and C in table 7.4). Some samples from other groups cluster with them: samples 28, 30, 33, 47 and 62. Samples 30 and 28 were plotted, in the scatterplot Figure 7.9, above the majority of the samples from groups E, C, and F. These might be more similar to group D in composition. Samples 33 and 62 were the sherds attributed to Group B but re-assessed during petrography (sections 5.3.4 and 5.3.6). Finally, sample 47 was mentioned as an outlier in section 7.3.2. The Blue Clay samples are spread across both the above clusters. However, more samples are clustering with the sherds from groups C, E and F.

Groups B and A cluster together, which is consistent with the microscopic and

petrographic interpretations of these sherds (section 5.3.5 and 5.3.7). They also cluster systematically with the Terra Rossa samples (LP).

S	OM	PLM	A	C	**S**	OM	PLM	A	C
1	D3		2	2	36	B2	5	3	3
2	D2		1	2	37	E	1.1	1	1
3	D3				38	D2			
4	D3	2.1	2	2	39	B1?		3	3
5	B1		3	3	40	C	1.1	1	1
6	D2?				41	D3			
7	E		1	1	42	D3		2	2
8	D1		2	2	43	B1		3	3
9	D2	2.1	2	2	44	C			
10	D1	2.1	2	2	45	C			
11	D1		1	1	46	B1	5	3	3
12	C	1.2	1	1	47	F?		2	2
13	B1	5	3	3	48	D2?	2.2	1	2
14	D3				49	D2			
15	E	1.1	1	2	50	E		1	2
16	E				51	D1			
17	D2		2	2	52	C	1.1	1	1
18	B1?	5	3	3	53	B1		3	3
19	D3		2	2	54	B?	5	3	3
20	E				55	D2			
21	D2	2.1	2	2	56	D3			
22	F?	1.1	1	2	57	E?			
23	C		1	1	58	D2	2.2	2	2
24	C				59	D2?			
25	D?	2.1	2	2	60	D3	2.1	2	2
26	D2		2	2	61	A	7	3	3
27	C	1.1	1	1	62	B1?	4	2	2
28	E		2	2	63	D2			

29	D2	1.2			64	F?	1.3	1	1
30	E?	1.1	2	2	65	D3?	3	1	1
31	E				66	?	1.1	1	2
32	B2		3	3	67	D?	1.1		
33	B2	6	2	2	68	A	7	3	3
34	B1	5			69	?	1.1	1	2
35	B?	5	3	3	70	B	5	3	3

S	Type	A	C	**S**	Type	A	C
DLA.A1	Terra Rossa?	1	1	NF.A1	Blue Clay	2	2
FC.A1	Uncertain	1	2	NF.B1	Blue Clay	1	2
GH.A1	Blue Clay	1	1	QL.A1	Blue Clay	1	1
GH.B1	Blue Clay	1	1	QL.B1	Blue Clay	1	2
GH.C1	Blue Clay	2	2	QR.A1	Blue Clay	1	1
GNB.A1	Blue Clay			QR.C1	Blue Clay	1	1
GNB.B1	Blue Clay			QR.D1	Blue Clay	1	1
GNB.D1	Blue Clay	1	1	RIH.A1	Uncertain	1	1
GNB.E1	Blue Clay			RIH.B1	Uncertain	1	2
GNB.F1	Blue Clay			RIH.D1	Uncertain	1	1
GT.A1	Blue Clay	1	1	RML.B1	Blue Clay	1	1
GT.B1	Blue Clay	1	1	RML.D1	Blue Clay		
LP.A1	Terra Rossa	3	3	RML.E1	Blue Clay	1	1
LP.E1	Terra Rossa	3	3	SLF.A1	Uncertain	2	2
MG.A1	Uncertain			SLF.B1	Uncertain	2	2
MG.B1	Uncertain			TL.A1	Blue Clay	1	1
MX.A1	Globigerina marl			TL.B1	Blue Clay	1	1
MX.D1	Globigerina marl			WSP.B1	Uncertain	2	2

Table 7.4: Table presenting the sherds and raw materials as classified by the Complete Link method (C) and Average Link method (A). The purple numbers are mismatches between methods. S: Samples.

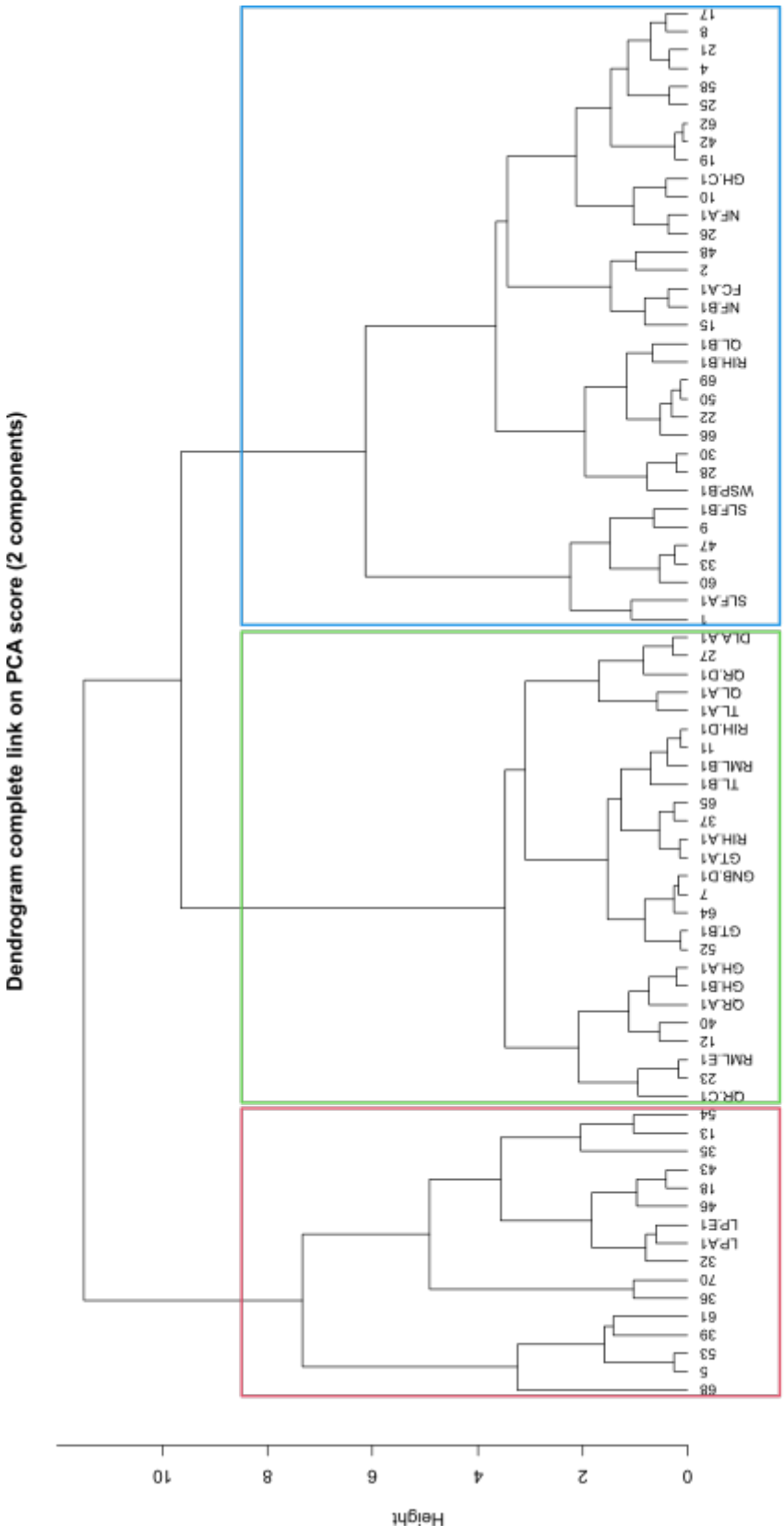


Figure 7.14: Dendrogram of HCA, complete link, using the PC scores, cut at three clusters as indicated by RStudio.

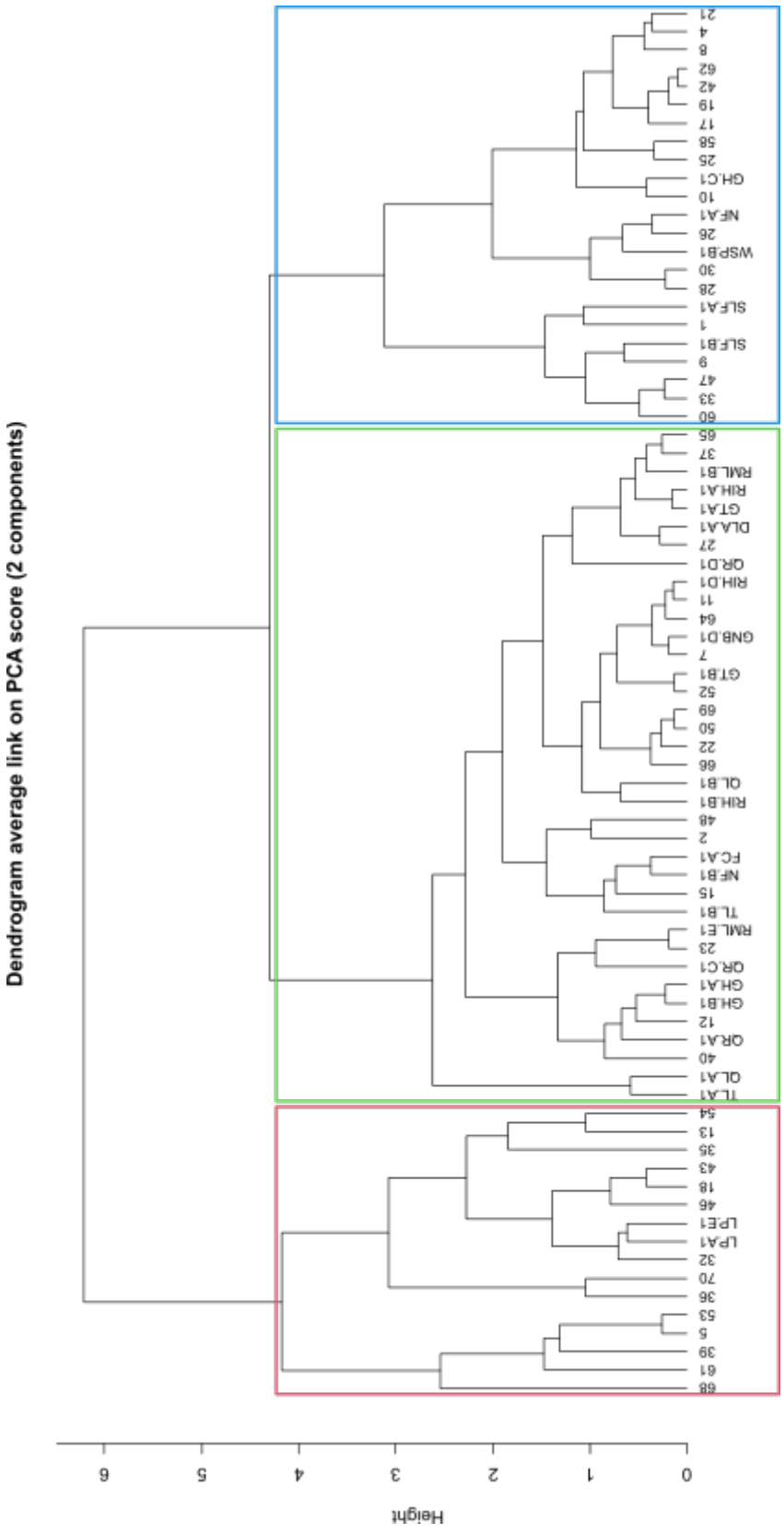


Figure 7.15: Dendrogram of HCA, average link, using the PC scores, cut at three clusters as indicated by RStudio.

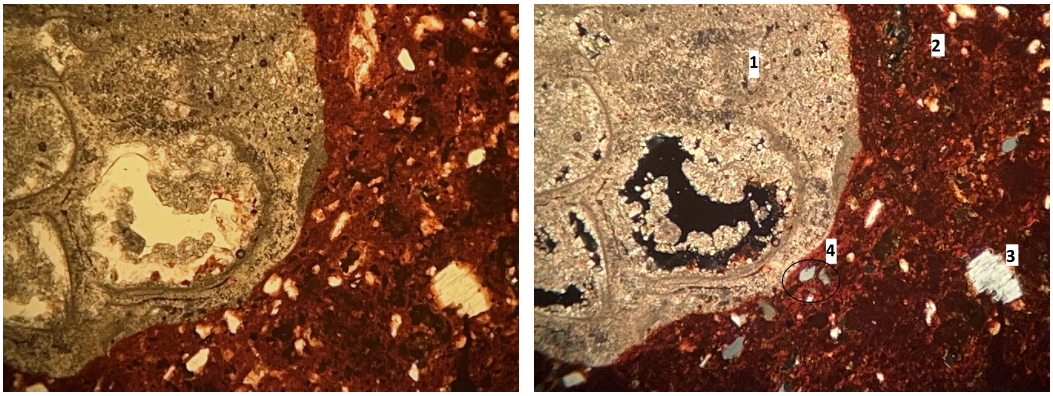
7.4 Terra Rossa experimental archaeology

To test the hypothesis of Terra Rossa being similar to Fabric 5 (Group B) as explored with PCA and HCA (sections 7.3.2 and 7.3.3), experimental samples were manufactured and analysed with PLM (section 6.3 for more details).

The raw material could be shaped in briquettes. Although it was plastic, it was hard to work because of its stickiness. The briquettes held together during firing (see Figure 7.16); however, upon re-hydration, they broke due to the large pieces of limestone.

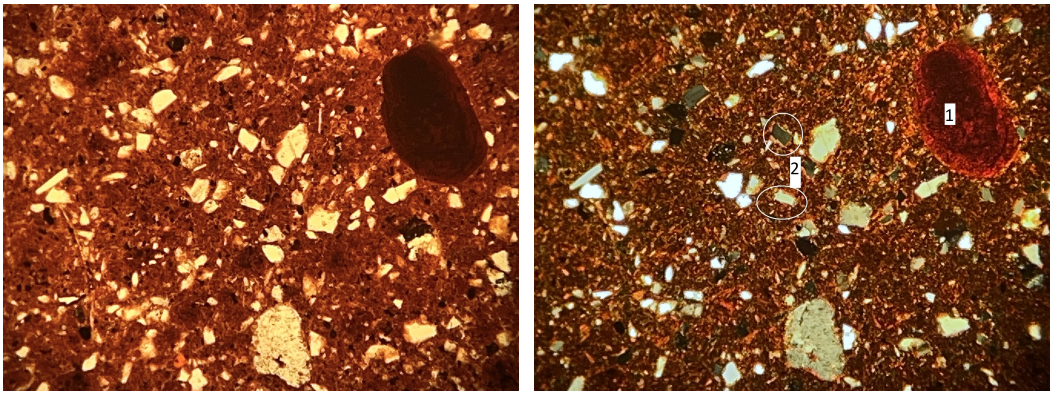


Figure 7.16: Photograph of manufactured briquettes after firing at 500°C. EA1 and FA1 were sent for petrographic analysis.



(a) (b)

Figure 7.17: LP A1 (Briquette FA1), PPL (a), XPL (b). FOV: 1.3 x 1 mm. 1: Sparitic limestone containing fossils or oolites; 2: Iron-rich matrix; 3: feldspar; 4: examples of fine quartz



(a) (b)

Figure 7.18: LP E1 (Briquette EA1), PPL (a), XPL (b). FOV: 1.3 x 1 mm. 1: glauconite, oxidised; 2: example of fine quartz

The PLM characteristics of the briquettes made of Terra Rossa from Ta'Lippija are explored in Table 7.5 and illustrated in Figure 7.18. LP.A1 was described as coarser than the other Terra Rossa. The sherds which can be compared with the Terra Rossa are from Group B/ Fabric 5. There is no direct match between the samples and the pottery sherds. However, there are similarities between the groundmass of the briquettes and some of the sherds (e.g. 13, 18, 54). Other samples from Fabric 5, such as samples 34, 35 or 46, have more frequent fine quartz than the briquettes. Samples 61, 68 and 70 have much finer and more abundant quartz (PLM).

The claystones (angular carbonates or chamotte) found in the sherds of Fabric 5 are

not naturally present in the Terra Rossa briquettes (PLM). As discussed in section 5.3.5, in Fabric 5, they could be a temper added by the potter. The material felt sticky and plastic when being worked, and potters can add temper to the raw material to enhance workability (Eramo 2020: 4). Terra Rossa is not excluded as potential raw material for some vessels. This is discussed in detail in section 8.2.

Briquettes	Component	Abundance
Both	Iron-rich matrix	
Both	fine-grained inclusions (angular quartz dominant on glauconite, feldspar, rare mica)	Moderately abundant
LP.E1 (briquette EA1)	carbonates as bioclasts: mollusc fragments, rare algae, other fossils; fossiliferous limestones	occasional
LP.A1 (briquette FA1)	carbonates as bioclasts: mollusc fragments, rare algae, other fossils; fossiliferous limestones	moderately rare

Table 7.5: Table presenting Dr Capelli's comments on the two Terra Rossa briquettes. The frequency is expressed in Dr Capelli's words.

Part IV

Discussion

Chapter 8

Raw material provenance

8.1 Blue Clays and San Leonardo clays

This section discusses the fabric groups described in section 5.3 and their possible raw materials (clays): Blue Clays and the clays/marls at San Leonardo.

8.1.1 Fabric 1

Fabric 1, equivalent to groups C and E-F, was observed through multiple techniques and was consistent in composition. This fabric is likely to be locally manufactured as it is consistent with the expected composition of Blue Clay. Looking at the XRF results, sherds from Fabric 1 have grouped well with most samples of Blue Clay, regardless of the grouping technique used, which supports local manufacture. This group is consistent with Anastasi (2019) fabric 1, Sagona (2015b) Crisp Ware and Bruno and Capelli (2000) "Generico" group. More broadly, limestone fragments or biomicrite inclusions are described in locally manufactured pottery across periods. The three major fabric groups observed in Bronze Age Baħrija pottery by Tanasi et al. (2020a: 125) contain microfossils, micrite and grog (maybe claystone?). Similarly, Palmer et al. (2018) looks at 17th-20th Maltese pottery. Fabric 2 from the Palmer paper, used for shapes common in Malta during the post-medieval

period, is rich in calcite and microfossils. In general, these characteristics are represented across time in Malta.

Sample 29, the inscribed sherd found in Fabric 1, shares characteristics of Blue Clays (limestone fragments, *foraminifera*, varying calcareous matrix, claystone). However, it is slightly different to the main group Fabric 1 because of the rare quartz and few iron-rich nodules. The clay source might differ slightly from the larger group.

A few volcanic minerals in Fabrics 1 and 2 are the results of volcanic eruptions and wind-transported (Dr Capelli, *pers. communication* 21/10/2022). These minerals are rare in the fabric, and a few volcanic minerals could be found in Malta's sedimentary geology. Therefore, these samples could be locally manufactured.

The chemical variations within Blue Clays can not be thoroughly investigated with the methodology used because of the lack of accuracy of the instrument and the missing LOI calculations. Samples taken from the same place but on different biostratigraphic levels are plotted across the PCA biplot (Figure 7.11). For example, clays from different stratigraphic levels in Gelmus Hill were spread across the PCA graph. There is, therefore, no evidence from this study that the assumptions for provenance studies can be proven within Maltese Blue Clays, i.e. that the variation between the composition of Blue Clay sources is greater than within a source. Consequently, the precise origin of the raw material within the Maltese islands can not be asserted.

The problem might be the definition of *clay source* in Malta. In this work, a clay source was understood as a clay hill or a geographical area (e.g. Gelmus Hill or Għajn Tuffieħa). A more systematic sampling methodology across and within the clay slopes and hills and more accurate instrumentation could investigate these variations to assess if raw materials could be assigned more precise locations.

A major limitation of these analyses is the need for foreign sherds and clays to compare the fabric and chemical composition. Marine deposits are common in the central Mediterranean, and there is, for now, a lack of discrimination with

samples from abroad (section 2.2.2). Because of the semi-quantitative nature of the analysis, it was impossible to include legacy dataset (e.g. Palmer et al., 2018).

8.1.2 Fabric 2

The stereo-microscopy and polarised light microscopy revealed iron-rich nodules in Fabric 2, equivalent to Group D, interpreted for now as limonite or Terra Rossa nodules. This fabric is the most common at Tas-Silġ in the assemblages, and Bechtold (2017: 125) proposes that at Żejtun, red inclusions become the major facies group in the 2nd century BCE. The working hypothesis is that those samples are not imported because of their firing defects, such as in sample 9 (see section 5.2.2), and typologically, there are no differences with fabric 1. Some characteristics, such as the common microfossils, are close to fabric 1. However, the fine quartz and the iron-rich nodules make it distinctive at all scales of analysis, including visually. No rock fragment excludes a local origin.

Iron oxides and hydroxides are found in the limestone layers of Malta (Soldati et al. 2015: 20). Soils derived from Coralline limestone (Upper and Lower) include Terra Rossa and Terra Fusca, which contain ferric hydroxides (Chatzimpaloglou et al. 2020: 31). Iron oxides have been discussed in the case of a study on ochre by Montalto et al. (2012: 1095) where they suggest different sources that could contain iron-rich material: calcitic red limestones, greensands, ooids and Terra Rossa. These iron nodules are, therefore, not incompatible with the literature on the geology of Malta, but they still need to be fully identified. More experimental archaeology would be needed to assess if these iron-rich nodules occur naturally in Blue Clays. They might be secluded in specific layers (e.g. close to the erosion of limestone), or particular deposition processes could have incorporated the nodules during the transport of sediments (e.g. gullies).

Regarding the chemical analysis, this fabric tended to group away from the bulk of the Blue Clay samples in PCA. In hierarchical clusters, however, the sherds have grouped with some of the blue clay samples. A clay sample from Gelmus Hill in Gozo (GH.C1), collected by Asciak (2019) close to the Greensand layers, is one of

the closest Blue Clay samples. There are variations across clustering methodology, and more tests could be carried out on this specific fabric group.

San Leonardo area

The two San Leonardo clay samples are close to some of the sherds from this fabric group with different clustering methods. These clay samples were extracted from the San Leonardo fort ditch. The geology of the area was described by Pedley (2011: 916). The landscape is today modified for fields, and it is impossible to access an exposed section.

These beds are one of the closest possible sources of clay close to Tas-Silġ and Żejtun (Figure 6.1). This raw material would be worth exploring further. It would additionally be interesting to look at contemporary assemblages from Northern Malta and see if fabric 2, with these iron-rich nodules, is as standard in the rest of the islands or if it is a southern phenomenon.

Provenance hypothesis

The main hypotheses around the raw material provenance for Fabric 2 are, therefore:

- These nodules are naturally occurring in some Blue Clay sources which have not been sampled / or are under-represented here,
  - This hypothesis could also include sources such as San Leonardo,
- These nodules occur in soils deriving from Blue Clay, and the formation processes have not been identified,
- Potters modified raw material to incorporate the nodules, although they do not have the shape and distribution of temper characteristics.
  - It is, for example, possible that the potters mixed Blue Clay they collected and Terra Rossa.
- The vessels are imported.

These hypotheses highlight that more research is needed on the chemical and mineral variations within the Blue Clay slopes and sources and how the erosion of other geological layers influences these sources.

8.1.3 The question of quartz in local materials

The question about the presence/absence of quartz grains as inclusions was raised. Quartz grains were observed in the experimental samples of Terra Rossa studied with petrography and are, therefore, definitely found in Malta.

The quartz content, the size of quartz grains and the frequency of the mineral in Maltese Blue Clays has yet to be studied in depth. XRD analysis performed by students on some Blue Clay samples as part of the CoFIPoMs project (University of Malta 2021) have suggested that quartz is one of the main minerals in some Blue Clay samples (Humann 2021: eg. 43, 48, Xuereb 2021: 71-74). Quartz was also mentioned by French and Taylor (2020) as a mineral found in Malta.

Looking at other petrographic analyses on pottery, the *generico* group from Bruno and Capelli (2000: 61) has a "*fine mass composed of angular quartz fragments and feldspars and rare micas*" (translated from Italian). Other fabric groups from other periods studied in Malta contain quartz grain observable with PLM, such as the Bronze Age Fabric A from Barone et al. (2015: 104) and are considered local. The local fabric groups in Palmer (2020: 582) also contained quartz.

Therefore, quartz fragments do not exclude a local provenance for Fabric 2, especially if mixed with Terra Rossa, which contains quartz. Further research would need to understand the distribution of quartz in Maltese clay sources and why some pottery might contain or might not contain it.

8.1.4 Fabrics 3, 4 and 6

These fabric groups are made of one sherd each. Only further sampling could clarify if they are outliers or if the group they are part of was not represented in the

assemblage. The provenance of Fabric 3 is not ascertained because of the large quartz grain. It does share some characteristics of Fabrics 1 and 2. There is no evidence that Fabric 4 and Fabric 6 are imported or non-Maltese.

8.2 Terra Rossa

This section considers the hypothesis that Terra Rossa soils were used to manufacture local pottery.

8.2.1 Fabric 5

Fabric 5, equivalent to group B, has an iron-rich matrix with fine quartz as well as biomicrite (or chamotte) and limestone fragments (section 5.3.5). Apart from one fragment of trachyte in sample 54, no rock fragment is incompatible with Maltese geology. This trachyte could result from air-borne volcanic minerals after an eruption.

The raw material of these sherds does not share the typical characteristics of Blue Clays and, more generally, of marine clays. Maltese geological units are formed by marine deposits (Magri 2006: 13) and marine clays tend to be rich in microfossils and have a calcium-rich matrix (Montana 2016: 93). These characteristics are not visible for this fabric group. Determining possible sources for this fabric used for certain cooking vessels was one of the main questions after reviewing the literature (section 2.3).

The arguments for these vessels to be locally produced were the inscriptions to Astarte on the vessels, the abundance of these vessels, and the local development of olla-shapes. The petrographic analysis indicates that both inscribed vessels of this group, as depicted in section 5.2.2, do not display a significant difference from the other sherds of the same fabric group. Therefore, it can be assumed that the inscribed vessels are made of the same material as the other olla-shaped vessels.

Based on the PCA and HCA analysis and the experimental briquettes, Terra Rossa cannot be excluded as a possible raw material for this fabric group and sherds 13, 18, and 54 compared the best. For the first time, an available raw material in Malta has been identified as similar to these cooking vessels. This study included only one source of Terra Rossa (Ta'Lippija), and the possibility of variations in this material (chemical and mineral) across the Maltese islands is unknown. The two samples chosen had differences, for example, in coarseness, despite being sourced close to each other. The composition of Terra Rossa and its formation in the Mediterranean has been the object of debate. However, it is generally agreed that it is a clayey material deriving from limestone (Durn 2003), in Malta Coralline limestone. More studies on the mineralogy and composition would be necessary.

8.2.2 Use of Terra Rossa in the Mediterranean

Looking at the history of pottery making in the Mediterranean, the use of iron-rich soils and Terra Rossa for making cooking vessels has a long history. The possible reasons for this choice are explored in section 9.2.

Preferential selection of raw materials for cooking vessels is essential in traditional pottery making. In a study of traditional pottery workshops in Mallorca, Day et al. (2015) describes how different types of vessels are made of different raw materials: cooking vessels manufactured by specific workshops with red Quaternary clay and water jars with white clay. Collecting the appropriate raw material for the vessels is part of the "true tradition" (Day et al. 2015: 61) of making the vessels, and part of the Pòrtol pottery reputation relies on these long-established traditions.

From the archaeological record, iron-rich clays have long been an appropriate material - at least perceived as such- for cooking vessels in the Mediterranean. Looking first at the vessels close to the olla/casseroles in Malta, Quercia (2002) cites the caccabé described by Bats (1988: 46). The latter traces this style back to vessels found in Athens and described by Thompson (1934: entry C70). In Thompson's digitised collection from the Athenian Agora, these cooking vessels (mostly chytra) are made with red clay, grey-brown clay, and grey clay and have



Figure 8.1: Photograph of vessel C70 from the Agora collection sitting on top of a brazier (American School of Classical Studies 1958)

mottled surfaces. For instance, C70 (Figure 8.1) or Agora Object: P 2393 (American School of Classical Studies 1958) is made of "coarse red clay".

These raw materials are not Terra Rossa; however, iron-rich red clays were used to make these forms of cooking vessels. Looking at Terra Rossa specifically, cooking vessels were manufactured with this material since the Iron Age in the southern Levant. In Jerusalem, for instance, Terra Rossa was preferred to the Moza marls because marls were inadequate to make cooking vessels (Ben-Shlomo 2019: 15).

In Syria, the tradition of "Brittle Ware", which included cooking vessels, starting from the Roman period, originated partly using Terra Rossa. Vokaer (2010) likewise cites this practice in Lebanon and Palestine from the Hellenistic to Byzantine periods. Other Terra Rossa vessels are known from Phoenician Cyprus (Waiman-Barak et al. 2021). In the central Mediterranean, closer to Malta, Terra Rossa was used during Punic times in Libya (Swift 2018). There would be likely compositional differences between the Terra Rossa of these places, however, these examples show that potting traditions for cooking vessels across the Eastern and

central Mediterranean have used similar soils. The reasons behind adopting a new raw material and these new vessels and the chronology are discussed in 9.2.

8.2.3 Fabric 7: two fine vessels

The two sherds of Fabric 7 from the Żejtun villa were classified as "local fine ware" for ZTN06/2107/9 and "Local cooking ware" for ZTN06/549/13 by Bechtold (2017). There was no direct match between the two fine vessels and any raw material. The groundmass looks similar to Fabric 5 which could indicate a similar type of raw material but refined, for instance, levigated. However, there is, for now, no direct evidence that these sherds are made from clay from Malta. No rock fragments contradict a Maltese origin.

This fabric is consistent with the descriptions of Fabric 4 in Anastasi (2019). The fabric is additionally consistent with the description of late Red Bricky Ware (or a refined version of Red Bricky ware) as described by Sagona (2015b: 74-77). In the description of Anastasi (2019: 37), it is mentioned that the black inclusions could be distinctive of local sources. However, these inclusions are not diagnostic of any geology, and the present analysis has not confirmed that they were markers of local geology.

Despite their fine and similar aspect, these two vessels have different functions. Fine wares become common in Malta from the 1st century BCE (Anastasi 2019: 58). Further sampling of fine wares in Malta could indicate if fine wares should be classified into several groups rather than one.

The quartz contained in these vessels does not have the characteristics of aeolian quartz, which would have ruled out a Maltese origin. For instance, Hasenzagl and Capelli (2020) have described the quartz in the ARS from the Sidi Khalifa workshop as opaque and rounded, which have been associated with quartz transported by the wind (aeolian). It is not the case for these sherds.

8.3 Other possible raw materials

Other raw materials might be worth exploring in Malta for further analysis and are described in this section in consideration of the results of the various analyses carried out. This topic was explored in section 2.1.

8.3.1 Marl samples

Globigerina marls derived sediments were mentioned in section 2.1.2. This raw material was investigated because some vessels, mentioned in section 5.2.2, were brittle and white and it was deemed that it would be worth exploring raw materials with even higher expected content of carbonates.

The XRF results of Globigerina marls were inconclusive, and most marls were outliers in the chemical analysis, even those collected close to Tas-Silġ. Following these preliminary results, globigerina marls are not conclusive raw materials for the pottery assemblages in Tas-Silġ and at the Żejtun villa.

A side project of CoFIPoMS had experimented with making marl briquettes using Globigerina Marl from St Peter's Pool ("pale grey marl" Cassar, 2002: 35), not analysed by petrography or XRF in this research. These briquettes held together during firing. The briquettes, however, crumbled afterwards, most likely due to rehydration of the calcium carbonate content (lime spalling) or because of the low content of clay. Only the low-fired briquette did not crumble. Some photos are available in the appendix C.3.

8.3.2 Other quaternary and alluvial deposits

Quaternary deposits in Malta have yet to be studied as pottery raw materials. Apart from Terra Rossa soils, other deposits could be of interest to studying the ceramic record in Malta. Quaternary deposits are younger than the five main geological layers, most known and found close to the coasts, in caves or valleys (Camilleri

Haber 2015: 9). The Quaternary started with the Ice Age in Europe (Hunt and Schembri 1999: 41) and displayed global climate shifts since then. Quaternary sediments were deposited on land after the tectonic uplift, which triggered the emergence of the Maltese islands. These deposits have not been sampled as part of this dissertation but came to be of interest when studying fabrics 4 and 5, which do not display marine clay characteristics.

Valley fills and systems (see Figure 8.2) could yield deposits with clayey content, including transported Terra Rossa. Hunt (1997: 105) mentions rare fluvial deposits with "fine-grained sediment deposition" in Malta. Some fluvial deposits on the sides of valleys are believed to have accumulated during the late Roman period and, therefore, would not have been available during the Late Punic and Early Roman periods. However, those are often difficult to date with precision: Hunt and Schembri (1999: 44) mention valley fills dating back to the Neolithic up to modern times. Other fluvial deposits which are mentioned are alluvial fans (Camilleri Haber 2015: 12), although these contain both fine-grained sediments and gravel (Hunt and Schembri 1999: 55).

More recently, the *FRAGSUS project* has sampled locations by coring in estuaries to understand past landscapes better. One core from Wied Żembaq has layers of alluvial brown to dark clays, including some likely deposited well before the Punic period (Hunt et al. 2020: 58). Adding that many valleys in Malta are cultivated or impacted by human activity, these deposits can be impossible to sample.

Cave deposits, as described by Hunt (1997: 107), could be of interest. Pedley (2011: 915) mentions Għar Dalam, Mnajdra Gap and Magħlaq Cave with "fluvial conglomerates, brown clays and speleothems", the deposit dates to the mid-Pleistocene.

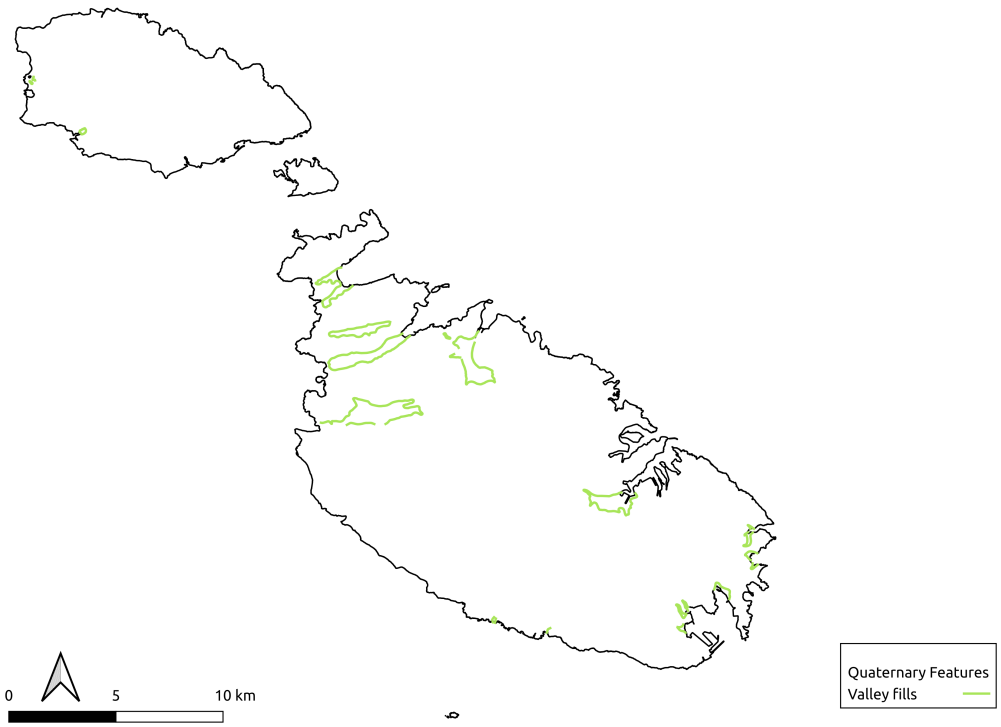


Figure 8.2: Map representing the boundaries for Quaternary deposits falling into the "Valley fills" category as mapped on the Planning Authority Geo-portal. The metadata lists these fills as "Low angle subaerial fanglomerate cones, Terra Rossas, local clays and alluvium" (Planning Authority 2021)

Chapter 9

Chaîne opératoire and technology

9.1 Summary of the chaînes opératoires

This section summarises the results on the stages of the *chaîne opératoire*, excluding raw material selection addressed in other sections.

9.1.1 Raw material treatment

After the clay is selected and collected, it can be processed in multiple ways. Some treatments do not leave direct evidence (Eramo 2020). Processing would have been necessary for the Blue Clays, which are found as large, broken lumps in the landscape in dry weather; as highlighted by the description of *pasturi* craftmen (Lanfranco 1978) in section 2.1. Clay lumps would need to break down and be homogenized (Roux 2019: 31). Blue Clay could have been crushed or soaked in water and dried (Roux 2019: 32-33).

There is no evidence for specific types of clay processing with Fabric 1 and that any components were purposely added as tempers. Fabrics 1 and 2 have varied natural inclusions, and nothing indicates the purification of the material. The variability between samples suggests a non-discriminatory strategy of clay collection and little subsequent treatment (Santacreu 2014: 245). Nothing suggests that a systematic

treatment was applied to the sherds to create a standard paste. However, a few samples, such as samples 60 and 4, are similar in section and could have been made from a similar paste (section 5.3.3).

Fabric 2, as mentioned in section 8.1, does not match directly with local raw materials. Therefore, the mix of several raw materials, clays and other sediments, or the addition of temper can not be excluded. Since the iron-rich inclusions shared visual and mineral similarities with the matrix of fabric 5, the hypothesis that Terra Rossa was included in the material, intentionally or not, is plausible. Determining clay mixing from natural homogeneity is not possible at this stage and is, more generally, difficult to investigate even with experimental archaeology (Ho and Quinn 2021: 10). Clay mixing can offer advantages such as improved workability (Eramo 2020: 7) or other properties such as decreasing shrinkage or improving strength (Ho and Quinn 2021: 1).

Fabric 5 was discussed in section 8.2.1. The limestone inclusions in fabric 5 are angular and were not noted in the samples of Terra Rossa studied in this work. Therefore, the tempering of the raw material by adding crushed rock fragments such as biomicrite or other limestones is, for now, the most plausible hypothesis to explain the presence of these inclusions. This shows a different process than the other groups and a will to modify the raw material properties. If Terra Rossa or similar material is used, then the difficulty to work the material because it was sticky could explain the need to add a temper.

The fabric from Fabric 5 is visually homogeneous. However, the chemical composition across the samples is not entirely homogeneous. Compared to other fabric groups, there was a more standardised way of making cooking fabrics (fabric 5) than other fabrics. However, there is no complete standardisation for this fabric, as variations are observable in shape, including wall thickness and chemical composition, and some variations were observed in the fabric. Santacreu (2014: 254) argues that low variability, or standardisation, can be caused by specific social or technical demands but that cooking vessels, because of their requirements, tend to have more fabric homogeneity.

Other temper additions include sherds with chamotte, such as in Fabric 6 (sample 33), where some inclusions are vitrified. However, this phenomenon is not widely spread in the assemblage, and chamotte is challenging to distinguish from marly fragments and other clay-based inclusions as explored in section 5.3.2.

Fabric 7 could be a case of local clay processing if it were of Maltese origin, which this work could not ascertain. Considering Malta's lack of known fine material, some material purification could have been carried out. Levigation is a process to remove a coarser fraction of the material (Santacreu et al. 2016: 68), which involves the use of tanks and is often associated with permanent production structures (Cuomo Di Caprio 2017b: 106), and pottery workshops knowledgeable in the techniques. No such structures have been positively identified in Malta; if these structures could be identified in the first place, the petrographic and chemical evidence would still need to be more conclusive to assert that these sherds were produced in workshops in Malta.

To summarise, there are different ways of treating raw materials for making pottery for the two archaeological sites. Plates and bowls do not have evidence of further clay treatment except for the possibility of mixing various materials for fabric 2. Cooking vessels, on the contrary, could have been tempered, resulting in a longer preparation process.

9.1.2 Manufacturing methods and implications

The interpretation of the evidence for manufacturing was not decisive. Both Sagona (2015b: 50) and Anastasi (2019) suggested that the local vessels were wheel-made. It is assumed that these claims were based on macroscopic features.

As described in section 5.2.2, some macroscopic traits of Fabric 1-4 and 6 suggest the use of a wheel, or what Roux (2019: 42, 48, 158) calls Rotary Kinetic Energy (RKE), which is the energy supplied when using rotary devices in general. Some sherds have characteristics which are often associated with the use of a wheel, such as string marks (Roux 2019: 179) and ribbing (e.g. Samples 2, 15). The

petrographic analysis showed no explicit evidence of wheel throwing in the fabrics 1-4 with a few exceptions such as sample 30 (see Section 5.3.2). Wheel-thrown vessels are expected to have elongated voids parallel to the walls (Roux 2019: 184) and preferred inclusion orientation (Santacreu 2014: 167). The type of inclusions present in these fabrics are large inclusions with irregular shapes, not elongated. These would not necessarily display orientation except for the biotite minerals (micas), but they are too rare to display patterns.

Manufacturing techniques are challenging to analyse because several actions can be performed as part of the *chaîne opératoire*. There are many variables during manufacturing, such as re-shaping, the potter's experience (Thér and Toms 2016), and types of devices which can influence the voids of the sherds. An example is wheel-coiling, where a vessel is first coiled and then finished on the wheel (Courty and Roux 1995). This combination of techniques might not leave clear-cut evidence and might exhibit macroscopic features of both. For instance, samples 7 and 30 could exhibit wheel-coiling traits because of the ribbing. However, fine topographic analysis of changes in the surface of the vessels was not performed here and would be necessary to confirm this hypothesis (Valentine Roux, *pers. comm. 11/04/2022*). Further research on this point could try different techniques, such as multiple sections of the vessels, X-Ray imaging, and surface analysis using topographical analysis using complete profiles.

One limitation of this study in understanding manufacture comes from the sampling design. Indeed, to gain typological information, rims were sampled. Rims can be shaped with techniques other than the vessel's main body. In the case of Tas-Silġ, the sherds were highly fragmented; therefore, most of them lacked an extended part of the wall to study. A paper published by Thér and Toms (2016) quantified the orientation of voids and inclusions to understand characteristics of manufacturing technique such as the differences between wheel-finished, wheel-shaped, and wheel-thrown vessels (Thér and Mangel 2020). Their study shows that results for the top part of the vessels could be less reliable than the samples taken from the bottom. This is explained mainly by the pressure to lift the clay mass when forming the vessel's base. Therefore, the fabric from the lower part of the wall could display

more orientation than the rims.

On the other hand, rare vessels had evidence of different techniques, such as coiling. No coiling joints were unambiguously observed. Fabric 5 exhibited large pores that seem to support that they were not thrown or turned, with some samples having a micro-structure indicating that they were handmade such as sample 35 (see section 5.3.5). However, no coiling joints were observed and other techniques have to be considered. Sample 70, however, had a thinner wall and elongated voids parallel to the walls, which tend to support the use of a wheel for throwing this vessel.

Fabric 7 was the only group with definitive evidence of wheel-throwing within the fabric, including elongated voids in the section and fabric containing only fine inclusions, suitable to be thrown (Roux 2019: 183 for the requirement of throwing on the wheel). However, these sherds are not provenanced with confidence; it can not be asserted that a workshop with a fast wheel was present in Malta. This question is significant because using the fast wheel necessitates motor skills that take much more time, with an extended knowledge transmission to acquire and maintain postures and gestures (Roux 2019: 261-262). These motor skills are generally associated with professional craft people with dedicated workshops and equipment.

To summarise, the microstructure contradicts the macroscopic evidence for wheel throwing for most sherds in the assemblage. However, the use of some rotary devices is still indicated by these visible marks, and before ruling out the use of the fast wheel, complete profiles should be studied with other methods. The cooking vessels for which the bases were unavailable are interpreted as handmade, with some exceptions, such as sample 70. Finally, more research needs to be done on the properties of the Blue Clays and how these might affect the action of the potter. Properties such as shrinkage directly influence both material choice and technological choice (Tite 2008: 223). One could attempt to get potters to turn Blue Clays and Terra Rossa to see how feasible some actions might be.

9.1.3 Surface treatment

Surface finish and treatments are different across the fabric groups and shapes. Some vessels have more regular finish lines, indicating a finish with a rotary device such as a wheel or a turntable. On the contrary, the least parallel striations, for example, in sample 65 (Fig. A.129), are similar to Roux (2019: 197, Fig. 3.52.d). These are characteristics of finishing the vessels when they are still wet using the fingers or a cloth. The plates, bowls and miniatures from Fabric 1 and 2 have been finished when wet, and little effort has been spent finishing the vessels, particularly the non-visible parts such as the bases or the non-visible surface, which sometimes have surface inclusions.

The cooking fabric 5 has burnished surfaces with more time investment. The relationship between surface treatment and the function of the vessel is explored in section 9.2.1.

Surface bleaching in bowls and plates

The white surface of some sherds (e.g. sample 7) was studied. By eye, it is difficult to assess if the white surfaces have a slip or if they became white during firing. All white/cream surfaces were first thought to have a slip; however, the petrography did not support this hypothesis even for homogeneous white layers on the vessel surface, such as sample 7 (Figure 5.10c).

Some samples have only part of their surface whitened, not creating a homogeneous surface colour. For example, the heterogeneity could result from an unintentional process in sample 9 (Figure 5.10d). This points to a lack of precise control on the firing conditions and the absence of a requirement for having homogenous-looking pottery at the sites.

Von der Crone and Maggetti (2002: 249) mention similar pottery from Tunisia and Israel and call this process salt water bleaching. In her dissertation, Humann (2022: 42,52) simplified the explanation of the phenomenon: the salt in water used

for preparing the paste increases the solubility of calcium carbonate in the clays, which then tends to accumulate on the vessel's surface, transported by the water during the evaporation while the vessels are drying.

Seawater is cited in Molera et al. (1998: 198-199) as one possible explanation: they also suggest that a lighter colour ceramic material can be obtained using calcareous clay fired between 700-1000°C, with systematic results at 950°C. They attribute the cream colour to the formation of pyroxenes, calcite dissociation and fewer iron oxides in the margins in the form of maghemite. A creamy layer could be achieved with high temperatures, long firing times, and reducing the atmosphere at the end of the firing, for example, by closing a kiln.

Only a few sherds were analysed for this dissertation; this questions the categories previously used for a white or cream slip in the literature. For instance, in describing the ceramic industry of the Punic Period, Sagona (2015a: 244) describes the slip from Crisp Ware as pale yellows to greys. Similarly, Quercia (2011: 434) describes a thick cream slip with decorated bands for the fifth century BCE, whilst in the late Punic period/ early Roman period (third and second century BCE), he describes an uneven floury slip (Quercia 2011: 437). This floury slip might only be caused by uncontrolled firing rather than slip. There is no evidence, however, that the Punic thick cream slip was not a slip, as this work does not contain samples of these earlier periods and further research could test this hypothesis.

Using seawater in Malta could be an economically rational choice if workshops are in the vicinity of direct access to the sea. Fresh water is scarce, and water would have been stored in cisterns or wells (Grima 2007: 36). Other reasons could lead potters to add salt directly to the paste, including functional reasons mentioned by Roux (2019: 38). For example, salt temper increases the porosity of the vessels. Santacreu (2014: 172) also cites the ethnographic use of saltwater to reduce spalling or lime spalling - and therefore breakage - which would have been common in calcite and limestone-rich clays. If seawater were partially or entirely used in ceramic production, then the firing temperatures might have been over-estimated during analysis as seawater might accelerate calcite dissociation (Molera

et al. 1998: 189).

The CoFIPoMS project attempted to make briquettes with sieved Blue Clay (sieved QL.B1) and seawater with oxidising atmosphere and 120 minutes of soaking time. These are compared with briquettes from Xuereb (2021: 52) manufactured from the same sieved clay and fired with similar conditions. The briquettes with salt water were lighter than those made with tap water (see Appendix Table C.17); however, no white surfaces were created. There seem to be differences in mineral composition, particularly calcite, possibly due to salt water. This can be observed by visually inspecting two XRD diffractograms in Figure C.4, which compares briquettes with and without seawater. Photos and details are available in Appendix C.3. This could be explained for several reasons:

- The briquettes were fired only up to 900°C, and the whitening might happen at higher temperatures or with a longer firing time
- The sieving process removed enough calcite to prevent the full whitening of the surface. Note that the clay was sieved because the experiment was not designed to compare with these sherds but to start testing Blue Clay's properties.
- This specific Blue Clay from Il-Qolla does not allow for the surface bleaching

More experimental briquettes with unsieved clay and different parameters might achieve different results. For now, therefore, this question can not be concluded.

9.1.4 Firing methods

Indicators of firing conditions were sought in the sherds. However, without the knowledge of the firing structures, it is impossible to describe the technology used at the time. When these structures are not found, there is little direct evidence of the firing process (Thér et al. 2019: 1148). Gosselain (1992) has long argued that making inferences about firing technology based on firing temperatures only is imprecise as many firing procedures might produce the same results. It is not possible to relate directly "thermal characteristics [...] to a specific firing

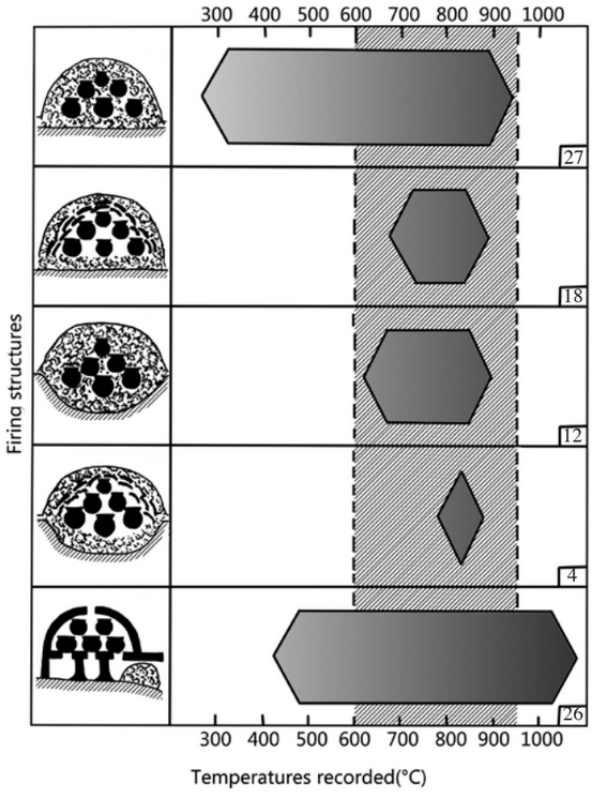


Figure 9.1: Ranges of temperatures achieved with different firing arrangements and procedures, from Gosselain (1992: 246) and Guo (2017: 182, Fig. 3). The grey area represents two-thirds of the data from the original experiments in Gosselain (1992).

procedure" (Smith 2001: 999). Different structures have a wide range of possible temperatures, illustrated in Figure 9.1. The strict opposition between open fires and kilns and their assumed results have long been dropped (Guo 2017), there are plenty of possible procedures and set-ups that can be implemented (Smith 2001: 999). Various firing procedures can be performed in the same structure according to the need (Thér et al. 2019: 1144).

Sagona (2015b: 51) indicates that Crisp Ware has varied colours across and on the same vessels. She explains this phenomenon due to stacking the pots in the kilns. There is no evidence supporting such a statement for now. Some sherds have oxidised margins and reduced cores, likely caused by the lack of diffusion of heat and oxygen through the core (Xuereb 2021: 81). This phenomenon can have varied causes (e.g. short soaking time), and was observed for the Maltese Phoenician amphorae (Anastasi et al. 2021).

Some samples from all fabric groups have dissociated carbonate inclusions and

more or less vitrified matrix, indicating that temperatures in a range of 800-900°C could be reached. Still, it was not systematically observed in the sherds. Initial vitrification occurs at around 800-850°C, and extensive vitrification is achieved for calcareous clays between 850-1050°C (Kiriatzi and Siddall 2022: 7). It is not impossible to reach these temperatures without a kiln (Smith 2001: 999).

The heterogeneity of fabrics 1-2, particularly in colour, indicates a lack of systematisation and control over the firing process for the mottled sherds. This could be intentional but not necessarily; there was no need or means to fire the pottery homogeneously. Mottled sherds could additionally be caused by contact with fuel (Santacreu et al. 2016: 105). Rice (2015: 172-180) highlighted that the lack of control is often associated with open fires and that not using structures like kilns can be more fuel efficient. The vessels within the fire would reach a high temperature more rapidly. It cannot be excluded that these vessels were fired in pits, bonfires or one-chamber kilns. Since the fabric groups are heterogeneous, having more than one technique across Malta is possible.

The yellow and green fabrics, mentioned in section 5.2.2, could be caused by over-firing. Indeed some sources mention that calcareous clay will turn green if over-fired; however, the process (and necessary temperature) is not explained in the literature (Grammatikakis et al. 2019: 2653). In this case, the green tint of the sample might be explained by a firing mistake. The miniature white vessels are more challenging to explain as they were homogeneously white.

Fabric 5 has homogeneous colours, although carbonates are more or less dissociated. Homogeneity of appearance might be achieved through greater control of the firing process. The homogeneous oxidation state across the fabric group also tends to point to (i) a structure in which oxygen is controlled and/or (ii) experienced potters who know how to control oxygen input and the firing procedure. However, more experiments should be conducted on the Terra Rossa soils: the briquettes presented in section 7.4 had homogeneous colours in cross-sections even at a firing temperature of 500°C. The homogeneity of colour might be caused by the raw material itself. In section 5.2.2, the possible presence

of soot was mentioned for some of the cooking vessels, and an alternative hypothesis was proposed: direct contact with fuel. If this is the case, a kiln with chambers would not be expected to have been used.

Santacreu (2014: 88) and Orton and Hughes (2013: 136) warn that wheel-thrown vessels should not be associated with fired-in kilns without evidence. Finer vessels tend to be more sensitive to changes in temperature, and the heating rate is less controllable in open fires; thus, for complete control of the firing process, a kiln would be expected to have been used (Santacreu et al. 2016: 173). Fabric 7 was most likely fired in a controllable environment, for example, a kiln, but it is challenging to assess the firing for other fabrics.

To summarise, there are many firing variations across and within the fabric groups, especially in Fabrics 1-2. Firing temperature can reach the temperature of carbonate dissociation and sometimes vitrification of the matrix. The heterogeneous-looking assemblages, colours and bleaching of the surface for bowls and plates suggest a lack of precise control of the firing conditions. Another unlikely possibility is the intentional variations in colour for different batches of pottery. On the contrary, Fabric 5 and 7 have homogeneous sections and colours, although fabric 5 also has different firing temperatures. These two groups seem to have been fired with more control.

9.2 Technology and implications

9.2.1 Intended function, vessel efficiency and raw material choice

Understanding the reasons behind specific technological choices is imbued with theoretical implications on how archaeologists perceive techniques, the transmission of knowledge, or agency (see section 1.1.3). The making of a pottery vessel is the result of the entanglement of factors such as raw material and environmental constraints, social demands, or available technology (Rice 2015: 212).

When looking solely at the functional aspect of a vessel and its properties, Santacreu (2014: 188) warns that many characteristics and parameters affect the diverse performances of ceramic vessels. It might be reductionist to single out only a few attributes to explain technological choices, and correlations between parameters and functions must be analysed with care (Tite et al. 2001: 321). Additionally, some effects of properties might not be culturally significant or appreciated (Whitbread 2016: 31, e.g. with a rounded shape for flameproof vessels).

Considering these limitations, vessels can still be designed around their intended function(s). The perception of performance, suitability and efficiency is unique to a socio-cultural context (Santacreu 2014: 187); however, one can test if some parameters are efficient in modern-day terms, assessing if patterns emerge and could help to understand the archaeological record. The study of raw material choice, manufacturing technique and function is explored with a case study of Fabric 5 in the next section.

Making a cooking pot in Roman Malta

The cooking vessels which make up fabric 5 (olle, casseroles) can be used as a case study to look at the link between technological choices at different stages of the *chaîne opératoire* and intended function. Discussing this is possible because this fabric was found only in cooking vessels. Not all the cooking vessels in the Punic-early Roman times are made of this fabric (Anastasi 2019: 77-81, catalogue of local cooking wares), but it seems that most of the vessels made of this fabric are cooking vessels. That this fabric is specifically made and used for specific forms of cooking vessels was already stated in Anastasi (2019: 39; Fabric 5) and Sagona (2015b: 75, Bricky Red Ware). Other cooking fabrics in the Late Punic - Early Roman assemblages have yet to be studied; the fabric of trays was looked at by Humann (2022) with SEM-EDS.

Moreover, because of their function, cooking vessels must have a set of properties making them suitable for this task, which is likely to dictate, to some extent,

technological choices (Whitbread 2015: 31). For example, cooking vessels must be resistant to thermal stress and shock, including temperature gradients between the different areas of the vessels (Müller 2016: 606,616).

This approach is worth exploring because the raw material differs from the bowl and plate fabrics. Mommsen et al. (2006: 86) had hypothesised that different requirements for cooking vessels could cause the differences they were observing in local "recipes". Based on the analysis in this research, the working hypothesis is that these vessels were made of tempered Terra Rossa, if locally made.

Looking first at the intended function, these vessels are described as cooking vessels based on the classification of Anastasi (2019), Quercia (2002), and Sagona (2002), in consideration of the shape of the vessel. The shape of a cooking vessel can facilitate specific cooking practices (Villing and Spataro 2015: 6). It was argued that these vessels had a shape for cooking semi-liquid or liquid foods such as soup or stew (Sagona 2002: 220-224; Quercia 2002: 410). The presence of a lid locator, indicating the use of a lid with the vessels, would support the possibility of boiling or heating at high temperatures. None of the examples in this research have a complete profile, however, comparative material for the *pentole* (Quercia 2002: 412) and *olle* (Quercia 2002: 408) have round bottoms, and Sagona (2015b: 74) states that round bottoms are usual for Bricky Red Ware vessels. Round vessels have been associated with direct contact with flames and using a brazier (Rice 2015: 413-414). The advantages are of these shapes are avoiding stress concentrations or offering a larger surface for heating (Whitbread 2015: 31). Direct contact with flames implies the necessity for the vessel and the fabric to withstand the thermal shock associated with this practice.

The hypothesis that these vessels would have been used to boil liquid food ingredients was supported for the site of Tas-Silġ by the organic residue analysis performed by Notarstefano (2012: 125,126). This research was conducted on similar shapes, close to the Greek *caccabé*, deemed typical in the Phoenician and Punic repertoire and suitable for boiling meat/fish sauce/stews. The organic residues concluded that both herbivore meat and fish were most likely cooked in

these vessels.

Surface treatments can be applied to cooking vessels to change their properties. Some vessels of fabric 5 are burnished, as stated in section 5.2.2. The burnishing could improve the heating of the content and waterproof the surfaces. This reduces the loss of the liquid content by absorption by the vessel by closing surface porosity (Whitbread 2015: 30). Sagona (2015b: 75) has argued that the light reflective surface was not burnishing but was caused by use, such as stirring. It is not possible for now to support/reject this hypothesis. The effect of surface treatment on the performance of the vessels is not straightforward as Santacreu (2014: 159) points out that polishing, for instance, can reduce the efficiency of heating. In any case, these vessels would suitably bring to boil a liquid as there is no open porosity on the inner surface (Santacreu 2014: 158).

Looking at the fabric itself, several characteristics could make it an efficient cooking fabric. The iron-rich vessels in the Mediterranean were mentioned in section 8.2. The petrography analysis suggested that the matrix has a high Fe/Ca ratio. Although it is not unique to this fabric, these vessels consistently have a high ratio. The scatterplot in Figure 7.2a confirmed that fabric 5 is depleted in calcium oxides explaining the bright red colours of the vessel. Using the Terra Rossa rather than the Blue Clays-derived soils could cause this pattern. Hein et al. (2008: 42) compared a Greek calcareous (14%wt) to a Greek non-calcareous clay using experimental briquettes. They concluded that focusing on conductivity alone, a non-calcareous clay fired at high temperature ($>$850 and even $>$ 1050°C) with a moderate amount of temper (not above the 20-30% range) had the best results in terms of heat conductivity. It is generally admitted that low calcium clays are better suited for cooking vessels (Degryse and Braekmans 2016: 257).

The naturally occurring quartz is not detrimental to cooking practice. Quartz is a conductive mineral and would conduct heat efficiently (Hein et al. 2008: 39). Quartz undergoes a displacive transformation at 573°C during firing and expands (Cuomo Di Caprio 2017a: 332). This creates micro-damages in the pottery, which

can be detrimental, but the crystals act as crack arrestors, increasing the toughness of a vessel and possibly its lifetime (Müller 2016: 616). Although it does not mean that the raw materials were chosen for these properties, the material composing these vessels seems to indicate they were efficient cooking pots, which potters might have learnt with experience. These are summarised in Figure 9.2.

The yellowish and pinkish white inclusions of these vessels had been described as "lime" (Anastasi 2019: 75) and the white inclusions as "crushed limestone rock" (Sagona 2015b: 74). The inclusions are calcium carbonates inclusions; however, "lime" would only apply to calcium carbonate that has dissociated, which means samples with a temperature above 850-900°C. The petrography in this dissertation has supported the identification of the inclusions as either biomicrite, marl fragments or, less likely, chamotte. Limestone rock fragments are often cited as a possible temper for cooking vessels because calcite has a similar thermal expansion coefficient to low-fired clay (Müller 2016: 618-619). Calcite is said to improve thermal resistance (Eramo 2020: 5) and have a reasonable heat transmission (Degryse and Braekmans 2016: 257). Crushed sherds, such as grog or chamotte, also have similar properties to the vessel, such as thermal expansion coefficient (Rice 2015: 424).

Since limestone, biomicritic limestones, and marls are easily found in Malta (see section 2.1), they could have been picked because of their availability rather than other properties. Tempering can increase heat transmission as a very fine vessel with aligned clay sheets, and porosity does affect the transmission of heat (Degryse and Braekmans 2016: 253). However, based on the experience of working the Terra Rossa soils, the tempers could have been selected to improve workability (see sections 9.1.1).

To summarise, these vessels and the material seem well suited to their intended function. This could be assessed further with material tests on the heat conductivity of sherds and experimental samples comparing Blue clay briquettes and Terra Rossa briquettes. This dissertation indicates that there might have been a preferential use of the iron-rich raw material, possibly Terra Rossa, for cooking vessels, and it

could have been more suited for specific food preparation techniques. If this trend is confirmed across the islands, this might be a specialised strategy of raw material procurement (Santacreu 2014: 245). This concept describes when potters choose a type of clay for specific vessels or depending on their function. It is to be noted that if these vessels were not made locally, this cooking fabric would still represent a deliberate choice of vessel procurement for import.

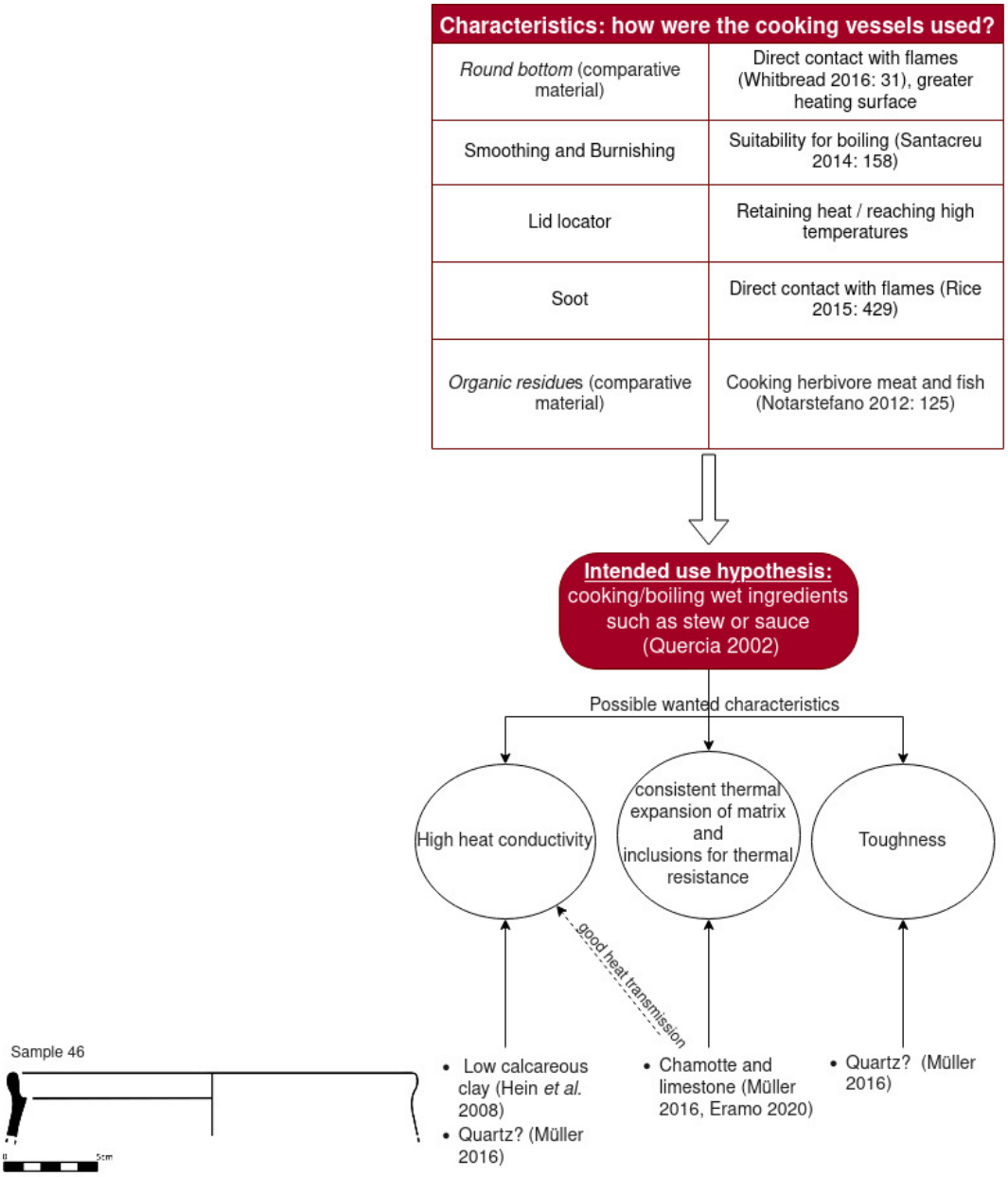


Figure 9.2: Graphic summary presenting the discussion on the relationship between fabric, shape, and intended use.

One interpretation of the cooking vessels at Tas-Silġ was that the vessels were only used a few times or reserved for ritual activities based on their low concentrations

of fatty acids (Notarstefano 2012: 127). Low concentrations of fatty acid could also be caused by the surface treatment of the vessels, as burnishing tends to close surface porosity (Correa-Ascencio and Evershed 2014: 1337). This limitation aside, if these vessels were only used a few times, they were still designed as suitable cooking vessels for boiling.

Implications on technological knowledge

This section takes an approach broader than the archaeological sites studied here. However, this question should be furthered when the cooking vessels of other sites are studied. For now, there is no evidence of using Terra Rossa soils for pottery in Malta before using the olla-shaped vessels. Terra Rossa has been mentioned recently as a possible base material for Red Skorba pottery, but the vessels have yet to be compared to local raw materials (Malone et al. 2020: 742). Terra Rossa also seems to have been one source of ochre (Montalto et al. 2012). In Malta, however, no conclusive evidence exists for vessels made with similar material in the Bronze Age or earlier. Most olla shapes in Sagona (2002) seem to appear during Period IV and be common after the 4th century BCE (Anastasi 2019: 77). Quercia (2002: 411) argues that these shapes became widespread in the occidental Punic world in the 5th century BCE. The hypothesis is that fabric 5 in Malta, which makes up these vessels, appears concomitantly with these shapes.

With the introduction of new forms, the *connaissance* and *savoir-faire* to make (or copy) these types of vessels might also have arrived in Malta, including raw material selection and procurement strategy. *Connaissance* describes the knowledge around practice, such as knowledge of raw material, while *savoir-faire* describes the practical knowledge of making (Bamforth and Finlay 2008: 2). Both of these aspects would have been necessary to make these vessels.

Several processes could explain an emerging technical knowledge of a shape or a raw material. For instance, local potters might have been trying to replicate vessels familiar in the Mediterranean with local materials and experimenting to find the best raw material. This hypothesis is hard to explore as there needs to

be more information on the variations within the cooking vessels across time and space. More research should be done on the variations of locally suitable available materials, such as the Terra Rossa soils.

Another explanation would be the case of mobile potters (even temporarily) replicating their knowledge with the closest material they find or, more generally, a case of knowledge transfer. Successful recognition of knowledge transfer from potters moving to a new location has been carried out in the Mediterranean. For example, as a parallel Aegina's potters successfully exported cooking vessels during the Bronze Age but they were then paralleled with locally available raw materials along the Euboean gulf, possibly by moving potters carrying their knowledge of the *chaîne opératoire* with them (Lis et al. 2020). Similarly, in 6th century Athens, the Aeginitan cooking vessel imports were slowly replaced by locally made pottery with very similar *chaîne opératoires* which could have been caused by migration of potters to Athens (Klebinder-Gauss and Strack 2015: 89). For the latter case, transitional vessels were identified. The Aegina example highlights that workshops would need to be identified as well as the techniques and the shapes which might have been inspired from - in clear, better identification of comparative material within the central Mediterranean and a refined chronology of the vessel's appearance and use of raw material.

A question remains: if these vessels are local, why not adopt this raw material for other vessels? A few hypotheses can be drawn from the literature on raw material variation. More research needs to be carried out before asserting one or the other. These are the following:

- Limited access to the source compared to the abundance of Blue Clay in the northern parts of the island
- Reluctance to change procedure (Santacreu 2014: 195) for other types of vessels for which Blue Clay might be suitable
- Difficulties to work the new raw material: the constraints of the material on certain steps of the *chaîne opératoire* might have required a certain technical investment (Santacreu 2014: 58);

Finally, this technical knowledge (or the use of selected imported vessels) seems to have picked up in Malta, meaning there was a demand for these vessels. The making of pottery is highly related to food culture, which can foster innovation, or on the contrary, continuity (Santacreu 2014: 272), specific cooking methods might have become more prominent concomitantly.

9.2.2 Workshops and archaeological sites

Skill, specialisation and workshops

Identifying the organisation of production based on ceramic assemblages is impossible, as the places where production activities take place have not been identified in Malta. Many markers of production (Santacreu 2014: 249) are missing in the known Maltese archaeological record, which would allow a more accurate understanding of the organisation of production and distribution around the islands. A few tentative comments can be made, keeping in mind the limitations highlighted by Santacreu (2014: 246-7) that the frameworks developed to understand production organisation are often imbued with the Western concepts of production.

First, if the wheel-turned or wheel-thrown vessels are made in Malta, then it is likely that workshops would have occurred in Malta as wheel-throwing requires training and equipment, as mentioned in section 9.1.2. Following the discussion of the knowledge transfer of working Terra Rossa and collection strategies, potters with access to workshops dedicated to these resource strategies could have been present around the island. This does not mean that these possible workshops would have exclusively worked these vessels. However, specific knowledge would have been required and transmitted in dedicated places, such as workshops (Rice 2015: 360).

The pottery from Tas-Silġ fabrics 1 and 2 had some characteristics such as uneven firing, uneven surface finish, and asymmetry cited across the dissertation, which suggests that there was not as much skilled work dedicated to these fabrics (Santacreu 2014: 257). This does not mean that the potters were not skilled, but

rather that there was no necessity to have highly standardised, homogeneously finished and fired pottery in this specific time and space.

The absence of evidence for a production structure such as a kiln prevents more interpretation of production organisation. Kilns have been described in post-medieval Malta as excavated in the rock or ground or as simple temporary structures (Palmer 2020: 448). Rock-cut features, such as the ones mentioned in Section 2.3.1, should also be investigated, although the ability to fire pottery in a Maltese limestone kiln should be tested. Palmer et al. (2018: 450-451) describe a year-long small-scale pottery production for early twentieth-century Malta, possibly a kin-based industry. Although it is impossible to extrapolate this organisation to the Roman period, similar modes of production and technology might not leave much material evidence. This is particularly true for household production and the industry or small localised workshops where firing, for instance, might not be performed in permanent structures or small structures (Peacock 1982).

In the lack of structural evidence of a kiln in Malta, one can still assess whether a kiln would be viable in the Maltese islands by studying specific locations. The example of Tal-Qares mentioned in Section 2.3.1 can help in discussing the viability of kilns. Tal-Qares is situated close to potential raw materials. Although it is built on the Attard member of Lower Coralline Limestone, the geological maps indicate that current fields across Wied ta' Għajn Riħana are located on underlying Blue Clay. Similarly, the valley itself could be catching plastic sediments. The water supply could be guaranteed by wells or cisterns at the site (Cutajar and Spiteri 2014: 7) and possibly water accumulating in the closeby valley. The site is associated with agricultural features (vine trenches) (Cutajar and Spiteri 2014). In classical times, olive oil was additionally being produced all over the islands in similar sites (Anastasi et al. 2022; Anastasi and Vella 2018). Peacock (1982: 25) mentions an ethnoarchaeological study on a pottery workshop in Tunisia where the olive production waste, among other possible farming waste, was used as fuel for pottery making. Production could be practiced only part of the year, particularly when coupled with agricultural activity (Peacock 1977b: 9).

Final points on the archaeological sites

Some final points can be mentioned when looking at the two archaeological sites, the sanctuary at Tas-Silġ and the Żejtun villa, separately. It has already been argued that the plates and bowls at Tas-Silġ did not need to be highly standardised and well-finished, although most of them were still efficient vessels (section 5.1.1). This is probably related to using the vessels at the site as offerings, possibly thrown away after use. It has also been stated that, despite the hypothesis of using the cooking vessels once, these were cooking vessels which seemed to be designed as efficient cooking vessels, with an emphasis on the type of meals which could be prepared (stew, soup, liquid food). No fine ware was identified in the two assemblages of Tas-Silġ

The assemblage at the Żejtun villa is more challenging to interpret because fewer samples were studied. No miniatures were found, which supports their ritual aspect at Tas-Silġ as mentioned in section 5.2.1, and the only diagnostic cooking vessel found was a fine ware from fabric 7. Undiagnostic sherds of possible cooking fabric were found at Żejtun (see appendix B.3)..

The fabric classification is overly dictated by the Tas-Silġ assemblages, and the Żejtun samples only sometimes fit well with the other samples. When undertaking the microscopic classification, the uncertainly classified samples, such as 66 or 69, were from the villa (appendix C.1). Unexpectedly, Samples 66 and 69 fit the petrographic classification. Petrographically, there were also outliers; for example, fabrics 3 and 4 are outliers to the classification and were sampled from the villa. If these differences were confirmed with more samples across the two archaeological sites. In that case, they could be caused by a chronological difference, the different activities at the archaeological sites or different ceramics sources. These differences might be a sample bias from the specific contexts chosen, and more samples could be analysed.

Conclusion

Research aims and summary

This dissertation set out to tackle four research aims: the review of literature on fabrics from the Punic-Roman period; the classification of pottery fabrics at the two archaeological sites using an interdisciplinary approach; the assessment of the variations between pottery fabrics, considering the differences in the *chaîne opératoire*, and their possible provenance.

Two major ware groups were investigated: Crisp Ware (Anastasi Fabric 1) and the Bricky Red Ware (Anastasi Fabric 5) in four stratigraphic assemblages from the Tas-Silġ sanctuary and the Żejtun villa. Plates, bowls and cooking vessels from the 3rd-1st century BCE were studied in detail. Seventy samples of these stratigraphic assemblages were recorded macroscopically and microscopically, and a smaller number of sherds were chosen for analysis with XRF (49 sherds) and PLM (34 sherds).

Geological samples from the Maltese Islands, including Blue Clay derived soils and Terra Rossa, were analysed with XRF and compared with the archaeological sherds. PLM analysis was carried out on Terra Rossa briquettes to strengthen the conclusion that this raw material could have been used in Malta. The main findings can be summarised as follows:

(i) Crisp Ware was subdivided into several fabric groups (Fabrics 1-4), with the major differences being the presence of quartz and limonitic nodules. These differences can be explained by either a different raw material choice or differences in the *chaîne opératoire*.

(ii) Fabric 1 is likely to be local. The question remains open for Fabric 2 for which there was no direct match in this case, although a mix of raw materials could have been used by the potter.

(iii) Bricky Red Ware was confirmed as a consistent group through the analysis, here Fabric 5.

(iv) Fabric 5 and the fine ware Fabric 7 are different from the other fabric

groups and have more elaborate *chaîne opératoires*, possibly more specialised potters, and different raw materials.

(v) Some samples from Fabric 5 had chemical and mineral similarities with the local raw material Terra Rossa. The knowledge and use of this raw material might have concurred with the appearance of specific cooking vessel shapes.

(vi) If Fabric 5 could be locally made with Terra Rossa, it is used for specific forms and worked differently than the Blue Clay materials. Different technological choices would have been made in the Late Punic-Early Roman periods according to the vessel's intended function and its context of use.

(vii) Most samples from Fabrics 1, 2, 5 and 7 had the same classification at the macroscopic scale down to the elemental scale. Outliers were noticed using petrography and XRF.

Main limitations

As observed throughout the dissertation, only 70 samples could be analysed in such detail. Several forms and fabric variations could not be sampled because of time and budget constraints. Similarly, only four stratigraphic assemblages were analysed, which might not be representative of the archaeological sites or time-period.

The lack of a precise characterisation instrument dedicated and calibrated for these materials has limited how the results can be interpreted. Moreover, no foreign raw materials or identified imported pottery sherds were analysed, which prevented a complete provenance study.

The Terra Rossa briquettes have exemplified the importance of experimental archaeology to better understand past manufacturing practices; additional time and budget could not be allocated to pursue this further.

Main contributions

This work contributes to several broader research questions besides a better understanding of the sourcing of pottery at the two archaeological sites. This work has produced a collection of microphotographs, photographs and drawings to build on the several classifications and providing to future research comparative material for Late Punic and Roman assemblages in Malta. This record will be made accessible when a suitable repository and means of dissemination are identified.

The research for this dissertation has established a petrographic classification which was not available for plates, bowls and cooking vessels for this period. It has also shown that even when using semi-quantitative methods for chemical characterisation, there is scope to classify fabrics and compare them with raw materials while always considering the significant limitations. Finally, it has been suggested that possible local raw materials would be used for specific fabric groups.

Recommendations for future work

Several ideas are proposed to tackle these limitations. To strengthen the fabric classifications, more samples should be analysed from the two archaeological sites and other sites. More forms should be studied, such as expanding the cooking vessel repertoire, fine wares, amphorae and storage vessels. The fabric of these vessels could have specific requirements not explored here. Different contexts, such as funerary contexts, could also be included to understand if the fabrics differ according to site type. Moreover, the chronological span of the study could be widened, both for these archaeological sites and across the Maltese islands, to understand how the fabric variations have evolved. Comparisons with environmental and pottery samples from Southern Sicily and places in close relationship with Malta, such as Tunisia, would allow the provenance hypotheses from this dissertation to be refined.

More geological samples should be analysed with more accurate characterisation techniques to assess the variations within Blue Clays stratigraphic layers and across space, as well as the variations of Terra Rossa in the Maltese islands. This could include using a WD-XRF calibrated for geomaterials using fused beads and pressed pellets to quantify both major, minor, and trace elements. Experimental archaeology could allow testing these materials, experimenting with different sources and processes, such as mixing or levigating and testing their properties, for instance, heat conductivity.

Dedicated research could target the different stages of the *chaîne opératoire*. This includes more experimental work on surface treatments and firing processes and more analysis, such as X-Rays imaging, to understand the manufacturing methods (Ina and Janet 2016). Modern potters could be involved in testing the limitations of the materials as research would benefit from their insights. Research on potters who used specific raw materials, most likely through their descendants in the case of Malta, could be carried out to understand the constraints of the clays on pottery manufacture (Fowler 2016: 471).

Finally, work must be done on distinct fabric groups and forms, such as fabric 5, which seems to be associated with specific forms and uses. Looking at chemical and mineral variations and changes in forms across time and space (within the islands and tracing them back outside the islands) will allow archaeologists to understand better the appearance and development of specific techniques in the Maltese islands. A better dating of these vessels and refined chronology across the islands would support understanding the development of this technical knowledge. Direct technique methods, such as thermoluminescence, could be considered as the vessels are now proven to contain quartz which is often the mineral used in this method (Blain 2016).

Bibliography

Abela, R. 2012. The Żejtun Roman villa: its past and present contexts. In: R. Abela, ed. *The Żejtun Roman villa: research, conservation, management.* Malta: Wirt iz-Żejtun, pp.75–85.

Aitchison, J., Barceló-Vidal, C., and Pawlowsky-Glahn, V. 2002. Some comments on compositional data analysis in archaeometry, in particular the fallacies in Tangri and Wright's dismissal of logratio analysis. *Archaeometry*, 44(2), pp.295–304.

Alderton, D. 2020. Carbonates (Ca, Mg, Fe, Mn). In: S. Elias, ed. *Encyclopedia of geology.* 2nd. Vol. 1, Mineralogy. Amsterdam: Academic Press, pp.382–394.

Amadasi Guzzo, M.G. 1993. Divinità fenicie a Tas-Silġ, Malta–I dati epigrafici. *Journal of Mediterranean studies*, 3(2), pp.205–214.

Amadasi Guzzo, M.G. 2011. *Il santuario di Astarte di Malta: le iscrizioni in fenicio da Tas-Silġ*. Roma: Sapienza Università di Roma.

American School of Classical Studies 1958. Agora object: p 2393. *Agora excavation* [Online], ASCSA digital collections. Available from: `https://agora.ascsa.net/id/agora/object/p%5C%202393` [Accessed September 5, 2022].

Anastasi, M. 2012. Pottery from the 1972 excavations at the Żejtun villa. In: R. Abela, ed. *The Żejtun Roman villa: research, conservation, management.* Malta: Wirt iz-Żejtun, pp.26–41.

Anastasi, M. 2019. *Pottery from Roman Malta*. Oxford: Archaeopress.

ANASTASI, M. 2010. *Coarse and fine wares: a contextual meaning of pottery in Late Punic and Roman Malta*. MA dissertation. University of Malta. Unpublished.

ANASTASI, M. 2015. *Small-island interactions: pottery from Roman Malta*. PhD thesis. University of Oxford. Unpublished.

ANASTASI, M. 2020. From vine to vat and beyond: the case of ancient Malta. In: M. BENTZ and M. HEINZELMANN, eds. *Proceedings of the 19th international congress of Classical archaeology, Cologne/Bonn 2018*. Archaeology and Economy in the Ancient World. Vol. 9. Heidelberg: Propylaeum, pp.89–101.

ANASTASI, M., BETTS C, J., and VELLA, N. 2022. From windlass to screw: olive pressing technology in the Maltese Islands in Antiquity. In: C. SERRACINO, ed. *Ardens Amat: Essays in Honour of Horatio Caesar Roger Vella*. Malta: Midsea Books, pp.39–62.

ANASTASI, M., CAPELLI, C., GAMBIN, T., and SOURISSEAU, J.-C. 2021. The Xlendi Bay shipwreck (Gozo, Malta): a petrographic and typological study of an Archaic ceramic cargo. *Libyan studies*, 52, pp.166–172.

ANASTASI, M. and VELLA, N. 2018. Olive oil production technology in Roman Malta. In: N. VELLA, A.J. FRENDO, and H.C. VELLA, eds. *The lure of the Antique: essays on Malta and Mediterranean archaeology in honour of Anthony Bonanno*, Ancient near eastern studies, Suplement 54. Leuven, Paris, Bristol: Peeters, pp.275–300.

ANASTASI, M. and VELLA, N. 2021. Pottery variability and site function: Late Punic and Early Roman ceramic assemblages from Ras ir-Raeb and other archaeological sites in the Maltese Islands. In: N. CHIARENZA, B. D'ANDREA, and A. ORSINGHER, eds. *LRBT dall'archeologia all'epigrafia studi in onore di Maria Giulia Amadasi Guzzo*, Semitica et classica, Supplementa 3. Turnhout: Brepols, pp.15–39.

ARNOLD, D. 1980. Localized exchange: an ethnoarchaeological perspective. *Models and methods in regional exchange, SAA papers*, 1, pp.147–150.

ARNOLD, D. 2011. Ceramic theory and cultural process after 25 years. *Ethnoarchaeology*, 3(1), pp.63–98.

ASCIAK, G. 2019. *Characterisation and identification of fossil and mineral inclusions in Roman pottery from one site in Victoria, Gozo.* MA dissertation. University of Malta. Unpublished.

ATTARD, A. 2010. Gozitan Christmas lore and traditions. *Gozo observer*, 23, pp.17–24.

BAMFORTH, D.B. and FINLAY, N. 2008. Introduction: archaeological approaches to lithic production skill and craft learning. *Journal of archaeological method and theory*, 15(1), pp.1–27.

BARBERA, G., BARONE, G., CRUPI, V., LONGO, F., MAJOLINO, D., MAISANO, G., MAZZOLENI, P., RANERI, S., TEIXEIRA, J., and VENUTI, V. 2014. A multi-technique approach for the determination of the porous structure of building stone. *European journal of mineralogy*, 26, pp.189–198.

BARONE, G., GULLÌ, D., MAZZOLENI, P., RANERI, S., and TANASI, D. 2010. Archaeometric identification of Maltese imports in Prehistoric Sicily: Żebbuġ phase pottery from Licata-Caduta (Agrigento). *Malta Archaeological Review*, 10, pp.23–30.

BARONE, G., MAZZOLENI, P., RANERI, S., TANASI, D., and GIUFFRIDA, A. 2015. Archaeometric characterization of Middle Bronze Age pottery from the settlement at Borġ in-Nadur. In: D. TANASI and N. VELLA, eds. *The Late Prehistory of Malta: essays on Borġ in-Nadur and other sites.* Oxford: Archaeopress, pp.99–112.

BATS, M. 1988. Vaisselle et alimentation à Olbia de Provence (v. 350-v. 50 av. J.-C.). Modèles culturels et catégories céramiques. *Revue archéologique de Narbonnaise*, 18(1), pp.5–72.

BAXTER, M.J. 2001. Statistical modelling of artefact compositional data. *Archaeometry*, 43(1), pp.131–147.

Baxter, M.J. 2016. *Multivariate analysis of archaeometric data an introduction*. Unpublished. Available from: https://www.academia.edu/7721938/Multivariate_Analysis_of_Archaeometric_Data_Lecture_Notes [Accessed December 4, 2022].

Baxter, M.J. and Freestone, I.C. 2006. Log-ratio compositional data analysis in archaeometry. *Archaeometry*, 48(3), pp.511–531.

Baxter, M.J. 2008. Cluster analysis for archaeometric data analysis (English translation). In: I. Liritzis, ed. *New technologies in the archaeognostic sciences*. Gutenberg Press. Athens, Greece, pp.445–481.

Baxter, M. 1995. Standardization and transformation in principal component analysis, with applications to archaeometry. *Journal of the Royal Statistical Society: Series C (applied statistics)*, 44(4), pp.513–527.

Bechtold, B. 2018. La distribuzione di anfore da trasporto maltesi fuori dall'arcipelago: nuovi dati. In: N. Vella, A.J. Frendo, and H.C. Vella, eds. *The lure of the Antique: essays on Malta and Mediterranean archaeology in honour of Anthony Bonanno*. Leuven, Paris, Bristol: Peeters, pp.257–273.

Bechtold, B. 2017. The pottery from selected stratigraphic units (4th-1st cent. BCE). In: Vella, N., Bonanno, A., Anastasi, M., Farrugia, R., Fenech, K., Mizzi, D., Verdonck, L., and Zammit, A. *A view from the countryside: the nature of the Late Punic and Early Roman activity at the Żejtun villa site, Malta*, Rivista di studi fenici, 45, pp.122–143.

Bechtold, B., Gassner, V., Trapichler, M., and Radbauer, S. 2020. *Facem: provenance studies on pottery* [Online]. Available from: https://facem.at/project/about.php [Accessed December 4, 2022].

Ben-Shlomo, D. 2019. Cooking pot production in Judah during the Iron Age II. *Judea and Samaria research studies*, 28(1), pp.5–36.

Bishop, R.L., Rands, R.L., and Holley, G.R. 1982. Ceramic compositional analysis in archaeological perspective. In: M. Schiffer, ed. *Advances in archaeological method and theory*. Vol. 5. New York: New York Academic Press, pp.275–330.

Blagg, T., Bonanno, A., and Luttrell, A. 1990. *Excavations at Ħal Millieri, Malta: A Report on the 1977 Campaign Conducted on Behalf of the National Museum of Malta and the University of Malta*. Malta: Malta University Press.

Blain, S. 2016. Direct dating methods. In: A. Hunt, ed. *The Oxford handbook of archaeological ceramic analysis*. Oxford: Oxford University Press, pp.671–690.

Bonanno, A. and Vella, N. 2012. Past and present excavations of a multi-period site. In: R. Abela, ed. *The Żejtun Roman villa: research, conservation, management.* Malta: Wirt iz-Żejtun, pp.8–25.

Bonanno, A. 1977. Distribution of villas and some aspects of the Maltese economy in the Roman period. *Journal of the faculty of arts*, 6(4), pp.73–81.

Bonanno, A. 2005. *Malta: Phoenician, Punic, and Roman*. Malta: Midsea books.

Bonanno, A. 2007. The Phoenicians and the Maltese Prehistoric cultural landscape. In: D. Barrowclough and C. Malone, eds. *Cult in context : reconsidering ritual in archaeology*. Oxford: Oxbow Books, pp.107–111.

Bonanno, A. 2008. Maltese wine pressing in antiquity. *Melita historica*, 15(1), pp.1–18.

Bonanno, A. 2011. The rise of a maritime strategic island : Malta under the Phoenicians & the Romans/. In: C. Cini, J. Borg, R. Grima, and D. Cilia, eds. *The maritime history of Malta : the first millennia*. Malta: The Salesians of Don Bosco Malta in collaboration with Heritage Malta, pp.37–71.

Bonanno, A. 2015. The figurative representations, scarabs and amulets. In: A. Bonanno and N. Vella, eds. *Tas-silġ, Marsaxlokk (Malta): archaeological excavations conducted by the University of Malta, 1996-2005.* Vol. I. Leuven: Peeters, pp.257–297.

Bonanno, A., Frendo, A.J., Vella, N., Bonnano, A., Mason, S., Sagona, C., Farrugia, R., Borda, K., Zammit, M.E., Stöger, H., et al. 2000. Excavations at Tas-Silġ, Malta: a preliminary report on the 1996–1998 campaigns conducted by the Department of Classics and Archaeology of the University of Malta. *Mediterranean archaeology*, 13, pp.67–114.

Bonanno, A. and Vella, N. 2015a. Introduction. In: A. Bonanno and N. Vella, eds. *Tas-silġ, Marsaxlokk (Malta): archaeological excavations conducted by the University of Malta, 1996-2005.* Leuven: Peeters, pp.1–16.

Bonanno, A. and Vella, N., eds 2015b. *Tas-silġ, Marsaxlokk (Malta): archaeological excavations conducted by the University of Malta, 1996-2005.* Vol. I. Leuven: Peeters.

Bonanno, A. and Vella, N., eds 2015c. *Tas-silġ, Marsaxlokk (Malta): archaeological excavations conducted by the University of Malta, 1996-2005.* Vol. II. Leuven: Peeters.

Bonifay, M. 2004. *Etudes sur la céramique romaine tardive d'Afrique*. Oxford: Archaeopress.

Bonzano, F. 2017. *Fanum Iunonis Melitense: l'area centrale del santuario di Tas-Silġ a Malta in età tardo-repubblicana*. Bari: Edipuglia.

Borg, H. 2005. *Neolithic pottery of Malta: a review of techniques, decoration and firing, including an exercise in experimental archaeology*. BA Disserttion. University of Malta. Unpublished.

Bourdieu, P. 1990. *Outline of a theory of practice*. Cambridge: Cambridge University Press.

Brogan, C. 2021a. *A potted history: Malta's earliest pottery tradition* [Online]. The Archaeology Society of Malta. Unpublished. Available from: `https://www.youtube.com/watch?v=swTTxTBSkQ8&ab_channel=TheArchaeologicalSocietyMalta` [Accessed December 4, 2022].

Brogan, C. 2021b. *MaltaPot: methods and analysis*. Webinar presentation. Webinar presentation. Pottery under the microscope: Taking stock of pottery fabric studies in Malta. University of Malta. Unpublished.

Brongniart, A. 1844. *Traité des arts céramiques ou des poteries: considérées dans leur histoire, leur pratique et leur théorie* [Online]. Vol. 1. Paris: Béchet jeune; Mathias (Augustin). Available from: `https://gallica.bnf.fr/ark:/12148/bpt6k67829t/f7.item.zoom` [Accessed December 4, 2022].

Bruno, B. 2009. *Roman and Byzantine Malta: trade and economy*, Maltese social studies. Malta: Midsea Books.

Bruno, B. and Capelli, C. 2000. Nuovi tipi di anfore da trasporto a Malta. *Atti della 6a giornata: le scienze della terra e l'archeometria*, pp.59–65.

Buxton, L.H.D. and Hort, A.V.D. 1921. 79. The modern pottery industry in Malta. *Man*, 21, pp.130–131.

Cachia, A. 2011. Orslika, a trip down memory lane. *Times of Malta* [Online]. Available from: `https://timesofmalta.com/articles/view/Orslika-a-trip-down-memory-lane.397160` [Accessed April 13, 2020].

Camilleri Haber, D. 2015. *Mapping Quaternary deposits in a Maltese valley*. BSc dissertation. University of Malta. Unpublished.

Cardona, D. 2021. Past, present, future: an overview of Roman Malta. *Open archaeology*, 7(1), pp.231–255.

Caruana, A.A. 1899. *Ancient pottery from the ancient pagan tombs and Christian cemeteries in the islands of Malta by AA Caruana: printed by order of His Excellency the Governor*. Malta: Government Printing Office.

Cassar, D. 2020. *An investigation into the one-dimensional compression properties of the reconstituted and intact Blue Clay of the Maltese Islands*. Master of Civil Engineering dissertation. University of Malta. Unpublished.

Cassar, J. 2002. Deterioration of the Globigerina limestone of the Maltese Islands. *Geological Society, London, special publications*, 205(1), pp.33–49.

Cazzella, A. and Recchia, G. 2007. Revisiting anomalies: new excavations at Tas-Silġ and a comparison with other megalithic temples in Malta. *Accordia research papers*, 10, pp.61–70.

Cazzella, A. and Recchia, G. 2012. Tas-silġ: the Late Neolithic megalithic sanctuary and its reuse during the Bronze Age and the Early Iron Age. *Scienze dell'antichità storia archeologia antropologia*, (18), pp.15–38.

Chatzimpaloglou, P., Schembri J., P., French, C., Ruffell, A., and Stoddart, S. 2020. The geology, soils and present-day environment of Gozo and Malta. In: C. French, C. Hunt, R. Grima, R. McLaughlin, S. Stoddart, and C. Malone, eds. *Temple landscapes: fragility, change and resilience of Holocene environments in the Maltese Islands*. Vol. 1, Fragility and sustainibility - studies on Early Malta, the ERC-funded FRAGSUS project. Cambridge: McDonald Institute for Archaeological Research, pp.19–34.

Ciasca, A. 1993. Some considerations regarding the sacrifical precincts at Tas-Silġ. *Journal of Mediterranean studies*, 3(2), pp.225–244.

Cilia, D. 2022a. *Globigerinoides ruber* [Online]. Available from: `https://foraminifera.eu/single.php?no=1000803&aktion=suche` [Accessed December 20, 2022].

Cilia, D. 2022b. *Nodosaria torsicostata* [Online]. Available from: `https://foraminifera.eu/single.php?no=1001294&aktion=suche` [Accessed December 20, 2022].

Cilia, D. 2022c. *Orbulina sp* [Online]. Available from: `https://foraminifera.eu/single.php?no=1001386&aktion=suche` [Accessed December 20, 2022].

Collett, L. 2012. *An introduction to drawing archaelogical pottery*, IfA professional practice paper, 10. Reading: Institute For Archaeologists.

Continental Shelf, M. 2022. *Geological map of the Maltese Islands (1:10,000)* [Online]. Available from: `https://experience.arcgis.com/experience/04736039724248fb8dc52615f1528e2e/page/Page/` [Accessed December 16, 2022].

Correa-Ascencio, M. and Evershed, R.P. 2014. High throughput screening of organic residues in archaeological potsherds using direct acidified methanol extraction. *Analytical methods*, 6(5), pp.1330–1340.

Courty, M.-A. and Roux, V. 1995. Identification of wheel throwing on the basis of ceramic surface features and microfabrics. *Journal of archaeological science*, 22(1), pp.17–50.

Cuomo Di Caprio, N. 2017a. *Ceramics in archaeology: from Prehistoric to Medieval times in Europe and the Mediterranean: ancient craftsmanship and modern laboratory techniques*. Vol. I. Rome: L'Erma di Bretschneider.

Cuomo Di Caprio, N. 2017b. *Ceramics in archaeology: from Prehistoric to Medieval times in Europe and the Mediterranean: ancient craftsmanship and modern laboratory techniques*. Vol. II. Rome: L'Erma di Bretschneider.

Cutajar, N. 2006. *Zebbiegh (ZBH2006)* [Online]. Malta: Superintendence of Cultural Heritage. Available from: http://www.fastionline.org/excavation/micro_view.php?item_key=fst_cd&fst_cd=AIAC_1159 [Accessed December 4, 2022].

Cutajar, N. and Spiteri, M. 2014. *Archaeological evaluation at Tal-Qares, Mosta i.c.w. Rationalisation Scheme Map 27, Site E* [Online]. Malta: Superintendence of Cultural Heritage Malta. Available from: https://culture.gov.mt/en/culturalheritage/Documents/form/Preliminary%5C%20Report%5C%20for%5C%20Archaeological%5C%20Evaluation%5C%20at%5C%20Tal-Qares,%5C%20Mosta.pdf [Accessed December 4, 2022].

Darvill, T. 2008. *The concise Oxford dictionary of archaeology*. Oxford: Oxford University Press.

Day, P.M., Cau Ontiveros, M.Á.C., Mas Florit, C., and Müller, N.S. 2015. A contextual ethnography of cooking vessel production at Portol, Mallorca (Balearic Islands). In: A. Villing and M. Spataro, eds. *Ceramics, cuisine and*

culture: the archaeology and science of kitchen pottery in the ancient Mediterranean world. Oxford: Oxbow Books, pp.37–48.

De Bonis, A., Bonis, B. de, Piacentini, D., and Scagliarini, F. 2019. Les inscriptions phéniciennes et puniques sur poterie de Tas-Silġ (Malte). In: A. FERJAOUI and F. REDISSI, eds. *La vie, la mort et la religión dans l'univers phénicien et punique: actes du VIIème congrès international des études phéniciennes et puniques*. Tunis: Institut National du Patrimoine, pp.1625–1640.

Debono, N. 2012. *Index properties of sediments from the Maltese stratigraphy, containing clay minerals*. Master of Civil Engineering dissertation. University of Malta. Unpublished.

Degryse, P. and Braekmans, D. 2016. Petrography: optical microscopy. In: A. Hunt, ed. *The Oxford handbook of archaeological ceramic analysis*. Oxford: Oxford University Press, pp.233–265.

Degryse, P. and Shortland, A.J. 2018. Characterization of ceramics. In: S. López Varela, ed. *The encyclopedia of archaeological sciences* [Online]. Wiley Online Library, pp.1–6. Available from: `https://onlinelibrary.wiley.com/doi/book/10.1002/9781119188230` [Accessed December 4, 2022].

Dietler, M. and Herbich, I. 1998. Habitus, techniques, style: an integrated approach to the social understanding of material culture and boundaries. In: M. Stark, ed. *The archaeology of social boundaries*. Washington: Smithsonian Institution Press, pp.232–263.

DiGeronimo, I., Grasso, M., and Pedley, H. 1981. Palaeoenvironment and palaeogeography of miocene marls from southeast sicily and the maltese islands. *Palaeogeography, palaeoclimatology, palaeoecology*, 34, pp.173–189.

Drennan, R. 2009. *Statistics for archaeologists: a common sense approach*, Interdisciplinary contributions to archaeology. New-York: Springer US.

Druc, I. 2013. What is local? looking at ceramic production in the Peruvian Highlands and beyond. *Journal of anthropological research*, 69(4), pp.485–513.

Durn, G. 2003. Terra rossa in the Mediterranean region: parent materials, composition and origin. *Geologia croatica*, 56(1), pp.83–100.

Eramo, G. 2020. Ceramic technology: how to recognize clay processing. *Archaeological and anthropological sciences*, 12(8), pp.1–24.

FACEM 2020. *M 114/3* [MALTA-C-2] [Online]. Available from: `https://facem.at/m-114-3` [Accessed January 11, 2022].

Farres, P. 2019. Palaeosoils: legacies of past landscapes, with a series of contrasting examples from Malta. In: R. Gauci and J. Schembri, eds. *Landscapes and landforms of the Maltese Islands*. Gewerbestrasse: Springer, pp.141–152.

Finch, A. and Allison, N. 2007. Coordination of Sr and Mg in calcite and aragonite. *Mineralogical magazine*, 71(5), pp.539–552.

Fort, R., Varas, M., Ergenç, D., Cassar, J., Anastasi, M., and Vella, N. 2022. The technology of ancient lime mortars from the Żejtun Roman Villa (Malta). In: *Preprint*. Research Square.

Fowler, C. 2010. From identity and material culture to personhood and materiality. In: *The Oxford handbook of material culture studies* [Online]. Available from: `https://www.oxfordhandbooks.com/view/10.1093/oxfordhb/9780199218714.001.0001/oxfordhb-9780199218714-e-15` [Accessed April 14, 2021].

Fowler, K.D. 2016. Ethnography. In: A. Hunt, ed. *The Oxford handbook of archaeological ceramic analysis*. Oxford: Oxford University Press, pp.469–486.

French, C., Hunt, C.O., Grima, R., McLaughlin, R., Stoddart, S., and Malone, C., eds 2020. *Temple landscapes: fragility, change and resilience of Holocene environments in the Maltese Islands*. Cambridge: McDonald Institute for Archaeological Research.

FRENCH, C. and TAYLOR, S. 2020. The geoarchaeology of past landscape sequences on Gozo and Malta. In: C. FRENCH, C. HUNT, R. GRIMA, R. MCLAUGHLIN, S. STODDART, and C. MALONE, eds. *Temple landscapes: fragility, change and resilience of Holocene environments in the Maltese Islands*. Vol. 1, Fragility and sustainibility - studies on Early Malta, the ERC-funded FRAGSUS project. Cambridge: McDonald Institute for Archaeological Research, pp.161–222.

FRENDO, A.J. and MIZZI, D. 2015. The Punic inscriptions. In: A. BONANNO and N. VELLA, eds. *Tas-Silġ, Marsaxlokk (Malta): archaeological excavations conducted by the University of Malta, 1996-2005.* Leuven: Peeters, pp.515–650.

GAMBIN, T., SOURISSEAU, J.-C., and ANASTASI, M. 2021. The cargo of the Phoenician shipwreck off Xlendi Bay, Gozo: analysis of the objects recovered between 2014–2017 and their historical contexts. *International journal of nautical archaeology*, 50(1), pp.3–18.

GAUCI, R. and SCERRI, S. 2019. A synthesis of different geomorphological landscapes on the Maltese Islands. In: R. GAUCI and J. SCHEMBRI, eds. *Landscapes and landforms of the Maltese Islands*. Gewerbestrasse: Springer, pp.49–65.

GLASCOCK, M. 1992. Characterization of archaeological ceramics at MURR by neutron activation analysis and multivariate statistics. *Chemical characterization of ceramic pastes in archaeology*, 7, pp.11–26.

GLASCOCK, M. 2016. Compositional analysis in archaeology. In: *The oxford handbook of topics in archaeology* [Online]. Available from: `https://academic.oup.com/edited-volume/43506/chapter/364131553` [Accessed December 4, 2022].

GOSSELAIN, O.P. 1992. Bonfire of the enquiries. pottery firing temperatures in archaeology: what for? *Journal of archaeological science*, 19(3), pp.243–259.

Gosselain, O.P. 2018. Pottery chaînes opératoires as historical documents. In: T. Spear, ed. *Oxford research encyclopedia of african history.* [Online]. Oxford University Press. Available from: https://oxfordre.com/africanhistory/view/10.1093/acrefore/9780190277734.001.0001/acrefore-9780190277734-e-208 [Accessed December 20, 2022].

Grammatikakis, I.E., Kyriakidis, E., Demadis, K.D., Cabeza Diaz, A., and Leon-Reina, L. 2019. Mineralogical characterization and firing temperature delineation on minoan pottery, focusing on the application of micro-Raman spectroscopy. *Heritage*, 2(3), pp.2652–2664.

Grech, J. 2019. *Characterisation of Roman pottery from Malta*. B. Eng. dissertation. University of Malta. Unpublished.

Greenacre, M. 2018. *Compositional data analysis in practice*. New York: CRC Press.

Grima, R. 2007. Landscape and ritual in Late Neolithic Malta. In: D. Barrowclough and C. Malone, eds. *Cult in context : reconsidering ritual in archaeology*. Oxford: Oxbow Books., pp.35–41.

Gualtieri, S. 2020. Ceramic raw materials: how to establish the technological suitability of a raw material. *Archaeological and anthropological sciences* [Online], 12(8). Available from: https://link-springer-com.ejournals.um.edu.mt/article/10.1007/s12520-020-01135-w [Accessed December 20, 2022].

Guo, M. 2017. Variability in pottery firing technology: choice or technical development? *Chinese archaeology*, 17(1), pp.179–186.

Hall, M. 2016. X-Ray Fluorescence-Energy Dispersive (ED-XRF) and Wavelength Dispersive (WD-XRF) Spectrometry. In: A. Hunt, ed. *The Oxford handbook of archaeological ceramic analysis*. Oxford: Oxford University Press, pp.343–381.

Hammer, Ø., Harper, D., and Ryan, P. 2001. PAST: paleontological statistics software package for education and data analysis. *Palaeontologica electronica*, 4(1).

Hasenzagl, C. and Capelli, C. 2020. Petrographic characterization of Late Roman African pottery from JW Salomonson's surveys: 2. the workshop of Sidi Aïch. *Antiquités africaines. L'Afrique du Nord de la protohistoire à la conquête arabe*, 56, pp.161–173.

Hazenfratz Marks, R. 2016. Evaluating data: uncertainty in ceramic analysis. In: A. Hunt, ed. *The Oxford handbook of archaeological ceramic analysis*. Oxford: Oxford University Press, pp.48–56.

Hein, A. and Kilikoglou, V. 2020. Ceramic raw materials, how to recognize them and locate the supply basins: chemistry. *Archaeological and anthropological sciences* [Online], 12(8). Available from: https://link-springer-com.ejournals.um.edu.mt/article/10.1007/s12520-020-01129-8 [Accessed December 20, 2022].

Hein, A., Müller, N.S., Day, P.M., and Kilikoglou, V. 2008. Thermal conductivity of archaeological ceramics: the effect of inclusions, porosity and firing temperature. *Thermochimica acta*, 480(1), pp.35–42.

Henderson, J. 2000. *The science and archaeology of materials: an investigation of inorganic materials*. London and New-York: Routledge.

Ho, J.W. and Quinn, P.S. 2021. Intentional clay-mixing in the production of traditional and ancient ceramics and its identification in thin section. *Journal of archaeological science: reports* [Online], 37. Available from: https://www.academia.edu/45652455/Intentional_clay_mixing_in_the_production_of_traditional_and_ancient_ceramics_and_its_identification_in_thin_section [Accessed December 20, 2022].

Hoard, R., O'Brien, M., Khorasgany, M., and Gopalaratnam, V. 1995. A materials-science approach to understanding limestone-tempered pottery from the midwestern united states. *Journal of archaeological science*, 22(6), pp.823–832.

Holmqvist, E. 2016. Handheld portable energy-dispersive X-Ray Fluorescence spectrometry (pXRF). In: A. Hunt, ed. *The Oxford handbook of archaeological ceramic analysis*. Oxford: Oxford University Press, pp.363–381.

HUMANN, A. 2021. *Characterisation of Maltese clay samples by classical analytical methods, XRD and micro- Raman*. Professional report. Hochschule Fresenius; Fresenius University of Applied Sciences. Unpublished.

HUMANN, A. 2022. *Analysis of Late Punic and Early Roman pottery sherds from Malta*. BSc dissertation. Hochschule Fresenius. Unpublished.

HUNT, A. 2017a. Introduction. In: A. HUNT, ed. *The Oxford handbook of archaeological ceramic analysis*. Oxford: Oxford University Press, pp.3–6.

HUNT, A., ed. 2017b. *The Oxford handbook of archaeological ceramic analysis*. Oxford: Oxford University Press.

HUNT, A. and SPEAKMAN, R.J. 2015. Portable XRF analysis of archaeological sediments and ceramics. *Journal of archaeological science*, 53, pp.626–638.

HUNT, C., FARRELL, M., FLOOD, R., FENECH, K., MCLAUGHLIN, R., TAYLOR, S., VELLA, N., and FRENCH, C. 2020. The sediment cores. In: C. FRENCH, C. HUNT, R. GRIMA, R. MCLAUGHLIN, S. STODDART, and C. MALONE, eds. *Temple landscapes: fragility, change and resilience of Holocene environments in the Maltese Islands*. Vol. 1, Fragility and sustainibility - studies on Early Malta, the ERC-funded FRAGSUS project. Cambridge: McDonald Institute for Archaeological Research, pp.43–63.

HUNT, C.O. 1997. Quaternary deposits in the Maltese Islands: a microcosm of environmental change in Mediterranean islands. *GeoJournal*, 41(2), pp.101–109.

HUNT, C.O. and SCHEMBRI, P.J. 1999. Quaternary environments and biogeography of the Maltese Islands. In: A. MIFSUD and V. SAVONA, eds. *Facets of Maltese Prehistory*. Malta: The Prehistoric Society of Malta, pp.41–75.

INA, B. and JANET, A. 2016. X-radiography of archaeological ceramics. In: A. HUNT, ed. *The Oxford handbook of archaeological ceramic analysis*. Oxford: Oxford University Press, pp.544–564.

John, C.M., Mutti, M., and Adatte, T. 2003. Mixed carbonate-siliciclastic record on the North African margin (Malta)—coupling of weathering processes and mid Miocene climate. *Geological Society of America Bulletin*, 115(2), pp.217–229.

Johnson, M. 2009. The theoretical scene, 1960-2000. In: C. Gosden, B. Cunliffe, and R. Joyce, eds. *The Oxford handbook of archaeology*. Oxford: Oxford University Press, pp.71–88.

Kaufman, L. and Rousseeuw, P.J. 2009. *Finding groups in data: an introduction to cluster analysis*. Oxford: John Wiley & Sons.

Kipfer, B.A. 2008. *Dictionary of artifacts*. Oxford: John Wiley & Sons.

Kiriatzi, E. and Siddall, R. 2022. *An introduction to ceramic petrology; part 2: petrology applications to ceramic studies.* Notes and Bibliography to support a course taught at the British School of Athens 20 June-1 July 2022. Athens: British School at Athens. Unpublished.

Klebinder-Gauss, G. and Strack, S. 2015. An Aeginetan potters' workshop in Athens. In: W. Gauss, G. Klebinder-Gauss, and C.v. Rüden, eds. *The transmission of technical knowledge in the production of Ancient Mediterranean pottery*. Vol. 54, International conference at the austrian archaeological institute at athens. Athens: Österreichisches Archäologisches Institut, pp.77–95.

Kolb, C.C. 2014. Provenance studies in archaeology. In: C. Smith, ed. *Encyclopedia of global archaeology*. New York: Springer, pp.6172–6181.

Kolb, C.C. 2020. Ceramic ecology. In: C. Smith, ed. *Encyclopedia of global archaeology*. Cham: Springer International Publishing, pp.2059–2067.

Lanfranco, G. 1978. The Maltese clay modelling tradition. *Heritage: an encyclopedia of Maltese culture and civilizatio*, 15, pp.292–297.

Lang, D. 1960. *Soils of Malta and Gozo*. (29). Colonial office. London: Colonial Research Studies.

Lis, B., Kiriatzi, E., Batziou, A., and Rückl, Š. 2020. Dealing with the crisis: mobility of Aeginetan-tradition potters around 1200 BC. *Annual of the british school at athens*, 115, pp.269–327.

López-García, P., Argote-Espino, D., and Fačevicová, K. 2018. Statistical processing of compositional data: The case of ceramic samples from the archaeological site of Xalasco, Tlaxcala, Mexico. *Journal of archaeological science: reports*, 19, pp.100–114.

Lucas, I. 2021. *The contribution of photogrammetry to the documentation and monitoring of an archaeological trench*. (Technical Report). Malta: ENSG; University of Malta.

Lutgens, F.K., Tarbuck, E.J., and Tasa, D.G. 2016. *Essentials of geology*. New York: W.W. Norton and Company.

Magri, O. 2006. A geological and geomorphological review of the Maltese Islands with special reference to the coastal zone. *Territoris*, 6, pp.7–26.

Malone, C., Brogan, C., and McLaughlin, R. 2020. Appendix to chapter 10. In: C. Malone, R. Grima, R. McLaughlin, E. Parkinson W, S. Stoddart, and N. Vella, eds. *Temple places excavating cultural sustainability in Prehistoric Malta*. Cambridge: McDonald Institute for Archaeological Research, pp.723–762.

Malta Environment and Planning Authority 2006. *South Malta local plan* [Online]. Malta: MEPA. Available from: `https://www.pa.org.mt/en/local-plan-details/south-malta-local-plan` [Accessed December 4, 2022].

MITA 2021. *Malta inspire geoportal; Maltese spatial data infrastructure* [Online]. Available from: `https://msdi.data.gov.mt/geoportal.html` [Accessed December 4, 2022].

Molera, J., Pradell, T., and Vendrell-Saz, M. 1998. The colours of Ca-rich ceramic pastes: origin and characterization. *Applied clay science*, 13(3), pp.187–202.

MOLITOR, M. 1988. *Pots and potters of Prehistoric Malta*. PhD thesis. Los Angeles: University of California. Unpublished.

MOMMSEN, H., BONANNO, A., BONAVITA, K.C., KAKOULLI, I., MUSUMECI, M., SAGONA, C., SCHWEDT, A., VELLA, N., and ZACHARIAS, N. 2006. Characterization of Maltese pottery of the Late Neolithic, Bronze Age and Punic period by neutron activation analysis. *Geological Society, London, special publications*, 257(1), pp.81–89.

MONTALTO, N.A., SHORTLAND, A., and ROGERS, K. 2012. The provenancing of ochres from the Neolithic Temple Period in Malta. *Journal of archaeological sciences*, 39(4), pp.1094–1102.

MONTANA, G. 2016. Ceramic raw materials. In: A. HUNT, ed. *The Oxford handbook of archaeological ceramic analysis*. Oxford: Oxford University Press, pp.87–100.

MONTANA, G. 2020. Ceramic raw materials: how to recognize them and locate the supply basins—mineralogy, petrography. *Archaeological and anthropological sciences*, 12(8), pp.1–19.

MONTANA, G., ONTIVEROS, M.Á.C., POLITO, A.M., and AZZARO, E. 2011. Characterisation of clayey raw materials for ceramic manufacture in ancient Sicily. *Applied clay science*, 53(3), pp.476–488.

MÜLLER, N. 2016. Mechanical and thermal properties. In: A. HUNT, ed. *The Oxford handbook of archaeological ceramic analysis*. Oxford: Oxford University Press, pp.603–625.

MUNSELL COLOR 2012. *Munsell soil color charts*. Grand Rapids, Michigan: Munsell Color X-Rite.

MURRAY, J. 1890. The Maltese Islands, with special reference to their geological structure: with geological map, two lithographic plates, and woodcuts. *Scottish geographical magazine*, 6(9), pp.449–488.

National Archives, G.S. n.d. *Historic photos catalogue* [Online]. Gozo. Available from: https://mgoz.gov.mt/en/nag/Documents/PAPhotoAlbums.pdf [Accessed December 15, 2022].

Notarstefano, F. 2012. Ricerche sui residui organici nella ceramica di età storica dal santuario di Tas-Silġ. In: E. Lippolis, ed. *Scienze dell'antichità*. Vol. 18. Roma: Sapienza Università di Roma, pp.119–130.

Orton, C. and Hughes, M. 2013. *Pottery in archaeology*. Cambridge: Cambridge University Press.

Pace, A., Cutajar, N., Mercieca Spiteri, B., Mifsud, C., and Spiteri, M. 2012. The Żejtun villa and its ancient landscape - three new archaeological discoveries. In: R. Abela, ed. *The Żejtun Roman villa: research, conservation, management.* Malta: Wirt iz-Żejtun, pp.60–73.

Palmer, R. 2020. Post-medieval Maltese earthenware and its makers: unearthing a forgotten industry. *International journal of historical archaeology*, 24(2), pp.422–455.

Palmer, R., Raneri, S., Mazzoleni, P., Vella, N., Barone, G., and Clercq, W. 2018. Neighbourly ties: characterizing local and Sicilian pottery in post-Medieval Malta. *Journal of archaeological science: reports*, 19, pp.575–587.

Papageorgiou, I. 2020. Ceramic investigation: how to perform statistical analyses. *Archaeological and anthropological sciences*, 12(9), pp.1–19.

PCRG 2010. *The study of Prehistoric pottery: general policies and guidelines* [Online]. 3rd. Vol. 1 and 2, Occasional papers. Prehistoric Ceramics Research Group. Available from: https://www.pcrg.org.uk/News_pages/PCRG%5C%20Gudielines%5C%203rd%5C%20Edition%5C%20(2010).pdf [Accessed December 4, 2022].

Peacock, D. 1970. The scientific analysis of ancient ceramics: a review. *World archaeology*, 1(3), pp.375–389.

PEACOCK, D. 1977a. Ceramics in Roman and Medieval archaeology. In: D. PEACOCK, ed. *Pottery and early commerce: characterisation and early trade in Roman and later ceramics*. London: Academic Press, pp.21–34.

PEACOCK, D., ed. 1977b. *Pottery and early commerce: characterisation and early trade in Roman and later ceramics*. London: Academic Press.

PEACOCK, D. 1982. *Pottery in the Roman world: an ethnoarchaeological approach*. London: Longman.

PEDLEY, M. 2011. The Calabrian Stage, Pleistocene highstand in Malta: a new marker for unravelling the Late Neogene and Quaternary history of the islands. *Journal of the geological society*, 168(4), pp.913–926.

PEDLEY, M. and CLARKE, M.H. 2002. *Limestone isles in a crystal sea: the geology of the Maltese Islands*. Malta: Publishers Enterprises Group.

PERRONE, A., FINLAYSON, J.E., BARTELINK, E.J., and DALTON, K.D. 2014. Application of Portable X-Ray Fluorescence (XRF) for sorting commingled human remains. In: B.J. ADAMS and J.E. BYRD, eds. *Commingled human remains*. San Diego: Academic Press, pp.145–165.

PIRONE, F.S. 2017. *Trade, interaction and change: trace elemental characterization of Maltese Neolithic to Middle Bronze Age ceramics using a Portable X-Ray Fluorescence Spectrometer*. PhD thesis. University of South Florida. Unpublished.

PIRONE, F.S. and TYKOT, R.H. 2017. Trace elemental characterization of Maltese pottery from the Late Neolithic to Middle Bronze Age. *Open archaeology*, 3(1), pp.202–221.

PLANNING AUTHORITY 2021. *Geological map of the Maltese Islands - Quaternary Feature* [Malta GeoPortal] [Online]. Available from: `https://msdi.data.gov.mt/geonetwork/srv/api/records/41575112-7335-482c-be78-971b8f48c344` [Accessed February 24, 2022].

POLLARD, M., BATT, C., STERN, B., and YOUNG, S. 2007. *Analytical chemistry in archaeology*. Cambridge: Cambridge University Press.

POLLARD, M. and HERON, C. 2008. *Archaeological chemistry*. Cambridge: Royal Society of Chemistry.

QUERCIA, A. 2002. La ceramica da fuoco del santuario di Tas-Silġ (Malta): tipi attestati e proposte interpretative. *Vicino oriente*, 3(2), pp.403–424.

QUERCIA, A. 2005. La ceramica Punico-Maltese del santuario di Tas-Silġ: analisi tipologica e funzionale. *Scienze dell'antichità storia archeologia antropologia*, 12, pp.335–354.

QUERCIA, A. 2011. Typological and morphological remarks upon some vessels in the repertoire of pottery in Punic Malta. In: C. SAGONA, ed. *Ceramics of the Phoenician-punic world*. Leuven: Peeters, pp.433–450.

QUINN, P. 2013. *Ceramic petrography: the interpretation of archaeological pottery & related artefacts in thin section*. Oxford: Archaeopress.

RANERI, S., BARONE, G., MAZZOLENI, P., TANASI, D., and EMANUELE, C. 2015. Mobility of men versus mobility of goods: archaeometric characterization of Middle Bronze Age pottery in Malta and Sicily (15th-13th century BC). *Periodico di mineralogia*, 84, pp.23–44.

RENFREW, C. 1977. Introduction: production and exchange in early state societies, the evidence of pottery. In: D.P. PEACOCK, ed. *Pottery and early commerce: characterization and trade in Roman and later ceramics*. London: Academic Press, pp.1–20.

RICE, P.M. 1987. *Pottery analysis: a sourcebook*. Chicago; London: University of Chicago Press.

RICE, P.M. 2015. *Pottery analysis: a sourcebook*. 2nd. Chicago; London: University of Chicago Press.

ROLLINSON, H.R. and PEASE, V. 2021. *Using geochemical data to understand geological processes*. Cambridge: Cambridge University Press.

ROSSI, A.M. 2015. *Making archaeology abroad. a postcolonial perspective in Malta.* PhD dissertation. University of College London. Unpublished.

ROSSIGNANI, M.P., AIROLDI, F., and GRASSI, E. 2011. *Missione archeologica italiana a Malta* [Online]. Università Cattolica del Sacro Cuore. Available from: https://amblavalletta.esteri.it/resource/2012/01/54486_f_amb61BROCHUREMalta.pdf [Accessed December 4, 2022].

ROUX, V. 2016. Ceramic manufacture: the *chaîne opératoire* approach. In: A. HUNT, ed. *The Oxford handbook of archaeological ceramic analysis*. Oxford: Oxford University Press, pp.233–265.

ROUX, V. 2019. *Ceramics and society: a technological approach to archaeological assemblages*. Gewerbestrasse: Springer.

RUVALCABA-SIL, J.L. 2018. PIXE and material analysis. In: *The encyclopedia of archaeological sciences* [Online]. Wiley Online Library. Available from: https://onlinelibrary.wiley.com/doi/book/10.1002/9781119188230 [Accessed December 4, 2022].

SAGONA, C. 2002. *The archaeology of Punic Malta*. Belgium: Peeters.

SAGONA, C. 2005. *Combined reports on the Tas-Silġ pottery: up to 2005*. Unpublished.

SAGONA, C. 2015a. *The archaeology of Malta: from the Neolithic through the Roman period*. Cambridge: Cambridge University Press.

SAGONA, C. 2015b. The pottery. In: A. BONANNO and N. VELLA, eds. *Tas-silġ, Marsaxlokk (Malta): archaeological excavations conducted by the University of Malta, 1996-2005.* Leuven: Peeters, pp.1–514.

SAID-ZAMMIT, G.A. 1993. The Punic tombs of the Maltese Islands. In: K. SCIBERRAS, ed. Proceedings of History Week. Malta: Malta Historical Society, pp.67–80.

Santacreu, D. 2010. Pastas desgrasadas con calcita y pastas desgrasadas con materia vegetal: aproximación experimental. *Boletín del laboratorio de petrología y conservación cerámica*, 2, pp.18–34.

Santacreu, D. 2014. *Materiality, techniques and society in pottery production: the technological study of archaeological ceramics through paste analysis*. Berlin: De Gruyter Open.

Santacreu, D., Trias, M.C., and Rosselló, J.G. 2016. Formal analysis and typological classification in the study of ancient pottery. In: A. Hunt, ed. *The Oxford handbook of archaeological ceramic analysis*. Oxford: Oxford University Press, pp.181–99.

Scerri, S. 2019. Sedimentary evolution and resultant geological landscapes. In: R. Gauci and J. Schembri, eds. *Landscapes and landforms of the Maltese Islands*. Gewerbestrasse: Springer, pp.31–47.

Schmidt, K. and Bechtold, B. 2013. Fabrics of Malta. *FACEM* [Online], 1, pp.1–6. Available from: `http://facem.at/map/production_site.php?id=61` [Accessed December 4, 2022].

Schramm, R. 2015. *X-Ray fluorescence analysis: practical and easy*. 2nd. Bedburg-Hau: FLUXANA.

Shackley, M.S. 2018. X-Ray Fluorescence Spectrometry (XRF). In: S. López Varela, ed. *The encyclopedia of archaeological sciences* [Online]. Wiley Online Library. Available from: `https://onlinelibrary.wiley.com/doi/book/10.1002/9781119188230` [Accessed December 4, 2022].

Shackley, M.S., ed. 2011. *X-Ray Fluorescence Spectrometry (XRF) in geoarchaeology*. New York: Springer New York.

Shepard, A.O. 1956. *Ceramics for the archaeologist*. Washington DC: Carnegie Institution.

Sheytanova, T. 2015. *A Monte Carlo study comparing three methods for determining the number of principal components and factors*. Unpublished Thesis. Sweden: Örebro University. Unpublished.

Shirvalkar, P. 2016. Analytical drawing. In: A. Hunt, ed. *The Oxford handbook of archaeological ceramic analysis*. Oxford: Oxford University Press, pp.217–230.

Shortland, A.J. and Degryse, P. 2020. Ceramics. In: M.P. Richards and K. Britton, eds. *Archaeological science: an introduction*. Cambridge: Cambridge University Press, pp.335–346.

Skibo, J.M. and Schiffer, M. 2008. *People and things: a behavioral approach to material culture*. Brooklyn: Springer Science & Business Media.

Smith, A.L. 2001. Bonfire II: the return of pottery firing temperatures. *Journal of archaeological science*, 28(9), pp.991–1003.

Soldati, M., Barbieri, M., Biolchi, S., Buldrini, F., Devoto, S., Forte, E., Furlani, S., Gualtieri, A., Lugli, S., Mantovani, M., Mocnik, A., Padovani, V., Pasuto, A., Piacentini, D., Prampolini, M., Remitti, F., Schembri, J., Tonelli, C., and Vescogni, A. 2015. *Multidisciplinary geological excursion in the open-air laboratory of the island of Malta. 11-18 november 2010. field-trip guide.* [Online]. Dipartimento di Scienze della Terra, Università degli Studi di Modena e Reggio Emilia. Unpublished. Available from: `https://www.academia.edu/83184018/Multidisciplinary_geological_excursion_in_the_open_air_laboratory_of_the_Island_of_Malta_11_18_November_2010_Field_Trip_Guide` [Accessed December 4, 2022].

Speakman, R.J., Little, N.C., Creel, D., Miller, M.R., and Iñañez, J.G. 2011. Sourcing ceramics with portable XRF spectrometers? A comparison with INAA using Mimbres pottery from the American Southwest. *Journal of archaeological science*, 38(12), pp.3483–3496.

Stoltman, J. 2001. The role of petrography in the study of archaeological ceramics. In: P. Goldberg, V. Holliday, and C. Ferring, eds. *Earth sciences and archaeology*. New York, Boston, Dordrecht, London, Moscow: Kluwer Academic; Plenum Publishers, pp.297–326.

Swift, K. 2018. Ceramics, clays and classification in Cyrenaica. *Libyan studies*, 49, pp.81–91.

Tanasi, D., Brunelli, D., Cannavò, V., and Levi, S.T. 2019. Archaeometric characterization of Prehistoric pottery from baħrija, Malta. *Journal of archaeological science: reports*, 27, pp.1–15.

Tanasi, D., Daniele, B., Cannavò, V., and Levi, S.T. 2020a. Baħrija pottery production from an archaeometric perspective. In: D. Tanasi and D. Cardona, eds. *The Maltese archipelago at the dawn of history: reassessment of the 1909 and 1959 excavations at Qlejga tal-Baħrija and other essays*. Oxford: Archaeopress, pp.121–136.

Tanasi, D., Tykot, R.H., Pirone, F.S., and Vella, N. 2020b. Non-destructive pXRF analysis of Middle Bronze and Iron Age pottery from Malta. In: D. Tanasi and D. Cardona, eds. *The Maltese archipelago at the dawn of history: reassessment of the 1909 and 1959 excavations at Qlejga tal-Baħrija and other essays*. Oxford: Archaeopress, pp.109–120.

Tartaron, T.F. 2013. *Maritime networks in the Mycenaean world*. Cambridge: Cambridge University Press.

Tassi, F., Bonini, M., Montegrossi, G., Capecchiacci, F., Capaccioni, B., and Vaselli, O. 2012. Origin of light hydrocarbons in gases from mud volcanoes and CH4-rich emissions. *Chemical geology*, 294, pp.113–126.

The British Museum 2019. *Pottery recording guide: a guide and protocol for recording pottery on the Portable Antiquities Scheme database* [Online]. Portable Antiquities Scheme. Available from: `https://finds.org.uk/counties/findsrecordingguides/wp-content/uploads/2019/03/Pottery-Guide-190312.pdf`.

THÉR, R. 2020. Ceramic technology. how to reconstruct and describe pottery-forming practices. *Archaeological and anthropological sciences* [Online], 12(8). Available from: https://link-springer-com.ejournals.um.edu.mt/article/10.1007/s12520-020-01131-0 [Accessed December 20, 2022].

THÉR, R., KALLISTOVÁ, A., SVOBODA, Z., KVĚTINA, P., LISÁ, L., BURGERT, P., and BAJER, A. 2019. How was Neolithic pottery fired? an exploration of the effects of firing dynamics on ceramic products. *Journal of archaeological method and theory*, 26(3), pp.1143–1175.

THÉR, R. and MANGEL, T. 2020. *Quantification of the orientation of aplastic components of a ceramic body as the tool for the identifi cation of the forming techniques utilising rotational kinetic energy: review of the current state of research* [Online]. Archaeological approaches to the study of the Potter's wheel. Unpublished. Available from: https://www.youtube.com/watch?v=aAbWjsHh3eg&list=PLqWUT1pOFU1NyRJvH8Morbgeh2NIejw97&index=3&ab_channel=EXARC [Accessed December 4, 2022].

THÉR, R. and TOMS, P. 2016. Quantification of the orientation and alignment of aplastic components of a ceramic body as a method for distinguishing among various means of using a rotational device in pottery forming. *Journal of archaeological science: reports*, 9, pp.33–43.

THOMPSON, H.A. 1934. Two centuries of Hellenistic pottery. *Hesperia: the journal of the american school of classical studies at athens*, 3(4), pp.311–476.

TITE, M.S., KILIKOGLOU, V., and VEKINIS, G. 2001. Strength, toughness and thermal shock resistance of ancient ceramics, and their influence on technological choice. *Archaeometry*, 43(3), pp.301–324.

TITE, M.S. 2008. Ceramic production, provenance and use—a review. *Archaeometry*, 50(2), pp.216–231.

Tite, M.S. 2016. History of scientific research. In: *The Oxford handbook of archaeological ceramic analysis*. Oxford: Oxford University Press, pp.7–16.

Trigger, B. 2006. *A history of archaeological thought*. 2nd. Cambridge: Cambridge University Press.

Trump, D.H. 2002. *Malta: Prehistory and temples*, Malta's living heritage. Malta: Midsea Books.

Turi, A., Picollo, M., and Valleri, G. 1990. Mineralogy and origin of the carbonate beach sediments of Malta and Gozo, Maltese Islands. *Bollettino della societa geologica italiana*, 109, pp.367–374.

University of Malta 2018. *Żejtun Roman Villa* [Department of Classics and Archaeology: Our research] [Online]. Available from: `https://www.um.edu.mt/arts/classics-archaeo/ourresearch/zejtunromanvilla` [Accessed December 4, 2022].

University of Malta 2020. *MaltaPot* [Online]. Available from: `https://www.um.edu.mt/projects/maltapot` [Accessed December 4, 2022].

University of Malta 2021. *CoFIPoMS* [Online]. Available from: `https://www.um.edu.mt/projects/cofipoms/potterysherds` [Accessed December 4, 2022].

Vella, J.S. 2003. *Soil survey and soil mapping in the Maltese Islands: the 2003 position*. (Research Report). European Soil Bureau, pp.235–244.

Vella, M. and Richard-Trémeau, E. 2021a. *Operating procedure for the sampling of clay using a hand auger set for the scope of archaeological research* [Online]. (Standard Operating Procedures CAR-018-01). University of Malta. Available from: `https://www.um.edu.mt/operatingprocedures/doc/CAR-018-01` [Accessed October 27, 2021].

Vella, M. and Richard-Trémeau, E. 2021b. *Operating procedures for the manufacturing of clay briquettes* [Online]. (Standard Operating Procedures CAR-017-01). University of Malta. Available from: https://www.um.edu.mt/operatingprocedures/doc/CAR-017-01 [Accessed October 27, 2021].

Vella, N. and Anastasi, M. 2019. Malta and Gozo. In: L.-R.C.D.B. R., ed. *The Oxford handbook of the Phoenician and Punic Mediterranean*. Oxford: Oxford University Press.

Vella, N., Bonanno, A., Anastasi, M., Bechtold, B., Farrugia, R., Fenech, K., Mizzi, D., Verdonck, L., and Zammit, A. 2017. A view from the countryside: the nature of the Late Punic and Early Roman activity at the Żejtun villa site, Malta. *Rivista di Studi Fenici*, 45, pp.109–143.

Vella, N., Mason, S., Farrugia, R., and Zammit, M. 2015. The stratigraphy. In: A. Bonanno and N. Vella, eds. *Tas-silġ, Marsaxlokk (Malta): archaeological excavations conducted by the University of Malta, 1996-2005.* Leuven: Peeters, pp.45–229.

Villing, A. and Spataro, M. 2015. Investigating ceramics, cuisine and culture – past, present and future. In: A. Villing and M. Spataro, eds. *Ceramics, cuisine and culture: the archaeology and science of kitchen pottery in the ancient Mediterranean world*. Oxford: Oxbow Books, pp.1–26.

Vokaer, A. 2010. Cooking in a perfect pot. shapes, fabric and function of cooking ware in late antique syria. In: S. Menchelli, S. Santoro, M. Pasquinucci, and G. Guiducci, eds. *LRCW3. Late Roman coarse wares, cooking wares and amphorae in the Mediterranean. archaeology and archaeometry. comparison between Western and Eastern Mediterranean*. BAR International Series, pp.115–129.

Von der Crone, M. and Maggetti, M. 2002. Experimental firing of clays using salt water. In: E. Jerem and K. Biro, eds. *31st international symposium*

on archaeometry, Budapest, april 26-may 2 1998. Vol. 1043 (I), BAR international series. Archaeopress, pp.249–255.

Waiman-Barak, P., Georgiadou, A., and Gilboa, A. 2021. Regional mineralogical and technological characterization of Cypriot Iron Age pottery: a view from Tel Dor. *Levant*, 53(2), pp.236–261.

Waksman, Y. 2016. Provenance studies. In: A. Hunt, ed. *The Oxford handbook of archaeological ceramic analysis*. Oxford: Oxford University Press, pp.148–162.

Whitbread, I. 1986. The characterisation of argillaceous inclusions in ceramic thin sections. *Archaeometry*, 28(1), pp.79–88.

Whitbread, I. 1995. *Greek transport amphorae: a petrological and archaeological study.* Fitch laboratory occasional paper, 4. Athens: The British School at Athens.

Whitbread, I. 2015. Materials choices in utilitarian pottery: kitchen wares in the Berbati valley, Greece. In: A. Villing and M. Spataro, eds. *Ceramics, cuisine and culture: the archaeology and science of kitchen pottery in the ancient Mediterranean world*. Oxford: Oxbow Books, pp.28–36.

Whitbread, I. 2016. Fabric description of archaeological ceramics. In: A. Hunt, ed. *The Oxford handbook of archaeological ceramic analysis*. Oxford: Oxford University Press, pp.200–216.

Wilkinson, I., Quinn, P., Williams, M., Taylor, J., and Whitbread, I. 2016. Ceramic micropalaeontology. In: A. Hunt, ed. *The Oxford handbook of archaeological ceramic analysis*. Oxford: Oxford University Press, pp.327–341.

Wilson, L. and Pollard, M. 2001. The provenance hypothesis. In: D.R. Brothwell and M. Pollard, eds. *Handbook of archaeological sciences*. Chichester; New York: John Wiley & Sons LTD, pp.507–518.

Xuereb, L. 2021. *A study on the firing of sourced Maltese clay into a usable product* [Online]. B. Eng. dissertation. University of Malta. Unpublished. Available from: `https://www.um.edu.mt/library/oar/handle/123456789/103123`.

ZWICK, W.R. and VELICER, W.F. 1986. Comparison of five rules for determining the number of components to retain. *Psychological bulletin*, 99(3), pp.253–259.

Appendices

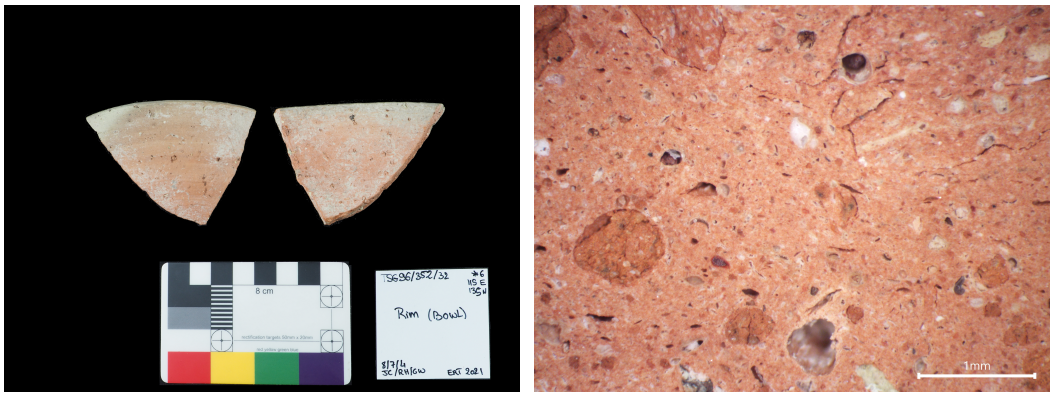
Appendix A

Pottery Catalogue

Notes for the catalogue

This catalogue presents the 70 sherds analysed. Most drawings of sherds from the Żejtun Villa are reproduced from Vella et al. (2017); however, the other drawings were produced for this dissertation. The diameter, thickness and colours were measured for this dissertation.

Sample 1 (TSG96/352/32)



(a) (b)

Figure A.1: (a) Photograph: interior; exterior (b) Microphotograph: ground sample

Description: Bowl, shape close to Anastasi (2019) D6, shapes dated from the 3rd century BCE onward. Lip close to Quercia (2011) shape 2:7, slightly flaring, but the body is convex and globular. Striations from surface finish visible on surfaces, heterogeneous in colour especially close to the rim where colour is greyish (due to firing?). Outer diameter: 18cm. Thickness: 5.4 - 7.1mm, including rim.

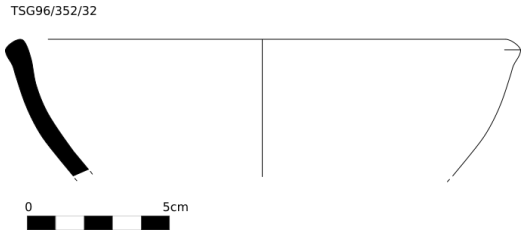


Figure A.2: Reconstructed bowl rim

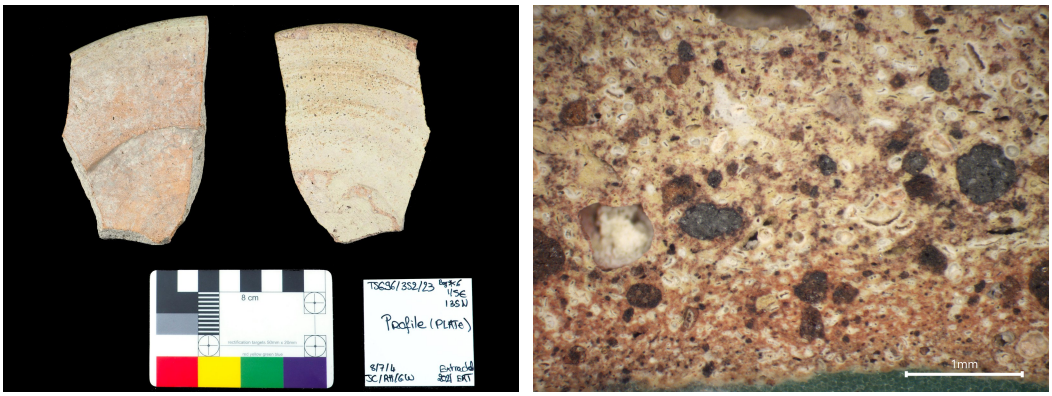
Internal surface	External surface	Core	Margins
2.5YR 6/6 light red	2.5YR 7/6 light red-5YR 6/6 reddish yellow. 5Y 7/2 light gray (rim)	2.5YR 6/6 light red	2.5YR 5/8 red

Table A.1: Munsell colours values

Macro	OM	PLM	HCA
Anastasi F1 with orange-brown rounded inclusions, some white inclusions	D3	-	HCA: Group 2; consistent with OM

Table A.2: Classifications of the sherd across this study. Numbering is independent in different methods.

Sample 2 (TSG96/352/23)



(a) (b)

Figure A.3: a) Photograph: interior; exterior (b) Microphotograph: ground sample

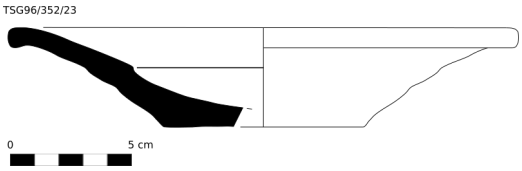


Figure A.4: Reconstructed plate

Description: Profile of plate, close to Sagona (2015b) 1:95:6, Anastasi (2019) D27.2 with a marked ribbing or Quercia (2011: 2nd-1st century shapes) B6. The base is poorly finished, with visible lumps of fired material on the edges and concentric striations (string marks?). Parallel lines are visible on the inner surface from the surface finish (wet-wiped?). The outer surface might be bleached or slipped with marked differences of colour between surfaces. Outer rim diameter: 21 cm. Thickness: 6.8-14mm, including base.

Internal surface	External surface	Core	Internal margins	External margins
5YR 6/4 light reddish brown	10YR 8/1 white (heterogeneous)	10YR 7/3 very pale brown (heterogeneous)	Ill defined	5YR 5/4 reddish brown

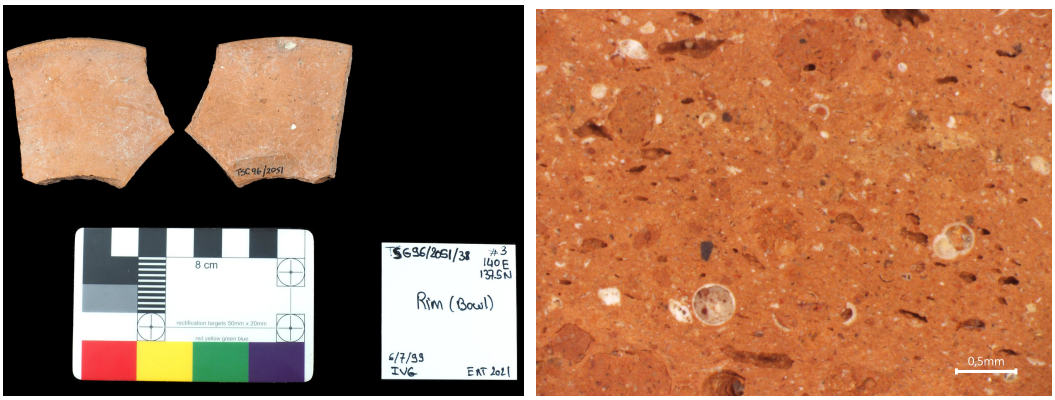
Table A.3: Munsell colours values

Macro	OM	PLM	HCA
Anastasi F1 with black to brown inclusions	D2	-	Conflicting (1 or 2)

Table A.4: Classifications of the sherd across this study. Numbering is independent in different methods.

This sherd was classified during PCA and HCA as uncertain.

Sample 3 (TSG96/2051/38)



(a) (b)

Figure A.5: a) Photograph: interior; exterior (b) Microphotograph: ground sample

Description: Open form, plate? or bowl?, close to Anastasi (2019) D26.2, D27.1. Flaring rim. Surfaces with visible finish lines. Softer vessel than the rest of the samples, probably due to low firing temperature (can be scratched with a nail). Outer diameter: 16cm, thickness: 5-6.2mm.

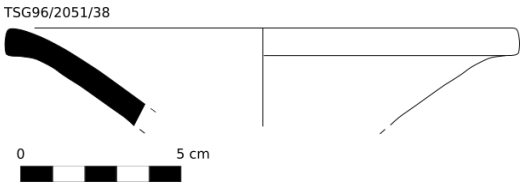


Figure A.6: Reconstructed vessel rim

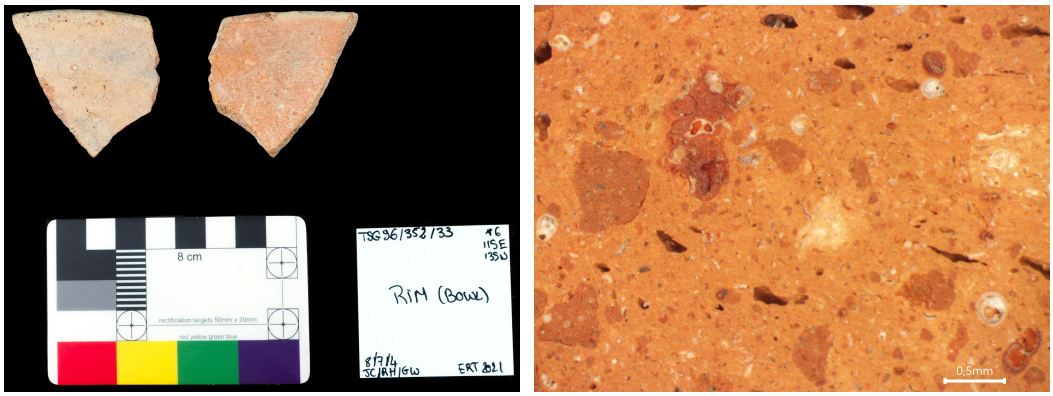
Internal surface	External surface	Core
2.5YR 6/6 light red	2.5YR 5/6 red	2.5YR 5/6 red

Table A.5: Munsell colours values

Macro	OM	PLM	HCA
Anastasi F1 with orange-brownrounded inclusions, some white inclusions	D3	-	-

Table A.6: Classifications of the sherd across this study

Sample 4 (TSG96/352/33)



(a) (b)

Figure A.7: (a) Photograph: interior; exterior (b) Microphotograph: ground sample

Description: Rim of bowl, shape close to Anastasi (2019) D6.2 and Quercia (2011) 2:7-8 with slightly flaring and everted rim. Ribbing on the outer wall. The outer surface and lip are whitened or bleached by firing (or unlikely slipped), markedly different in colour from the inner surface. Outer diameter: 19cm. Thickness: 6.5-8.2mm, including rim.

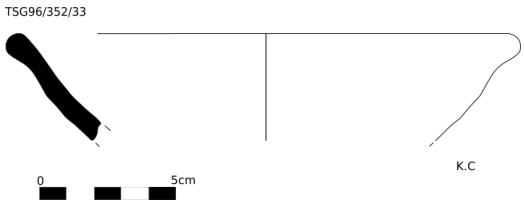


Figure A.8: Reconstructed bowl rim, drawing by Kellian Coste

Internal surface	External surface	Core
2.5YR 5/6 red (HT)	5YR 7/2 pinkish gray (HT)	5YR 5/6 yellowish red

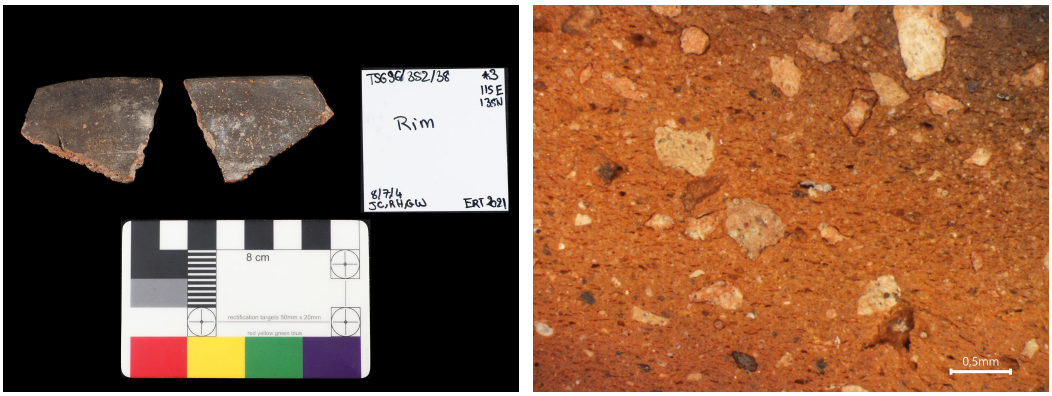
Table A.7: Munsell colours values; HT: heterogeneous

Macro	OM	PLM	HCA
Anastasi F1 with orange-brown rounded inclusions, some white inclusions	D3	Fabric 2.1	Group 2

Table A.8: Classifications of the sherd across this study. Numbering is independent in different methods.

The classification of this sherd was consistent across techniques, with the other samples containing predominantly iron-rich inclusions and carbonate inclusions.

Sample 5 (TSG96/352/38)



(a) (b)

Figure A.9: (a) Photograph: interior; exterior (b) Microphotograph: ground sample

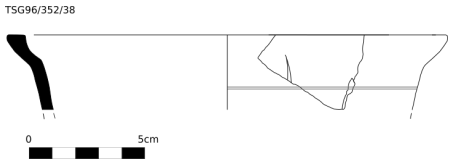


Figure A.10: Reconstructed inscribed vessel

Description: Tegame/Casserole, interpreted by Quercia (2002) as a cooking vessel. Shape close to Quercia (2002) C:3, but the wall goes inward in the lower part of the remaining vessel; and Sagona (2015b) 1:111:1-1:112:1. Parallel and regular striations. Surface inclusions are prevalent on the inner surface but not on the outer surface (difference of surface treatment?). One incised stroke is visible and was likely incised before firing. Outer diameter: around 19cm (a small rim part remains). Thickness: 5.2-6.6mm.

Internal surface	External surface	Core
10YR 4/2 dark grayish brown (heterogeneous)	5YR 3/1 very dark gray (rim) - 10YR 4/2 dark grayish brown	2.5YR 4/8 red

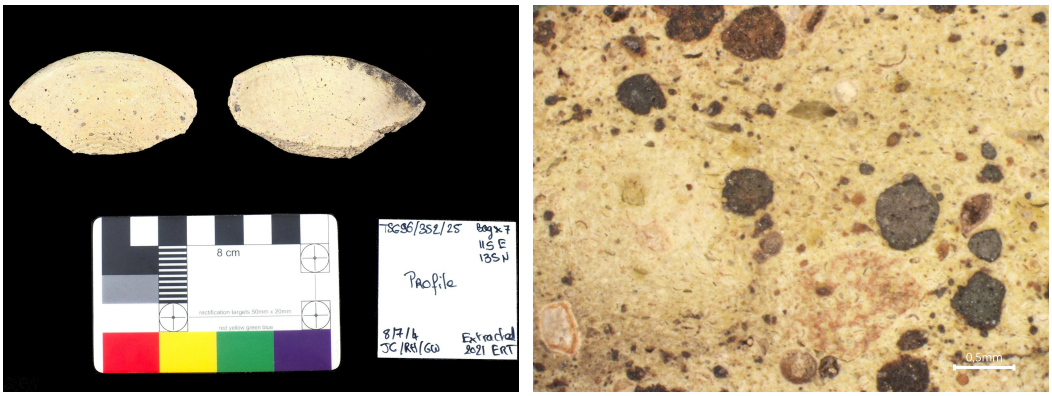
Table A.9: Munsell colours values

Macro	OM	PLM	HCA
Anastasi F5	B	-	3

Table A.10: Classifications of the sherd across this study. Numbering is independent in different methods.

The classification of this sherd was consistent through techniques, grouping systematically with other cooking vessels.

Sample 6 (TSG96/352/25)



(a) (b)

Figure A.11: Figure A.9: (a) Photograph: interior; exterior (b) Microphotograph: ground sample

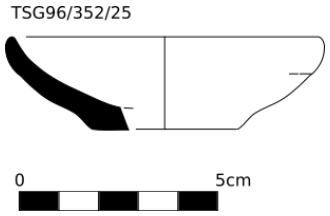


Figure A.12: Reconstructed bowl

Description: Profile of miniature bowl, close to Sagona (2015b) 1:61:14, Quercia (2002) 3:5 but lacks the fully inverted rim. Similar to sample 38 but more globular. Rim is pointy. The surface was cracked and powdery, and the sherd was brittle. A possible incised line was noticed but is likely to a damage as the sherd is powdery and brittle. Parallel striations on the inner surface (wet-wiped?) and a dark patch (soot?) on the part of the rim are visible. Outer rim diameter: 9 cm. Thickness ranges from 6.2 to 7.4mm, including the base.

Internal surface	External surface	Core
2.5Y 8/2 pale brown	2.5Y 8/6 yellow	2.5Y 8/3 pale brown

Table A.11: Munsell colours values

Macro	OM	PLM	HCA
Anastasi F1 with white matrix	D2?	-	-

Table A.12: Classifications of the sherd across this study. Numbering is independent in different methods.

Sample 7 (TSG96/2051/39)



(a) (b)

Figure A.13: (a) Photograph: interior; exterior (b) Microphotograph: ground sample

Description: Bowl, shape close to Sagona (2015b) 1:65:15 and Anastasi (2019) D.6.6 with everted rim. The sherd is whitened/bleached due to firing (or less likely slipped), quite homogeneous in colour with stark contrast with the fabric colour. Finish lines are visible, regular and parallel. Outer diameter: 20cm and thickness: 4 to 7mm.

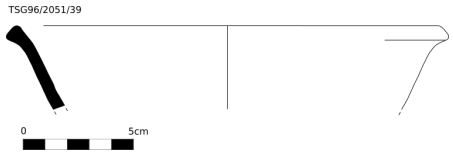


Figure A.14: Reconstructed bowl rim

Internal surface	External surface	Core
2.5Y 8/2 pale brown	2.5Y 8/2 pale brown	2.5YR 5/8 red

Table A.13: Munsell colours values

Macro	OM	PLM	HCA
Anastasi F1 with predominantly white inclusions	E	-	1

Table A.14: Classifications of the sherd across this study. Numbering is independent in different methods.

Sample 8 (TSG96/2051/32)



(a) (b)

Figure A.15: (a) Photograph: interior; exterior (b) Microphotograph: ground sample

Description: Bowl, 2 fragments of the vessel joining, shape close to Sagona (2015b) 1:66:6-7 and Anastasi (2019) D.8.2. Rounded lip, the rim is everted and wall slightly ribbed on the outer part. The inner surface has visible black inclusions whilst the outer surface has been treated differently as nearly no inclusions are visible (smoothened?). The finish lines are visible. Outer diameter: 18cm and thickness: 5-7.1mm.

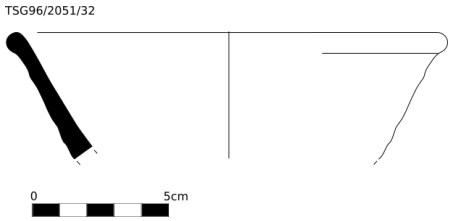


Figure A.16: Reconstructed bowl rim

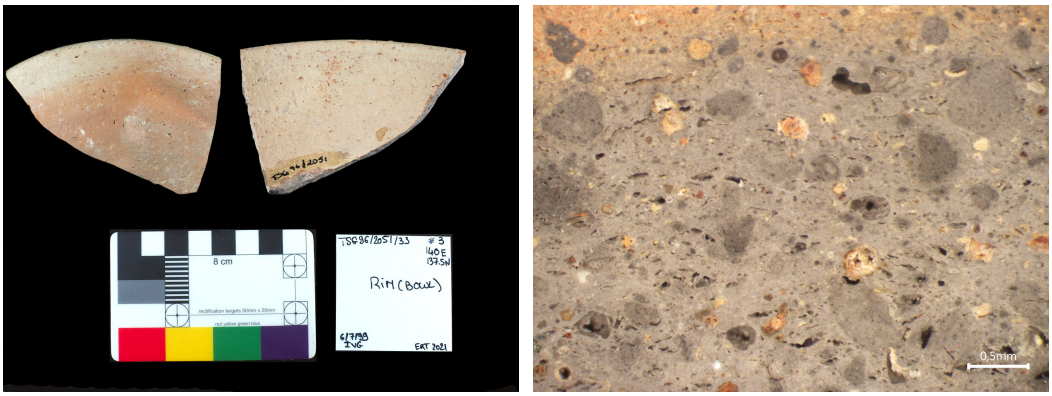
Internal surface	External surface	Core	Internal margins	External margins
2.5Y 8/2 - 7/3 pale brown	10YR 6/2 light brownish gray	10YR 6/1 gray	2.5YR 6/8 light red	2.5Y 7/3 pale brown

Table A.15: Munsell colours values

Macro	OM	PLM	HCA
Anastasi F1 with black to brown inclusions	D1	-	2

Table A.16: Classifications of the sherd across this study. Numbering is independent in different methods.

Sample 9 (TSG96/2051/33)



(a) (b)

Figure A.17: (a) Photograph: interior; exterior (b) Microphotograph: ground sample

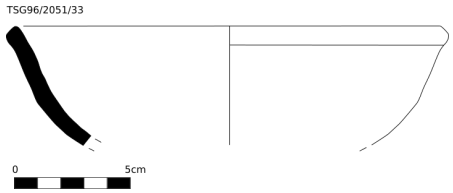


Figure A.18: Reconstructed bowl rim

Description: Bowl, variation of Quercia (2011) 2.7, although upper body is not as concave; and Sagona (2015b) 1:66 shapes. External margins in the section are very thin. Surfaces are mottled, and the inner surface looks like it could be slipped (surface inclusions seem covered), although it could be whitened by firing. Some irregular finish lines/striations, particularly on the outer surface below the rim. An air bubble/blister is visible in the middle of the sherd. Outer diameter: 19cm and thickness: 5.9-7.4mm.

Internal surface	External surface	Core	Margins
10YR 8/2 very pale brown	10YR 8/2 very pale brown - 7.5YR 6/3 light brown - 5YR 6/6 reddish yellow	GLEY 1 5/N in parts	5YR 6/6 reddish yellow

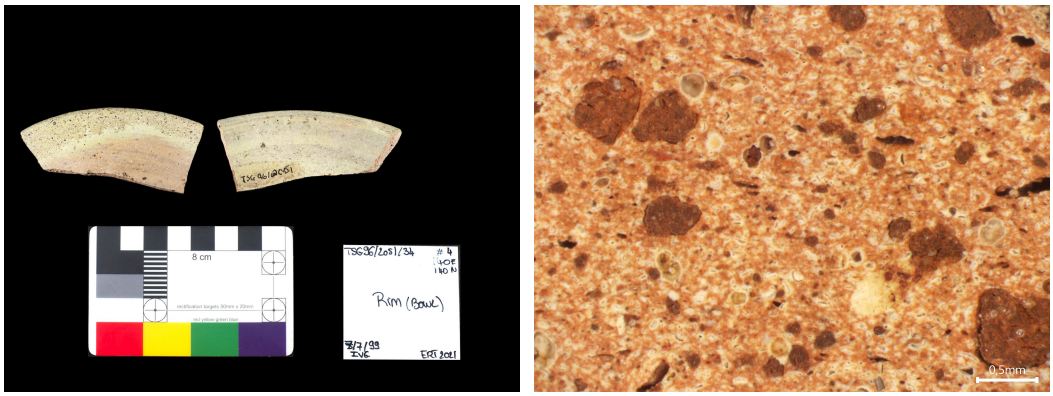
Table A.17: Munsell colours values

Macro	OM	PLM	HCA
Anastasi F1 with black to brown inclusions	D1	2.1	2

Table A.18: Classifications of the sherd across this study. Numbering is independent in different methods.

The classification of S9 was consistent with all techniques, grouping with sherds having iron-rich inclusions.

Sample 10 (TSG96/2051/34)



(a) (b)

Figure A.19: (a) Photograph: interior; exterior (b) Microphotograph: ground sample

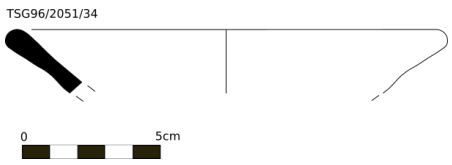


Figure A.20: Reconstructed bowl rim

Description: Bowl, shape close to Anastasi (2019) 6.5. The rim has a bulb shape. Part of the surface looks slipped (thin wash), stopping below the rim on the outer surface. The surface was more likely bleached or whitened because of firing. The contrast between the whitish and non-white area can be seen in Figure A.19a on the outer surface of the sherd, where inclusions are visible on top and non-visible on the bottom part. Outer diameter: 16cm and thickness: 5.1-8.1mm.

Internal surface	External surface	Core	Margins
5Y 7/3 pale yellow - 5Y 6/1 gray	5Y 7/3 pale yellow - 10Y 6/3 pale brown	5YR 6/6 reddish yellow	2.5 7/3 pale brown

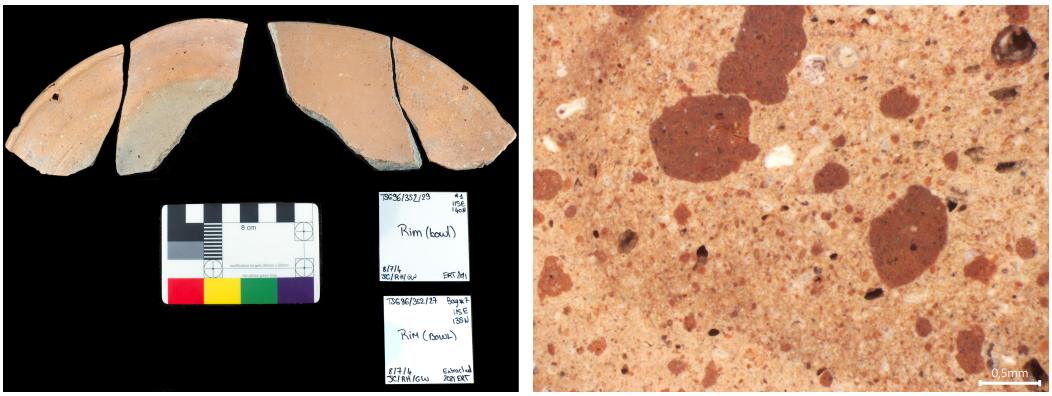
Table A.19: Munsell colours values

Macro	OM	PLM	HCA
Anastasi F1 with orange-brown rounded inclusions, some white inclusions	D1	2.1	2

Table A.20: Classifications of the sherd across this study. Numbering is independent in different methods.

The classification of S9 was consistent with all techniques, grouping with sherds having iron-rich inclusions.

Sample 11 (TSG96/352/27,29)



(a) (b)

Figure A.21: (a) Photograph: interior; exterior (b) Microphotograph: ground sample

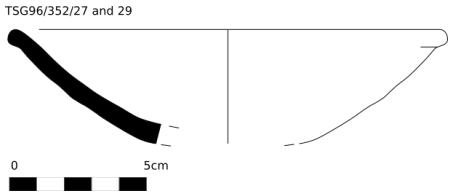


Figure A.22: Reconstructed bowl rim

Description: These were originally two samples which were found to be joining mid-study. Bowl rim, shape close to Sagona (2015b) 1:66:2, Quercia (2011) 2:7 and Anastasi (2019) D6, found in 3rd century BCE contexts and onward. Flaring rim with rounded lip. Striations on surfaces are not perfectly parallel, two strokes on the outer surface, similar to brush strokes, stand out. The change of colour in the outer surface could be caused by the firing process, the grey part was harder than the pink part (note taken when crushing). No surface inclusions visible suggesting surface treatment such as smoothing/wet-wiping or brushing (Roux 2016: 198-199). Outer diameter: 16cm. Thickness: 3.9-8.1mm endgroup

Internal surface	External surface	Core	Margins
5YR 6/6 reddish yellow	2.5YR 7/6 light red to 5YR 7/6 reddish yellow; 10YR 6/2 light brownish gray	2.5Y 6/4 light yellowish brown	OEM: 5YR 6/6 reddish yellow, IEM: GLEY 1 4/N Dark grey for 29

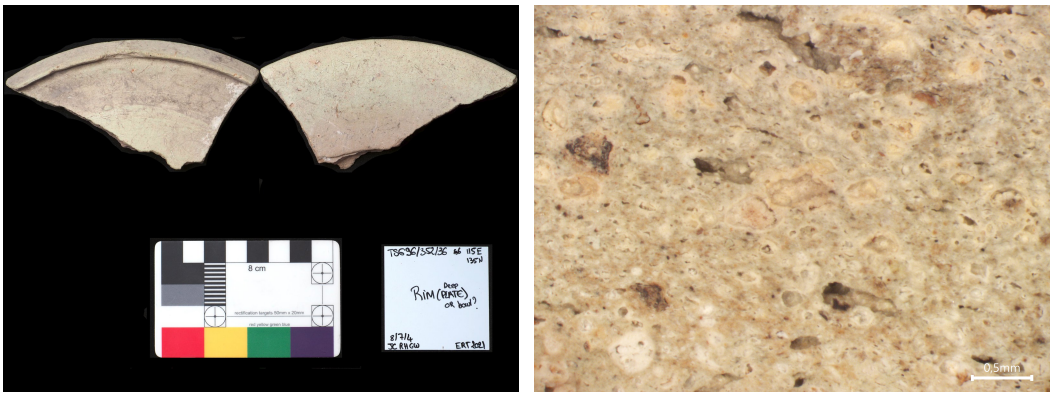
Table A.21: Munsell colours values; OEM: Outer external margin; IEM: Inner external margin

Macro	OM	PLM	HCA
Anastasi F1 with black to brown inclusions but fresh break in the grey part	D1	-	1

Table A.22: Classifications of the sherd across this study. Numbering is independent in different methods.

The classification of S11 was not consistent with all techniques, grouping with sherds having iron-rich inclusions microscopically but with Group 1 with XRF.

Sample 12 (TSG96/352/36)



(a) (b)

Figure A.23: (a) Photograph: interior; exterior (b) Microphotograph: ground sample

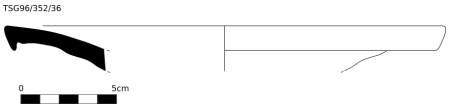


Figure A.24: Reconstructed vessel

Description: Open form, deep plate or bowl. The shape of the rim (triangular and flaring) is close to Anastasi (2019) D29.1 or more likely Sagona (2015b) 1:98:2-3. The sherd feels powdery compared to other sherds but the material is not as brittle as other sherds with whitish matrices (eg. sample 6). The outer surface has striations from the surface finish and variations in colour whereas the inner surface does not (difference in surface treatment). Outer diameter: 23cm. Thickness: 8.1-9.1mm.

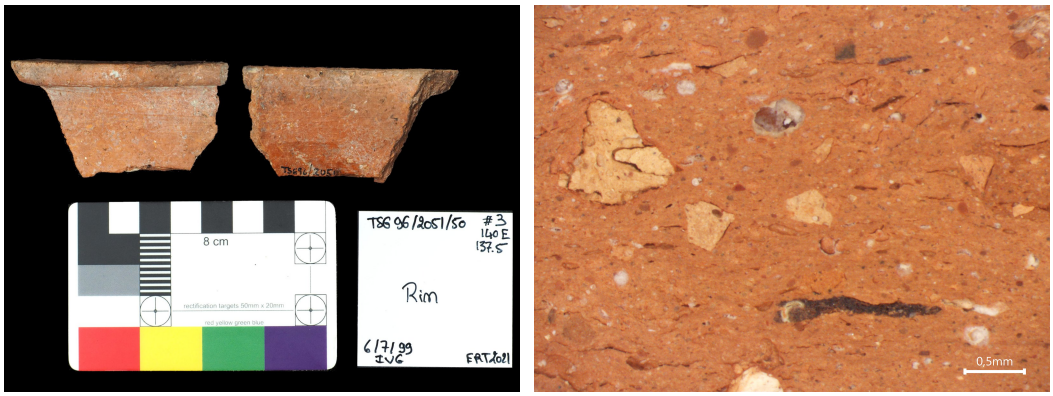
Internal surface	External surface	Core
5Y 8/2 pale yellow, some10Y 7/2	5Y 8/2 pale yellow, some 10Y 7/2	heterogeneous 5YR 7/4 pink

Table A.23: Munsell colours values

Macro	OM	PLM	HCA
Anastasi F1 with white matrix	C	1.2	1

Table A.24: Classifications of the sherd across this study. Numbering is independent in different methods.

Sample 13 (TSG96/2051/50)



(a) (b)

Figure A.25: (a) Photograph: interior; exterior (b) Microphotograph: ground sample

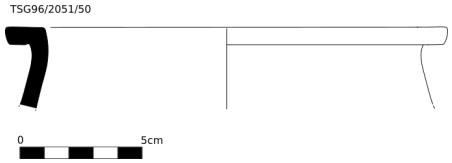


Figure A.26: Reconstructed vessel rim

Description: Olla, shape close to Quercia (2002) A1 cooking vessels, Anastasi (2019) C1.1-C1.2 and Sagona (2015b) 1:119:1-6. Flat-top everted rim. The finish lines are not fully parallel and regular (smoothened/wiped?). Dark patches on the surface (firing, use or post-depositional?) and within the section sometimes (noticed when the surface was removed). Outer diameter: 18cm and thickness: 5.8-6.5mm.

Internal surface	External surface	Core
2.5YR 5/6 red	2.5YR 5/6 red	2.5YR 5/8 red

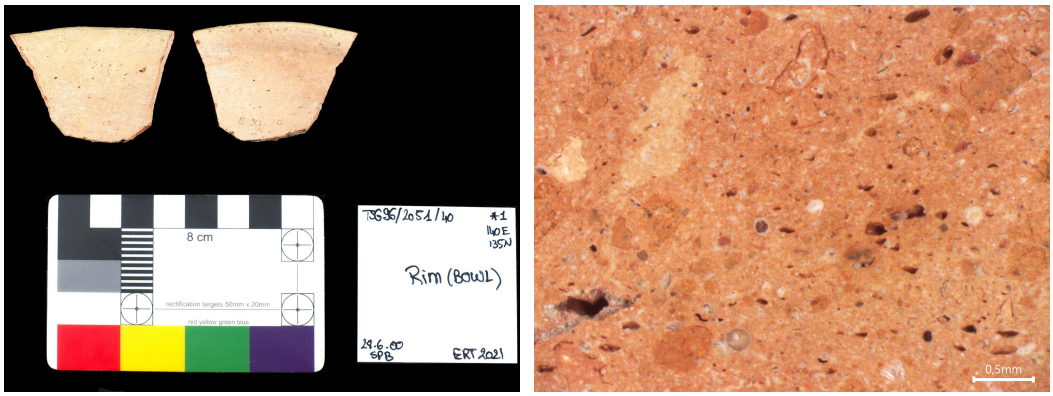
Table A.25: Munsell colours values

Macro	OM	PLM	HCA
Anastasi F5	B1	5	3

Table A.26: Classifications of the sherd across this study. Numbering is independent in different methods.

The classification of S13 was not consistent with all techniques, grouping with sherds having iron-rich matrix, and fine quartz. This sherd contains a greater amount of microfossils.

Sample 14 (TSG96/2051/40)



(a) (b)

Figure A.27: (a) Photograph: interior; exterior (b) Microphotograph: ground sample



Figure A.28: Reconstructed bowl rim

Description: Bowl, shape close to Anastasi (2019) D6.4 with a rounded, slightly flaring rim. Surface whitened or bleached? (or slipped? inclusions seem "covered" due to the visible striations), homogeneous in colour on the inner surface. Thin regular surface lines are visible from the surface finish, possibly wiping with fingers or a clothe. Outer diameter: 17cm, thickness: 5.4-6.6mm.

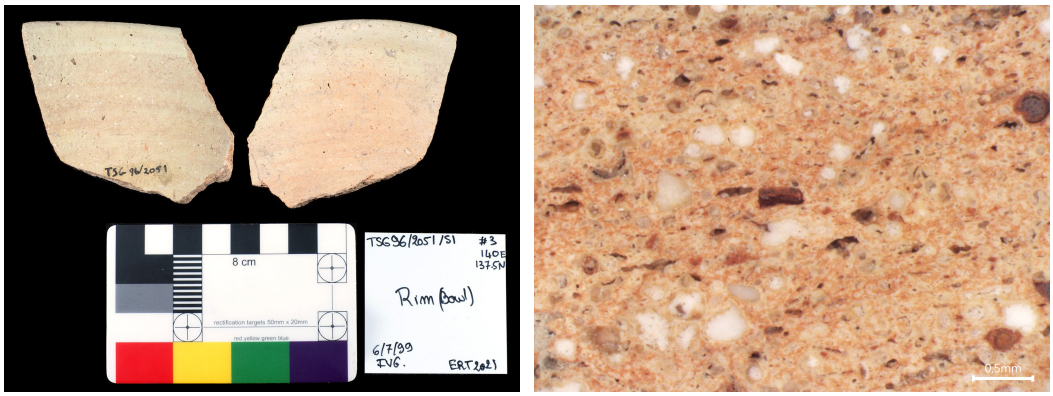
Internal surface	External surface	Core	Margins
10YR 8/2 very pale brown	10YR 8/2 very pale brown	5YR 6/6 reddish yellow	2.5YR 6/8 red

Table A.27: Munsell colours values

Macro	OM	PLM	HCA
F1 with orange-brown rounded inclu- sions,some white inclusions	D3	-	-

Table A.28: Classifications of the sherd across this study. Numbering is independent in different methods.

Sample 15 (TSG96/2051/51)



(a) (b)

Figure A.29: (a) Photograph: interior; exterior (b) Microphotograph: ground sample

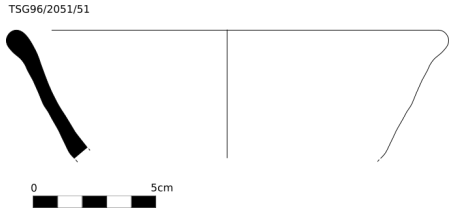


Figure A.30: Reconstructed bowl rim

Description: Bowl, shape close to Anastasi (2019) D6:5, slightly flaring rounded rim. Light ribbing of the wall (outer part). Colours and the horizontal bands as seen on the inner surface (see left of Fig. A.29a) suggest the application of a layer of slip/wash on the surfaces although the white colour could be from whitening or bleaching during firing. Surface finish lines visible. Inner diameter: 17cm, thickness: 5.4-8mm.

Internal surface	External surface	Core
2.5Y 7/3 light brown - 5Y8/2 pale yellow	5Y8/2 pale yellow - 7.5YR 7/3	5YR 7/6 reddish yellow

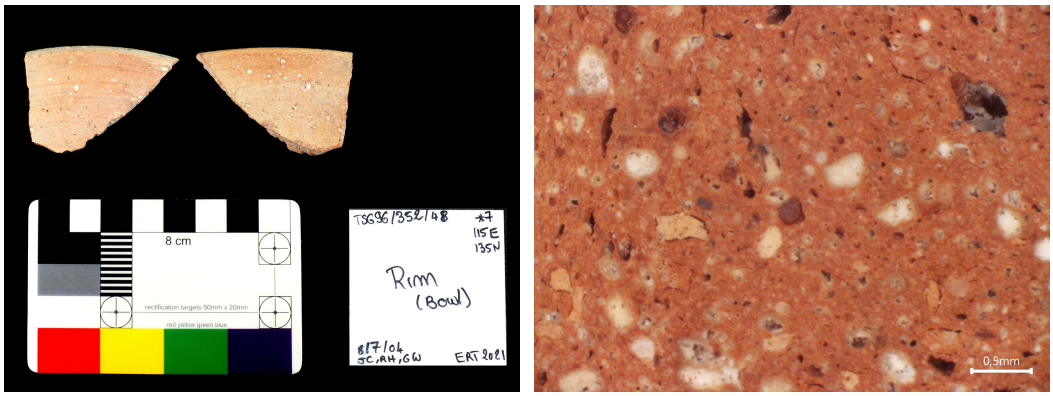
Table A.29: Munsell colours values

Macro	OM	PLM	HCA
Anastasi F1 with predominantly white inclusions	E	1.1	Conflicting classification

Table A.30: Classifications of the sherd across this study. Numbering is independent in different methods.

This sample did not clearly classify with the XRF and is for now treated as an outlier of both XRF groups 1 and 2.

Sample 16 (TSG96/352/48)



(a) (b)

Figure A.31: (a) Photograph: interior; exterior (b) Microphotograph: ground sample

Description: Bowl, shape close to Anastasi (2019) D7 suggested to be a parallel/development to Quercia (2011) 2.8. Rim is triangular. Surfaces are whitened or slipped (less likely) and striations from surface finish are visible, regular and parallel. Some white inclusions are visible on the surface. Inner diameter: 14cm, thickness: 4.3-7.3mm.

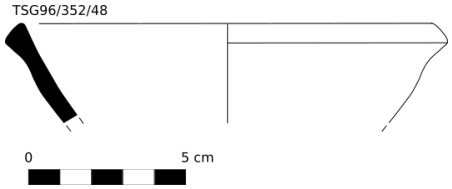


Figure A.32: Reconstructed bowl rim

Internal surface	External surface	Core
7.5 YR 7/3 Pink	5YR 6/4 light reddish brown	2.5YR 4/8 red

Table A.31: Munsell colours values

Macro	OM	PLM	HCA
Anastasi F1 with predominantly white inclusions	-	-	-

Table A.32: Classifications of the sherd across this study. Numbering is independent in different methods.

Sample 17 (TSG96/352/28)



(a) (b)

Figure A.33: a) Photograph: interior; exterior (b) Microphotograph: ground sample

Description: Rim of bowl. Deep form, the closest comparison is Sagona (2015b) 1:71:1-2 with a rounded rim and ribbed wall thickening at the bottom of the body. Surfaces have parallel and regular striations from the surface finish (wet-wiping?).One inscribed line is visible, and although no "lumps" of clays are visible on the edge of the inscription, therefore inscribed at an uncertain stage of production.

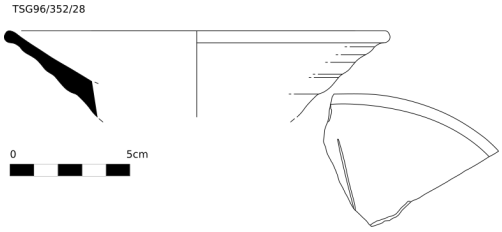


Figure A.34: Reconstructed bowl rim

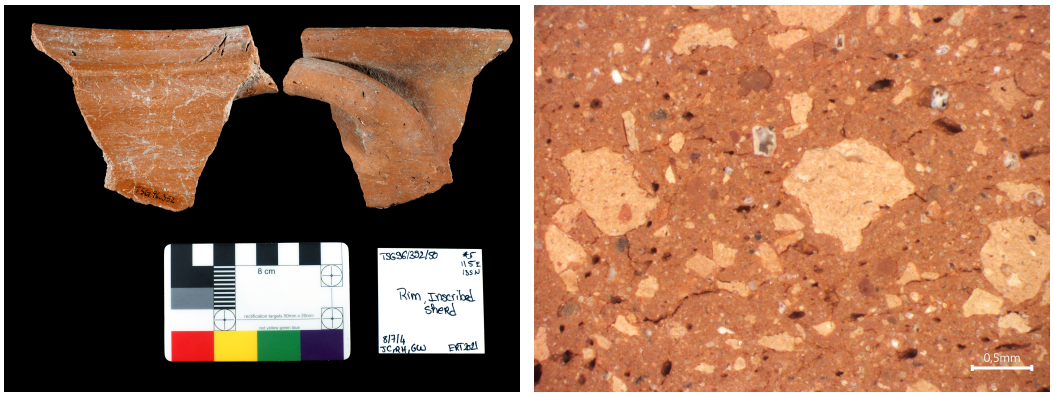
Internal surface	External surface	Core	Margins
10YR 7/3 very pale brown	2.5Y 7/3 pale brown	Gley 1 5/N gray	Very thin 10YR 6/4 light yellowish brown

Table A.33: Munsell colours values

Macro	OM	PLM	HCA
Anastasi F1 with black to brown inclusions, some white inclusions	D2	-	2

Table A.34: Classifications of the sherd across this study. Numbering is independent in different methods.

Sample 18 (TSG96/352/50)



(a) (b)

Figure A.35: (a) Photograph: interior; exterior (b) Microphotograph: ground sample

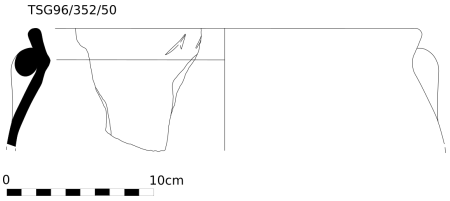


Figure A.36: Reconstructed inscribed rim

Description: Olla, Quercia (2002: III-II BCE) B1, and parallels in Sagona (2015b) 1:112:5. Shape associated with cooking vessels. Rounded lip, offset (lid locator?) and globular body. The handle is a "horizontal loop handle" (Sagona 2015b: 75). Parts of the surfaces and rim are lustrous and smooth, sightly burnished for the inner surface. Irregular striations close to the bottom of the handle, likely from attaching the handle and smoothing with fingers. Striations from the finish are irregular. The inscription would read "LT" with a T visible and a possible "L" (pers. comm. Prof. A Frendo 24th November 2021). Manufacture technique is unclear; the hypothesis is that the vessel was handmade. Inner diameter: 25cm. Thickness: 6.2-8mm.

Internal surface	External surface	Core
2.5YR 5/6 red	2.5YR 5/6 red	5YR 5/6 yellowish red

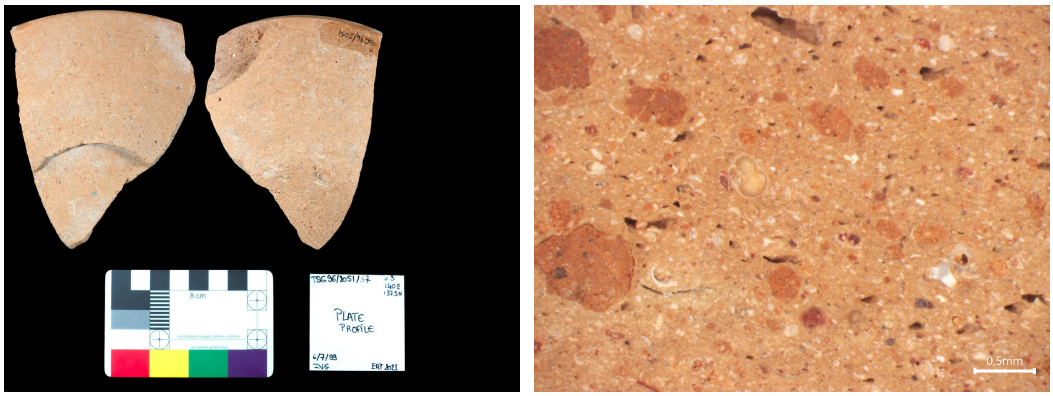
Table A.35: Munsell colours values

Macro	OM	PLM	HCA
Anastasi F5	B	5	3

Table A.36: Classifications of the sherd across this study. Numbering is independent in different methods.

The classification of this sherd is consistent with all techniques, grouping with the other cooking vessels

Sample 19 (TSG96/2051/37)



(a) (b)

Figure A.37: (a) Photograph: interior; exterior (b) Microphotograph: ground sample

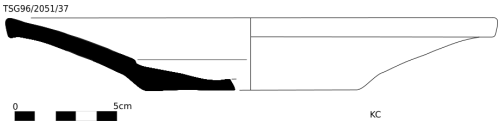


Figure A.38: Reconstructed plate, drawn by Kellian Coste

Description: Profile of plate, shape close to Anastasi (2019) D26, D27.6-8 and Quercia (2011) 2.8. The rim is flaring. The base has irregular concentric striations (string cut marks?) and is flat. The vessel was smoothed/wet-wiped, and striations were visible. Outer rim diameter: 24 cm and thickness: 5.2-10.7mm.

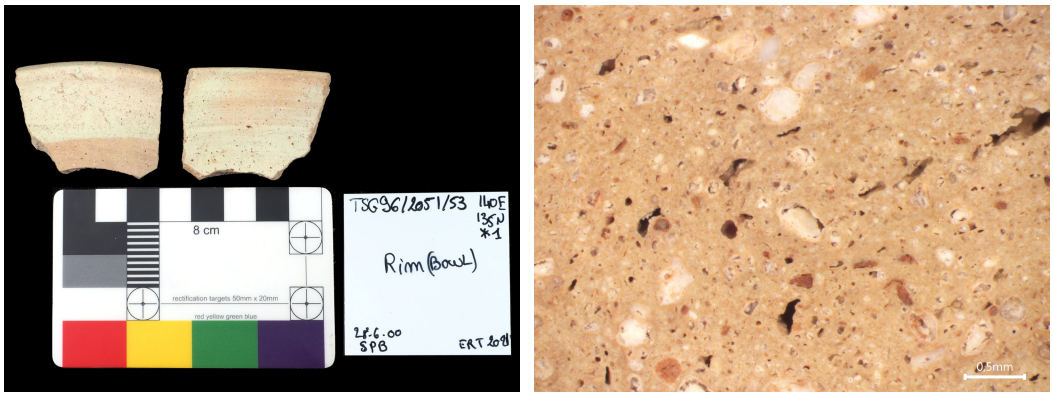
Internal surface	External surface	Core
5YR 6/6 reddish yellow	5YR 6/6 reddish yellow	5YR 6/6 reddish yellow

Table A.37: Munsell colours values

Macro	OM	PLM	HCA
Anastasi F1 with orange-brown rounded inclusions, some white inclusions	D3	-	2

Table A.38: Classifications of the sherd across this study. Numbering is independent in different methods.

Sample 20 (TSG96/2051/53)



(a) (b)

Figure A.39: (a) Photograph: interior; exterior (b) Microphotograph: ground sample

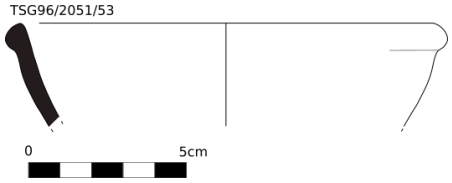


Figure A.40: Reconstructed bowl rim

Description: Bowl, shape close to Sagona (2015b) 1:68:4-5 or variant of Anastasi (2019) D6 and samples from this dissertation such as sample 23. The surface colour suggests a slip/a wash would have been applied as the outer surface has a clear separation between a cream and pink colour (Figure A.39a). Finish lines (from the application? wiping?) are visible. The sherd has a chalky/powdery feel. Inner diameter: 13cm and thickness: 4.2-6.9mm.

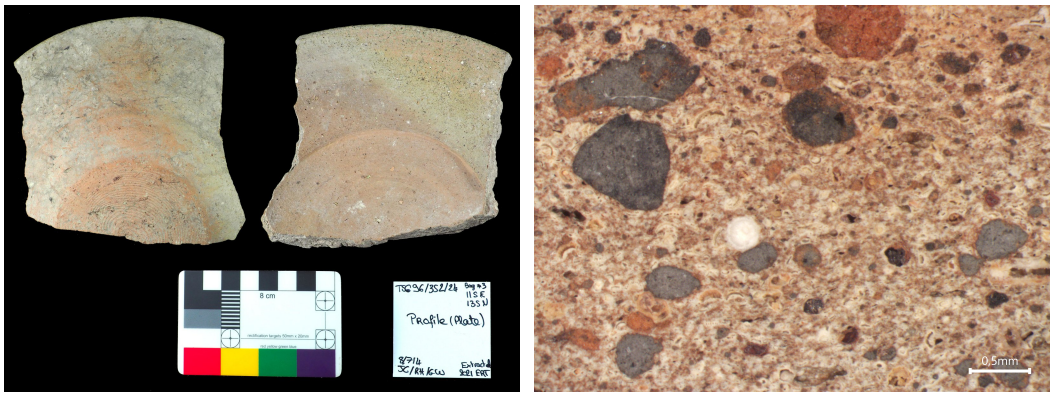
Internal surface	External surface	Core	Margins
5Y 8/2 Pale yellow	2.5Y 8/2 pale brown and 7.5 YR 7/4 pink	10YR 6/3 pale brown	7.4 7/3- 6/3 but too thin

Table A.39: Munsell colours values

Macro	OM	PLM	HCA
Anastasi F1 white inclusions	-	-	-

Table A.40: Classifications of the sherd across this study. Numbering is independent in different methods.

Sample 21 (TSG96/352/24)



(a) (b)

Figure A.41: (a) Photograph: interior; exterior (b) Microphotograph: ground sample



Figure A.42: Reconstructed plate

Description: Profile of plate, close to Anastasi (2019) D26. The rim is less flaring than sample 2, for instance. The base has visible striations (concentric/ellipsoidal), and thin parallel striations are visible on both surfaces. Inclusions are visible on the inner surface (harsh feel), but the outer surface was smoothed (smooth feel). Post-depositional processes could have caused grey marks and patches. The variations in colour in surfaces could be caused by the firing and/or bleaching of parts of the surfaces. Outer rim diameter: 23cm. Thickness: 6-13mm, including base.

Internal surface	External surface	Core
Range 10YR 7/3 very pale brown and 7.5YR 7/4 pink	5YR 7/4 pink, 7/5YR 6/3 light brown in areas.	10YR 6/3 pale brown

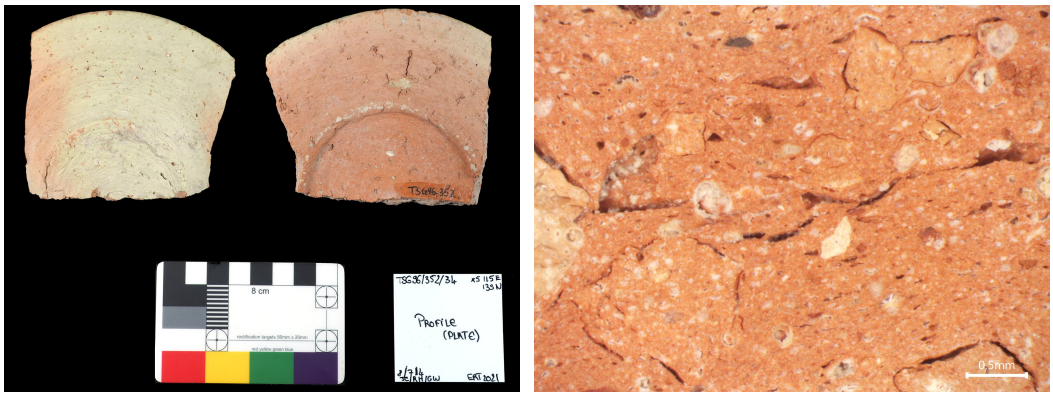
Table A.41: Munsell colours values. Surfaces and core are heterogeneous in colour.

Macro	OM	PLM	HCA
Anastasi F1 with black to brown inclusions	D2	2.1	2

Table A.42: Classifications of the sherd across this study. Numbering is independent in different methods.

The classification of this sherd is consistent with all techniques, grouping with the other sherds with iron-rich inclusions. This sherd was analysed by CRB laboratory and has multiple readings with XRF as it was used to assess precision and accuracy.

Sample 22 (TSG96/352/34)



(a) (b)

Figure A.43: a) Photograph: interior; exterior (b) Microphotograph: ground sample

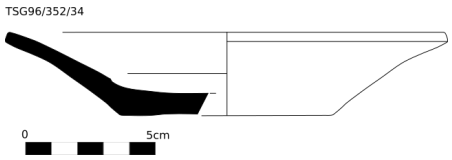


Figure A.44: Reconstructed plate profile

Description: Profile of plate, shape close to sample 21 and reference within entry A. Whitened surface, with a possible cream slip, applied on the outer surface and rim (less likely due to heterogeneity). Striations (not entirely regular and parallel) on surfaces and concentric striations on the base are visible. Post-depositional processes could have caused one prominent surface inclusion surrounded by cracks or lime-spalling. In the fresh break, the margins are very thin. Outer diameter: 17cm. Thickness: 4.8-12.9mm, including rim and base.

Internal surface	External surface	Core	Margins
2.5YR6/6 light red and 5YR 7/4 pink	7.5YR 7/4 pink - 2.5Y 8/3 pale brown	2.5YR6/6 light red	thin, close to 5YR 7/6 reddish yellow

Table A.43: Munsell colours values

Macro	OM	PLM	HCA
Anastasi F1 with white inclusions	F?	1.1	Conflicting classification

Table A.44: Classifications of the sherd across this study. Numbering is independent in different methods.

Sample 23 (TSG96/2051/45)



(a) (b)

Figure A.45: (a) Photograph: interior; exterior (b) Microphotograph: ground sample

Description: Bowl, rim close to sherds studied in this dissertation such as sample 40. Almond-shaped rounded body. Surface pores are visible and the sherd is brittle. Surfaces are white and homogeneous in colour, surface finish lines are thin and parallel. Inner diameter: 13cm, thickness: 4.2-7.2mm.

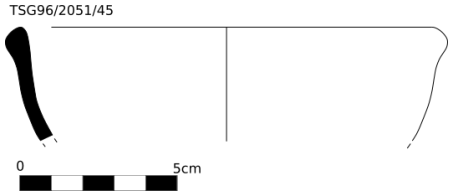


Figure A.46: Reconstructed bowl rim

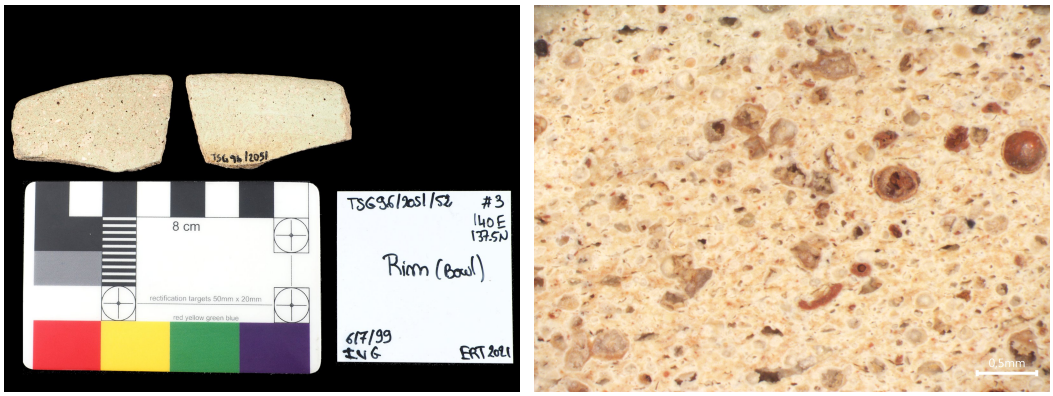
Internal surface	External surface	Core
2.5Y 8/2 pale brown	2.5Y 8/2 pale brown	2.5YR 8/3 pale brown

Table A.45: Munsell colours values

Macro	OM	PLM	HCA
Anastasi F1 with white matrix	C	-	1

Table A.46: Classifications of the sherd across this study. Numbering is independent in different methods.

Sample 24 (TSG96/2051/52)



(a) (b)

Figure A.47: (a) Photograph: interior; exterior (b) Microphotograph: ground sample

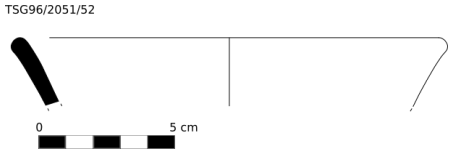


Figure A.48: Reconstructed bowl rim

Description: Bowl, shape close to illustrations in Sagona (2015b) 1:66 with a rounded rim and Anastasi (2019) D8?. The texture is rough and the surfaces are irregular. Inclusions are visible on one of the surfaces, whilst the other surface has nearly none, which could suggest a different treatment such as a slip or smoothing/wet-wiping with care. The sherd could have been altered by post-deposition, hence the rough greenish surface. Inner diameter: 16cm and thickness: 4.6 to 6.2mm.

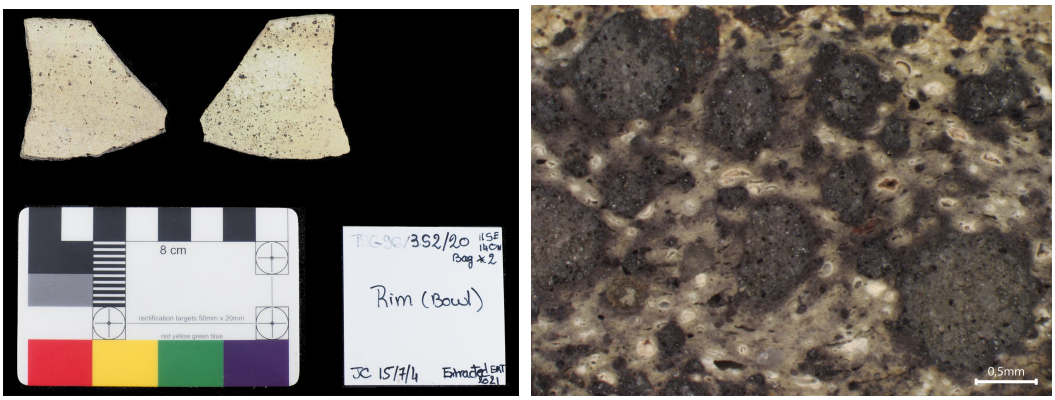
Internal surface	External surface	Core
5Y 8/2 Pale yellow	5Y 7/3 Pale yellow	5Y 7/3 Pale yellow

Table A.47: Munsell colours values

Macro	OM	PLM	HCA
Anastasi F1 with white matrix	C	-	-

Table A.48: Classifications of the sherd across this study. Numbering is independent in different methods.

Sample 25 (TSG96/352/20)



(a) (b)

Figure A.49: (a) Photograph: interior; exterior (b) Microphotograph: ground sample



Figure A.50: Section of the bowl rim

Description: Bowl, shape close to Sagona, 2015b 1:65:16 which is described as partly grey/green, Quercia (2011) 2:7, Anastasi (2019) D6.6 and Bechtold (2017) 8:5. Flaring rounded rim. Black rounded inclusions visible on the sherd surface, parallel striations (finish lines) on the outer surface with a lighter colour close to the rim (different surface treatment?). On the lip, this extra layer of material is remaining and seems to be flaking. Rim is too small to establish diameter. Thickness: 4.4-6.8mm.

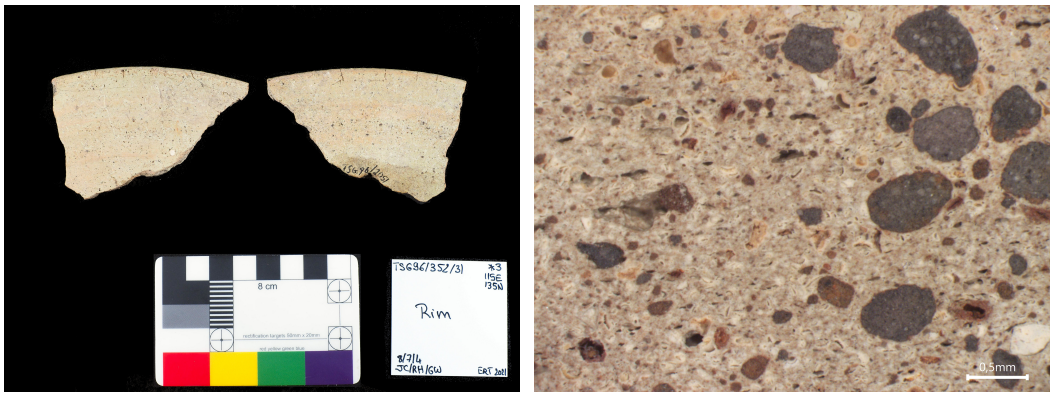
Internal surface	External surface	Core
5Y 8/3 pale yellow	5Y 8/2 pale yellow	5Y3/1 very dark grey and pale yellow

Table A.49: Munsell colours values

Macro	OM	PLM	HCA
Anastasi F1 with white matrix	D?	2.1	2

Table A.50: Classifications of the sherd across this study. Numbering is independent in different methods.

Sample 26 (TSG96/352/31)



(a) (b)

Figure A.51: (a) Photograph: interior; exterior (b) Microphotograph: ground sample



Figure A.52: Reconstructed plate rim

Description: Plate form, as shallow as illustrations in Sagona (2015b) 1:97:2 but larger. Anastasi (2019) D.26.2 has a similar rim but is deeper. Slightly ribbed walls and flaring triangular rim. A brittle material, cracks can be observed on the surfaces close to the rim. Visible inclusions on surfaces and light striations were observed on the outer surface. Outer diameter: 29cm. Thickness: 5.4-10.1mm including lip.

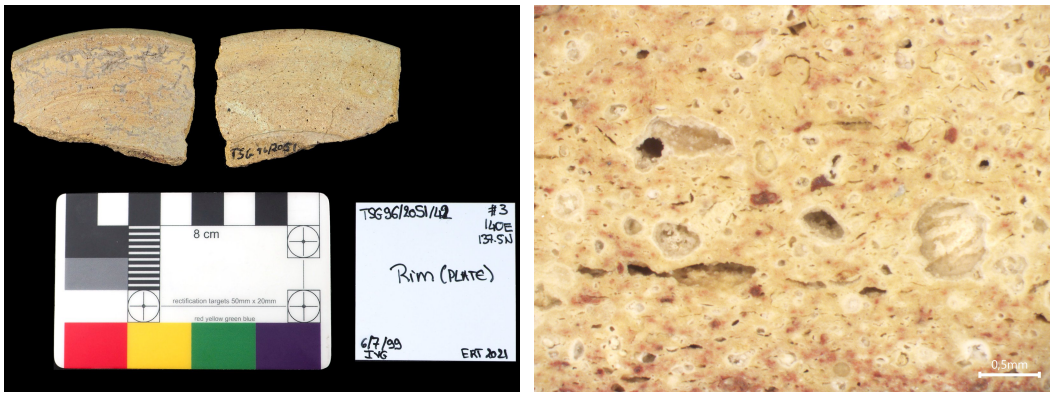
Internal surface	External surface	Core	Margins
2.5Y 7/4 pale brown - 5Y 8/2 pale yellow	2.5Y 7/4 pale brown - 5Y 8/2 pale yellow.	10YR 7/1 light gray	5YR 6/6 reddish yellow

Table A.51: Munsell colours values, surfaces have colour range

Macro	OM	PLM	HCA
Anastasi F1 with black to brown inclusions	D2		2

Table A.52: Classifications of the sherd across this study. Numbering is independent in different methods.

Sample 27 (TSG96/2051/42)



(a) (b)

Figure A.53: (a) Photograph: interior; exterior (b) Microphotograph: ground sample

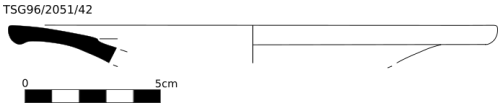


Figure A.54: Reconstructed plate rim

Description: Plate, close to Anastasi (2019) 26.3-27.1?. Shallow form with parallels like in Sagona (2015b) 1:89:8?, 1:92:5, 1:96:3 but smaller. Surface is powdery and the material is very brittle (break with hand pressure). Flaring rim. Surface striations (finish lines) are regular and parallel. Post-depositional deposit visible on outer surface. Outer diameter: 18cm, thicknes: 5-7mm

Internal surface	External surface	Core
2.5Y 7/4-8/4 pale brown	2.5Y 7/4-8/4 pale brown	2.5 Y 8/6 yellow

Table A.53: Munsell colours values

Macro	OM	PLM	HCA
Anastasi F1 with white matrix	C	1.1	1

Table A.54: Classifications of the sherd across this study. Numbering is independent in different methods.

Sample 28 (TSG96/352/47)



(a) (b)

Figure A.55: (a) Photograph: interior; exterior (b) Microphotograph: ground sample

Description: Bowl, shape close to Anastasi (2019) D6.6 but with a straighter and more vertical wall. The triangular rim is slightly everted. Surfaces are heterogeneous in colour and whitened through the firing process or slipped (less likely but there is a clear difference in colour between fabric and surface). Inner diameter: 16cm and thickness 4.8-7.6mm.

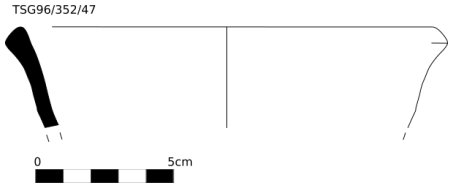


Figure A.56: Reconstructed bowl rim

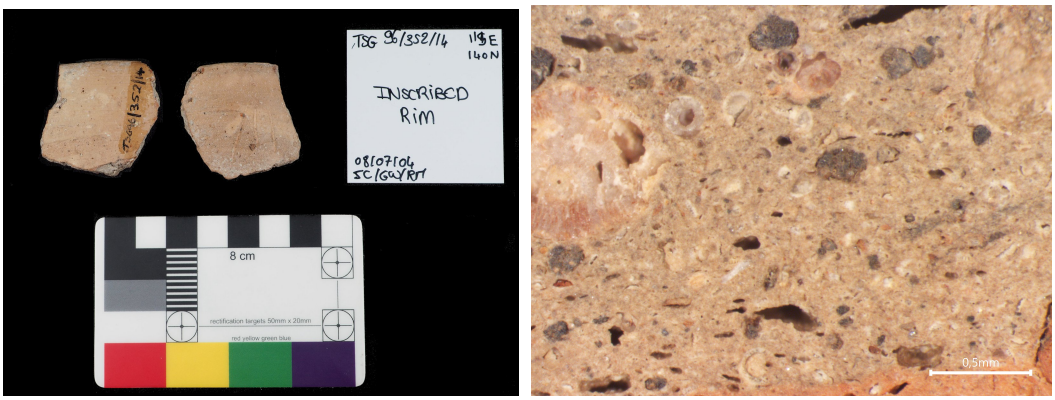
Internal surface	External surface	Core	Margins
10YR8/3 very pale brown - 2.5YR 6/6 light red	10YR8/3 very pale brown	2.5Y 4/1 dark gray	2.5YR 6/6 light red

Table A.55: Munsell colours values

Macro	OM	PLM	HCA
Anastasi F1 with predominantly white inclusions	E	-	2

Table A.56: Classifications of the sherd across this study. Numbering is independent in different methods.

Sample 29 (TSG96/352/14)



(a) (b)

Figure A.57: (a) Photograph: interior; exterior (b) Microphotograph: ground sample

Description: Bowl, shape close to illustrations in Sagona (2015b) 1:67:2 or 1:67:6 with straight rim. Some straight walls, everted, observed at Żejtun by Bechtold (2017) 9:4, 9:8. Surface finish lines visible on the surfaces, particularly on the inner surface suggesting wiping (or smoothing), for example, with a cloth (Roux 2016: 200,203 figures 3.54b or 3.57b, unlikely from slip application). Inscription made pre-firing interpreted as "LT" (Frendo and Mizzi 2015: 598) on the outer surface. Outer diameter: 12 cm. Thickness: 4.7-6.2mm.

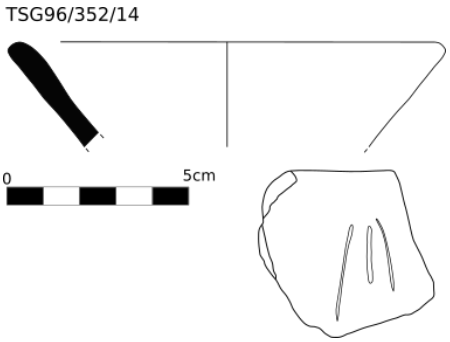


Figure A.58: Reconstructed bowl

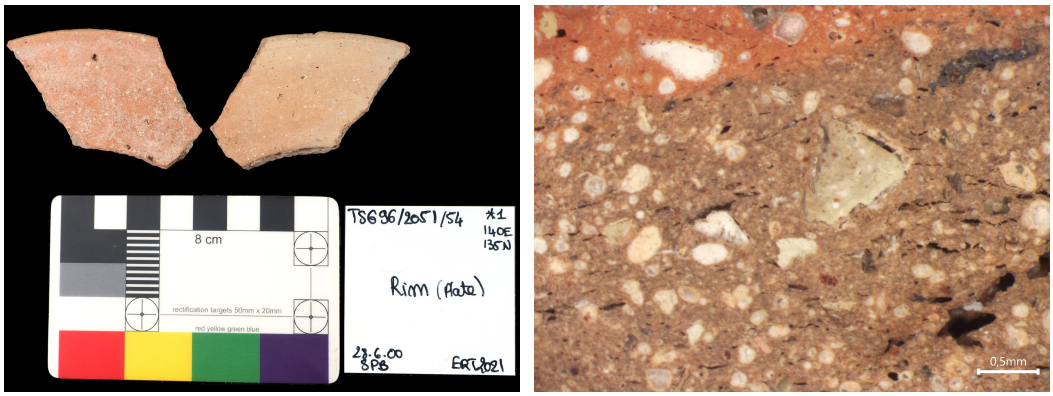
Internal surface	External surface	Core	Margins
7.5YR 7/4 pink, hues closer to 8/4	7.5YR 7/4 pink	10YR 6/3 pale brown	2.5YR 6/8 light red

Table A.57: Munsell colours values

Macro	OM	PLM	HCA
Anastasi F1 with black to brown inclusions	D2	1.2	-

Table A.58: Classifications of the sherd across this study. Numbering is independent in different methods.

Sample 30 (TSG96/2051/54)



(a) (b)

Figure A.59: (a) Photograph: interior; exterior (b) Microphotograph: ground sample

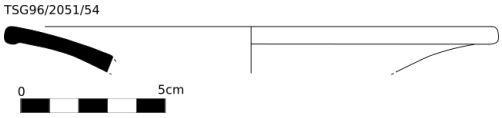


Figure A.60: Reconstructed plate rim

Description: Plate, shape close Quercia (2011) 1:4-5, Anastasi (2019) D26 but with a slightly different rim attitude, and illustrations Sagona (2015b) 1:95:5-6, rounded flaring rim. The inner surface is smoother with a lighter colour (whitened?), and striations are visible on both surfaces (particularly on the outer surface) from the surface finish (wet-wiping?). Outer diameter: 17cm and thickness 5.5-6.3mm.

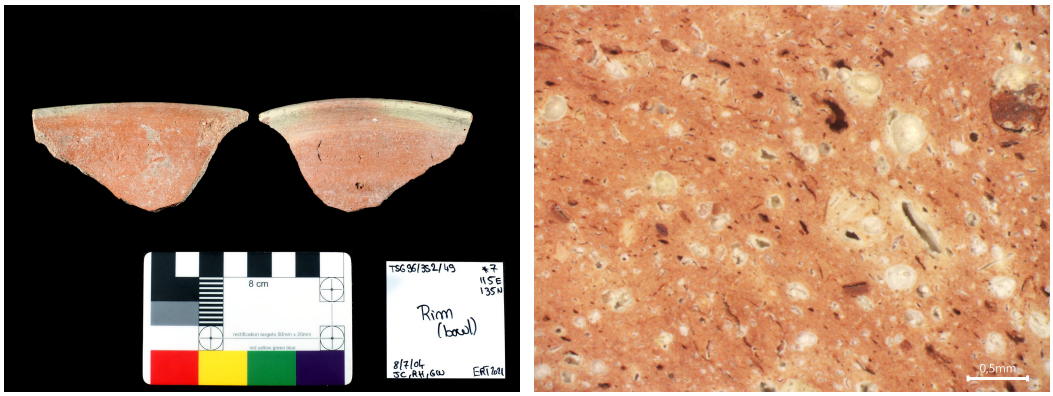
Internal surface	External surface	Core	Margins
5YR 7/6 reddish yellow	2.5YR 5/8 red	10YR 5/3 brown	2.5YR 5/8 red

Table A.59: Munsell colours values

Macro	OM	PLM	HCA
Anastasi F1 with predominantly white inclusions	E?	1.1	2

Table A.60: Classifications of the sherd across this study. Numbering is independent in different methods.

Sample 31 (TSG96/352/49)



(a) (b)

Figure A.61: (a) Photograph: interior; exterior (b) Microphotograph: ground sample

Description: Bowl, shape close to Anastasi (2019) D6.3, D9? and Quercia (2011) 2.7 and 2.8. Rim is flaring and everted. Whitening of parts of the rim (less likely slip), irregular and creating heterogeneity in colour. Striations are visible on both surfaces from the surface finish. Outer diameter: 19cm and Thickness: 4.6-6.3mm.

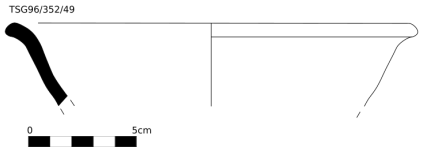


Figure A.62: Reconstructed bowl rim

Internal surface	External surface	Core
2.5YR 6/6 light red	2.5Y 8/2 pale brown (rim) - 2.5YR 6/6 light red	2.5YR 5/8 red

Table A.61: Munsell colours values

Macro	OM	PLM	HCA
Anastasi F1 with predominantly white inclusions	-	-	-

Table A.62: Classifications of the sherd across this study. Numbering is independent in different methods.

Sample 32 (TSG96/2051/49)



(a) (b)

Figure A.63: (a) Photograph: interior; exterior (b) Microphotograph: ground sample



Figure A.64: Section of vessel rim

Description: Olla, shape close to Anastasi (2019) C3 with a slightly different lip (no concavity). The offset (lid locator?) can be noted. The diameter was not established due to damages to the rim, however, these vessels are often around 20cm or larger (Anastasi 2019: 79, see vessels C3). Surfaces were damaged, likely by post-depositional processes. Striations (finish lines) are visible on the inner surfaces. The outer surface is darker (use?). Thickness: 4.2-6.7mm

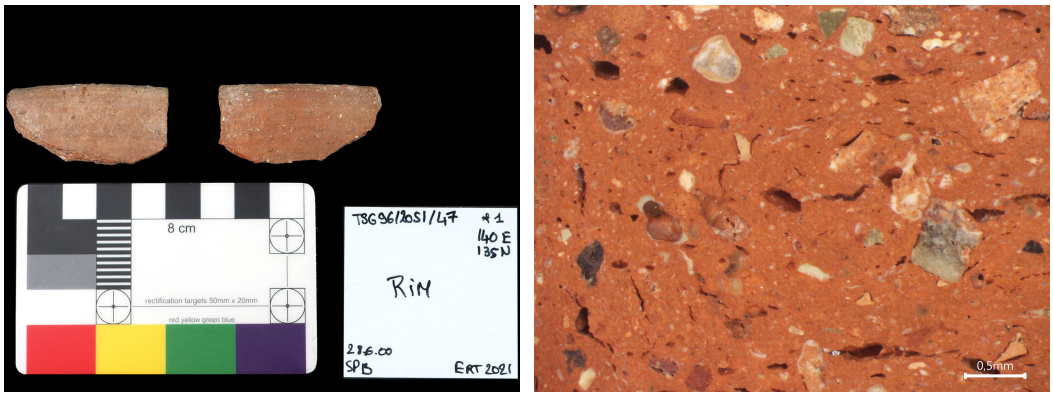
Internal surface	External surface	Core colour
5YR 4/3 reddish brown	2.5YR 4/2 weak red	2.5YR 5/8 red

Table A.63: Munsell colours values

Macro	OM	PLM	HCA
Anastasi F5	B1	-	3

Table A.64: Classifications of the sherd across this study. Numbering is independent in different methods.

Sample 33 (TSG96/2051/47)



(a) (b)

Figure A.65: (a) Photograph: interior; exterior (b) Microphotograph: ground sample



Figure A.66: Reconstructed bowl rim

Description: Bowl, shape close to typical round flaring rim, such as Quercia (2011) 2.7 and vessels illustrated in Sagona (2015b) 1:65, 1:66 despite a larger diameter, however, these shapes are often described as "Crisp Ware" whereas the fabric is different here. This sherd is part of a small group of sherds with a similar fabric in SU TSG96/2051, which are likely to come from the same vessel. Small white/yellow inclusions are visible on surfaces; the texture is irregular and rough (post-deposition, feel eroded with lumps on the surface as seen in Figure **??**). Visible striations on the surfaces. Inside diameter: 20cm and thickness: 4.8-7.7mm

Internal surface	External surface	Core
2.5YR 4/6 red	2.5YR 4/6 red	2.5YR 5/8 red

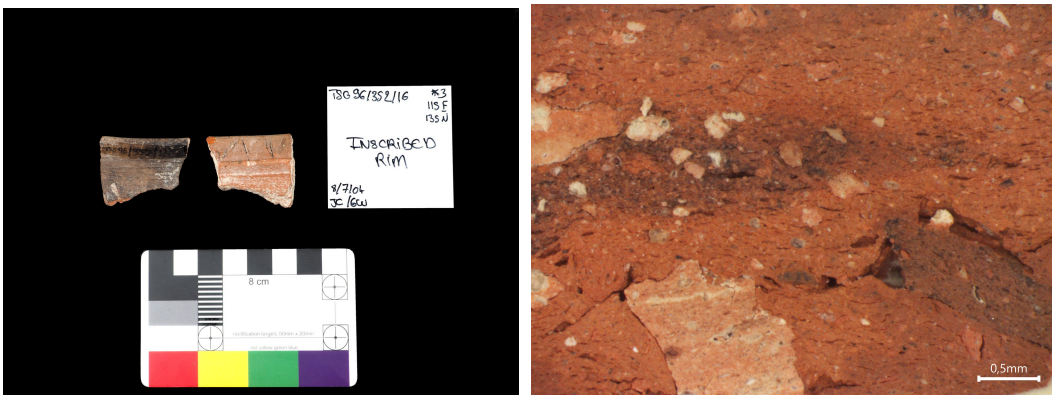
Table A.65: Munsell colours values

Macro	OM	PLM	HCA
Anastasi F5	B?	6	2

Table A.66: Classifications of the sherd across this study. Numbering is independent in different methods.

This sherd is, after analysis, considered an outlier (Fabric 6) which would need to be compared with more sherds from the archaeological site?

Sample 34 (TSG96/352/16)



(a) (b)

Figure A.67: (a) Photograph: interior; exterior (b) Microphotograph: ground sample

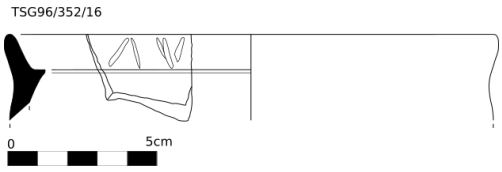


Figure A.68: Reconstructed vessel

Description: Olla (Anastasi 2019) / pentola (Quercia 2002), forms interpreted as cooking vessels. Shape close to Quercia (2002: B2-3), and vessels in Sagona (2015b: 1:114:6/7, 1:115:1) at Tas-Silġ, including other inscribed sherds. Slightly everted upper wall with a step (lid locator). Surface finish line is visible but not fully parallel, probably from smoothing-wiping. Inscription on the inner part of the rim interpreted as [L']ST[RT] Frendo and Mizzi (2015: 598, also see Figure 5.12a), inscribed pre-firing (fired lumps of clay on edges visible) and likely after the surface finish. Soot (?) / blackening on the outer surface suggests contact with fire or ash (from use?). Wall thickness: 4.4-6.8mm. Inside diameter over 16cm.

Internal surface	External surface	Core	Margins
2.5YR 4/6 red	5YR 4/3 reddish brown (and black lines)		

Table A.67: Munsell colours values

Macro	OM	PLM	HCA
Anastasi F5	B	5	-

Table A.68: Classifications of the sherd across this study. Numbering is independent in different methods.

Sample 35 (TSG96/352/40)



(a) Photograph of both surfaces



(b) Microphotograph of ground sample, x30

Figure A.69: (a) Photograph: interior; exterior (b) Microphotograph: ground sample

Description: Olla, handmade. Shape close to vessels in Sagona (2015b) 1:113:5. Crumbles easily when cut. Rounded lip and offset (lid locator). The surfaces are burnished, and the finish is light reflective. Striations from the surface finish are visible. Rim is too flat for a reading of diameter. Thickness 8.1-11.9mm.

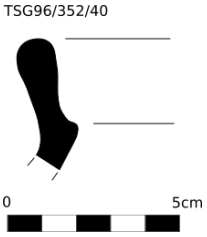


Figure A.70: Drawing of rim

Internal surface	External surface	Core	External margins
2.5YR 4/4 reddish brown	2.5YR 4/4 reddish brown	5Y 4/1 dark gray	2.5YR 6/8 red

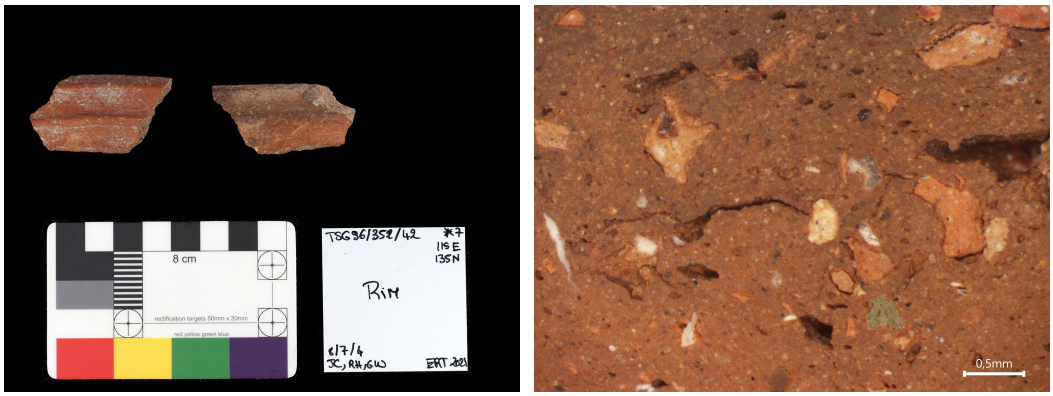
Table A.69: Munsell colours values

Macro	OM	PLM	HCA
Anastasi F5	B?	5	3

Table A.70: Classifications of the sherd across this study. Numbering is independent in different methods.

The classification of this sherd is consistent with all techniques, grouping with the other cooking vessels.

Sample 36 (TSG96/352/42)



(a) (b)

Figure A.71: (a) Photograph: interior; exterior (b) Microphotograph: ground sample



Figure A.72: Reconstructed vessel rim

Description: Olla, with lid-locator. The closest shape is Anastasi (2019) C3.2 suggests that the shape could be an evolution of Quercia, 2002 type B. Other parallels are found in Sagona (2015b) 1:116:2, 1:115:3. Darker patches are visible on the outer surface (use?). The inner surface is smooth and light reflective (burnished?). Inner diameter: 18cm. Thickness: 6.5-8.4mm.

Internal surface	External surface	Core
2.5YR 5/6 red	2.5YR 5/6 red	2.5YR 4/8 red

Table A.71: Munsell colours values

Macro	OM	PLM	HCA
Anastasi F5	B2?	5	3

Table A.72: Classifications of the sherd across this study. Numbering is independent in different methods.

The classification of this sherd is consistent with all techniques, grouping with the other cooking vessels.

Sample 37 (TSG96/2051/56)



(a) (b)

Figure A.73: (a) Photograph: interior; exterior (b) Microphotograph: ground sample

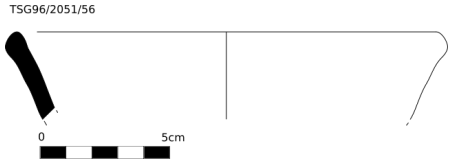


Figure A.74: Reconstructed bowl rim

Description: Bowl, shape close to other shapes in TSG96/2051 and likely variations of Anastasi (2019) D6 and parallels illustrated in Sagona (2015b) 1:67:1. Rim is almond shaped. The outer surface is whitened (less likely slipped?), and white inclusions are visible on both surfaces. The sherd difficult was hard to cut, and differences were observed in the fabric between the lip and the rest of the rim visible macroscopically. Inner diameter: 16cm and thickness: 5.2-8mm.

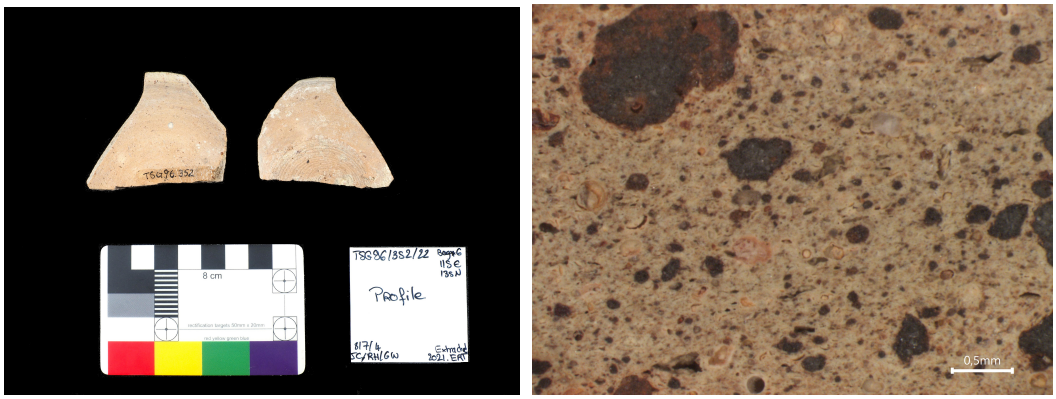
Internal surface	External surface	Core	Margins
2.5 YR 5/6 red	7.5YR 7/4 pink	2.5 YR 6/6 light red	2.5 YR 5/6 red

Table A.73: Munsell colours values

Macro	OM	PLM	HCA
Anastasi F1 with predominantly white inclusions	E	1.1	1

Table A.74: Classifications of the sherd across this study. Numbering is independent in different methods.

Sample 38 (TSG96/352/22)



(a) (b)

Figure A.75: (a) Photograph: interior; exterior (b) Microphotograph: ground sample

Description: Profile of miniature bowl, form close to Quercia (2011) 3:5 but lacking the inverted lip, dated 2nd century BCE, and illustration in Sagona (2015b) 1:61:14. Rounded rim, slightly concave at the lower part of the body. The flat base has concentric striations (string marks?). Lip is whitened. Thickness: 3.8-10.8mm.

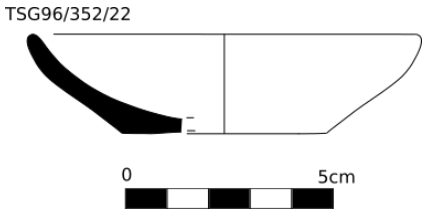


Figure A.76: Profile of sherd

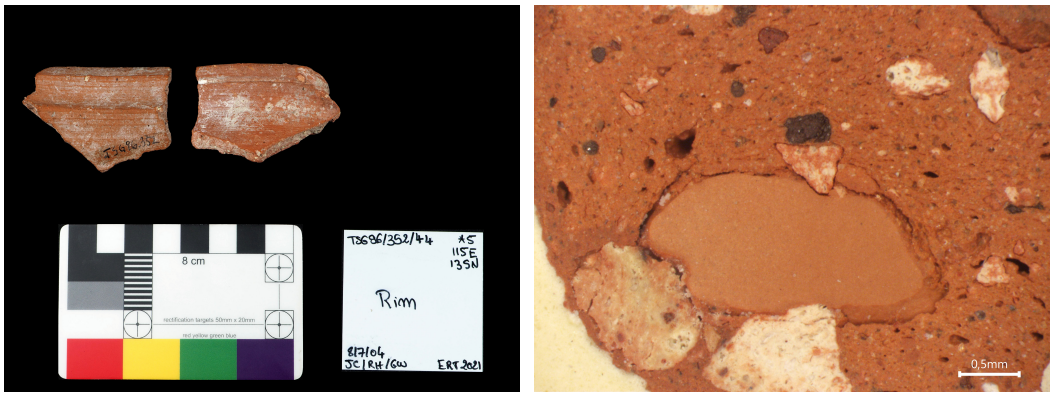
Internal surface	External surface	Core colour	Margins
7.5YR7/3 pink	7.5YR7/3 pink	2/5U 7/3 pale brown	very thin, 7.5 7/4

Table A.75: Munsell colours values

Macro	OM	PLM	HCA
Anastasi F1 with black to brown inclusions	D2	-	-

Table A.76: Classifications of the sherd across this study. Numbering is independent in different methods.

Sample 39 (TSG96/352/44)



(a) (b)

Figure A.77: (a) Photograph: interior; exterior (b) Microphotograph: ground sample

Description: Olla/cooking vessel, shape close to illustrations in Sagona (2015b: 163, 204), for instance, 1:111:3, although this one does not have burning evidence. Offset (lid locator) and groove on the exterior. Striations visible (parallel and regular), smooth surfaces. Outer diameter: 20cm, thickness: 4.6-5.1mm.

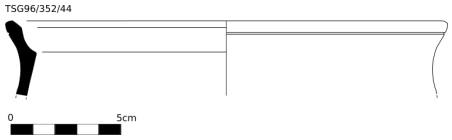


Figure A.78: Reconstructed vessel rim

Internal surface	External surface	Core
2.5YR 5/6 red	2.5YR 4/4 reddish brown	2.5YR 5/8 red

Table A.77: Munsell colours values

Macro	OM	PLM	HCA
Anastasi F5	B?	-	3

Table A.78: Classifications of the sherd across this study. Numbering is independent in different methods.

Sample 40 (TSG96/2051/44)



(a) (b)

Figure A.79: (a) Photograph: interior; exterior (b) Microphotograph: ground sample

Description:
Bowl, shape close to Quercia (2011) 2.7? and some comparative vessels illustrated in Sagona (2015b) 1:68:4-5 with similar dimensions. Rounded flaring rim. The Colour of the outer surface is bright white, which contrasts with the cream inner (slip?). Inner diameter: 12cm and thickness: 5-7mm.

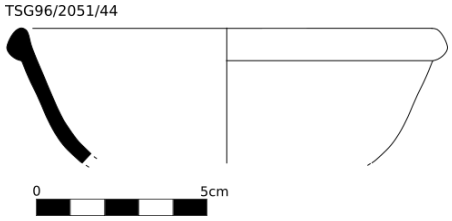


Figure A.80: Reconstructed bowl rim

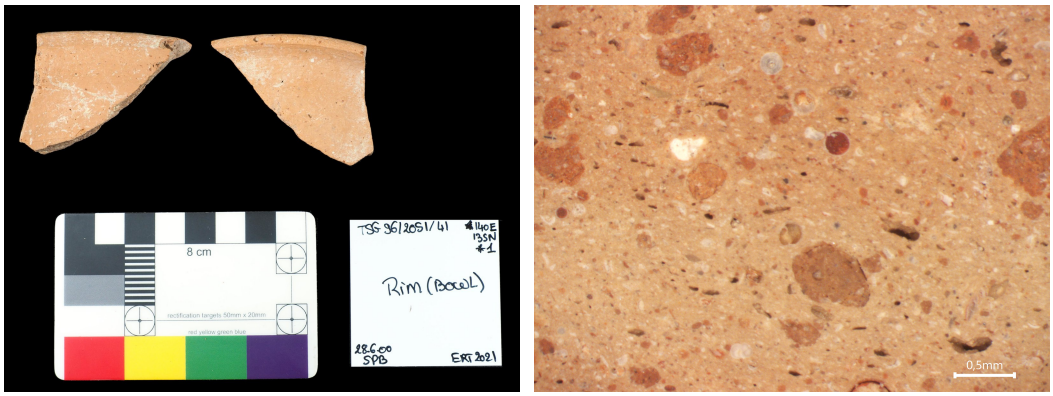
Internal surface	External surface	Core
7.5YR 8/4-7/4 pink	2.5 Y 8/3-8/4 pale brown	5Y 8/2 Pale yellow to 7.5YR8/4 pink

Table A.79: Munsell colours values

Macro	OM	PLM	HCA
Anastasi F1 with white matrix	C	1.1	1

Table A.80: Classifications of the sherd across this study. Numbering is independent in different methods.

Sample 41 (TSG96/2051/41)



(a) (b)

Figure A.81: (a) Photograph: interior; exterior (b) Microphotograph: ground sample

Description: Bowl, shape close to Anastasi (2019) D6.3, D9? and Quercia (2011) 2.7 and 2.8. Flaring and everted rim. Finish lines are visible, particularly close to the rim and outer surface. Surface inclusion is only rarely visible. Outer diameter: 20 cm and thickness: 6-7.5mm.

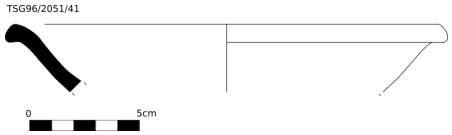


Figure A.82: Reconstructed bowl rim

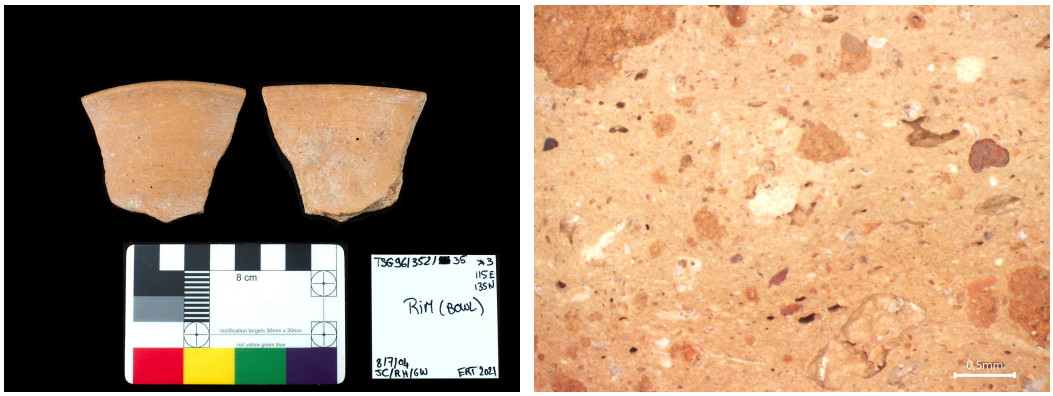
Internal surface	External surface	Core colour
5YR 7/6 reddish yellow	5YR 7/6 reddish yellow	5YR 7/6 reddish yellow

Table A.81: Munsell colours values

Macro	OM	PLM	HCA
Anastasi F1 with orange-brow rounded inclusions, some white inclusions	D3	-	-

Table A.82: Classifications of the sherd across this study. Numbering is independent in different methods.

Sample 42 (TSG96/352/35)



(a) (b)

Figure A.83: (a) Photograph: interior; exterior (b) Microphotograph: ground sample

Description: Bowl, shape close to sample 4 and related shape of sample 41, and references within catalogue entries. Close to Quercia (2011) 2:6-7. Thin striations are visible from the surface finish, particularly on the outer surface. Outer diameter: 18cm: 6.4-7.8mm including rim.

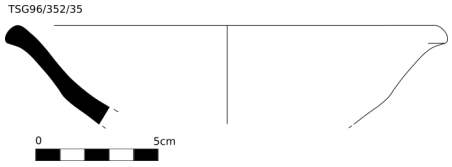


Figure A.84: Reconstructed bowl rim

Surfaces	Core	Margins
5YR 6/6 reddish yellow	7.5YR 7/6 reddish yellow	5YR 6/6 reddish yellow

Table A.83: Munsell colours values

Macro	OM	PLM	HCA
Anastasi F1 with orange-brown rounded inclusions,some white inclusions	D3	-	2

Table A.84: Classifications of the sherd across this study. Numbering is independent in different methods.

Sample 43 (TSG96/352/45)



(a) (b)

Figure A.85: (a) Photograph: interior; exterior (b) Microphotograph: ground sample

Description: Olla, shapes close to Quercia (2002) B and parallel found in Sagona (2015b) 1:114:6. Rounded lip and offset (for the lid). Surfaces are light reflective (burnished? and smooth, and striations from surface finish are visible, regular and parallel. Outer diameter: 18cm and thickness: 3.1-4.9mm.



Figure A.86: Reconstructed vessel rim

Internal surface	External surface	Core colour
2.5YR 4/6 red	2.5YR 4/6 red	7.5YR 3/3

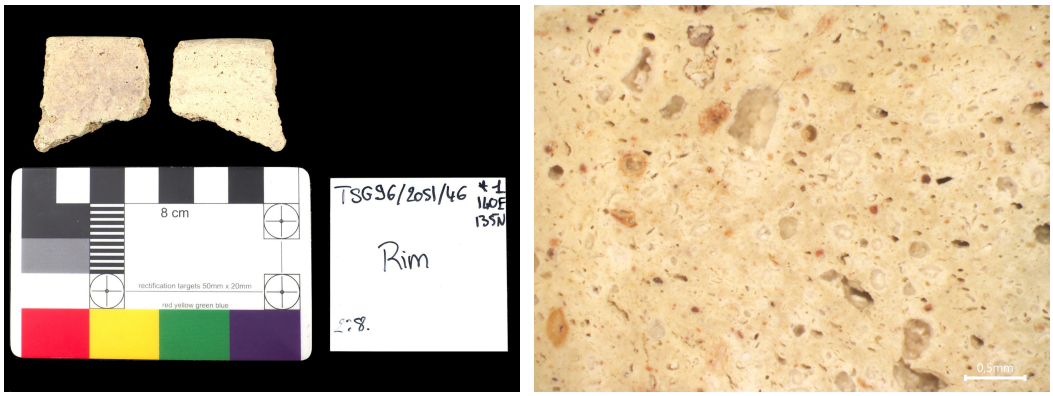
Table A.85: Munsell colours values

Macro	OM	PLM	HCA
Anastasi F4 or 5	B1	-	3

Table A.86: Classifications of the sherd across this study. Numbering is independent in different methods.

other cooking vessels.

Sample 44 (TSG96/2051/46)



(a) (b)

Figure A.87: (a) Photograph: interior; exterior (b) Microphotograph: ground sample

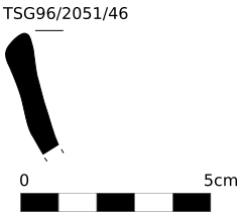


Figure A.88: Analytical drawing

Description: Bowl, shape close to Sample 37 and references within. Pointy rims are also found in shapes like vessels illustrated in Sagona (2015b) 1:59:2, 1:64:1, 1:70:4. However, the wall is less straight. It is possible that this is a residual sherd closer to shapes of Quercia (2011) 2.4-5. Margins are challenging to assess. Parallel lines (finish lines) are visible. The surfaces are smooth and the outer surface is bright white. The material is brittle and breaks easily. Rim is too small to assess the diameter. Thickness: 4.5-8.8mm.

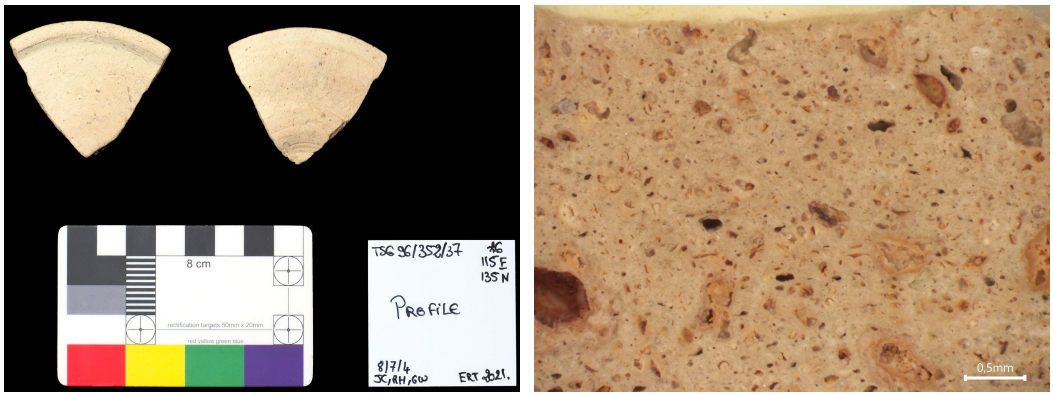
Internal surface	External surface	Core
2.5YR 8/2 pale brown, 7/1 light gray	2.5YR 8/2 pale brown	2.5YR 8/3 pale brown

Table A.87: Munsell colours values

Macro	OM	PLM	HCA
Anastasi F1 with white matrix	C	-	-

Table A.88: Classifications of the sherd across this study. Numbering is independent in different methods.

Sample 45 (TSG96/352/37)



(a) (b)

Figure A.89: (a) Photograph: interior; exterior (b) Microphotograph: ground sample

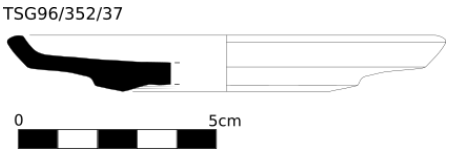


Figure A.90: Reconstructed plate

Description: Plate, miniature. Close to shapes in Sagona (2015b) 1:65:13, 1:64:6. Concentric marked striations on the base (string marks) and the edge of the base are irregular. The plate is not flat based and the wall has a carination. Slightly oblique / everted rim. The outer surface is powdery and has finish marks such as striations close to the base. On the contrary, the inner surface was smoothed and is light reflective. Outer rim diameter: 11cm. Thickness: 5-8mm including base and rim.

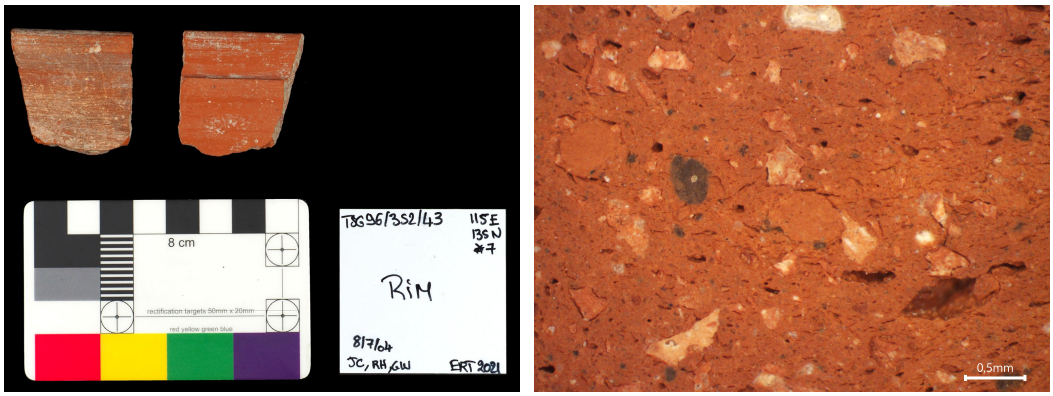
Internal surface	External surface	Core
2.5Y/2 8/ pale yellow	10YR 8/3 pale brown	10YR 7/4 very pale brown

Table A.89: Munsell colours values

Macro	OM	PLM	HCA
Anastasi F1 with white matrix	C	-	-

Table A.90: Classifications of the sherd across this study. Numbering is independent in different methods.

Sample 46 (TSG96/352/43)



(a) (b)

Figure A.91: (a) Photograph: interior; exterior (b) Microphotograph: ground sample

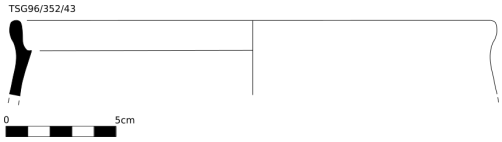


Figure A.92: Reconstructed vessel rim

Description: Olla, close to Quercia (2002) B3 and parallels found in Sagona (2015b) 1:113:5, 1:114:3. Close in shape to other samples such as Sample 45 and 43. Rounded lip and offset (for a lid). Lustrous/light reflective on the inside (burnished? less likely slipped), very thin and regular striations on the outside from surface treatment. The outer diameter is 22cm and the thickness: is 4.5-6.2mm.

Internal surface	External surface	Core
2.5YR 5/8 red	2.5YR 4/3 reddish brown, 2.5YR 5/8 red	2.5YR 4/3 reddish brown

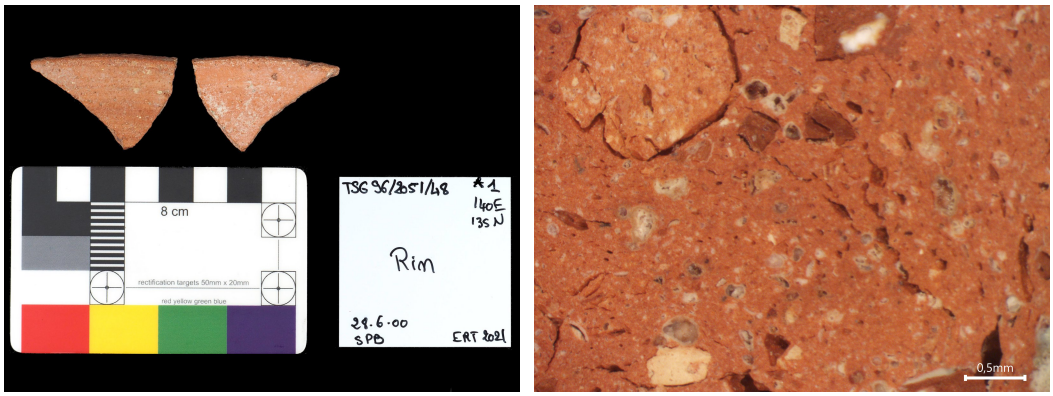
Table A.91: Munsell colours values

Macro	OM	PLM	HCA
Anastasi F4 or F5	B	5	3

Table A.92: Classifications of the sherd across this study. Numbering is independent in different methods.

The classification of this sherd is consistent with all techniques, grouping with the other cooking vessels.

Sample 47 (TSG96/2051/48)



(a) (b)

Figure A.93: (a) Photograph: interior; exterior (b) Microphotograph: ground sample

Description: Bowl, shape close to Anastasi (2019: D) 6 - D8?, with a straighter wall, and from illustrations in Sagona (2015b) 1:67:1, 1:59:2?, or close to sample 37. Pointy, triangular rim. White inclusions are visible on the surfaces as well as striations from the surface finish. Outer diameter: 15cm and thickness 4.8-6.4mm.

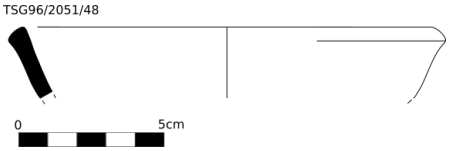


Figure A.94: Reconstructed bowl rim

Internal surface	External surface	Core
2.5YR 6/6 light red	2.5YR 6/6 light red	2.5YR 4/8red

Table A.93: Munsell colours values

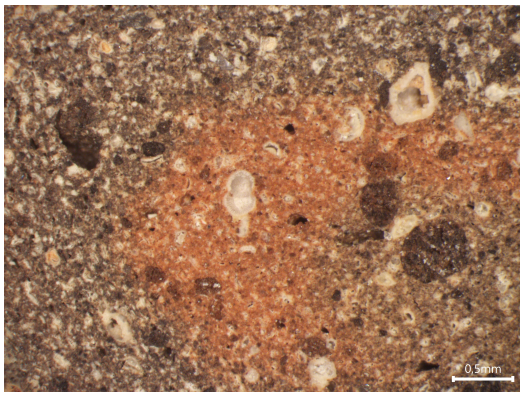
Macro	OM	PLM	HCA
Anastasi F1 with predominantly white inclusions	F?	-	2

Table A.94: Classifications of the sherd across this study. Numbering is independent in different methods.

Sample 48 (TSG96/352/26)



(a) Photograph of both surfaces



(b) Microphotograph of ground sample, x30

Figure A.95: (a) Photograph: interior; exterior (b) Microphotograph: ground sample

Description: Rim of plate, closest comparative material is Sagona (2015b) 1:95:1; 1:97:1 or shapes D27 from Anastasi (2019) but shallower. The triangular rim is flaring and the bottom part of the body is slightly convex. The inner surface and whole rim is slipped and the slip is flaking at places. Striations visible on both surfaces Outer diameter: 17cm. Thickness: 4.8-6.8mm.

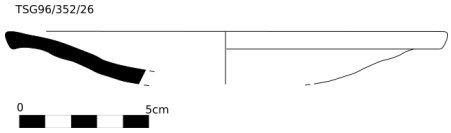


Figure A.96: Reconstructed plate rim

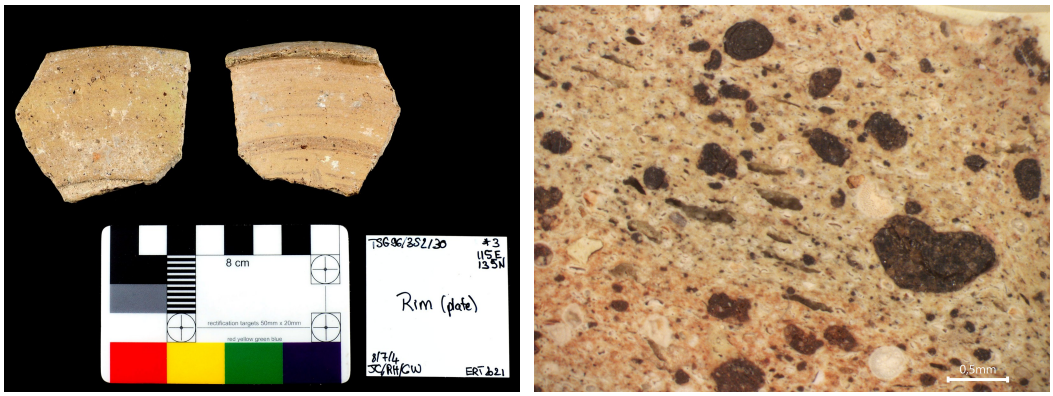
Internal surface	External surface	Core
7.5YR 7/6 reddish yellow	7.5YR 5/2 brown	10YR 5/2 grayish brown

Table A.95: Munsell colours values

Macro	OM	PLM	HCA
Anastasi F1 with black to brown inclusions	D2?	2.2	Conflicting classification

Table A.96: Classifications of the sherd across this study. Numbering is independent in different methods.

Sample 49 (TSG96/352/30)



(a) (b)

Figure A.97: (a) Photograph: interior; exterior (b) Microphotograph: ground sample

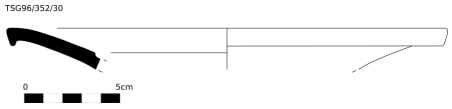


Figure A.98: Reconstructed plate rim

Description: Rim of plate, shape close to illustrations Sagona (2015b) 1:97:1-3 and Anastasi (2019) type D27.2-3, rim attitude closer to D27.2. Triangular with a deep point, flaring rim. Striations (smoothing/wet-wiping?) and some inclusions are visible on both surfaces. The darker lines on the outer surface as observed in Figure A.97a on the right, could be decorative. Additional external margins are difficult to observe. Outer diameter: 23 cm, thickness: 6-9.8mm.

Surfaces	Core	Margins
10YR 7/3 very pale brown	5YR 7/6 reddish yellow	5Y 7/3 pale yellow

Table A.97: Munsell colours values

Macro	OM	PLM	HCA
Anastasi F1 with black to brown inclusions	D2	-	-

Table A.98: Classifications of the sherd across this study. Numbering is independent in different methods.

Sample 50 (TSG96/352/46)



(a) (b)

Figure A.99: (a) Photograph: interior; exterior (b) Microphotograph: ground sample

Description: Bowl, parallels found in Sagona (2015b) 1:70:5-6. The ribbed outer surface and a rounded lip. The rim is irregular (see Fig. A.100) and the surfaces are mottled. The surfaces obtained their colour through whitening during firing or less likely slip. Striations are visible on the inner surface. Inner diameter: 14 cm and thickness: 4.8-7.8mm.

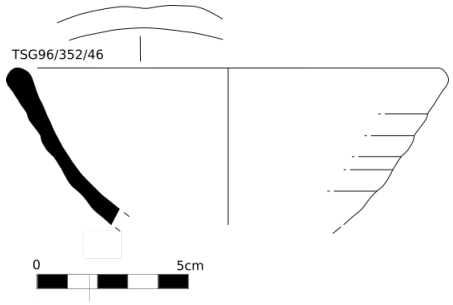


Figure A.100: Reconstructed bowl rim

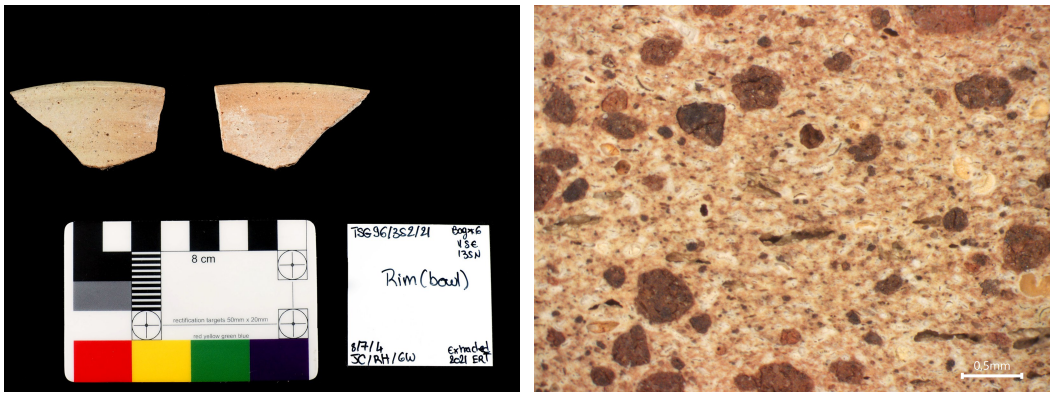
Internal surface	External surface (range)	Core
2.5Y 8/3 pale brown	2.5Y 8/2 pale brown -grey patches - 5YR 6/6 reddish yellow	2.5YR 5/8 red

Table A.99: Munsell colours values

Macro	OM	PLM	HCA
Anastasi F1 with predominantly white inclusions	E	-	Conflicting classification

Table A.100: Classifications of the sherd across this study. Numbering is independent in different methods.

Sample 51 (TSG96/352/21)



(a) (b)

Figure A.101: (a) Photograph: interior; exterior (b) Microphotograph: ground sample

Description: Bowl, form close to illustrations in Sagona (2015b) 1:67:5, and types Anastasi (2019) D6.3 and Quercia (2011) 2.7. Shape common in Tas-Silġ and Żejtun villa (Anastasi 2019: 105). Surfaces are whitened, and striations are visible. The outer diameter of 17cm, thickness: is 3.9-6.1mm including the rim.

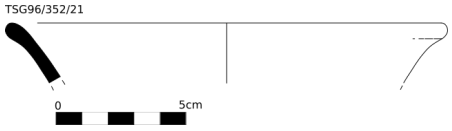


Figure A.102: Reconstructed bowl

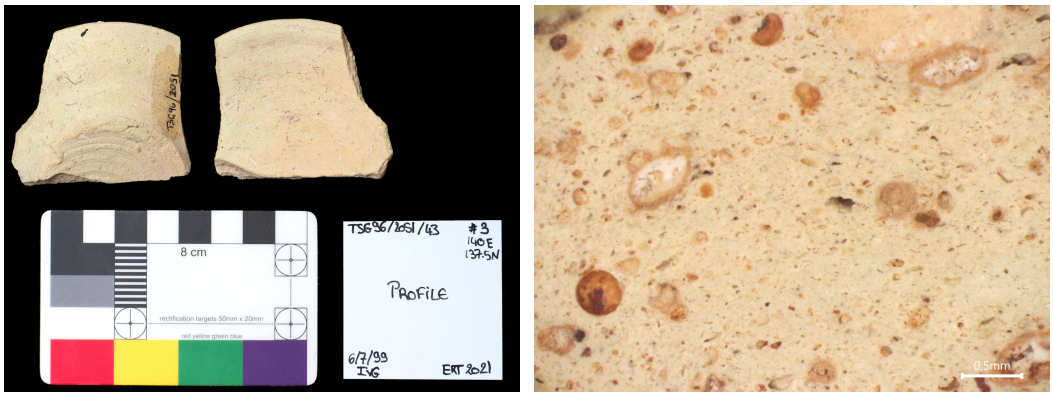
Internal surface	External surface	Core	Margins
7/5YR 6/4 light brown	2.5Y 7/3 pale brown	7.5YR6/2 pinkish gray	5YR 7/6 reddish yellow

Table A.101: Munsell colours values

Macro	OM	PLM	HCA
Anastasi F1 with black to brown inclusions	D1	-	-

Table A.102: Classifications of the sherd across this study. Numbering is independent in different methods.

Sample 52 (TSG96/2051/43)



(a) (b)

Figure A.103: (a) Photograph: interior; exterior (b) Microphotograph: ground sample

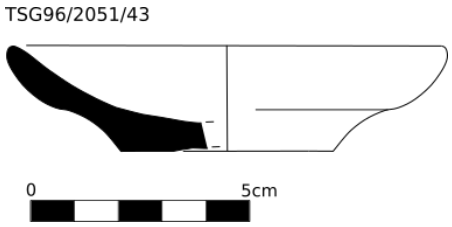


Figure A.104: Reconstructed bowl

Description: Profile of bowl (miniature), shape close Quercia (2011: 3.5) and illustrations from Sagona (2015b: 1:62:3,5,7). Pointed rim, concave lower part of the body. The base has an irregular edge and concentric striations (string cuts?). The inner surface has striations from the surface finish. The outer surface has been smoothed or wet wiped. Some short grooves on the outer surface are not-parallel to the rim, but it is unclear if they could be damaged or from the surface finish. Outer rim diameter: 10 cm, thickness: 5-7mm.

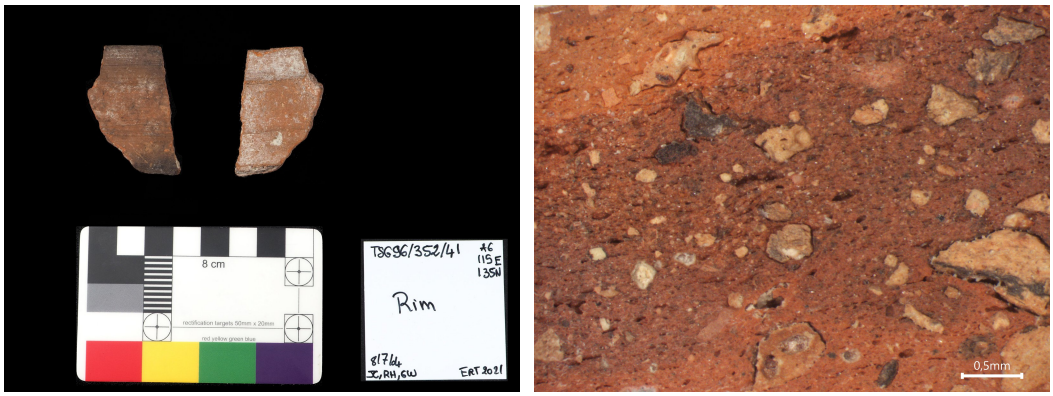
Internal surface	External surface	Core	Margins
2.5Y 8/2 pale brown-10YR 7/4 very pale brown	2.5Y 8/2 pale brown	10YR 8/4 - 7/4 very pale brown	Irregular 2.5Y 8/2 pale brown

Table A.103: Munsell colours values

Macro	OM	PLM	HCA
Anastasi F1 with white matrix	C	1.1	1

Table A.104: Classifications of the sherd across this study. Numbering is independent in different methods.

Sample 53 (TSG96/352/41)



(a) (b)

Figure A.105: (a) Photograph: interior; exterior (b) Microphotograph: ground sample

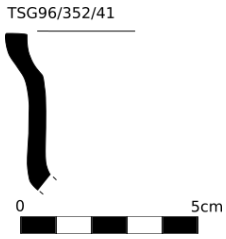


Figure A.106: Drawing of rim

Description: Tegame/Casserole; shapes of tegame such as form C in Quercia (2002) do not have a straight lip combined with a convex wall. Parallels are found in Tas-Silġ such as Sagona (2015b) 1:111:1. Finish lines are visible on both surfaces with one deeper groove. Darker patches are visible which could have been caused by use as a cooking vessel. Outer diameter was not possible to establish due to some damage to the rim. Thickness: 4.2-6.4mm.

Internal surface	External surface	Core	Margins
2.5 YR 5/6 red	2.5YR 4/4 reddish brown - 5YR 4/4 reddish brown	2.5YR 4/3 reddish brown	2.5YR 5/8 red

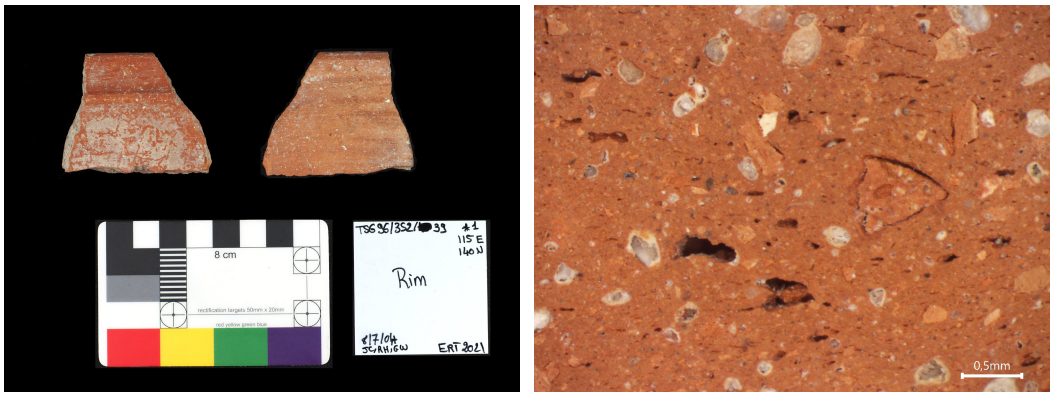
Table A.105: Munsell colours values

Macro	OM	PLM	HCA
Anastasi F5	B	-	3

Table A.106: Classifications of the sherd across this study. Numbering is independent in different methods.

The classification of this sherd is consistent with all techniques, grouping with the other cooking vessels.

Sample 54 (TSG96/352/39)



(a) (b)

Figure A.107: (a) Photograph: interior; exterior (b) Microphotograph: ground sample

Description: Olla, shape close to Quercia (2002) B2/B3 and Sagona (2015b) 1:113:6-1:114:7. Offset and rounded rim. Very smooth surfaces, inner surface is burnished. Surface finish striations are visible. Post deposition residue on inner surface. Outer diameter: 18cm and thickness: 6.5-8.1mm.

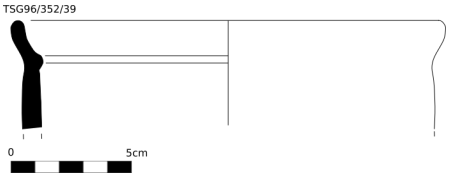


Figure A.108: Reconstructed vessel rim

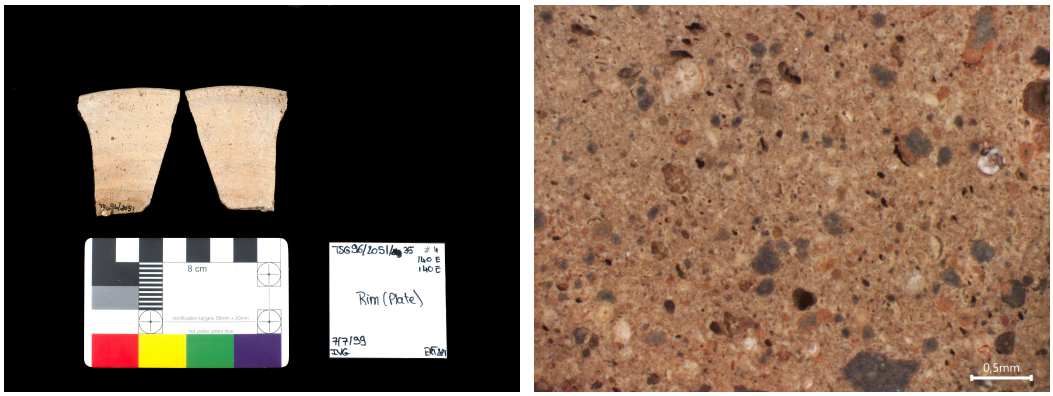
Internal surface	External surface	Core colour
2.5YR 5/6 red	2.5YR 5/6 red	2.5 YR 5/8 red

Table A.107: Munsell colours values

Macro	OM	PLM	HCA
Anastasi F5	B?	5	3

Table A.108: Classifications of the sherd across this study. Numbering is independent in different methods.

Sample 55 (TSG96/2051/35)



(a) (b)

Figure A.109: (a) Photograph: interior; exterior (b) Microphotograph: ground sample

Description: Plate, shape close to Anastasi (2019) D27.2 and Quercia (2011) 1.7-8 which are common in Tas-Silġ. Flaring triangular rim (but rounded angles) similar to sample 49. The surfaces, cream colour are likely cream slipped, or whitened. The finish lines are visible. Outer diameter: 21cm and thickness: 4.8-9.7mm.



Figure A.110: Reconstructed plate rim

Surfaces	Core	Margins
7.5YR 7/3 pink - 6/3 light brown	7.5YR6/2 pinkish gray	5YR 6/4 light reddish brown

Table A.109: Munsell colours values

Macro	OM	PLM	HCA
Anastasi F1 with black to brown inclusions	D2	-	-

Table A.110: Classifications of the sherd across this study. Numbering is independent in different methods.

Sample 56 (TSG96/2051/36)



(a) (b)

Figure A.111: (a) Photograph: interior; exterior (b) Microphotograph: ground sample

Description: Bowl, shape close to illustrations in Sagona (2015b) 1:70:6 or 1:71:1, or close to Quercia (2011) type 2.7 but smaller. Shape similar to samples 8 or 15. Wall is ribbed on the outer surface. Upper internal surface is whitened (less likely slipped), and striations from surface finish are visible. Outer diameter: 13cm and thickness: 5-7.2mm.

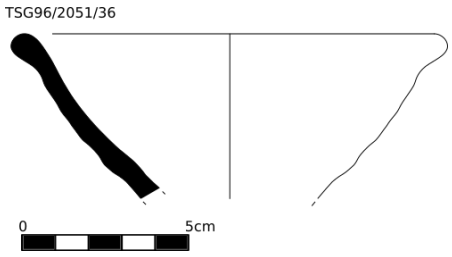


Figure A.112

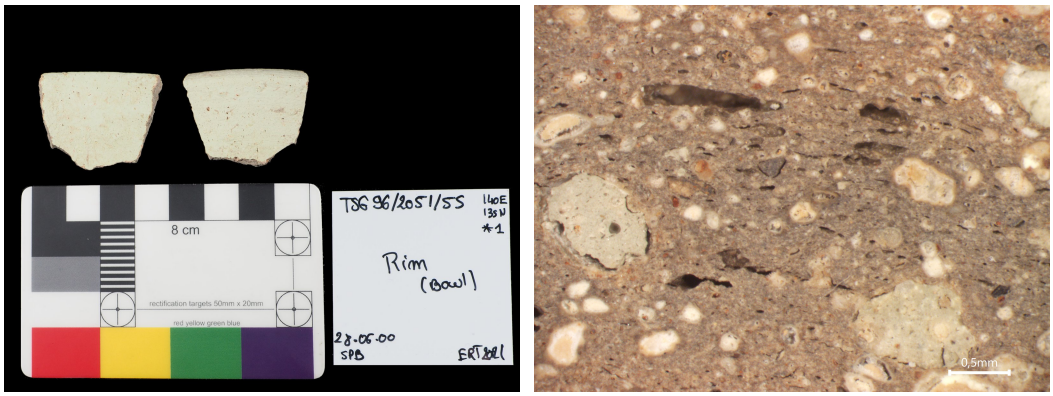
Internal surface	External surface	Core
5YR 6/4 light reddish brown - uneven	2.5YR 6/6-5/6 light red, 7.5YR 8/3 pink (rim)	2.5 YR 5/8 red

Table A.111: Munsell colours values

Macro	OM	PLM	HCA
Anastasi F1 with predominantly white inclusions	D3	-	-

Table A.112: Classifications of the sherd across this study. Numbering is independent in different methods.

Sample 57 (TSG96/2051/55)



(a) (b)

Figure A.113: (a) Photograph: interior; exterior (b) Microphotograph: ground sample

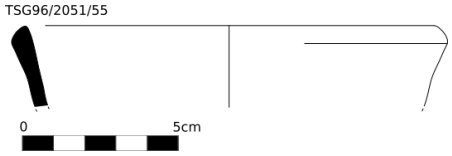


Figure A.114: Reconstructed bowl rim

Description: Bowl (jug?), shape close to other samples in SU TSG96/2051 such as sample 44 and references in the entry. Pointy rim. Cream slip(?) or slurry on both surfaces suggested by difference in colour between the core and surfaces, the inclusions are covered. The Surface finish lines are visible (application?). Inner diameter: 13 cm and thickness: 3.5- 6.4mm.

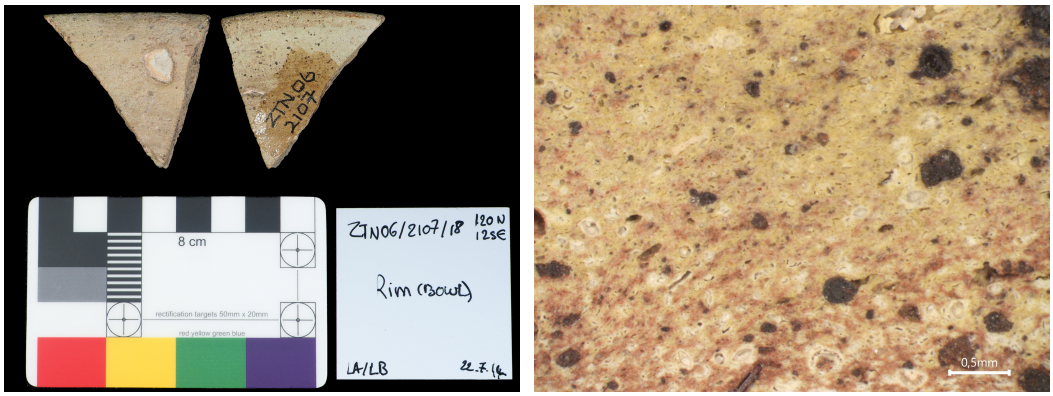
Surfaces	Core colour	Margins
5Y 8/2 pale yellow	2.5Y4/1 dark gray	YR5/6 yellowish red? (very thin)

Table A.113: Munsell colours values

Macro	OM	PLM	HCA
Anastasi F1 with predominantly white inclusions	E?	-	-

Table A.114: Classifications of the sherd across this study. Numbering is independent in different methods.

Sample 58 (ZTN06/2107/18)



(a) (b)

Figure A.115: (a) Photograph: interior; exterior (b) Microphotograph: ground sample

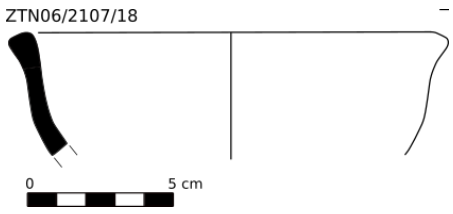


Figure A.116: Reconstructed vessel rim

Description: Bowl, shape close to Quercia (2011) 2.7 and Anastasi (2019) D6.6. Sherd classified as special find in 2021 for this work. Everted rim, slightly flaring. Inner surface has a cavity, which could have been caused by a dislodged surface inclusion. Some surface finish lines are visible, surfaces are irregular with fired lumps of surplus material (from before firing). Surface inclusions, mostly black, are visible on the outer surface and not on the inner surface (where they look covered).Outer diameter: 15cm and thickness: 6mm.

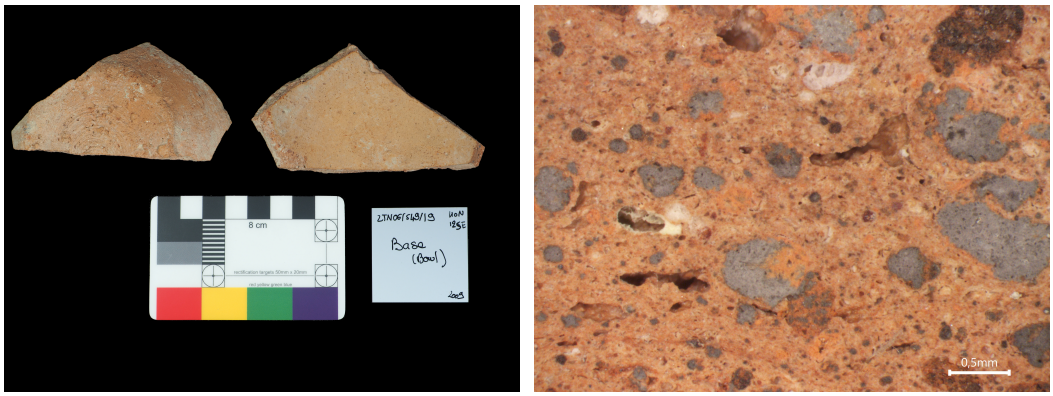
Internal surface	External surface	Core	Margins
2.5Y 7/3 Pale brown	5Y 8/2 Pale yellow	5Y 6/2 light olive gray	7.5YR 6/3 light brown

Table A.115: Munsell colours values

Macro	OM	PLM	HCA
Anastasi F1 with black to brown inclusions	D2	2.2	2

Table A.116: Classifications of the sherd across this study. Numbering is independent in different methods.

Sample 59 (ZTN06/549/19)



(a) (b)

Figure A.117: (a) Photograph: interior; exterior (b) Microphotograph: ground sample

Description:

Only base of the set, most probably from a bowl. Base has string marks and was not smoothed and surface finish lines are visible. Special Find extracted in 2021. Base diameter: 7cm, thickness: 6.1-9.2mm.

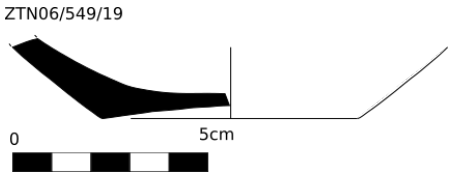


Figure A.118: Reconstructed vessel rim

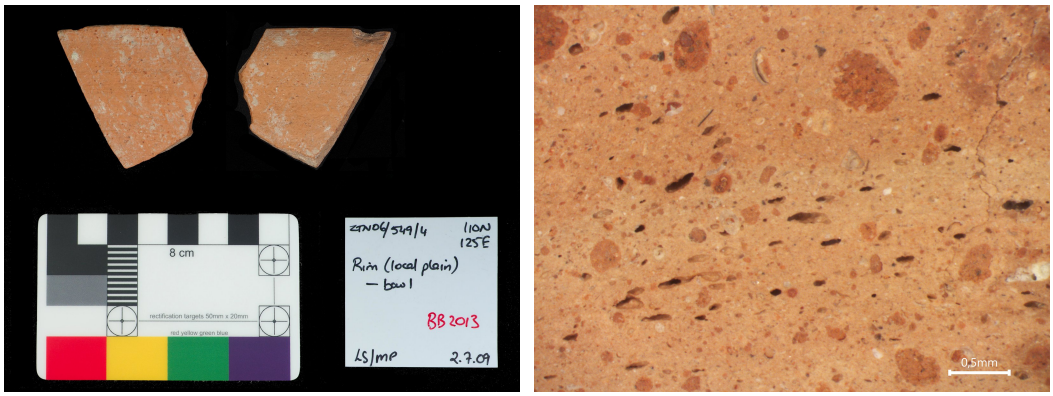
Internal surface	External surface	Core	Margins
7.5YR 7/4 pink	5YR 7/6 reddish yellow	5YR 5/4 reddish brown	2.5YR 6/6 light Red

Table A.117: Munsell colours values

Macro	OM	PLM	HCA
Anastasi F1 with black to brown inclusions (orange matrix)	D2?	-	-

Table A.118: Classifications of the sherd across this study. Numbering is independent in different methods.

Sample 60 (ZTN06/549/4)



(a) (b)

Figure A.119: (a) Photograph: interior; exterior (b) Microphotograph: ground sample

Description: Bowl, studied by Bechtold (2017). Unclear comparative material from the publication. Rim is pointy. Parallel striations on surfaces (wet wiped? smoothened?) are visible from the surface finish, indicating most likely a wet finish. Diameter: 18cm, Thickness: 6mm.

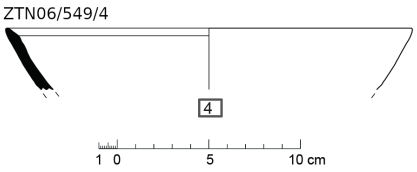


Figure A.120: Reconstructed vessel rim

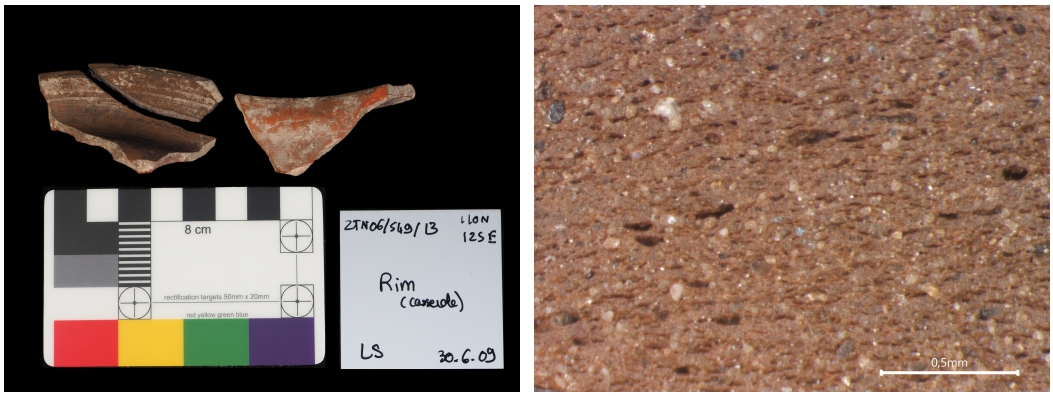
Surfaces	Core colour	Margins
2.5YR 7/6 Light red	7.5 YR 7/4 pink	2.5YR 6/8 Light red

Table A.119: Munsell colours values

Macro	OM	PLM	HCA
Anastasi F1 with orange-brown rounded inclusions,some white inclusions	D3	2.1	2

Table A.120: Classifications of the sherd across this study. Numbering is independent in different methods.

Sample 61 (ZTN06/549/13)



(a) (b)

Figure A.121: (a) Photograph: interior; exterior (b) Microphotograph: ground sample

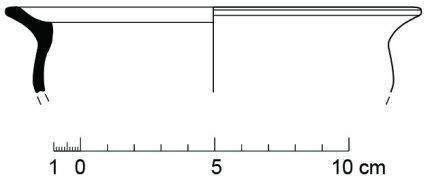


Figure A.122: Reconstructed vessel from Bechtold (2017)

Description: Olla/Pot, two joining fragments studied by Bechtold (2017: 133) who cites Quercia (2002) B5, Sagona (2015b) 1:115:3 and Anastasi (2012) 5.41 as comparative material. Shapes from Anastasi (2019) C3 can also be cited, with the offset for a lid. Darker patches particularly on the outer surface could be from use as a cooking vessel. Parallel and regular striations are visible, very thin (razed?). A deep groove is visible on the outer surface on the everted part of the rim. Outer diameter: 18cm and thickness: 3.5mm.

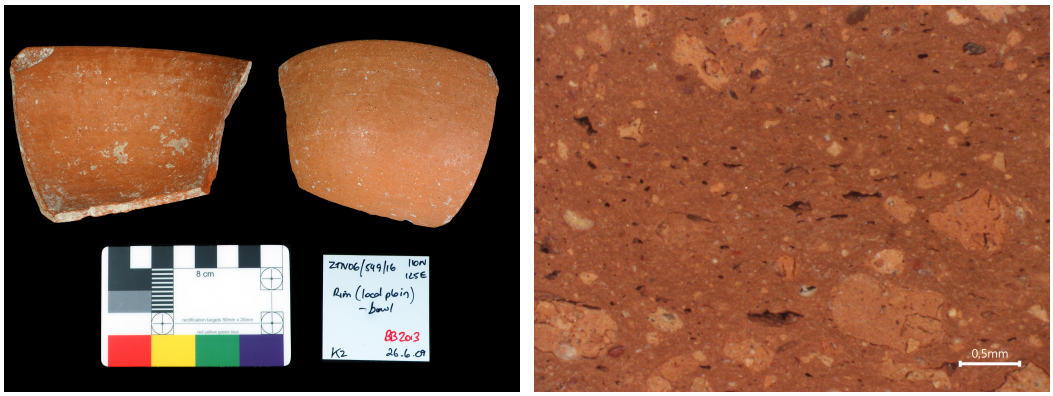
Internal surface	External surface	Core colour (heterogeneous)
2.5YR 5/6 Red	2.5YR 4/6 Red	2.5 YR 5/8

Table A.121: Munsell colours values

Macro	OM	PLM	HCA
Anastasi F4 (fine)	A	7	3

Table A.122: Classifications of the sherd across this study. Numbering is independent in different methods.

Sample 62 (ZTN06/549/16)



(a) (b)

Figure A.123: (a) Photograph: interior; exterior (b) Microphotograph: ground sample

Description: Bowl, studied by Bechtold (2017) who cites Quercia (2011) 2.3, slightly earlier forms. Globular body and pointy rim. Surfaces are smoothed, some surface finish lines are visible but no inclusions are visible on the surfaces. Outer diameter: 15cmm and thickness: 6mm.

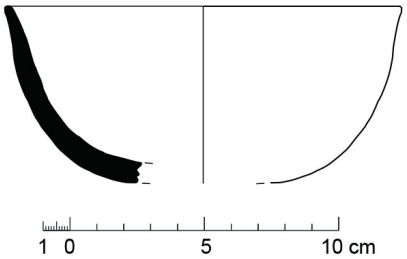


Figure A.124: Reconstructed vessel from Bechtold (2017)

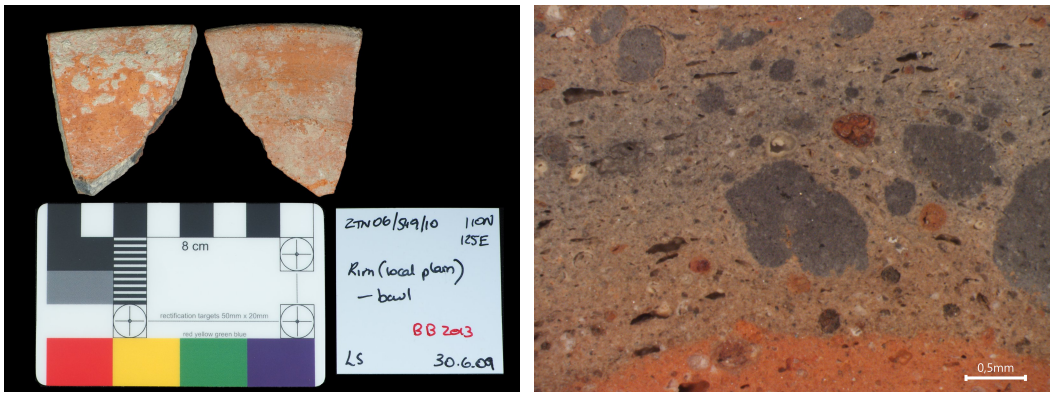
Internal surface	External surface	Core
2.5YR 6/6 light red	2.5YR 5/8 red	2.5YR 4/8 red

Table A.123: Munsell colours values

Macro	OM	PLM	HCA
Anastasi F1 with predominantly white inclusions	B?	4	2

Table A.124: Classifications of the sherd across this study. Numbering is independent in different methods.

ZTN06/549/10 (sample 63)



(a) (b)

Figure A.125: (a) Photograph: interior; exterior (b) Microphotograph: ground sample

Description:

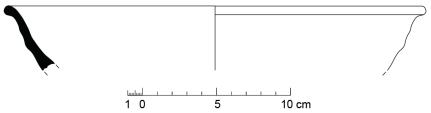


Figure A.126: Reconstructed vessel from Bechtold (2017)

Bowl, studied by Bechtold (2017: 133) with comparative given for all bowls Quercia (2011) 2.7, shapes from 2nd-1st centuries BCE, and Anastasi (2019) 3.24-25. Outer surface is ribbed. Strong colour difference between surfaces and core, probably due to firing conditions. Striations on surfaces visible. Outer diameter: 20cm and max thickness: 6.5mm

Internal surface	External surface	Core	Margins
2.5YR 6/8 Light Red	2.5 YR 6/6 light red	Gley 4/	7.5YR 5/4 brown

Table A.125: Munsell colours values

Macro	OM	PLM	HCA
Anastasi F1 with black to brown inclusions	D2	-	-

Table A.126: Classifications of the sherd across this study. Numbering is independent in different methods.

Sample 64 (ZTN06/2107/6)



(a) (b)

Figure A.127: (a) Photograph: interior; exterior (b) Microphotograph: ground sample

Description: Rim of a bowl, shape close to Quercia (2011) 2.8 according to Bechtold (2017: 135) but also close to Anastasi (2019) D6 and D8 shapes with everted walls. Surfaces are whitened irregularly, few surface inclusions visible (most are covered creating irregular surfaces). Striations, not fully parallel or regular, are visible on both surfaces.. On outer surface, striations perpendicular to the rills can be noted but it is unclear when those were performed (post-deposition?). Outer diameter: 18cm and max thickness: 6.5mm.

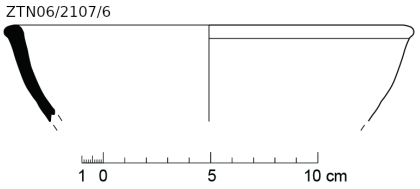


Figure A.128: Reconstructed vessel from Bechtold (2017)

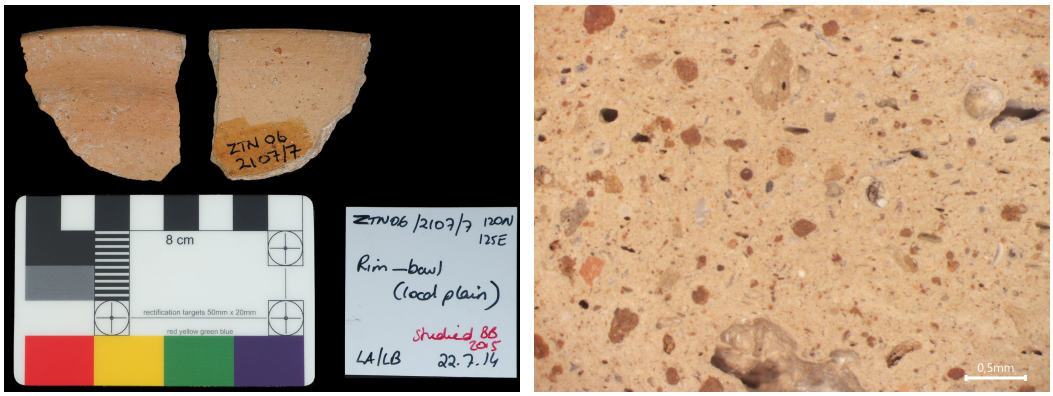
Internal surface	External surface	Core
2.5YR 6/6 - 2.5Y 8/2 pale brown	2.5 YR 6/6 light red	2.5YR 5/8 red

Table A.127: Munsell colours values, heterogeneous colours

Macro	OM	PLM	HCA
Anastasi F1 with predominantly white inclusions (large)	F?	1.3	1

Table A.128: Classifications of the sherd across this study. Numbering is independent in different methods.

ZTN06/2107/7 (sample 65)



(a) (b)

Figure A.129: (a) Photograph: interior; exterior (b) Microphotograph: ground sample

Description: Rim of bowl, shape close to Quercia (2011) 2.8 according to Bechtold (2017: 135) and Anastasi (2019) D8 shapes with everted walls and slightly flaring rim. Striations are visible, not fully parallel. On the outer surface, other marks, not parallel to the rim, are also visible (possibly wet-wiped?). No surface inclusions visible. Outer diameter: 17cm and max thickness: 6.4mm.

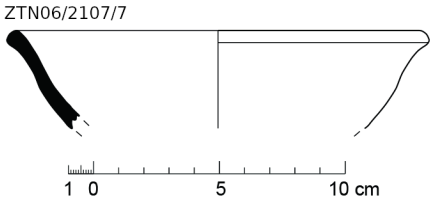


Figure A.130: Reconstructed vessel from Bechtold (2017)

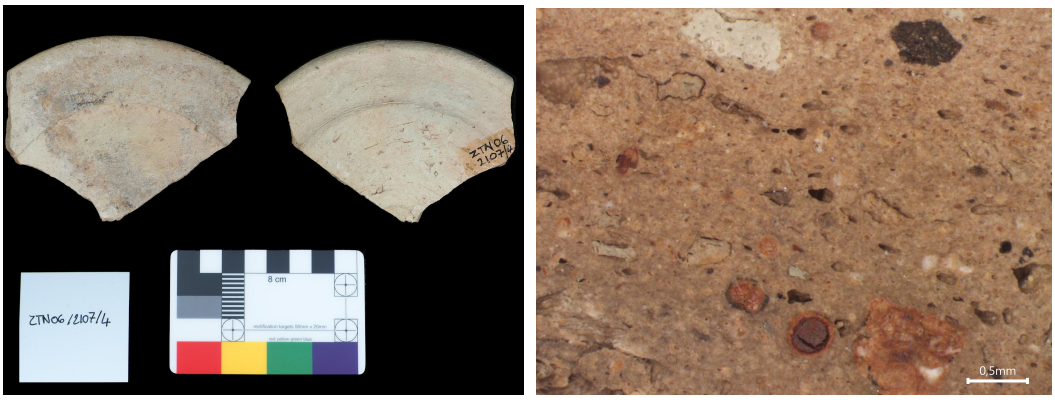
Internal surface	External surface	Core
7.5YR 7/4 pink	7.5YR 7/6 reddish yellow	7.5YR 6/4 Light brown

Table A.129: Munsell colours values

Macro	OM	PLM	HCA
Anastasi F1 with orange-brown rounded inclusions	D3?	3	1

Table A.130: Classifications of the sherd across this study. Numbering is independent in different methods.

Sample 66 (ZTN06/2107/4)



(a) (b)

Figure A.131: (a) Photograph: interior; exterior (b) Microphotograph: ground sample

Description: Profile ofa plate. Bechtold (2017: 135) cites Quercia (2011) 1.6 for comparative shapes and Sagona (2015b) 1:93:7, 1:97:6 in Tas-Silġ with 1st century BCE dates. Surfaces are whitened, or slipped but this was not revealed through analysis, with a contrast in colour between the surfaces and the fabric, some finish striations visible on outer surfaces. Rim on the outer part is irregular and the base is irregular with marks (string marks?). Outer diameter: 17cm and thickness: 5.5-7mm.

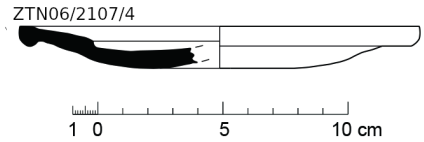


Figure A.132: Reconstructed vessel from Bechtold (2017)

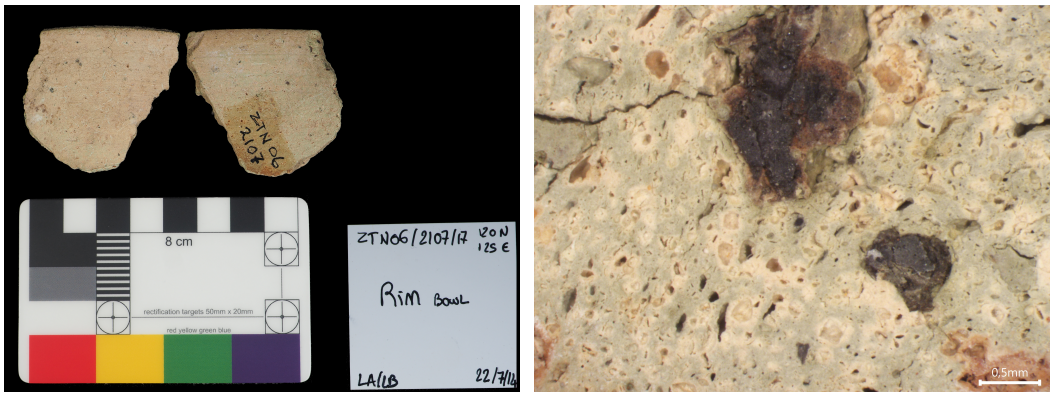
Surfaces	Core colour	Margins
10YR 8/2 very pale brown	10YR 5/3 brown	5YR 7/4 pink

Table A.131: Munsell colours values

Macro	OM	PLM	HCA
Anastasi F1 with predominantly white inclusions (large)	?	1.1	conflicting classification

Table A.132: Classifications of the sherd across this study. Numbering is independent in different methods.

Sample 67 (ZTN06/2107/17)



(a) (b)

Figure A.133: (a) Photograph: interior; exterior (b) Microphotograph: ground sample

Description: Bowl, shape close to D6 in Anastasi (2019). The sherd was extracted as special find in 2021. Straight wall. The greenish tint suggests a sherd over-fired. Material is brittle and breaks easily; breaks can be seen in the microphotograph Figure A.133b. Outer diameter: 20 cm and thickness: 4-6mm

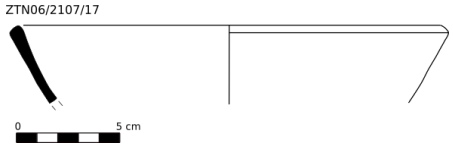


Figure A.134: Reconstructed vessel rim

Internal surface	External surface	Core
10YR 8/3 very pale brown (rim)- 5Y 8/2 pale yellow	10YR 8/2 Very pale brown	5Y 7/2 light gray with some pink areas

Table A.133: Munsell colours values

Macro	OM	PLM	HCA
Anastasi F1 with white matrix	D?	1.1	Removed because strong outlier

Table A.134: Classifications of the sherd across this study. Numbering is independent in different methods.

Sample 68 (ZTN06/2107/9)



(a) (b)

Figure A.135: (a) Photograph: interior; exterior (b) Microphotograph: ground sample

Description: Bowl, carinated (Bechtold 2017: 135). No comparative material given in publication. Carinated bowls are found in Anastasi (2019) D.11, D12. The everted rim is similar to (Quercia 2011) 2.7, but not the carination. Smooth surface and parallel and regular striations (trimming/shaving?). Rim is too small to estimate diameter. Thickness: 5.1mm.

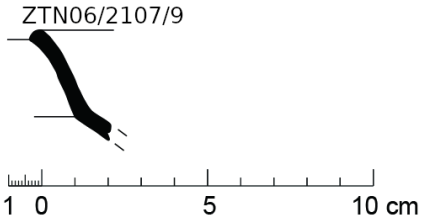


Figure A.136: Reconstructed vessel from Bechtold (2017)

Internal surface	External surface	Core
2.5YR 4/4 Reddish Brown	2.5YR 4/3 Reddish brown (rim), 2.5YR 5/8 red	2.5YR 5/8 Red

Table A.135: Munsell colours values

Macro	OM	PLM	HCA
Anastasi F4	A	7	3

Table A.136: Classifications of the sherd across this study. Numbering is independent in different methods.

Sample 69 (ZTN06/549/6)



(a) (b)

Figure A.137: (a) Photograph: interior; exterior (b) Microphotograph: ground sample

Description: Bowl or basin, studied by Bechtold (2017). No comparative material given in publication. Surfaces are whitened althought they were first thought to be slipped. Visible striations on surfaces, mostly parallel. On inner part, surface is also light-reflective. Inner diameter: 15cm; max thickness: 9mm.

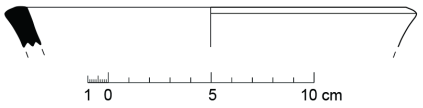


Figure A.138: Reconstructed vessel from Bechtold (2017)

Internal surface	External surface	Core	Margins
5YR 8/3 Pink	10YR 8/2 pale brown	2.5Y 5/1 Grey	2.5YR 5/8 red

Table A.137: Munsell colours values

Macro	OM	PLM	HCA
Anastasi F1 with predominantly white inclusions	?	1.1	Conflicting classification

Table A.138: Classifications of the sherd across this study. Numbering is independent in different methods.

Sample 70 (TSG96/2051/61)



(a) (b)

Figure A.139: (a) Photograph: interior; exterior (b) Microphotograph: ground sample

Description: Olla, shape close to Anastasi (2019) C3 with everted rim and offset for a lid. Fine compared to the other cooking vessels in the sample set. Smooth inner surface (burnished?), striations visible from surface finish. Outer surface has surface inclusions visible. Outer diameter: 21cm and thickness: 2.4-10.3mm.

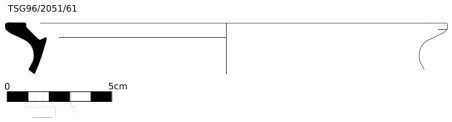


Figure A.140: Reconstructed vessel rim

Internal surface	External surface	Core
2.5YR 5/6 red	2.5YR 4/4 reddish brown	2.5YR 5/9 red

Table A.139: Munsell colours values

Macro	OM	PLM	HCA
Anastasi F4?	B?	5	2

Table A.140: Classifications of the sherd across this study. Numbering is independent in different methods.

Appendix B

Samples and SU lists

B.1 Results table and catalogue data (Digital Appendix)

B.2 Descriptions of diagnostic sherds for sampling (Digital Appendix)

B.3 SU summary

B.3.1 Tas-Silġ

Sagona's sheet general data			
Bag	Ware	Count report	Recounted?
1	Crisp Ware	57	5 missing probably
1	Crisp Ware coarse	6	SF, coarse difficult
1	Bricky Red Ware	1	to identify
1	Imported	1	Import not found.
1	Crisp Ware	61	
1	Crisp Ware, poorly fired	3	
1	Crisp Ware, coarse	6	
1	Coarse Ware [Punic; hand-made]	2	
1	Bricky Red Ware	9	
1	Dross	1	
2	Crisp Ware	7	Matches
2	Crisp Ware	9	
2	Dross	4	2 identified
3	Crisp Ware	189	Yes
3	Crisp Ware, painted	1	Matches

3	Crisp Ware, poorly fired	5	Matches
3	Bricky Red Ware	11	Missing 1
3	Pink Buff Ware, imported	1	Matches
3	Crisp Ware	181	
3	Crisp Ware, poorly fired	5	
3	Bricky Red Ware	32	
3	Coarse Ware [Punic; hand-made]	13	
3	Micaceous Ware, imported	1	
3	Dross	5	
4	Borg in-Nadur	1	Not identified
4	Crisp Ware	11	3 missing
4	Crisp Ware	12	
4	Crisp Ware, coarse	5	
4	Bricky Red Ware	7	
6	Coarse Ware [Punic; hand-made]	1	Hard to identify
6	Crisp Ware	76	Not all found
6	Crisp Ware, gritty variant	1	
6	Crisp Ware, poorly fired	34	
6	Bricky Red Ware	4	
6	Crisp Ware	89	
6	Crisp Ware, poorly fired	37	
6	Coarse Ware [Punic; hand-made]	55	
6	Bricky Red Ware	20	
6	Dross	12	
7	Anastasi Fabric 7		10
7	Anastasi Fabric 1		109
7	Anastasi Fabric 5 (or 4?)		13
7	Anastasi Fabric 7		8
7	Anastasi Fabric 5 (or 4?)		21
7	Import?		2
7	Anastasi Fabric 1		125
5	Anastasi Fabric 1		130
5	Anastasi Fabric 5 (or 4?)		6
5	Anastasi Fabric 7		2
5	Anastasi Fabric 1		80
5	Anastasi Fabric 5 (or 4?)		17
5	Anastasi Fabric 7		6
	Assumed total diagnostic	677	
	Assumed Total	1505	

Table B.1: Assessment of SU 352 bags against Sagona (2015b) and preliminary unpublished counts by Sagona (2005). Bags 7 and 5 had not been quantified for the available preliminary report that was consulted. They were therefore quantified according to macroscopic classification by Anastasi (2019). The pink cells are the bags are the diagnostic bags. These quantifications do not account for sherds which might join.

Macroscopic description	Count
Unclassified	415
Crisp Ware/ Anastasi F1 with orange brown, rounded inclusions, some white inclusions	51
Crisp Ware/ Anastasi F1 with black to brown inclusions	68
Crisp Ware/ Anastasi F1 with white matrix	29
Crisp Ware/ Anastasi F1 with predominantly white inclusions	44
Coarse Fabric - Anastasi Fabric 7? Coarser version of Crisp Ware?	22
Coarse Fabric - Anastasi Fabric 7? Coarser version of Crisp Ware?	48
Total	677

Table B.2: Macroscopic counts for diagnostic sherds for TSG96/352 used for sampling, used for Figure 5.3

Bag	Ware	Count report
1	Anastasi Fabric 1/ Crisp Ware	103
1	Anastasi Fabric 1/ Crisp Ware	73
1	Anastasi Fabric 7	2
1	Anastasi Fabric 5/ Bricky Red Ware	6
2	Anastasi Fabric 1/ Crisp Ware	76
2	Anastasi Fabric 5/ Bricky Red Ware	1
2	Anastasi Fabric 7	3
2	Anastasi Fabric 1/ Crisp Ware	96
2	Anastasi Fabric 7	2
2	Anastasi Fabric 5/ Bricky Red Ware	13
3	Anastasi Fabric 1/ Crisp Ware	94
3	Anastasi Fabric 5/ Bricky Red Ware	4
3	Anastasi Fabric 7	2
3	Anastasi Fabric 1/ Crisp Ware	135
3	Anastasi Fabric 7	7
3	Anastasi Fabric 5/ Bricky Red Ware	2
3	? Imported	2
4	Anastasi Fabric 1/ Crisp Ware	34
4	Anastasi Fabric 7	1
4	Anastasi Fabric 1/ Crisp Ware	28
4	Anastasi Fabric 7	5
4	Anastasi Fabric 5/ Bricky Red Ware	13
4	? Imported	1
	Assumed total diagnostic	318
	Assumed Total	703

Table B.3: Assessment of SU 2051 bags which were not counted in Sagona (2005). They were therefore quantified according to macroscopic classification by Anastasi (2019). The pink cells are the diagnostic bags. These quantifications do not account for sherds which might join.

Macroscopic description	Count
Crisp Ware/ Anastasi F1 with orange brown, rounded inclusions, some white inclusions	71
Crisp Ware/ Anastasi F1 with black to brown inclusions	29
Crisp Ware/ Anastasi F1 with white matrix	17
Crisp Ware/ Anastasi F1 with predominantly white inclusions	63
Bricky red ware/ Anastasi F5	5
Coarse Fabric - Anastasi Fabric 7? Coarser version of Crisp Ware?	6
Not identified	127
Total	318

Table B.4: Macroscopic counts for diagnostic sherds for TSG96/2051 used for sampling, used for Figure 5.3

B.3.2 Żejtun

Anastasi Fabric 1 / Crisp Ware	Diagnostic	16
	Non Diagnostic	22
Anastasi Fabric 4/ Late Red Bricky Ware	Diagnostic	2
	Non Diagnostic	7
Anastasi Fabric 5 / Bricky Red Ware	Non Diagnostic	7
Anastasi Fabric 7	Diagnostic	3
	Non Diagnostic	22
Imported?	Non Diagnostic	3
Unclassified	Non Diagnostic	6
	Total Diagnostic	21
	Total	88

Table B.5: Summary SU for ZTN06/549

Anastasi Fabric 1 / Crisp Ware	Diagnostic	12
	Non Diagnostic	10
Anastasi Fabric 4	Diagnostic	2
	Non Diagnostic	1
Anastasi Fabric 5	Diangostic	1
	Non Diagnostic	5
Anastasi Fabric 7	Diagnostic	3
	Non Diagnostic	27
	Total Diagnostic	18
	Total	61

Table B.6: Summary SU for ZTN06/2107

Macroscopic description	Count
Unclassified	2
Crisp Ware/ Anastasi F1 with orange brown, rounded inclusions, some white inclusions	9
Crisp Ware/ Anastasi F1 with black to brown inclusions	6
Crisp Ware/ Anastasi F1 with white matrix	2
Crisp Ware/ Anastasi F1 with predominantly white inclusions	9
Bricky red ware/ Anastasi F5	5
Coarse Fabric - Anastasi Fabric 7? Coarser version of Crisp Ware?	6
Total	39

Table B.7: Sherds description and macroscopic classification for diagnostic sherds for the Żejtun assemblages (combined)

B.4 Geological samples

Sample name	Location	Island	Type of rm	Reason to analyse	E	N	Coordinate system	El.	Procedure	Sampling date	Initials
DLA.A1	Delimara (Kalanka Bay)	Malta	Terra Rossa? Terra fusca?	Investigate red soils	460198	3964575	UTM84	-	Surface collection	03/03/21	ERT, JB, MV
FC.A1	Fort Chambray	Gozo	Uncertain	Re-analysis of material	436248	3986608	ED50?	42	MaltaPot collection		CB, JB
GH.A1	Gelmus Hill	Gozo	Blue Clay	Sample diversity	431215	3989738	ED50	85	Vella and Richard-Trémeau (2021a)	26/08/20	ERT, JB, MV, AA
GH.B1	Gelmus Hill	Gozo	Blue Clay	Re-analysis of material	431236	3989619	ED50?	¡100	Asciak (2019: 54)	2018	GA
GH.C1	Gelmus Hill	Gozo	Blue Clay	Re-analysis of material	431171	3989645	ED50?	100	Asciak (2019: 54)	2018	GA
GNB.A1	Ġnejna Bay	Malta	Blue Clay	GT and GNB case study	-	-	-	-	-	21/10/00	NCV, KCB, CS
GNB.B1	Ġnejna Bay	Malta	Blue Clay	GT and GNB case study	-	-	-	-	-	21/10/00	NCV, KCB, CS
GNB.D1	Ġnejna Bay	Malta	Blue Clay	GT and GNB case study	-	-	-	-	-	21/10/00	NCV, KCB, CS

Sample name	Location	Island	Type of rm	Reason to analyse	E	N	Coordinate system	El.	Procedure	Sampling date	Initials
GNB.E1	Ġnejna Bay	Malta	Blue Clay	GT and GNB case study	-	-	-	-	-	21/10/00	NCV, KCB, CS
GNB.F1	Ġnejna Bay	Malta	Blue Clay	GT and GNB case study	-	-	-	-	-	21/10/00	NCV, KCB, CS
GT.A1	Għajn Tuffieħa	Malta	Blue Clay	GT and GNB case study	441101	3976504	ED50	31	Vella and Richard-Trémeau (2021a)	28/08/20	ERT, JB, LX
GT.B1	Għajn Tuffieħa	Malta	Blue Clay	GT and GNB case study	440860	3976280	ED50	28	Vella and Richard-Trémeau (2021a)	28/08/20	ERT, JB, LX
LP.A1	Ta'Lippija	Malta	Terra Rossa	Investigate red soils	441335.38	3975967.22	UTM84	81	Opportunistic collection	02/06/2022	JB
LP.E1	Ta'Lippija	Malta	Terra Rossa	Investigate red soils	441246.91	3975958.6	UTM84	88	Opportunistic collection	02/06/2022	JB
MG.A1	Imġiebaħ	Malta	Uncertain	Location diversity	444153.96	3980633.39	UTM84	-	Opportunistic collection	18/10/20	JB
MG.B1	Imġiebaħ	Malta	Uncertain	Location diversity	444138.21	3980667.21	UTM84	-	Opportunistic collection	18/10/20	JB
MX.A1	Marsaxlokk	Malta	Globigerina marl	Investigate marls	459332	3966126	UTM84	3	Surface colletction with trower	03/03/21	ERT, JB, MV

Sample name	Location	Island	Type of rm	Reason to analyse	E	N	Coordinate system	El.	Procedure	Sampling date	Initials
MX.D1	Marsaxlokk	Malta	Globigerina marl	Investigate marls	459339	3966117	UTM84	0	Surface colletction with trower	14/05/21	LG, JB, ERT
NF.A1	In-Nuffara	Gozo	Blue Clay	Sample diversity	434666	3988817	ED50	124	Vella and Richard-Trémeau (2021a)	26/08/20	ERT, JB, MV, AA
NF.B1	In-Nuffara	Gozo	Blue Clay	Sample diversity	434617	3988788	ED50	115	Vella and Richard-Trémeau (2021a)	26/08/20	ERT, JB, MV, AA
QL.A1	Il-Qolla	Malta	Blue Clay	Sample diversity	444586	3973175	ED50	189	Vella and Richard-Trémeau (2021a)	28/08/20	ERT, JB, LX
QL.B1	Il-Qolla	Malta	Blue Clay	Sample diversity	444631	3973112	ED50	187	Vella and Richard-Trémeau (2021a)	28/08/20	ERT, JB, LX
QR.A1	Il-Qarraba	Malta	Blue Clay	GT and GNB case study	440664.45	3976184.02	UTM84	-	Opportunistic collection	02/10/21	ERT
QR.C1	Il-Qarraba	Malta	Blue Clay	Rich in iron nodule	440659.4	3976184.05	UTM84	-	Opportunistic collection	02/10/21	ERT

Sample name	Location	Island	Type of rm	Reason to analyse	E	N	Coordinate system	El.	Procedure	Sampling date	Initials
QR.D1	Il-Qarraba	Malta	Blue Clay	Rich in posidonia	440722.1	3976183.63	UTM84	-	Opportunistic collection	02/10/21	ERT
RIH.A1	Ras Il-Ħamrija	Malta	Uncertain	Close to sites of interest	-	-	-	-	-	12/11/00	NCV, KCB, CS
RIH.B1	Ras Il-Ħamrija	Malta	Uncertain	Close to sites of interest	-	-	-	-	-	12/11/00	NCV, KCB, CS
RIH.D1	Ras Il-Ħamrija	Malta	Uncertain	Close to sites of interest	-	-	-	-	-	12/11/00	NCV, KCB, CS
RML.B1	Ramla Bay	Gozo	Blue Clay	Re-analysis of material	435786	3991224	ED50	0	MaltaPot	-	CB, JB
RML.D1	Ramla Bay	Gozo	Blue Clay	Re-analysis of material	435174	3991328	ED50	0	MaltaPot	-	CB, JB
RML.E1	Ramla Bay	Gozo	Blue Clay	Washed clay after storm	435375.57	3990992.55	UTM84		Opportunistic collection	15/11/21	ERT
SLF.A1	San Leonardo area	Malta	Uncertain	Close to sites of interest	-	-	-	-	-	21/10/00	NCV, KCB, CS
SLF.B1	San Leonardo area	Malta	Uncertain	Close to sites of interest	-		-	-	-	21/10/00	NCV, KCB, CS

Sample name	Location	Island	Type of rm	Reason to analyse	E	N	Coordinate system	El.	Procedure	Sampling date	Initials
TL.A1	Ta' Leveċa	Gozo	Blue Clay	Sample diversity	430844	3991198	-	140	Vella and Richard-Trémeau (2021a)	26/08/20	ERT, JB, MV, AA
TL.B1	Ta' Leveċa	Gozo	Blue Clay	Sample diversity	430876	3991186	-	134	Vella and Richard-Trémeau (2021a)	26/08/20	ERT, JB, MV, AA
WSP.B1	Wied tal-Isperanza	Malta	Uncertain	Fine pool of clay	-	-	-	-	Opportunistic	-	JB

Table B.8: Geological samples analysed in this dissertation. N: Northing; E: Easting; El: Elevation; rm: Raw materials; -: missing information.

Appendix C

Macroscopy and Fabric analysis tables and supplement

C.1 Microscopy

The microscopic classification was carried out according to the methodology described in section 4.3. The preliminary descriptions of the samples are presented here. The samples which had been uncertainly classified are also presented. Note that these comments were made before PLM and XRF analysis.

G	Macroscopic group	Relationship?
A	\Anastasi F4/Sagona Late Bricky Red Ware	Similar raw material?
B	Anastasi F5/Sagona Red Bricky Ware	
C	Anastasi F1/Crisp Ware with white to greyish matrix	Closely related in raw material
D	Anastasi F1/Crisp Ware with red inclusions or orange inclusions, some white inclusions and Anastasi F1 Crisp Ware with black/brown inclusions	
E	Anastasi F1/Crisp Ware with white inclusions	
F?	Anastasi F1/Crisp Ware with white inclusions	

Table C.1: Table of equivalence between the microscopic groups, the macroscopic groups and the hypothesis, before analysis, of their relationships

C.1.1 Group A

S		68	61
M		Orange	Dark brown
Inclusions	Very fine to medium black/brown rounded to sub-rounded	Frequent	Frequent
	Medium white (varied shape)	Few	Few
	Micro-fossil remains	One large 0.77mm	Rare
	Medium to coarse orange rounded	Very rare	
	Very fine angular grey / transparent	Dominant at higher magnification	Dominant at higher magnification
	Very fine white (mostly \textless{}0.05)	Common at higher magnification	Common at higher magnification
V		Macro to meso voids elongated (not abundant)	Macro to meso voids elongated (not abundant)

Table C.2: Group A samples

C.1.2 Group B

Group B had been classified into two subgroups which were dropped early in the analysis (and therefore not reported). This means that the tables contain different inclusions.

S		5	34	43	53
M		Brownish orange, darker area close to wall (use)	Brown core and brownish orange margins	Dark brown	Light brown margins and dark brown core
Inclusions	Dissociation	Rare to few dissociated fine inclusions (micro-remains?)			
	Light pink to whitish	Frequent < 1.6mm	Few < 1.35mm	Few < 0.87mm	Frequent < 0.37mm
	Light pink with no inclusions inside	Common < 0.2mm	Common < 0.3mm		Common < 0.4mm
	Irregular brown	Rare < 0.7mm, mostly < 0.22mm	Rare < 0.33mm	Few < 0.97mm	Rare < 0.51mm
	White angular	Common < 0.63mm	Common < 0.7mm	Common < 0.75mm	Few < 0.52 mm
	Large grey		One 0.5mm		
	Dark red /brown	Common < 0.25mm		Rare / Few 0.09mm	Rare / Few 0.4mm
	Fine white and grey including Angular transparent reflective inclusion	Common			
	Others		Smaller dark grey inclusions < 0.1mm		Angular transparent reflective inclusions, large inclusions of varied colours
V		Meso channels and meso vesicles	Macro channels	Macro and meso channels and vesiclefs	Meso and macro channels

Table C.3: Table with descriptions of individual samples of Group B (Part 1). S: Samples; M: Matrix: v: Voids

S		39	62	46	18	70
M		Orange	light brown	brownish orange	light brown	Brownish orange
Inclusions	Dissociation	Rare to few dissociated fine inclusions (micro-remains?)				
	Light pink to whitish	Common < 1.2mm	Hard to distinguish dominant, angular < 0.94mm	Frequent < 0.63mm, angular but irregularly shaped	Dominant in coarse and fine fraction < 0.9mm	
	Light pink with no inclusions inside					Common (< 1.67mm)
	Irregular brown	Few < 0.33mm		Rounded, rare < 0.4mm	Few < 0.3	
	White angular					
	Large grey	One 0.79mm				
	Dark red /brown	Rare / few	Rare		Few red (< 0.4mm) and rare black (< 0.06mm)	Few (< 0.23mm
	Fine white and grey including Angular transparent reflective inclusion	Common				
	Others	Large (2.44mm) rounded brown inclusions (same colour as matrix)		Numerous black round inclusions $<$ 0.33mm), inclusions same colour than the matrix	Rare rounded white dissociated inclusions;	
V		Meso and macro channels	meso channels and vughs	Meso vesicles	Macro voids and meso channels	Few meso channels, mostly fine elongated voids / cracks

Table C.4: Table with descriptions of individual samples of Group B (Part 2). S: Samples; M: Matrix: v: Voids

S		36	32	33
M		Brownish orange to brown	Brownish orange to brown	Orange
	Dissociation	Rare to few dissociated fine inclusions		
Inclusions	Irregular light pink to whitish	Frequent$<$ 1.06mm	Frequent (?) $<$ 0.83mm	Common < 0.96mm
	Irregular brown	One large	Few < 0.71mm angular black	Light brown
	White angular or large grey	Common < 1.23mm	Rare (not as clear-cut in terms of colour)	Few/Rare < 1.05mm
	Homogeneous dark red /brown	Few /Common < 0.12mm	Rare (more black ones) < 0.55mm	Rare < 0.65mm
	white and grey < 0.15mm	Common (?)	Common (?)	Larger common inclusions < 0.23mm
	Green (angular)	Few < 0.5mm	Rare	Common (?)
	Others	Two linear white inclusions	Small black rounded inclusions (?) visible at x50, in general darker inclusions	Few angular
V		Macro vugh in rim and meso vesicles	Macro vughs and meso channels and vesicles	Rounded white inclusions and larger red inclusions

Table C.5: Table with descriptions of individual samples of Group B (Part 3). S: Samples; M: Matrix: v: Voids

Uncertain classifications group B

Sample 39 is not classified certainly due to the large inclusions close to the margin of the rim. These are rounded inclusions sizing up to 2.44mm of the same colour as the matrix but homogeneous in composition, similar to the rare ones observed in Sample 43. The sherd was difficult to sample because of its shape: breaking off a sub-sample perpendicular to the rim was nearly impossible because of the everted rim.

Sample 13 was not classified certainly due to the colour of the matrix, which is lighter than the others. Macroscopically, however, the texture of the matrix is very similar to the rest of the group and Group A. The cream-white angular inclusions are similar to the ones in sample 5. This sample does not have angular pinkish inclusions. A few white inclusions and micro-fossils (including dissociated) are visible and a few black rounded inclusions.

Sample 18 differs slightly from the group because of the higher abundance of cream-coloured inclusions than any other samples. The cream-colour inclusions are similar to those from sample 13, which is the main inclusion in this particular sherd. Differences with the group include.

- Only a few angular white inclusions (< 0.6mm), lacks the numerous white and grey inclusions
- foraminifera and other micro-remains are more prevalent than in the other samples.
- The sample is richer in fine inclusions

The primary type of inclusion of sample 18 was tested using a Mohs kit, and the point of hardness 3 scratched the inclusion while 2 did not. This supports the hypothesis that these inclusions are calcite or have a similar hardness.

C.1.3 Group C

S		23	24	40	52
M		Greenish white	Cream	Greenish white	Cream
Inclusions	Dissociation ?	Yes, Including micro remains			
	Larger white inclusions	Rare < 0.9mm	Rare < 0.9mm	Rare	
	Rounded red/brown inclusions	< 0.07mm	Few larger, < 0.2mm	Few < 0.18mm	Few < 0.18mm
	brown / red inclusions				
	Others			Sea urchin spine? one angular beown inclusion	
	V	Meso elongated close to wall (sub parallel) and close to the rim (not parallel), vesicles at higher magnfication and meso to macro vughs close to rim	One macro vugh, mostly meso channels	Mostly meso channels sub parallel to the wall except in the rim part	Meso channels

Table C.6: Table with descriptions of individual samples of Group C (Part 1). S: Samples; M: Matrix: v: Voids

S		45	12	44	27	67
M		Cream	Greenish white	Yellowish white with red spots	Yellowish white	Greenish white to green
Inclusions	Dissociation ?	Yes, Including micro remains				
	Larger white inclusions		Grey equant sub-angular, Few< 0.3	Rare, one large (1.3mm)		
	Rounded red/brown inclusions	Rare/few $< 0.9mm$	Rare/few $< 0.12mm$	Few < 0.12mm	Rounded and angular < 0.17mm	
	brown / red inclusions		Irregularly shaped rare < 0.63mm	Irregularly shaped rare / Few $< 1.3m$m	linear rare < 1.4mm	
			Sea urchin spine ?, Rare angular light pink inclusion (< 0.5mm)			
V	Others	Some macro voids seen in freh break< 1.73, all types of meso voids, numerous vesicles compared to other samples	Elongated voids,< 0.43mm and vesicles at high magnification	Mostly meso channels, but a few meso vughs and frequent vesicles close to the rim	Mostly meso channels, Large cracks from sample preparation visible	

Table C.7: Table with descriptions of individual samples of Group C (Part 2). S: Samples; M: Matrix: v: Voids

Uncertain classifications, group C

- Sample 44: has rare large brown and pink inclusions (claystone?) which are not found in other samples.
- Sample 27 has numerous very small red inclusions and seems to have more oxidation across the sherd

C.1.4 Group D

Uncertain classification, group D

- Sample 6: has a different matrix, very similar in colour and texture Group C.
  - The fabric is brittle
  - The sample has numerous cracks and can be broken easily, however.
  - It is classified in D because of the prevalent dark, irregularly shaped inclusions.
- Sample 48: was set aside because the matrix's colour is different from the other sherds. The sherd, however, shares the characteristics of D1 and D2 with large, dark, irregularly shaped inclusions and the most predominant foraminifera. It, therefore, most likely represents differences in firing conditions.
- Sample 59: was set aside because the black irregular inclusions differed from the rest of the samples.
  - The matrix of this sherd is oxidised, and the inclusions are still grey/black. This differs from D1 and D2 where the colour appears to follow the oxidation of the matrix. There is a possibility that these black inclusions are different from the ones above
  - The sample also has irregularly shaped reddish brown and brown inclusions.
  - rare macro voids are visible, and the predominant voids are meso vughs.
- Sample 25: has a matrix of colour similar to Group C and sample 6.
  - The abundance of black inclusions, mostly rounded, makes it visually stand out. The black inclusions also contain smaller inclusions, but visually, assessing if they are the same type of inclusions as the rest of this subgroup is challenging.
  - The foraminifera content appears similar to the rest of the sherds.
- Sample 65 :
  - The reddish brown inclusions are finer than in all the other samples of D (mostly ranging 0.3-0.4mm), with one large one (1.39mm). They are rather angular.
  - The foraminiferal content is closer to D1 with elliptical and elongated micro-remains.
  - Other inclusions include rare white and grey inclusions.

S		8	10	51	21	26
M		Light orange to light grey	Grey / yellowish grey to pinkish orange	Grey / yellowish grey to pinkish orange	Greyish brown	Grey to pinkish orange
Inclusions	Dissociation	Incommplete	Yes			
	Micro-fossils	Dominant / frequent				
	Irregular reddish brown	Dominant / frequent < 1.27mm	Dominant / frequent < 1.56mm	Dominant / frequent < 1mm	Few < 0.7mm	Common < 0.8mm
	Irregular black		In reduced margins			Frequent (< 1.1mm)
	Irregular black and brown				Very rare < 1.4mm	
	Small rounded to sub-rounded black (same as above?) < 0.2mm	Few	Elongated, few	Few	Few	common
	Transparent / grey angular	Very rare				
	non dissociated white		Very rare < 0.53		Few	Common < 0.4mm
	Others	1 long linear inclusion with microfossils inside (2.77mm) and 1 grey linear inclusions (0.57mm)	1 elongated angular grey inclusion			
V		Meso vughs and vesicles, some channels	Mostly meso elongated voids and meso vughs/ vesicles	Macro and meso elongated voids and vugh. Vesicles at higher magnification	Meso channels and vughs	Meso channels and vughs

Table C.8: Group D1-3 (Part 1) microscopic characteristics

	Sample	58	49	2	38	29
	Matrix colour	Brownish pink to yellow	Grey / yellowish grey to pinkish orange	Yellowish green to pinkish orange	Brownish grey	Brownish grey to orange
Inclusions	Dissociation	Yes				
	Micro-fossils	Dominant / frequent	Dominant / frequent	Dominant / frequent	Dominant / frequent	Frequent
	Irregular reddish brown	Few < 0.65mm	Few < 0.61mm	Few < 0.9mm	Few < 1.1mm	Common but more orange < 0.85mm
	Irregular black	Dominant < 0.98	Dominant < 1.1mm	Dominant < 1.53mm	Dominant < 0.77mm	Frequent (< 1.1mm)
	Irregular black and brown			Rare	Rare < 0.57mm	
	Small rounded to sub-rounded black (could be the same as larger inclusions) < 0.2mm	Common	Few	Common	Common	Few
	Transparent / grey angular			Shiny transparent very rare < 0.15mm		
	Non-dissociated white		Very rare	Rare	Rare/Few	
	Others		Small grey inclusions			Meso channels
	Predominant voids	Meso vesicles in rim and elongated voids parallel to margins	Meso channels	Meso channels and smaller vesicles	Few macro and meso elongated voids	

Table C.9: Group D1-3 (Part 2) microscopic characteristics

S		55	9	17	63	11
M		Light brown	Grey and orange (m)	Grey and light brown(m)	Grey and orange (m)	Light pinkish brown, darker margins (slip?)
Inclusions	Dissociation	Yes	Not fully	Yes		Not fully
	Micro-fossils	Frequent				
	Irregular reddish brown	Rare < 0.73mm	Common in m < 0.87mm	Common	Common? < 1.06mm	Dominant < 1.89mm
	Irregular black	Dominant < 0.9mm	Dominant < 0.63mm	Dominant $<$ 0.88mm	Dominant < 1.28mm	
	Irregular black and brown	Very rare $<$ 0.91mm				
	Rounded to sub-rounded black < 0.2mm	Few	Few ? 0.04mm	x at high magnification	x at high magnification	Rare 0.05mm
	Transparent / grey angular		Very rare $<$ 0.24mm	Rare	Rare	
	Non-dissociated white		Few? angular to sub-rounded < 0.13mm		Few not fully dissociated	Few equant < 0.25mm and elongated 0.45mm
	Others	large white inclusion : contamination?	Equant sub-Angular red inclusions < 0.21mm	Few red patches	Red patches and angular red inclusions	Very rare? Cream coloured inclusions < 2.85mm
V		Meso channels and vughs in the rim	Meso elongated and few vesicles, few macro (vughs and channels)	Meso elongated and vughs in wall	Meso elongated and vesicles	Meso channels (parallel to the wall) and vesicles

Table C.10: Group D1-3 (Part 3) microscopic characteristics. m= margins

S		3	4	14	19	41
M	Matrix colour	Orange	Orange	Pinkish orange	Pinkish orange	Light brown
Inclusions	Dissociation (microfossils)	Well preserved		Some dissociated, frequent microfossils	Well preserved shape, some start of dissociation	Well preserved
	Irregular light brown / orange	Dominant	Dominant < 1.65mm but majority < 1mm	Dominant < 1.16mm	Dominant < 0.65mm	Dominant < 1.1mm
	White	Rare in coarse (< 1.05mm, common in fine	Rare angular < 0.26mm	Rare angular, not dissociated fully < 0.45mm	Rare 0.37mm	Rare < 0.28mm
	Transparent shiny	Rare				
	Black inclusions	Very rare < 0.15mm	Few, equant subrounded < 0.07mm	Rare < 0.11mm	Rare 0.043mm	Rare 0.070mm
	Others	One angular red inclusion (0.4mm)		small red rounded		Red rounded inclusions, High magnification: large number of small inclusions of varied colours (grey, brown, black)
V		Few macro vughs and mostly meso channels	Meso channels and vesicles	Meso channels and vesicles	Meso channels and vughs	Meso channels and vughs

Table C.11: Group D1-3 (Part 3) microscopic characteristics.

S		42	56	60	1
M	Matrix colour	Light pinkish brown	Orange	Light pinkish brown	Light orange pink
Inclusions	Dissociation (microfossils)	Some microfossils dissociated	Microfossils dissociatd	Well preserved micro remains	Carbonates partly dissociated
	Irregular light brown / orange	Dominant < 1.41mm	Harder to see, Frequent to Dominant 0.88mm	Dominant < 1.12mm	Dominant $<$ 2mm, different colours from pink to brown
	White	Rare < 0.56mm	One large (2.75mm) cream	Very rare at high magnification	Common elongated subangular to angular $<$ 0.98mm and in fine fraction
	Transparent shiny	Rare			
	Black inclusions	Rare < 0.12mm	Rare / Few rounded < 0.2mm	Very rare $<$ 0.11mm	Rare 0.1mm
	Others	Red rounded inclusions, High magnification: a large number of small inclusions of varied colours	Red rounded inclusions, High magnification: a large number of small inclusions of varied colours		Greenish white inclusions? Red equant sub-rounded inclusions
V		Meso vughs (rim part)	Meso channels and vesicles	Meso channels	Meso elongated voids

Table C.12: Group D1-3 (Part 3) microscopic characteristics.

C.1.5 Group E

S		15	16	20	31	28
M		Pink to greenish grey?	Reddish orange	Light pink	Orange-pink	Brownish orange and grey
Inclusions	Dissociation	x	x (not fully?)			
	Micro-fossil	Frequent < 1.058mm	x	x	Dominant	x
	Bright white mostly elongated	Frequent	Frequent < 0.79mm	Frequent < 0.88 mm	Few or Common? < 0.5mm	subrounded, dominant (0.4mm and coarser)
	Transcluscent	Few (red patches)	Common	Common (higher mag)		Grey inclusions? varied shape
	Red mostly rounded	Rare < 0.51mm	Common (higher magnification)	Few (angular and patches)		Red patches or rounded inclusions sometimes within microfossils
	brown angular		Rare?		Few at high magnification < 0.43mm	common Angular red, brown and orange inclusions < 0.36mm
	Angular cream	Rare linear inclusions (dark) in margin	Frequent? < 0.86mm			Few < 0.72mm but mostly around 0.3mm
	Others					Two linear grey inclusions 0.23mm
V		meso vughs	Few macro vughs, Meso elongated voids or vughs in the wall and vesicles in rim	Meso elongated in wall and planar + vesicles following flaring rim		A few macro voids (rim part) mostly meso channels

Table C.13: Group E (Part 1) microscopic characteristics, x= present

S		50	7	57	30
M		Orange to greyish brown	Orange (and cream margin)	Grey core, pink inner margins and cream slip	brown core and orange margins
Inclusions	Dissociation	x (not fully?)	x	x	Dominant white, angular or rounded; partly dissociated foraminifera (< 0.47mm)
	Micro-fossil	x	x (Dominant?)	x	
	Bright white mostly elongated	inclusions, difficult to differentiate. Dominant < 0.72mm	White inclusions, difficult to differentiate to micro-fossils	Dominant elongated rounded (< 0.72mm)	
	Red mostly rounded	One large (1.5mm) angular, common rounded < 0.3mm	Few < 0.4mm	Common rounded (< 0.55mm)	Common reddish brown rounded inclusions(< 0.32mm)
	brown angular	Rounded frequent? < 0.22mm		Few	
	Angular cream		Frequent < 0.5mm		Few Coarse yellowish white to white inclusions (< 2.09mm)
	Others			Frequent Greenish white inclusions, mostly angular (< 0.96mm)	Green rather angular inclusions (< 0.64mm), rare black inclusions including an elongated/linear inclusions (0.85mm)
V		Meso vesicles	Meso channels, one large vugh		mostly meso vughs and elongated voids

Table C.14: Group E (Part 2) microscopic characteristics, x= present

Uncertain classification or variations?

- Sample 57 is different from the rest of the group as it has these coarse angular greenish-grey inclusions, which the other samples do not have.
- Sample 30 also has coarse inclusions (from angular to rounded), yellowish-white, and white inclusions. This sample also has green inclusions similar to the ones seen in B2, which makes it stand aside.
- The specificity of Sample 37 is dealt with in the next section and is not included in the table.
- The inclusions of sample 31 seemed different at first as there were none of the translucent inclusions, and most of the white inclusions (mostly hollow from dissociation) had the shapes of micro-fossils. However, this group is now the "best match".
- The classification of sample 7 is more uncertain as most white inclusions could be micro-fossils rather than other white inclusions (calcite, crushed limestone etc.). The angular inclusions are white.

C.1.6 Group F?

S		22	64	47
M		Light pinkish orange	Orange	Orange
Inclusions	Dissociation	x	x not fully	x
	Micro-fossil	x	x	x
	Coarse angular cream inclusion	Common < 1.74mm	Dominant < 1.41mm	Few < 0.6mm, not angular
	Light pink inclusions, sub-angular to sub-rounded	Dominant < 1.06mm	Common < 1.544	Common < 1.58mm
	Others	Common < 0.54mm	Angular brown and red inclusions < 0.4mm	Few large red inclusions < 1.22mm
V		few mega and macro planar voids from inclusions, meso channels	mostly meso vesicles, elongated voids across	Meso vughs and a few mega channels

Table C.15: Group F microscopic characteristics

Unclassified or uncertain

Sample 66 has only a few coarse inclusions visible, which range from angular white and grey to elongated rounded dark brown. The matrix is greyish brown. It does not contain the number of micro-fossils groups D and E have.

Sample 69 has not been classified due to the small black spots, which might be either contamination or inclusions.

C.2 Petrographic raw data

G	S	Mic. G	Form	Site	Fe/Ca	FQ	F	LM	C or B	Fe+qz	T°	2nd	Other comments and inclusions
1,1	15	E	Bowl	TSG	x	-	xxx	xx			x		
1.1	37	E	Bowl	TSG	xxx	-	xxx	xx		x	x		rare glauconite, biotite
1.1	30	E?	Plate	TSG	xxx	-	xxx	xx	- ?		xx		sandwich
1.1	69	E	Bowl or Basin	ZTN	xxx	-	xxx	x			xx	x	sandwich, little whitened surface, 1 fragment of marl with foraminifera and a mollusc
1.1	7	E	Bowl	TSG	xxx	-	xxx	x			xx		whitened surface
1.1	22		Plate	TSG	xxx	-	xxx	x	- ?	-	xx		little whitened surface
1.1	66	?	Plate	ZTN	xx	-	xx	x	- ?	x	xxx		little whitened surface
1.1	27	C	Plate	TSG	x	-	xx	x			xxx		
1.1	40	C	Bowl	TSG	x	-	xxx	x			xxx		
1.1	52	C	Small bowl	TSG	x	-	xx	x			xxx	x	finer variant?
1.2	29	D	Inscribed Bowl	TSG	xxx	x	xxx	x	- ?	x	xxx		sandwich
1.3 ?	64	F?	Bowl	ZTN	xx	xx	xx	x	xx	-	xxx	-	rare glauconite;yellow bio-claystone fragments; No chamotte but biomicrite fragments. A few comparisons with gr. 1 except for the frequent quartz
1.4?	12	C	Plate?	TSG	x	xx	xxx	xx	-	-	xx	x	partly similar to gr 1 except for the frequent quartz?
2.1	60	D3	Bowl	ZTN	xx	x	xx			xxx	x		sandwich

G	S	Mic. G	Form	Site	Fe/Ca	FQ	F	LM	C or B	Fe+qz	T°	2nd	Other comments and inclusions
2.1	4	D3	Bowl	TSG	xx	x	xx	-		xxx	xx		
2.1	10	D1	Bowl	TSG	xx	x	xx			xxx	xxx		whitened surface
2.1	21	D2	Plate	TSG	xx	x	xx	-		xxx	xxx		rare biotite
2.1	25	D?	Bowl	TSG	x	x	xx			xxx	xxx		limonite particularly frequent; highly fired; biotite (scattered, rare)
2.1	9	D2			xx	x	xx			xxx	xxx	x	
2.2	58	D2	Bowl	ZTN	x	xxx	xx			xxx	xxx		1 volcanic rock (trachyte?); more fine quartz, no coarser qtz grains. More fired than 60.
2.2?	48	D2?	Plate	TSG	xxx	xx	xx	x		xxx	xx	x	little whitened surface
3	65	D	Bowl	ZTN	x	x	xx		xx	xxx	x	x	Metamorphic quartz, not expected in Malta; optically active matrix, 1 large quartz
4	62	D			xx	x	xx		xxx		xx		Outlier to be moved from here. In this case chamotte cannot be excluded, biomicrite is rarer; chamotte/ temper grainsize is finer than usual; optically active matrix

G	S	Mic. G	Form	Site	Fe/Ca	FQ	F	LM	C or B	Fe+qz	T°	2nd	Other comments and inclusions
5.1	46	B	olla	TSG	xxx	xxx	x	x	xx		xx		pure red clay nodules; More oriented - wheel thrown?
5.1	34	B	inscribed olla	TSG	xxx	xxx	x	x	xxx		xxx		rare pure red clay nodules; sandwich
5.1	70	B			xxx	xxx	x	x	xx		xxx		Wheel trown?
5.1	35	B	olla	TSG	xxx	xxx	x	x	xxx		xxx		sandwich; chamotte = red bio-claystone fragments; More or less calcareous rock fragment
5.1	18	B	inscribed olla	TSG	xx	xxx	x	x	xxx	-	x	x	chamotte = yellow claystone fragments, + pure red clay rounded nodules; Chamotte: either rock fragment or chamotte? Natural or intentional ?
5.1	36	B			xxx	xxx	x	x	xxx		x		1 clinopyroxene
5.1	13	B			xxx	xx	x	x	xxx		xx		No evidence of wheel throwing
5.2	54	B			xxx	xxx	xx	xxx	xx		x		more visible/abundant calcareous components1 biotite, 1 plagioclase, 1 trachyte (volcanic rock)

G	S	Mic. G	Form	Site	Fe/Ca	FQ	F	LM	C or B	Fe+qz	T°	2nd	Other comments and inclusions
6	33	B	Bowl	TSG	xxx	x	x	x	xx	x	xx	x	1 vitrified fragment; chamotte = yellow and rare red claystone; One over fired rock fragments; Big voids, clay matrix purer.
7	61	A	Olla	ZTN	xxx	xxx					xxx		wheel-thrown; Fe-rich clay nodules
7	68	A	Bowl	ZTN	xxx	xxx					xxx		wheel-thrown; Fe-rich clay nodules

Table C.16: Petrographic table by Capelli, the groups were created and discussed extensively. x; xx; xxx stands for the relative frequencies of inclusions except for the temperatures. G: Group; S: Sample number; Mic. G: Microscopic group; Fe/Ca matrix: clay matrix ratio composition; FQ: Fine Quartz; F: fossils; LM: Limestone; C or B: Chamotte or Biomicrite; Fe+qz: Iron and quartz nodules (Limonite); T°: Firing temperature; 2nd: Secondary alteration (post-depositional).

C.3 Experimental Archaeology supplement

C.3.1 Marl-derived soils from Saint Peter's Pool

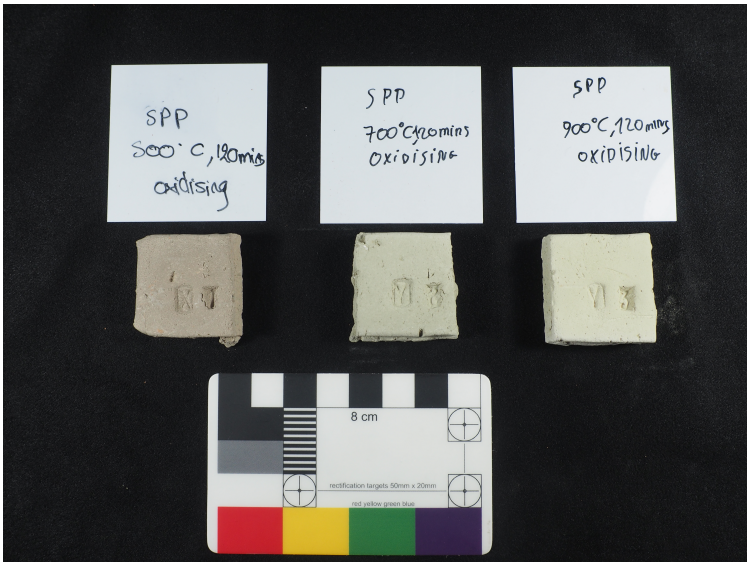


Figure C.1: Briquettes made of marl-derived soils fired at 500, 700 and 900°C in an oxidising atmosphere. The soaking time was 120 minutes.



Figure C.2: Microphotographs of experimental briquettes, unground sections, fired respectively at 500, 700 and 900°C.

These briquettes were made with another marl-derived soil collected close to Saint Peter's Pool. This marl was not tested in this dissertation. However, it was part of an internship project led by Kellian Coste and supervised by myself to assess the materials' plasticity and behaviour when fired. More briquettes must be manufactured to ensure that Marsaxlokk's marls tested in this dissertation have the same behaviour.

The sediment was plastic when wet, and the water of plasticity was less than 25% compared to around 40% for sieved Blue Clay from Il-Qolla (sieved QL.B1). The briquettes withstood firing, although, at 900°C, they became very chalky and had cracks. After a few days, most probably upon rehydration, the briquettes started to turn to powder.

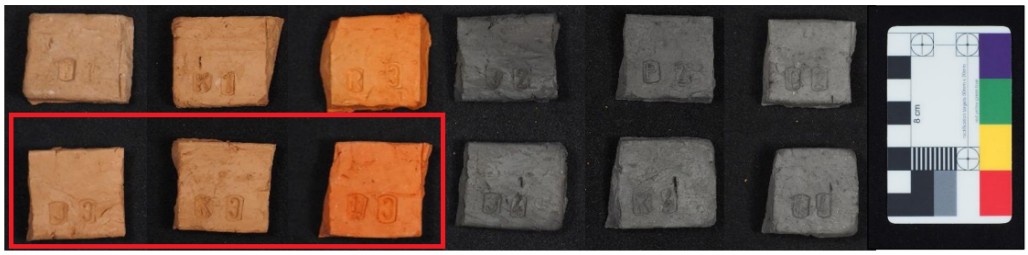
C.3.2 Salt water vs tap water

These experimental briquettes were made as part of the CoFIPoMS project (University of Malta 2021). The briquettes with tap water were manufactured for a dissertation (Xuereb 2021), and the briquettes with salt water were manufactured by Kellian Coste. The same clay was used, finely sieved down to $63\,\mu m$, wet sieved simultaneously. Different furnaces were used. However, the heating rate, atmosphere, and soaking time (120 mins) were the same. Only the cooling rate might have differed.

The diffractograms in Figure C.4 present the mineral composition of the briquettes fired at 700°C. To better observe the changes related to the surface bleaching, the same could be carried out with the 900°C which were manufactured. The peaks have not been fully identified. However, the differences can be visually assessed. The main peak difference seems to be in the peak labelled by Xuereb (2021: 72) as calcite, which peaks at angles 26.4-26.5. This could be caused by a faster dissociation of the calcite, although it is still unclear. It seems, however, that seawater has an impact on the calcite in these briquettes.

Water	C°	Munsell Colour	Recording
Tap	500	5YR 5/6 yellowish red	Recorded by Xuereb (2021)
	700	2.5YR 6/6 light red - 5/6 red	
	900	2.5YR 4/8 -5/8 red	
Salt	500	5YR 7/6 reddish yellow	Recorded by Coste (2021)
	700	5YR 6/4 light reddish brown to 6/6 reddish yellow	
	900	2.5YR 6/6 light red	

Table C.17: Table with the Munsell record of briquettes, maximum temperature (soaking temperature)

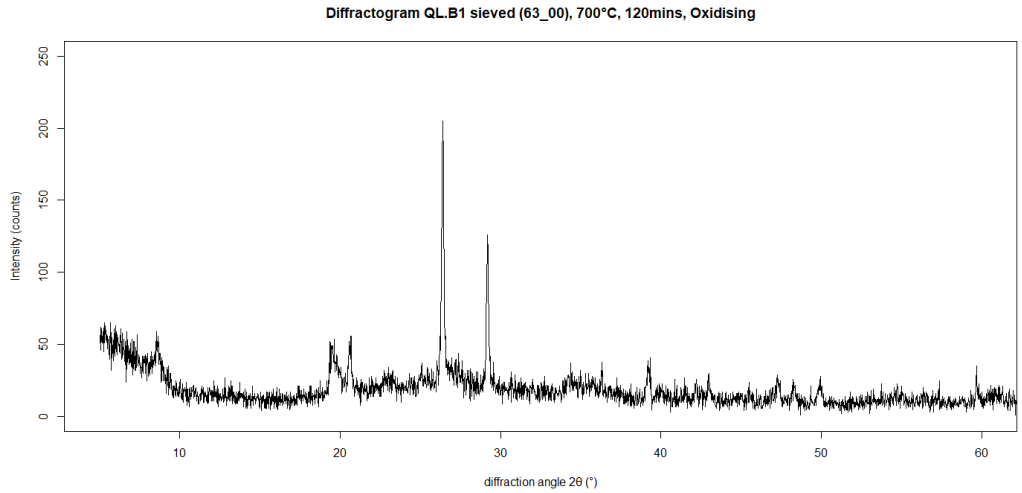


(a) Photos of the briquettes made with tap water. The bottom line, the first three briquettes are the ones of interest, fired with a soaking time of 120°C. Photos taken by the author and Luke Xuereb but photomontage made by Xuereb (2021: 43). From left to right on the bottom line: 500, 700 and 900°C.

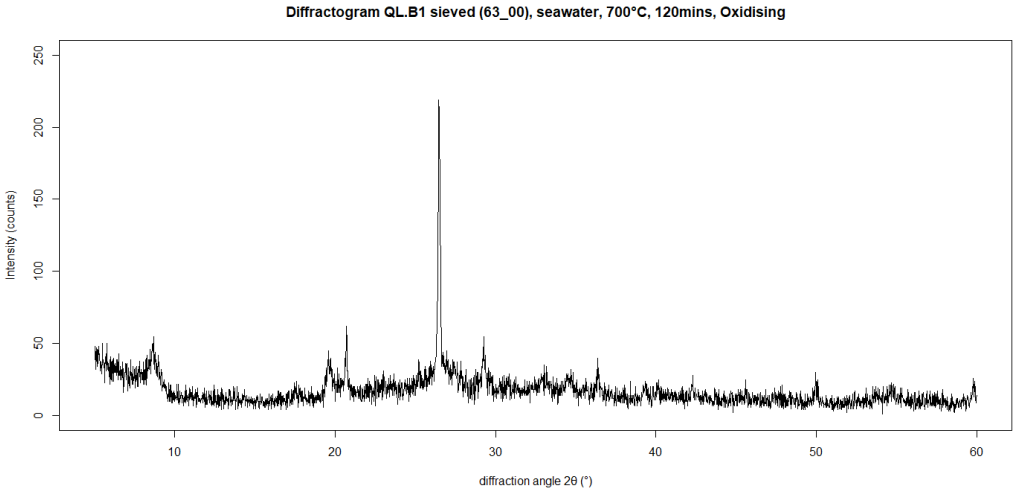


(b) Photos of briquettes manufactured with seawater. Photos were taken by Kellian Coste.

Figure C.3



(a) Diffractogram of the briquette made with tap water, fired at 700°C. XRD reading from Xuereb (2021), diffractogram produced with R for this dissertation.



(b) Diffractogram of the briquette made with seawater, fired at 700°C. XRD reading carried out by Kellian Coste and the author, diffractogram produced with R for this dissertation.

Figure C.4

Appendix D

Data analysis supplement

D.1 Analytical techniques

D.1.1 XRF

In atoms, electrons are present in shells around the nucleus. Inner electrons have lower energy than outer electrons. The X-Ray tube generates primary X-Rays directed toward the sample. As a reaction to this excess of energy, the atoms lose an electron which leaves a gap in their inner shell. This gap is then filled by one of the outer electrons, which must lose some excess energy. This process creates radiation energy which is different from one element to another (Henderson 2000: 15). This allows the software attached to the instrument, the analyser, to identify and quantify the different elements within a sample (Rice 1987: 393-394). This process is illustrated in Figure D.1. XRF can be performed on both geological samples and powdered archaeological material for bulk analysis.

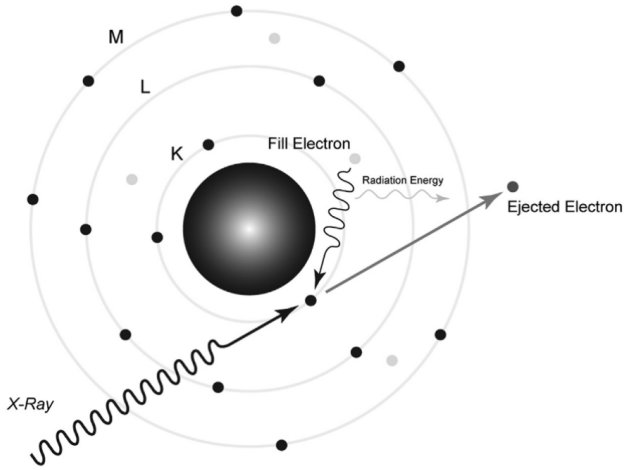


Figure D.1: Diagram extracted from Perrone et al. (2014: 146). This diagram shows an atom with, a nucleus and the electron shells around. The X-Ray ejects one of the inner electron and its position is filled by an outer electron. This generates an energy which is specific to the element and therefore can be recognised by the analyser.

D.2 X-Ray Fluorescence Results

D.2.1 CRB GmbH result

D.2.2 Six samples test, XRF

Table D.2 presents the raw data used for the graphs in the six samples test (section 6.1.4) to ensure repeatability.

D.2.3 Spearman Correlation full results

Parameter	Unit	TL.B1 (035790)	SPP.A1 (035791)	QL.B1 (035792)	G2005 (035793)	Sample 21 (035794)
SiO2	MA-%	42,36	11,86	40,04	36,85	52,84
Al2O3	MA-%	15,31	3,15	14,64	13,13	17,95
Fe2O3	MA-%	6,29	1,44	5,65	5,50	7,07
TiO2	MA-%	759	226	715	657	933
P2O5	MA-%	177	348	199	248	297
SO3	MA-%	3,06	2,39	0,77	0,11	0,10
CaO	MA-%	11,80	39,95	14,78	21,51	13,20
MgO	MA-%	2,12	2,02	1,78	1,55	1,86
K2O	MA-%	2,22	0,61	2,09	1,50	2,70
Na2O	MA-%	0,28	0,90	0,18	0,25	0,56
Mn	µg/g	269	115	244	281	512
Sc	µg/g	< 14	< 14	< 14	< 14	19
V	µg/g	125	29	113	82	123
Cr	µg/g	138	51	121	102	159
Co	µg/g	< 20	< 20	< 20	< 20	< 20
Ni	µg/g	43	28	43	38	69
Cu	µg/g	< 25	< 25	< 25	< 25	< 25
Zn	µg/g	87	52	86	70	102
Ga	µg/g	21	7	16	16	24
As	µg/g	< 8	< 8	< 8	< 8	< 8
Rb	µg/g	104	19	96	72	120
Sr	µg/g	402	975	432	333	482
Y	µg/g	23	13	21	23	46
Zr	µg/g	147	71	135	121	257
Nb	µg/g	18	8	16	15	20
Mo	µg/g	< 50	< 50	< 50	< 50	< 50
Sn	µg/g	< 60	< 60	< 60	< 60	< 60
Ba	µg/g	154	< 44	121	222	286
La	µg/g	< 33	< 33	< 33	< 33	< 33
Ce	µg/g	18	< 18	< 18	24	46
Pr	µg/g	< 5	< 5	< 5	< 5	< 5
Nd	µg/g	< 14	< 14	< 14	< 14	29
Sm	µg/g	< 5	< 5	< 5	< 5	6
Hf	µg/g	4	< 3	4	4	7
Ta	µg/g	< 30	< 30	< 30	< 30	< 30
W	µg/g	< 50	< 50	< 50	< 50	< 50
Pb	µg/g	18	< 15	19	< 15	25
Bi	µg/g	< 30	< 30	< 30	< 30	< 30
Th	µg/g	< 20	< 20	< 20	< 20	< 20
U	µg/g	< 10	< 10	< 10	< 10	< 10
LOI	MA-%	15,48	36,98	19,02	18,56	2,27

Table D.1: Table presenting CRB GmbH results for the five samples sent. "$<$" means value smaller than practical detection limit.

	7a	15a	18a	35a	46a	69a
Al_2O_3	13.4	10.4	13.2	12	13.3	12.9
As_2O_3	0	0	0.0007	0.0003	0.0007	0
BaO	0.0036	0	0.0105	0.0233	0.0189	0
Bi_2O_3	0.0022	0.0032	0.0027	0.0024	0.0026	0.0033
Br	0.0052	0.0064	0.0056	0.0064	0.0068	0.0085
CaO	15.4	25.7	5.49	3.89	3.48	18.2
CdO	0.0011	0.0014	0.0012	0.0014	0.0018	0.0014
CeO_2	0	0	0	0	0	0
Cl	0.393	0.276	0.361	0.356	0.324	0.386
CoO	0	0	0.0149	0.0133	0.0202	0
Cr_2O_3	0	0	0	0	0	0.0199
Cs_2O	0	0	0	0	0	0
CuO	0.0006	0.0044	0.005	0.0025	0.0045	0.0018
$Fe2O3$	6.74	5.71	7.11	7.45	7.59	6.49
Ga_2O_3	0.0018	0.0027	0.0032	0.0026	0.0036	0.0029
GeO_2	0	0	0.0005	0.0001	0.0005	0
I	0	0.0001	0	0	0	0
K_2O	2.41	2.23	2.78	2.63	2.77	2.48
La_2O_3	0	0	0	0	0	0
MgO	3.9	5.25	2.76	1.75	2.65	3.57
MnO	0.0408	0.0535	0.101	0.154	0.145	0.0481
MoO_3	0.0005	0.0006	0.0008	0.0006	0	0.0004
Na_2O	14.3	11.3	9.28	5.76	6.81	8.45
Nb_2O_5	0.0029	0.0022	0.0044	0.0044	0.0042	0.0028
Nd_2O_3	0	0	0.0185	0.0173	0.0367	0.0112
NiO	0.0015	0.0049	0.0043	0.004	0.0069	0.0041
P_2O_5	0.819	0.97	0.649	0.613	0.643	0.734
PbO	0.005	0.005	0.0054	0.0053	0.0055	0.0055
Pr_6O_11	0	0	0	0	0	0
Rb_2O	0.016	0.0115	0.0132	0.0154	0.0158	0.0153
$Sb2O3$	0.0038	0.0035	0.0038	0.0034	0.0039	0.0031
SeO_2	0.0008	0.0016	0.0011	0.0011	0.0009	0.0014
SiO_2	41.1	36.7	56.6	63.6	60.6	45.3
SnO_2	0.0127	0.0127	0.0113	0.0121	0.0123	0.0118
SO_3	0.47	0.688	0.431	0.394	0.376	0.504
SrO	0.068	0.0641	0.028	0.0252	0.0201	0.069
Ta_2O_5	0	0	0	0	0	0
TeO_2	0.0025	0.003	0.0026	0.0026	0.003	0.0016
TiO_2	0.784	0.648	1.03	1.09	1.1	0.742
V_2O_5	0	0	0.0127	0.0335	0.0239	0
WO_3	0	0	0	0	0	0
Y_2O_3	0.0031	0.0038	0.0048	0.0049	0.0049	0.0031
ZnO	0.012	0.0154	0.0118	0.0113	0.0114	0.013
ZrO_2	0.0338	0.0246	0.0651	0.0706	0.0699	0.033

Table D.2: Six samples data for the primary test as mentioned in section 6.1.4. Sample 15 was re-analysed in a subsequent analysis to ensure the data was correct.

	Al2O3	CaO	Cr2O3	CuO	Fe2O3	Ga2O3	K2O	MgO	MnO	Nb2O5	NiO	P2O5	Rb2O	SiO2	SO3	SrO	TiO2	Y2O3	ZnO	ZrO2
Al2O3		0.06	**0.03**	0.49	**0.00**	0.06	0.08	*0.05*	0.24	**0.00**	0.68	0.29	**0.00**	0.89	0.19	0.66	**0.01**	**0.01**	*0.05*	0.25
CaO	-0.26		**0.03**	0.30	**0.00**	0.15	0.23	**0.00**	**0.00**	**0.00**	0.24	**0.00**	0.16	**0.00**	**0.00**	**0.00**	**0.00**	**0.00**	**0.00**	**0.00**
Cr2O3	0.30	-0.30		0.56	**0.01**	**0.01**	0.33	0.69	0.38	0.27	**0.03**	0.54	**0.00**	0.09	0.32	**0.01**	*0.05*	0.54	0.12	0.56
CuO	0.10	-0.15	0.08		0.36	0.00	**0.00**	0.56	*0.05*	0.10	**0.00**	0.07	0.08	0.38	0.29	0.19	0.42	0.06	**0.00**	0.31
Fe2O3	0.64	-0.54	0.37	0.13		**0.05**	**0.02**	0.38	**0.00**	**0.00**	0.39	**0.00**	**0.01**	**0.01**	**0.02**	**0.00**	**0.00**	**0.01**	0.31	*0.05*
Ga2O3	0.26	-0.20	0.38	0.81	0.28		**0.00**	0.69	0.34	**0.04**	**0.00**	0.09	**0.00**	0.32	0.77	0.15	0.17	0.06	**0.00**	0.56
K2O	0.25	-0.17	0.14	0.54	0.32	0.55		0.66	0.71	0.20	**0.00**	0.10	**0.00**	0.61	0.21	0.30	0.35	0.69	0.19	0.97
MgO	0.28	0.65	-0.06	-0.08	-0.13	-0.06	0.06		**0.00**	**0.00**	0.10	**0.00**	0.61	**0.00**	**0.00**	**0.00**	**0.00**	**0.01**	**0.00**	**0.00**
MnO	0.17	-0.78	0.13	0.27	0.51	0.14	0.05	-0.62		**0.00**	0.27	**0.00**	0.92	**0.00**	**0.00**	**0.00**	**0.00**	**0.00**	**0.02**	**0.00**
Nb2O5	0.40	-0.69	0.16	0.23	0.50	0.29	0.18	-0.45	0.68		0.25	**0.00**	0.16	**0.00**	**0.00**	**0.00**	**0.00**	**0.00**	0.08	**0.00**
NiO	0.06	-0.17	0.30	0.78	0.12	0.89	0.44	-0.23	0.16	0.17		0.09	**0.00**	0.20	0.86	0.15	0.38	0.15	**0.00**	0.53
P2O5	-0.15	0.86	-0.09	-0.26	-0.47	-0.24	-0.23	0.68	-0.76	-0.63	-0.24		0.17	**0.00**	**0.00**	**0.00**	**0.00**	**0.00**	**0.02**	**0.00**
Rb2O	0.40	-0.20	0.41	0.25	0.34	0.51	0.68	0.07	-0.01	0.20	0.39	-0.20		0.45	0.94	0.40	0.32	0.76	0.11	1.00
SiO2	-0.02	-0.94	0.24	0.13	0.35	0.14	0.07	-0.77	0.75	0.61	0.18	-0.82	0.11		**0.00**	**0.00**	**0.00**	**0.00**	**0.00**	**0.00**
SO3	-0.19	0.73	-0.14	0.15	-0.32	0.04	0.18	0.55	-0.51	-0.49	0.03	0.61	-0.01	-0.72		**0.00**	**0.00**	**0.00**	**0.00**	**0.00**
SrO	-0.06	0.93	-0.34	-0.18	-0.50	-0.20	-0.15	0.67	-0.76	-0.60	-0.21	0.80	-0.12	-0.93	0.68		**0.00**	**0.00**	**0.00**	**0.00**
TiO2	0.35	-0.92	0.28	0.12	0.60	0.20	0.13	-0.55	0.76	0.72	0.13	-0.77	0.14	0.81	-0.67	-0.84		**0.00**	**0.00**	**0.00**
Y2O3	0.36	-0.52	0.09	0.27	0.37	0.26	-0.06	-0.34	0.66	0.82	0.21	-0.51	0.04	0.44	-0.46	-0.45	0.56		0.73	**0.00**
ZnO	0.27	0.45	0.22	0.40	0.14	0.53	0.18	0.46	-0.33	-0.24	0.45	0.32	0.23	-0.55	0.51	0.42	-0.40	-0.05		**0.00**
ZrO2	0.16	-0.82	0.08	0.15	0.27	0.08	-0.01	-0.62	0.79	0.80	0.09	-0.69	0.00	0.80	-0.66	-0.74	0.81	0.72	-0.58	

Table D.3: Table presenting the results of correlation analysis. The upper triangle presents the p values for the correlation test, with bold values being statistically significant. The lower pink triangle presents the correlation coefficient (spearman) being tested, between -1 and 1.

D.2.4 Multivariate Analysis datasets

PCA: Dataset 1 supplement

	PC 1	PC 2	PC 3	PC 4
Al2O3	0.234	0.350	0.688	-0.362
CaO	-0.956	0.006	0.039	0.171
Cr2O3	0.232	0.354	0.177	-0.375
CuO	0.175	0.783	-0.148	0.435
Fe2O3	0.480	0.329	0.484	-0.427
Ga2O3	0.185	0.891	-0.037	0.302
K2O	0.074	0.646	-0.513	-0.434
MgO	-0.637	0.220	0.503	-0.101
MnO	0.817	-0.261	0.213	0.186
Nb2O5	0.817	0.192	0.215	0.184
NiO	0.204	0.810	-0.219	0.354
P2O5	-0.855	-0.112	0.242	0.074
Rb2O	0.346	0.603	-0.309	-0.520
SiO2	0.936	-0.179	-0.244	-0.024
SO3	-0.702	0.217	-0.066	0.128
SrO	-0.918	0.039	0.107	0.090
TiO2	0.928	-0.172	0.151	0.024
Y2O3	0.633	0.193	0.383	0.444
ZnO	-0.426	0.683	0.365	0.124
ZrO2	0.885	-0.290	0.062	0.214

Table D.4: Table of loadings for each variables for the first 4 PCs for PCA of pottery sherd

S	G	Al2O3	CaO	Cr2O3	CuO	Fe2O3	Ga2O3	K2O	MgO	MnO	Nb2O5	NiO	P2O5	Rb2O	SiO2	SO3	SrO	TiO2	Y2O3	ZnO	ZrO2
1	D	0.336	0.335	-0.035	2.887	-0.365	3.609	0.507	0.208	-0.354	1.475	3.016	0.153	0.789	-0.446	0.183	0.684	-0.457	1.368	1.8	0.027
2	D	-0.507	-0.166	0.676	-0.347	-0.483	-0.23	0.176	-1.484	-0.342	-0.92	1.002	0.051	0.555	0.537	-0.824	-0.028	-0.39	-0.292	-0.53	-0.277
4	D	0.268	-0.132	0.764	0.131	0.558	0.266	0.733	-0.165	-0.31	-0.006	0.213	-0.247	0.607	0.016	0.054	0.166	-0.283	0.115	0.409	-0.389
5	B	-0.567	-1.408	0.028	-0.534	-0.029	-0.683	-1.131	-0.808	1.894	0.586	-0.841	-1.317	-0.337	1.68	-1.371	-1.448	1.526	0.5	-1.205	2.28
7	E	1.004	0.497	-1.803	-1.322	0.334	-1.366	0.335	1.136	-0.748	-0.489	-1.308	0.518	0.661	-0.888	0.068	0.945	-0.404	-1.498	-0.397	-0.703
8	D	1.382	0.357	-0.389	-0.023	0.69	0.005	0.683	0.464	-0.314	0.204	-0.257	-0.312	1.058	-0.751	-0.302	0.55	-0.171	0.691	0.236	-0.163
9	D	0.731	-0.287	1.38	1.477	1.171	2.032	1.035	0.374	-0.098	1.036	1.882	-0.607	1.436	-0.087	0.468	-0.407	-0.234	1.842	1.401	0.03
10	D	0.868	-0.042	1.275	-0.756	-0.256	-0.497	0.205	0.682	-0.529	0.13	-0.56	0.574	0.797	-0.189	-0.929	0.294	-0.239	0.148	-0.343	-0.123
11	D	-0.228	0.766	-1.803	0.389	-1.199	-0.953	0.568	0.714	-0.282	-0.955	-0.583	-0.141	-0.374	-0.804	3.769	1.039	-0.72	-0.441	-0.394	-0.3
12	C	-1.566	1.084	-0.479	-0.236	-2.021	-0.637	-0.717	0.76	-0.798	-1.468	-0.409	2.483	-1.424	-0.71	0.281	0.547	-1.432	-0.189	-0.524	-0.244
13	B	0.028	-0.643	0.858	-0.568	0.953	-0.504	0.511	-0.421	1.265	0.278	-0.306	-0.334	0.135	0.547	0.191	-0.463	0.629	-0.219	-0.762	0.236
15	E	-0.739	0.188	0.215	-0.408	-0.478	-0.568	-0.08	0.147	0.273	-0.562	-0.355	1.021	-0.615	-0.058	0.234	0.023	-0.362	-0.205	-0.647	0.005
17	D	0.572	-0.05	1.152	0.316	-0.151	0.539	0.461	0.096	-0.446	0.17	1.002	0.019	0.754	-0.095	0.455	0.304	-0.202	0.026	0.215	-0.136
18	B	0.225	-1.04	-1.803	1.231	0.278	0.245	0.705	-0.046	0.108	1.407	-0.053	-0.76	-0.412	0.887	-0.433	-0.998	0.928	0.541	-0.854	0.616
19	D	-0.097	-0.307	-0.234	1.422	0.481	0.483	1.925	-0.229	-0.311	-0.866	0.737	-0.516	-0.004	0.185	0.009	-0.571	-0.415	-0.313	1.332	-0.414
21	D	1.494	0.118	-0.233	-0.316	0.56	-0.134	0.461	0.018	-0.285	-0.132	0.203	-0.026	0.806	-0.437	-0.811	0.279	-0.129	0.755	-0.059	-0.134
22	F	0.181	0.602	0.881	-0.989	-0.637	-0.867	0.375	0.618	-0.703	-0.866	-0.883	0.506	0.375	-0.67	0.245	0.519	-0.894	-1.463	-0.483	-0.744
23	C	-1.221	1.823	-0.338	-1.281	-0.693	-0.915	-2.393	0.443	-0.686	-0.125	-1.297	1.191	-2.267	-1.366	0.672	1.405	-1.394	0.324	0.48	-0.968
24	C	0.532	1.781	0.255	1.437	-0.599	-0.408	-1.374	3.761	-0.554	-1.669	-0.061	2.138	-1.675	-2.283	2.242	1.086	-1.228	0.131	2.608	-1.092
25	D	-0.535	-0.271	0.664	0.341	-0.456	0.828	0.249	-1.005	-0.355	-0.312	1.266	-0.744	0.385	0.581	-1.286	0.015	-0.249	0.282	-0.078	-0.283
26	D	2.401	0.494	0.65	-0.794	0.268	-0.294	0.081	0.949	-0.536	-0.047	-0.43	0.765	-0.083	-1.067	-0.145	0.95	-0.256	0.151	-0.092	-0.405
27	C	-0.421	0.942	-0.03	-0.935	-0.027	-0.759	-1.101	-0.017	-0.639	-0.033	-1.12	0.839	-1.646	-0.732	0.432	0.539	-0.809	0.123	-0.22	-0.852
28	E	-1.696	0.882	0.778	0.761	-0.322	0.271	0.34	0.678	-0.331	-1.255	0.261	0.682	0.753	-0.638	0.533	0.104	-1.456	-0.665	1.052	-1.13
30	E	-1.028	0.845	1.006	0.226	-0.025	0.604	0.403	0.96	-0.654	-1.216	0.236	0.572	0.214	-0.825	0.87	0.323	-0.204	-1.225	1.092	-1
32	B	1.036	-1.373	1.072	0.459	0.716	0.241	0.689	-0.145	-0.098	1.21	-0.07	-0.607	0.633	1.054	-0.939	-1.349	1.037	0.208	-0.845	0.682
33	B	1.265	-0.672	1.225	0.22	2.087	0.696	1.416	0.188	-0.561	-0.617	0.274	-0.48	1.757	0.114	0.785	-0.539	0.001	-1.255	1.666	-0.83
35	B	-1.053	-1.287	-1.803	-0.285	0.395	-0.621	0.302	-0.971	0.81	1.177	-0.26	-1.101	0.056	1.522	-0.817	-1.162	1.063	0.434	-1.31	0.748
36	B	0.736	-1.307	1.175	1.16	1.063	0.757	-0.842	-0.498	2.488	1.673	0.712	-0.453	-0.391	1.125	-0.518	-1.299	2.328	1.172	1.05	1.086
37	E	-3.236	1.815	-0.342	-0.19	-1.299	-0.667	0.362	-2.422	-0.613	-0.767	0.099	0.542	0.018	-0.727	1.449	0.787	-0.878	-0.66	-0.277	-0.812
39	B	0.459	-1.387	0.927	-0.33	0.699	-0.596	-1.158	-0.716	3.348	0.81	0.025	-1.158	-0.215	1.379	-0.954	-1.471	1.77	1.531	-0.344	1.613
40	C	0.048	1.805	-0.848	-1.694	0.223	-1.027	-2.026	0.794	-0.646	-1.025	-0.891	1.813	-2.285	-1.757	0.845	1.685	-0.747	-0.472	1.546	-1.102
42	D	1.412	0.027	-0.591	0.724	0.207	0.656	1.188	0.816	-0.351	1.172	-0.083	-0.116	0.456	-0.516	0.34	0.226	-0.12	1.274	0.707	0.064
43	B	0.076	-1.16	0.486	1.474	0.461	-0.006	0.571	-0.561	0.16	1.201	-0.342	-0.328	0.321	1.101	-0.727	-1.132	0.929	0.069	-1.265	0.766
46	B	0.023	-1.339	-1.803	0.867	0.756	0.623	0.566	-0.202	0.703	0.959	1.065	-0.896	0.21	1.208	-0.92	-1.37	1.198	0.498	-1.207	0.748
47	D	0.767	0.21	0.558	0.47	1.956	1.366	1.21	0.418	-0.334	1.691	0.039	-0.382	1.929	-0.679	0.941	0.236	-0.284	0.942	1.691	-0.371
48	D	-0.959	-0.107	0.408	-1.022	-0.013	-0.879	0.261	-0.798	-0.34	-0.365	-0.537	-0.451	0.304	0.417	-0.935	-0.1	-0.344	0.009	-0.722	-0.095
50	E	-1.462	0.778	-1.803	0.345	-1.29	0.239	0.306	0.111	-0.842	-1.422	0.332	-0.089	0.077	-0.386	0.065	0.307	-0.904	-1.75	0.602	-1.092
52	C	-0.943	1.545	-1.071	0.822	-1.411	0.308	-0.546	-0.597	-0.635	-1.093	0.596	0.607	-2.24	-1.077	1.485	1.397	-0.733	-1.342	0.795	-0.623
53	B	-0.176	-1.416	0.145	-0.907	0.448	-0.869	-0.259	-2.422	1.19	0.887	-1.154	-1.093	0.045	1.75	-1.133	-1.398	1.753	0.806	-1.564	1.723

S	G	Al2O3	CaO	Cr2O3	CuO	Fe2O3	Ga2O3	K2O	MgO	MnO	Nb2O5	NiO	P2O5	Rb2O	SiO2	SO3	SrO	TiO2	Y2O3	ZnO	ZrO2
54	B	-0.804	-0.471	-0.505	-0.054	-0.563	-0.449	0.299	-1.243	-0.059	0.444	0.109	-0.731	-0.225	0.821	-0.015	-1.031	0.462	0.125	-1.546	0.404
58	D	-0.608	-0.181	1.145	0.152	-1.601	0.806	0.465	-0.333	-0.7	0.334	1.29	0.202	0.298	0.446	-0.868	-0.18	-0.056	0.187	-0.442	0.274
60	D	0.542	0.166	-0.701	2.397	-0.669	3.065	0.358	-0.145	-0.183	1.007	2.749	-0.812	0.581	-0.204	0.177	0.708	-0.43	1.56	0.958	0.118
61	A	0.831	-1.653	0.654	-1.163	1.155	-1.028	-1.467	-1.047	2.446	1.475	-1.33	-1.942	-0.267	1.645	-1.572	-1.773	1.932	1.288	-0.99	2.591
62	B	0.534	-0.747	0.919	-0.182	1.946	0.314	1.106	0.042	-0.52	-1.05	-0.093	-0.798	0.823	0.403	-0.191	-0.742	-0.101	-1.924	0.808	-1.023
64	F	-0.221	0.326	0.036	-1.694	-1.264	-0.905	0.288	0.937	-0.834	-0.444	-0.894	1.675	0.548	-0.392	0.686	0.469	-0.45	-0.904	-0.699	-0.34
65	D	-0.804	0.596	-1.803	-0.693	-1.157	-0.732	-0.055	0.074	-0.555	-0.996	-1.019	0.406	0.362	-0.362	1.282	1.825	-0.527	-1.177	-0.613	-0.648
66	Unc.	0.064	0.654	0.45	-0.28	-0.733	-0.228	-0.07	1.038	-0.701	-1.426	-0.318	0.661	-0.039	-0.728	0.238	0.761	-0.699	-1.988	-0.208	-0.82
67	Unc.	0.893	1.325	-1.658	-1.694	0.378	-1.089	-3.099	1.337	-0.704	-0.924	-2.045	2.414	-2.905	-1.423	-0.845	1.99	-0.725	-0.186	0.008	-0.863
68	A	-0.868	-1.709	-1.063	-0.632	-1.602	-1.029	-1.824	-1.313	2.216	0.955	-1.036	-2.053	-0.734	2.285	-1.403	-1.841	2.052	1.043	-1.852	3.367
69	Unc.	-0.1	0.741	0.258	-0.65	-0.898	-0.161	0.177	0.623	-0.682	-0.916	-0.163	-0.302	0.149	-0.705	0.079	0.783	-1.043	-1.784	-0.313	-0.844
70	B	1.127	-1.546	1.098	0.266	2.456	1.148	-1.181	-0.799	1.733	1.685	1.591	-1.039	0.247	1.299	-1.143	-1.646	2.362	1.81	0.328	1.444

Table D.5: Dataset 1 after normalization, variable selection and standardization. Final data used for PCA. S: Sample; G: OM groups.

PCA: Dataset 2 supplement (PCA1)

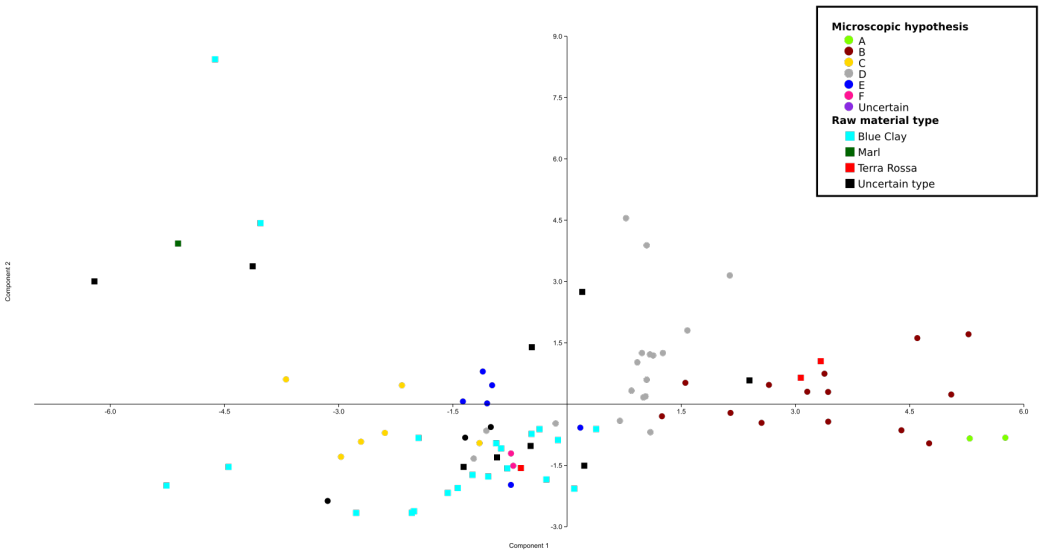


Figure D.2: PCA 1 for dataset 2 before removing the outliers. The other output is not presented.

PCA: Dataset 2 supplement (PCA2)

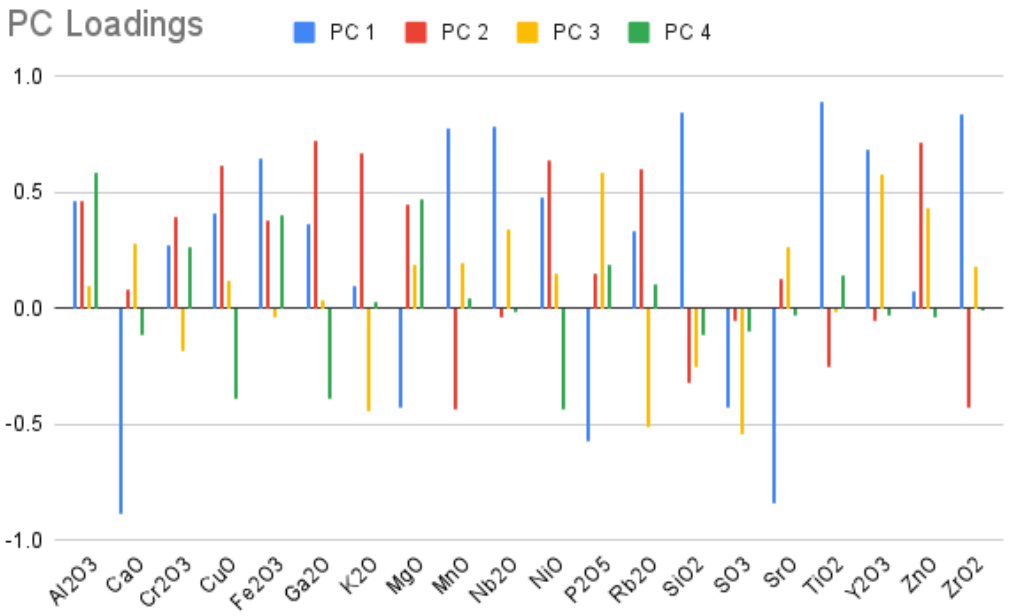


Figure D.3: Loading plot for the PCA 2 (without outliers) of Dataset 2

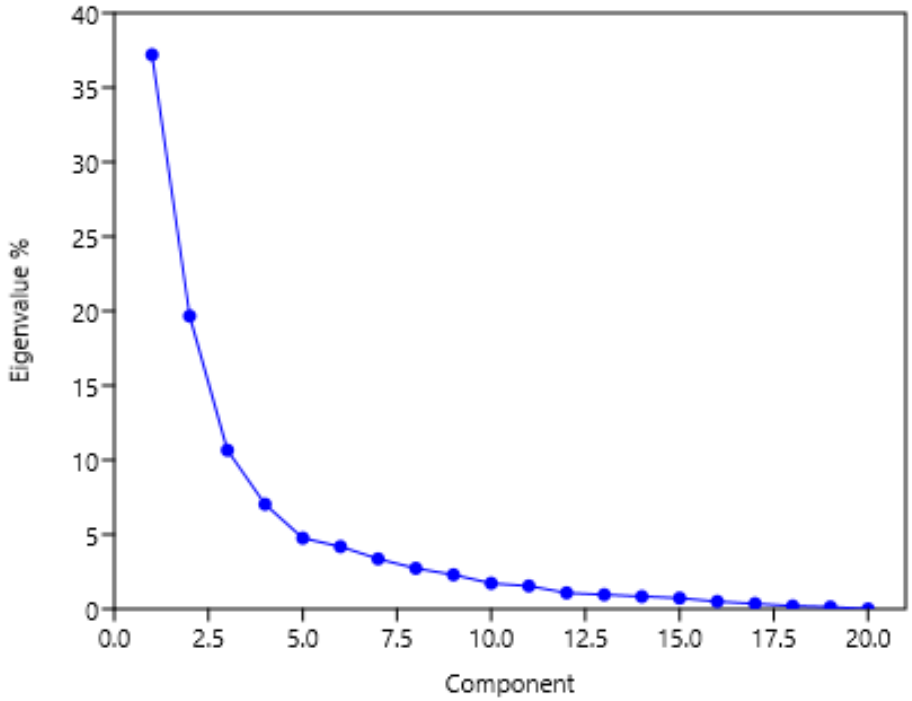


Figure D.4: Screeplot for the PCA 2 (without outliers) of Dataset 2

PC	Eigenvalue	% variance	Cumulative sum of % variance
1	7.44024	37.2	37.2
2	3.93251	19.7	56.9
3	2.13218	10.7	67.5
4	1.40583	7.0	74.6
5	0.952485	4.8	79.3
6	0.837771	4.2	83.5
7	0.67271	3.4	86.9
8	0.546313	2.7	89.6
9	0.459425	2.3	91.9
10	0.344813	1.7	93.6

Table D.6: Eigenvalues for the 10 first PCs (out of 20) as well as variance and cumulative variance (in %)

S	G	Al2O3	CaO	Cr2O3	CuO	Fe2O3	Ga2O3	K2O	MgO	MnO	Nb2O5	NiO	P2O5	Rb2O	SiO2	SO3	SrO	TiO2	Y2O3	ZnO	ZrO2
1	D	545	250	-119	2,339	-179	3,998	533	369	-151	1,733	2,956	544	824	-438	-387	782	-315	1,504	2,030	297
2	D	-193	-271	584	-156	-286	-205	106	-1,772	-137	-638	1,124	414	521	666	-620	-7	-240	247	-223	-31
4	D	485	-235	670	213	649	337	825	-103	-101	266	406	34	588	81	-417	208	-122	555	684	-152
5	B	-246	-1,561	-57	-300	122	-701	-1,583	-917	2,373	852	-553	-1,330	-629	1,949	-747	-1,580	1,873	847	-876	2,729
7	E	1,129	417	-1,867	-908	448	-1,449	310	1,543	-593	-212	-977	1,009	658	-934	-414	1,072	-256	-666	-95	-491
8	D	1,460	273	-469	94	768	52	760	693	-106	474	-21	-49	1,170	-780	-499	634	1	992	518	92
9	D	890	-397	1,279	1,252	1,200	2,271	1,215	579	137	1,297	1,924	-424	1,657	-35	-321	-427	-69	1,863	1,644	301
10	D	1,010	-142	1,175	-471	-82	-498	143	970	-347	401	-296	1,081	834	-150	-644	351	-73	580	-43	135
11	D	50	697	-1,867	412	-928	-997	612	1,010	-69	-673	-318	170	-677	-840	442	1,176	-604	134	-93	-55
12	C	-1,120	1,027	-558	-70	-1,667	-651	-1,048	1,068	-649	-1,181	-159	3,513	-2,030	-734	-365	631	-1,391	325	-218	4
13	B	275	-766	763	-326	1,004	-505	538	-427	1,667	547	-65	-76	-20	677	-385	-488	884	303	-448	522
15	E	-396	97	127	-203	-281	-575	-225	292	553	-284	-111	1,650	-987	-2	-375	50	-210	314	-337	273
17	D	751	-150	1,054	356	12	637	473	228	-254	440	1,124	373	777	-44	-325	362	-33	488	497	121
18	B	447	-1,179	-1,867	1,061	398	315	788	47	368	1,665	165	-619	-725	1,058	-530	-1,082	1,214	878	-537	933
19	D	165	-417	-316	1,209	579	575	2,365	-184	-102	-586	883	-309	-199	270	-428	-608	-268	231	1,578	-179
21	D	1,558	24	-315	-132	651	-100	474	129	-73	141	397	316	844	-427	-617	334	48	1,040	231	123
22	F	409	526	786	-651	-424	-903	363	888	-543	-585	-590	994	289	-689	-373	600	-797	-639	-179	-535
23	C	-819	1,795	-419	-876	-474	-956	-3,213	666	-523	148	-967	1,867	-3,117	-1,470	-274	1,582	-1,349	714	753	-777
25	D	-218	-380	571	375	-262	953	200	-1,167	-151	-36	1,364	-599	302	716	-727	41	-86	682	213	-38
26	D	2,351	414	558	-501	388	-275	-17	1,307	-355	226	-179	1,324	-301	-1,135	-463	1,077	-93	583	200	-169
27	C	-118	880	-115	-609	124	-784	-1,544	84	-471	239	-806	1,418	-2,317	-759	-330	622	-703	562	76	-652
28	E	-1,234	817	684	699	-141	344	318	964	-125	-970	450	1,218	776	-654	-306	140	-1,417	-35	1,307	-952
30	E	-650	779	909	287	125	708	398	1,321	-488	-931	428	1,078	81	-864	-229	383	-35	-459	1,345	-811
32	B	1,157	-1,524	975	466	791	311	768	-78	137	1,470	149	-424	622	1,247	-647	-1,470	1,334	626	-528	1,004
33	B	1,358	-796	1,126	282	2,022	808	1,707	344	-383	-338	462	-263	2,071	191	-248	-573	191	-482	1,900	-628
35	B	-671	-1,436	-1,867	-108	503	-634	268	-1,123	1,156	1,437	-23	-1,054	-122	1,772	-619	-1,263	1,363	797	-979	1,075
36	B	895	-1,456	1,076	1,007	1,102	875	-1,209	-525	3,039	1,929	861	-228	-699	1,326	-549	-1,415	2,759	1,356	1,305	1,441
37	E	-2,582	1,786	-423	-35	-1,019	-684	346	-2,960	-441	-487	302	1,039	-171	-754	-95	897	-779	-32	21	-608
39	B	652	-1,539	832	-143	775	-606	-1,617	-801	4,005	1,074	235	-1,126	-471	1,611	-650	-1,605	2,143	1,628	-44	2,010
40	C	292	1,776	-924	-1,195	349	-1,078	-2,739	1,111	-478	-742	-597	2,659	-3,141	-1,910	-234	1,892	-635	111	1,785	-921
42	D	1,486	-71	-669	671	334	765	1,413	1,139	-148	1,432	137	202	393	-516	-351	275	58	1,433	972	337
43	B	317	-1,304	396	1,249	562	40	616	-605	426	1,461	-98	-69	220	1,299	-598	-1,230	1,215	520	-934	1,096
46	B	271	-1,489	-1,867	781	827	729	609	-150	1,035	1,222	1,181	-793	76	1,420	-642	-1,494	1,512	845	-879	1,075
47	D	922	119	467	474	1,904	1,542	1,441	635	-128	1,946	248	-137	2,293	-699	-212	286	-124	1,182	1,924	-133
48	D	-589	-210	319	-676	136	-916	215	-905	-135	-89	-275	-226	197	531	-646	-87	-190	475	-409	165
50	E	-1,029	709	-1,867	378	-1,010	308	274	247	-699	-1,136	515	235	-96	-370	-415	365	-807	-856	871	-910
52	C	-575	1,506	-1,144	746	-1,119	384	-827	-650	-466	-810	755	1,122	-3,082	-1,147	-86	1,573	-619	-548	1,058	-404
53	B	96	-1,569	59	-588	550	-905	-456	-2,960	1,582	1,150	-837	-1,043	-136	2,027	-692	-1,525	2,124	1,079	-1,224	2,128
54	B	-454	-588	-584	70	-358	-445	264	-1,468	180	712	312	-583	-484	985	-433	-1,118	699	563	-1,207	704

S	G	Al2O3	CaO	Cr2O3	CuO	Fe2O3	Ga2O3	K2O	MgO	MnO	Nb2O5	NiO	P2O5	Rb2O	SiO2	SO3	SrO	TiO2	Y2O3	ZnO	ZrO2
58	D	-282	-287	1,047	230	-1,289	929	479	-316	-539	603	1,386	606	190	564	-630	-175	128	610	-139	564
60	D	725	74	-778	1,962	-453	3,402	340	-78	41	1,269	2,713	-685	554	-166	-389	809	-284	1,650	1,215	395
61	A	978	-1,816	561	-785	1,185	-1,079	-2,017	-1,219	2,992	1,732	-997	-2,125	-539	1,909	-793	-1,940	2,321	1,444	-669	3,065
62	B	718	-875	823	-28	1,895	391	1,307	159	-337	-767	128	-668	867	516	-474	-798	78	-989	1,071	-836
64	F	56	239	-49	-1,195	-987	-945	251	1,292	-689	-167	-600	2,483	513	-377	-271	545	-307	-216	-388	-99
65	D	-454	520	-1,867	-422	-891	-755	-193	199	-376	-714	-714	866	272	-343	-133	2,047	-391	-423	-304	-431
66	Unc.	306	581	360	-104	-510	-203	-212	1,419	-540	-1,140	-77	1,191	-245	-755	-375	868	-582	-1,037	88	-617
68	A	-510	-1,874	-1,136	-376	-1,290	-1,080	-2,478	-1,556	2,734	1,218	-729	-2,267	-1,141	2,628	-754	-2,015	2,454	1,258	-1,503	3,904
69	Unc.	163	671	170	-390	-659	-130	107	895	-519	-634	65	-36	-2	-729	-411	892	-961	-883	-14	-643
70	B	1,237	-1,705	1,000	317	2,353	1,304	-1,647	-905	2,191	1,940	1,659	-975	124	1,521	-694	-1,800	2,796	1,839	606	1,827
TL.A1	BC	-3,191	795	-1,867	-1,195	-2,160	-147	-821	-668	-24	-227	-484	-521	-409	220	301	583	-1,196	-74	-1,193	265
TL.B1	BC	-1,442	-328	106	-421	300	25	-470	-260	-628	-541	-285	-642	185	388	4,048	-71	-500	-1,069	-583	-688
NF.B1	BC	-638	176	511	-94	-85	-124	171	-1,562	-605	-1,109	-147	-371	-17	140	833	84	-202	-882	-276	-556
GH.B1	BC	-132	1,056	173	-405	345	-1,596	-236	718	-516	-1,306	-1,647	118	-356	-1,093	-399	1,321	-1,051	-497	-1,189	-769
FC.A1	Unc.	43	-694	419	-253	-674	-215	491	331	-810	-1,609	-501	-562	594	726	-434	-588	173	-1,425	-848	-760
GH.A1	BC	-2,223	549	363	78	-1,907	-71	-730	49	-497	-1,396	-8	-485	-573	122	1,145	981	-1,665	-1,338	-930	-791
GT.A1	BC	-1,085	838	-1,867	-1,195	-407	-730	-285	245	-529	-972	-493	-180	-319	-536	-316	772	-451	-912	-749	-793
GT.B1	BC	253	198	332	-1,195	-319	-196	-75	844	-592	-1,562	-372	-395	-49	-635	2,753	770	-586	-1,648	-729	-840
NF.A1	BC	-706	-686	1,438	126	1,113	740	293	260	-585	-1,386	408	-368	844	444	2,973	-372	-621	-1,131	312	-877
QL.A1	BC	-1,961	1,464	-150	-1,195	153	-1,769	-1,087	-511	-630	1,209	-1,647	168	-80	-879	-353	-130	-353	461	-1,995	-484
RIH.D1	Unc.	-755	390	213	-48	-763	-50	-293	-73	-385	-1,517	-1,647	204	-41	-120	-405	326	-918	-1,124	138	-507
WSP.B1	Unc.	-466	1,554	1,418	1,343	-53	-284	-678	-85	-337	793	-527	-24	62	-1,354	-428	-291	-931	-54	3,543	-751
DLA.A1	TR	-1,337	909	38	-602	-320	-881	-677	-285	-504	-200	-1,647	187	-60	-487	-380	106	-645	-358	-893	-496
QR.D1	BC	-461	203	-352	-1,021	-185	-1,023	399	-2,960	-456	-55	-1,159	-630	456	167	1,644	903	-205	-965	-830	-793
GH.C1	BC	1,044	-669	376	121	4	750	353	600	-677	-150	132	-496	412	200	1,887	-200	550	-1,042	174	-277
QR.A1	BC	651	717	-1,867	-1,195	-410	-310	530	1,499	-503	-1,277	-1,647	-120	-226	-1,384	2,316	1,106	-519	-1,327	-481	-700
QR.C1	BC	-1,368	2,368	-789	-1,195	-1,647	-950	-435	1,454	-535	-1,490	-1,647	-566	-1,210	-2,251	815	-374	-752	-1,802	-1,795	-1,158
RIH.A1	Unc.	-959	438	-1,867	-1,195	-1,311	-17	-45	-844	-653	-237	-152	-791	-141	-359	2,830	701	-633	-1,100	-333	-829
RIH.B1	Unc.	321	62	473	-433	-1,391	151	289	136	-800	-765	-266	-59	122	-120	-100	289	-147	-1,178	-622	-755
RML.B1	BC	-658	609	219	-346	-1,411	-540	80	-242	-609	-219	-604	-794	-155	-435	863	873	-441	-887	-595	-751
RML.E1	BC	-401	1,008	27	-1,195	-1,503	-1,333	-454	775	-652	-1,036	-1,647	-155	-559	-1,011	1,532	623	-1,431	-1,170	-1,520	-760
SLF.B1	Unc.	1,421	-1,213	1,795	597	1,681	575	2,140	323	-777	-311	1,862	-813	1,835	655	-652	-1,640	1,048	-1,546	642	-292
SLF.A1	Unc.	721	936	1,175	5,358	1,111	1,112	14	628	-768	-654	2,144	-1,506	1,419	-1,213	-571	-976	58	-1,929	382	-901
LP.A1	TR	913	-1,357	1,170	443	1,775	654	1,184	16	228	575	647	-695	763	965	-160	-1,803	303	1,072	-583	826
LP.E1	TR	360	-1,818	393	1,099	1,809	904	516	-339	621	321	801	-983	934	1,690	-402	-1,900	192	1,167	-229	734
QL.B1	BC	652	297	-618	-476	24	406	58	943	-583	-187	-162	-366	245	-588	337	427	-227	-770	92	-652
GNB.D1	BC	385	254	1,513	-1,195	-1,215	1,001	-32	279	-695	-596	-1,647	-452	-58	-494	1,700	685	-302	-1,464	-533	-895

Table D.7: Dataset 2 after normalization, variable selection, standardization and outlier removal. Final data used for PCA. S: Sample; G: OM groups.

Sample	PC 1	PC 2	PC 3	PC 4
1	1.8588	4.5686	2.5034	-2.8324
2	0.50369	-0.027806	-0.32975	-0.95687
4	0.78351	1.422	0.1287	0.29993
5	4.3098	-3.7755	0.19211	0.099379
7	-2.0728	0.091845	0.48338	2.3095
8	0.42335	1.5443	0.7185	1.2419
9	2.9262	3.9305	0.73215	-0.45996
10	-0.016161	0.70709	0.64217	1.8326
11	-2.0939	-0.31913	0.68409	-0.13058
12	-3.5545	-0.98808	2.8683	-0.34468
13	2.1488	-0.7659	-0.21609	0.98247
15	-0.59465	-0.8732	1.2678	0.344
17	0.76055	1.7896	0.42998	0.08599
18	2.874	-0.6459	0.45773	-0.50926
19	0.93372	2.2063	-0.24332	-0.80701
21	0.65391	1.0882	0.74849	1.0797
22	-1.9927	0.41955	-0.00074299	1.4743
23	-3.7837	-1.9025	4.0909	0.24138
25	1.2628	0.76778	-0.057016	-1.5539
26	-0.82406	1.1805	1.7389	2.4788
27	-2.0005	-1.3051	2.4081	0.61425
28	-1.7535	2.0211	0.62885	-0.53938
30	-1.5368	2.0802	0.66197	0.15066
32	3.6099	0.31919	-0.61609	0.96863
33	1.4956	3.5182	-1.3561	1.4649
35	3.298	-2.4591	-0.40686	-0.72207
36	5.4834	-0.50838	1.8914	0.18052
37	-2.3198	-0.9595	0.33956	-2.8117
39	5.3334	-2.7677	1.023	0.74441
40	-4.0803	-0.87268	4.4092	1.3995
42	1.0804	2.0193	1.3908	0.70929
43	3.2391	-0.42938	-0.35166	0.051575
46	3.8389	-0.51574	-0.062881	-0.82042
47	1.7124	3.6066	0.57312	0.83684
48	0.30907	-0.99357	-0.38972	0.076091
50	-2.1571	0.67077	0.24758	-1.6518
52	-2.8414	-0.19302	2.5937	-2.0992
53	4.5309	-3.6307	-0.68	0.006815
54	1.8073	-1.7516	-0.44522	-1.0634
58	0.92144	0.75186	0.44234	-1.2319
60	1.979	3.269	1.8131	-2.9508
61	5.8642	-4.0977	0.34355	1.4711
62	0.98929	2.0655	-1.6631	1.1851
64	-2.0463	-0.17639	0.72545	1.5657
65	-2.5229	-0.79342	0.50397	-0.13125

Sample	PC 1	PC 2	PC 3	PC 4
66	-2.3476	0.8033	0.52645	0.91299
68	5.2242	-6.0107	0.30395	-0.95992
69	-2.0212	0.65697	-0.018584	0.32689
70	6.5021	-0.27791	1.25	0.3387
TL.A1	-2.2411	-2.9912	-0.25406	-2.7486
TL.B1	-1.4752	-0.69621	-2.9298	-0.9218
NF.B1	-0.93457	-0.3191	-1.6455	-0.87143
GH.B1	-2.9574	-0.84132	-0.16578	1.5691
FC.A1	-0.65644	-0.062105	-2.2454	0.48107
GH.A1	-3.1094	-1.0008	-1.3406	-2.0902
GT.A1	-2.5767	-1.3459	-0.29076	-0.25979
GT.B1	-2.7575	-0.09424	-2.31	0.75814
NF.A1	-0.68045	1.5146	-2.928	-0.22388
QL.A1	-1.7048	-2.7597	0.20257	0.3746
RIH.D1	-2.1177	-0.46222	-0.6086	-0.0098077
WSP.B1	-0.96813	1.9697	1.7205	-0.34959
DLA.A1	-1.9184	-1.5722	-0.2164	0.17648
QR.D1	-1.2546	-1.6941	-2.355	-0.67081
GH.C1	0.076407	1.1213	-1.7374	0.43247
QR.A1	-3.5069	-0.39204	-1.3119	1.2843
QR.C1	-4.7281	-1.9519	-1.0453	0.25103
RIH.A1	-2.5045	-1.2139	-1.8164	-1.6663
RIH.B1	-1.4705	0.12667	-1.0992	0.089982
RML.B1	-2.0514	-0.71513	-1.1734	-0.59953
RML.E1	-3.8292	-1.7207	-1.3252	0.73528
SLF.B1	2.5105	3.4224	-2.5489	1.0951
SLF.A1	0.78731	4.5873	-1.0447	-1.6546
LP.A1	3.3964	1.1	-1.1018	0.80991
LP.E1	3.9519	0.83453	-0.99675	-0.18521
QL.B1	-1.178	0.74345	-0.41594	0.58553
GNB.D1	-2.1991	-0.044648	-1.9418	0.71116

Table D.8: PC Scores for Dataset 2, PCA 2 (without the outliers). Only PC1 and PC2 were used for the HCA.

D.2.5 Data Transformation tables (Digital appendix)

D.2.6 Method assessment: precision (Digital appendix)

D.2.7 Method assessment: accuracy (Digital appendix)

D.2.8 Raw data (Digital appendix)